MODELING OF A COUNTER-CURRENT ADSORPTION PROCESS FOR REMOVAL AND RECOVERY OF DISSOLVED ORGANICS FROM AQUEOUS EFFLUENTS

by

ROBERT CHARLES COPCUTT
B.Sc. (Chem. Eng.)

Submitted to the University of Cape Town in fulfilment of the requirements for the degree Master of Science in Engineering

(February 1988)

The continuous counter-current ion exchange process previously developed at UCT was investigated as a means of removing sodium, chlorides and other ions from paper pulp bleaching effluents. These ions would be recovered as re-usable by products in the proposed process. Preliminary tests on effluents from SAPPI's paper mills at Enstra in Springs and Ngodwana in the Eastern Transvaal indicated a problem with the recovery of the chlorides from the anion resin. The effluents contained organic compounds with a COD of about 1 g/l. These organics caused fouling of the anion resin when it was regenerated with lime. The most promising way found to relieve this fouling problem was to include an adsorption step between the cation and anion exchange steps. This project was initiated to investigate adsorption and then to develop a model for the design of the required adsorption step.

The first question was what compounds caused the anion resin to foul when regenerated with lime. The formation of calcium oxalate with a very low solubility was the most likely source of trouble. Other compounds such as long chained carboxylic acids and anthraquinone were also identified as foulants, but they could be easily removed from the effluent by polymeth-acrylic adsorbents such as XAD-8; oxalic acid could not be so easily removed. The method used for analysing the foulants was to convert any carboxylic acids to methyl or n-butyl esters. This was done while the foulants were adsorbed on the anion resin. During this derivatization process compounds desorbed from the resin and were dissolved in the reactant solution. The compounds in solution were analysed by gas liquid chromatography/mass spectrometry.

Spectrophotometric analysis was favoured and extensively used for conc-entration measurement because of its high precision, ready availability and its speed. However, this method suffered from interference caused by impurities coming from the experimental apparatus and the XAD-8. Some use was made of HPLC but the technique was less precise, much slower and less readily available.

Isotherms for the adsorption of organic compounds from bleaching effl-uents on a number of adsorbents have been tested by previous workers. Their conclusion, which was verified in this work, was that activated carbon could reduce the organic load in the effluents to a lower level than the polymeric adsorbents could. However, the polymeric adsorbents

were much more readily regenerated with alkaline solutions than the activated carbon. XAD-8 was selected for further study in this work because it was the easiest adsorbent to regenerate with sodium hydroxide. Isotherms for the adsorption of selected pure compounds on XAD-8 were also measured.

The Dubinin isotherm equation was used to model the adsorption of pure compounds. This equation had a number of distinct advantages over all other isotherm equations tested. It was accurate without being too complicated and it permitted re-arrangement of the dependent variable. It allowed the modeling of temperature effects and the prediction of unknown isotherms. The Freundlich isotherm was used to model the adsorption of bleaching effluents because the multicomponent nature of the effluents made the Dubinin equation unsuitable.

Experiments were performed to determine the rate of adsorption of bleaching effluents and of pure compounds on XAD-8. A 0.025 l spinning basket was built for this purpose. It is recommended that further work on adsorption isotherms and kinetics would be more suitably undertaken on a 0.02 m I.D. by 0.02 m long micro-column. This is because it would suffer less from the release of impurities, and because the flow of fluid through the bed could be well regulated.

A mathematical model for predicting the rate of adsorption in the batch experiments was developed. It assumed diffusion through a thin boundary layer around each particle followed by solid phase diffusion through the particle. Particle porosity was accounted for as well as the concentration dependence of the solid phase diffusion. The model was solved numerically using the Crank-Nicolson finite difference technique. The Crank-Nicolson analogs were solved using Gauss-Seidel iteration. The diffusion coefficients that best fitted the experimental data were found using the Nelder-Mead search algorithm.

This numerical model was adapted to another computer program for the design of continuous counter-current contactors. A graphical method for column design was also presented. It was not as accurate or versatile as the numerical design method but could be used to provide quick answers. It could also be used if sufficient computer power was not available for the numerically intensive computer programs.

A pilot plant was under construction to test the ion exchange/adsorption treatment of the bleaching effluent. The flow rate in the plant was to be 0.29 l/s. On the basis of the work performed, the author was able to make the following recommendations for the adsorption section which was still to be designed: XAD-8, or a similar polymethacrylic macroporous adsorbent, should be used. The adsorbent should be loaded in a series of fluidized beds where it could be periodically moved counter-current to the effluent; a horizontal arrangement of the Cloete-Streat contactor would be suitable. The contactor could be built with 6 fluidized beds (stages) initially and more stages could be added later if required. Each stage should be 1 m high and 0.4 m diameter. At the proposed flow rate, the up-flow of the effluent would cause 122% fluidization in the XAD-8 beds. If 85% removal of organics was found to be sufficient, the XAD-8 would have to be pulled-down (moved counter-current to the effluent) every 132 minutes. The resin would require about 0.01 l/s of 0.1 N sodium hydroxide for regeneration. This would also be carried out in a 6 stage contactor, but the stages would be 0.18 m ID and 2.5 m high. The rinsing of the adsorbent would be carried out in the first 3 stages and the last 3 stages would be for contact with the sodium hydroxide. The alkaline stream from the regeneration contactor would have an organic load 25 times that of the original bleach effluent.

The slow kinetics of adsorption on activated carbon and the difficulty of regenerating it means that its use was only recommended as a last resort.

Acknowledgements

The help of the following people and institutions is gratefully acknowledged. They have given me the opportunity to study a promising aspect of pollution control which is becoming increasingly important in the modern world.

I would like to express my appreciation to the following for their assistance and support during the project:

Mr. B.A. Hendry who initiated the project and who has provided much assistance;

Professor B.D.A. Paddon for his valuable help and support;

the CSIR, FRD for their bursary;

SAPPI Limited for their financial support of the experimental work;

all the Chemical Engineering Department staff and my fellow postgraduates for making work in the Department worth-while;

the South African Water Information Centre for the literature search;

Miss B. Williams of the Chemistry Department for the Mass Spectroscopic analyses;

Mr M. Birkett of SAPPI for performing the HPLC analyses;

the Electron Microscope Unit in the Physics Department for their time and the use of their equipment.

a	Constant for various isotherms	-
a_i	Isotherm constant for one compound	-
A	Absorbence of light	-
A_{ij}	Isotherm constant relating two solutes	-
b	Constant for various isotherms	-
B	Affinity coefficient	$[(KJ/mole)^k]$
C	Liquid concentration	[g adsorbate /l solution]
C_0	Initial liquid phase concentration	[g/l]
C_e	Equilibrium liquid concentration	[g/l]
C_1	Concentration of solution in stage 1	[g/l]
$C_{n,p}$	Concentration of solution leaving CCC	[g/l]
C_p	Concentration of pore solution	[g/l]
$C_{p,av}$	Pore concentration averaged over whole particle	[g/l]
C_s	Liquid phase conc on outside surface of adsorbent	[g/l]
C_{sat}	Concentration of saturated solution	[g/l]
d	Particle or bead diameter	[m]
D_p	Pore diffusion coefficient	$[m^2/s]$
D_q	Surface diffusion coefficient	$[m^2/s]$
D_s	Surface diffusion coefficient incorporating pore diff.	$[m^2/s]$
D_t	Diameter of column	[m]
e	Ultraviolet extinction coefficient	[l/mole/cm]
F	Flow rate into fluidized stage	[l/s]
F_s	Flow rate of adsorbent	[g/s]
g	Gravitational constant (9.8)	$[m/s^2]$
G	Gibb's free energy	[KJ/mole]
H	Henry's isotherm constant	[l/g]
i	Index	-
I	Intensity of light transmitted through cuvette	-
I_0	Original intensity of light	-
j	Index	-
k	Constant used for isotherms	-
k_f	Freundlich isotherm constant	-
K	Rate constant	$[s^{-1}]$
K_D	Distribution coefficient	[]
$K_{i,max}$	Maximum adsorption energy for compound i	-
$K_{i,min}$	Minimum " " " "	-
K_p, K_q	Empirical rate constants	-
K_s	Film transfer coefficient	[m/s]
L	Path length of light through cuvette	[cm]

m	Dosage of adsorbent	[g/l]
M	1 + total number radial steps in adsorbent particle	
M_l	Mass of solution in contacting system	[g]
M_r	Skeletal mass of adsorbent (ie dry mass)	[g]
n	Number of components	-
n_f	Freundlich isotherm exponent	-
N	Variable defined by equation 6.4	-
N_a	Flux per unit area due to diffusion	[Kg/s m^2]
P	Partial pressure of gas	[N/m^2]
P_o	Saturated vapour pressure of gas	[N/m^2]
q	Concentration on adsorbent	[g adsorbed /g dry resin]
q_{av}	Average solid phase concentration	[g/g]
q_e	Equilibrium solid phase concentration	[g/g]
q_{max}	Maximum of q (used as a parameter)	-
$q_{n,p+1}$	Concentration of adsorbent entering CCC	[g/g]
Q	Ultimate uptake capacity	[g/g]
r	Radial distance from particle centre	[m]
Γ	Grouping of descritization steps	-
R	Gas constant (0.0083144)	[KJ/mole]
R_p	Radius of adsorbent particle	[m]
t	Time	[s]
T	Temperature	[K] or [°C]
U_c	Superficial velocity of fluid	[m/s]
U_i	Free falling velocity at infinite dilution	[m/s]
U_o	Free falling velocity of particles in fluid	[m/s]
V_b	Gross volume of batch reactor	[l]
V_f	Gross volume of fluidized bed stage	[l]
V_l	Volume of liquid held within a resin bead	[l]
V_p	Volume of the pores within adsorbent particles	[l]
V_r	Volume of the matrix of adsorbent particles	[l]
x	Distance	[m]
X	Mole fraction of solute	-

Greek characters

α	Concentration dependence factor	
δ	Thickness of diffusion film	[m]
ϵ	Adsorption potential (Polanyi theory)	[KJ K/mole]
ϵ_i	Adsorption potential for component i	[KJ K/mole]
ϵ_1	Polanyi potential for pure solvent	[KJ K/mole]

ϵ_{s1}	Polanyi potential of solute adsorbing from solvent	[KJ K/mole]
ϵ_s	Polanyi potential for pure solute	[KJ K/mole]
ϵ	Voidage assuming solid adsorbent particles	-
ϵ_a	Settled bed voidage on a mass basis	-
ϵ_p	Particle voidage	-
ϵ_s	Settled bed voidage on a volume basis	-
ϵ_v	Voidage assuming porous adsorbent particles	-
ϵ_f	Fluidized bed voidage	-
$\emptyset$	Adsorption volume	[l/g resin]
$\emptyset_0$	Maximum adsorption volume	[l/g resin]
ρ	Density of solute in bulk phase	[Kg/m^3]
ρ_a	Effective density of beads $= \frac{M_r + \rho_f V_p}{V_r + V_p}$	[Kg/m^3]
ρ_f	Density of fluid	[Kg/m^3]
ρ_s	Density of dry adsorbent $= \frac{Mr}{V_r + V_p}$	[Kg/m^3]
∇	Molecular volume	[l/mole]
$\tilde{\nabla}$	Corrected molecular volume	[l/mole]
γ	Tortuosity factor	-
μ	Viscosity of fluid	[kg m/s]
λ	Wavelength of light	[nm]
Υ	Polarizability correction factor	-

Dimensionless groups

$\bar{C}$	Dimensionless liquid phase concentration	C/C_0
Dg_b	Solute distribution parameter for batch systems	$\rho_s q_s / C_0$
Dg_f	Solute distribution parameter for flow through systems	$\rho_s q_s (1-\epsilon_f)/C_0 \epsilon_f$
N_f	Dimensionless diffusivity parameter	$D_s t Dg_f / R_p^2$
$\bar{q}$	Dimensionless solid phase concentration	q/q_s
$\bar{r}$	Reduced radial coordinate	r/R_p
Re	Renolds number	$U_0 d \rho_f / \mu$
Sh_b	Sherwood number for batch systems	$K_s R_p / D_s Dg_b$
St_f	Stanton number modified for flow through systems	$K_s (1-\epsilon_f) \tau / R_p \epsilon_f$
$\bar{t}$	Dimensionless time (Batch system)	$D_s t / R_p^2$
τ	Hydraulic retention time	V_f / F
Tm	Dimensionless time (Flow through system)	$t / \tau Dg_f$

Chapter 1

INTRODUCTION

SAPPI (South African Pulp and Paper Industries) operates a paper mill at Ngodwana in the Eastern Transvaal which produces about 6000 m^3/day of bleach plant effluent, containing substantial quantities of pollutants. It also operates a mill at Enstra in Springs that has a similar pollution problem. These effluents need to be treated so that they can be re-used or safely discarded. This report is concerned mainly with the removal of the organic pollutants from these effluents.

1.1) History of Ion Exchange research at UCT.

Early research at UCT on the use of Ion Exchange for effluent treatment was conducted with funding from the Water Research Commission (WRC) and studied the use of multiple NIMCIX (National Institute for Metallurgy Continuous Ion-Exchange) contactors. The NIMCIX columns built in the Department consisted of a series of up to 12 stages placed vertically on top of each other. Each stage was separated by a perforated plate. Resin was loaded into the column from the top. When sufficient resin had been introduced into all stages, the loading cycle (or regeneration cycle in the regeneration column) was begun. The liquid stream was introduced at the bottom of the column, and the upward flowing liquid fluidized the beds of resin. In the load columns, the flow was sufficient to cause the resin bed to expand to about twice its settled bed volume (100% fluidization). After a suitable period the up-flow was stopped and the beds were given about 2 minutes to settle. Water was then pumped through a catch pot full of resin and into the top of the column. This had the effect of loading the top column with more resin and moving the resin in all stages down to the previous stage. The resin from the bottom (first) stage was caught in another catch pot. The up-flow cycle was then started again. The overall effect was that the resin moved counter-current to the liquid stream it was being contacted with.

The application of these NIMCIX columns was the desalination of secondary sewage effluents for potable water reclamation. Experience with these vertical columns demonstrated that regenerants such as a concentrated lime slurry could be utilized. Several novel processes were investigated which enhanced water recovery and reduced regeneration costs associated with treatment of effluents by ion exchange. Flow-sheets were developed which achieved cost effective chemical waste recovery and avoided pollution, making ion exchange an economical desalination process.

1.2) The SAPPI effluent treatment program

The WRC project was completed in 1981 and further work was undertaken from 1982 onwards on behalf of SAPPI and studied the use of a weak anion resin for chloride recovery from the pulp bleaching effluents.

The paper-making process involves chemically pulping the wood and then removing the lignin from the cellulose. The cellulose is the major component of paper and the lignin is a coloured polymeric material that is removed by a process called bleaching. The bleaching is performed in several stages. SAPPI have found that they can recycle all of their bleach effluents except one. At Enstra it is the combined effluent from two stages where the pulp is treated with chlorine dioxide (called D1/D2 effluent). At Ngodwana it is the effluent from a stage where the pulp is treated with chlorine and chlorine dioxide (called D/C effluent). The effluents contain sodium and chloride ions, smaller quantities of sulphate, calcium and other ions and a complex mixture of various organics. A flow-sheet was proposed that combined effluent desalination and chemical recovery whereby the sodium would be removed by a strong cation resin such as Duolite C26. The cation resin would be regenerated with sulphuric acid and the sodium sulphate thus produced can be re-used. The chlorides could then be removed with a weak anion resin, (eg Duolite A368). Sodium hydroxide and calcium hydroxide (lime) were considered as alternative regenerants.

Sodium chloride produced by using sodium hydroxide would only be useful if electrolysis to produce sodium hydroxide and chlorine were economically attractive. Lime regeneration would produce calcium chloride as a by-product. Calcium chloride has a limited solubility of 46.08 weight

percent in water at 25 °C and could be crystallized out of a concentrated regenerant stream. The solid byproduct would then have a resale value. However, experiments showed that the weak anion resin was very quickly fouled when lime was used as the regenerant, but not when sodium hydroxide was used. This fouling was caused by the combined effects of the calcium and the organics in the effluent and was believed to be due to insoluble calcium-organic compounds.

To make the use of lime possible it was proposed to add an adsorption step before the anion exchange step to remove the organics that caused the fouling. Research was begun at UCT to find a suitable adsorbent for this purpose. Various activated carbons and charged and uncharged polymeric adsorbents were screened. Amberlite XAD-8 was found to be the most suitable. Although it did not have the high capacity of the activated carbons, it displayed faster kinetics of adsorption and could be easily regenerated by a very weak alkaline solution such as 0.1 N sodium hydroxide. A highly concentrated spent regenerant stream with potential for calorific value recovery could be produced. Figure 1.1 shows the proposed flow-sheet. (Reproduced with permission from Hendry (1984)).

Although processes for bleach plant effluent treatment with XAD-8 had been reported before, these overseas applications were for colour removal rather than for chemical recovery. Incineration of the organics in the regenerant waste stream, and the subsequent heat recovery, was desirable and could only be achieved if the stream was of sufficient concentration. Previous experience with Cloete-Streat type continuous counter-current contactors encouraged the study of this method of operation for the adsorption step as well as for the cation and anion steps. This contactor incorporated certain properties not possessed by any other, which allow the required concentrating performance to be achieved.

1.3) Horizontal CCIX system.

Because of the interest in building a medium scale continuous counter current ion-exchange (CCIX) plant, the feasibility of the proposed ion exchange flow-sheets in a horizontal lay-out was investigated. The horizontal arrangement had the advantage of not needing the expensive support structures required for the vertical arrangement in addition to easier access for operators.

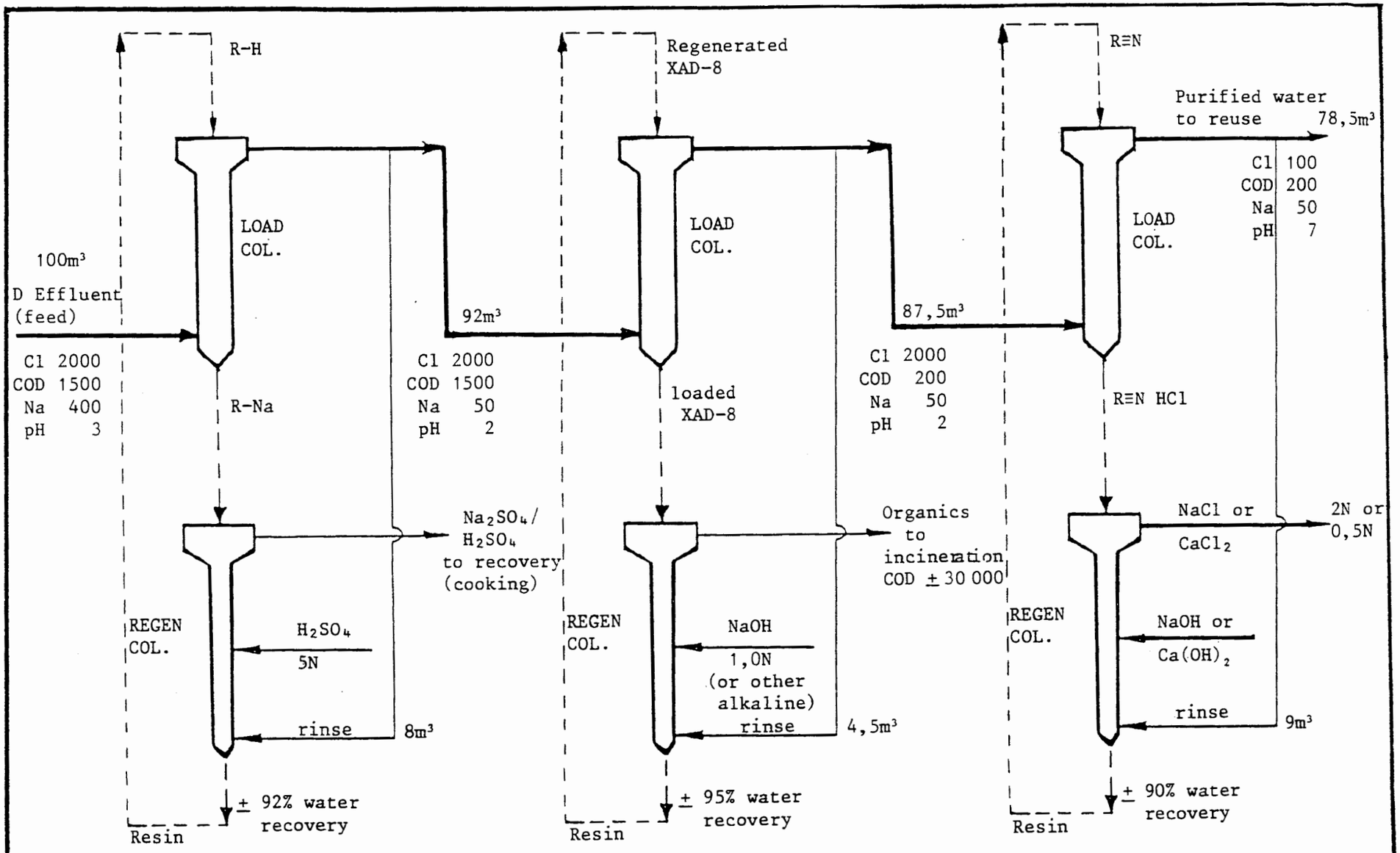

Figure 1.1 Flow-sheet of ion exchange/adsorption process for chloride, water and organic calorific value recovery from bleach effluent

Experiments carried out with three 0.09 m diameter horizontal stages showed that the operating pressures could be lower than in the vertical system. It was proposed that a theoretical cost comparison should be made before any more work is done on this topic. The detailed report on this work can be found in appendix 5.

1.4) Adsorption process model and identity of foulants

To design a Cloete-Streat type continuous counter-current contactor (CCC) the use of a process model is desirable. This process model would be used to calculate the number and size of the stages required for a given adsorber performance. This is of particular interest with respect to multi-component operations because of the competition between compounds for adsorption sites.

To generate data for the process model, it was considered preferable to find 'model organics' for adsorption studies, so an attempt was made to identify the anion resin foulants. Literature research begun by this author early in 1985 indicated that oxalic acid was the most probable foulant because of the low solubility of calcium oxalate (see appendix 6). A later experiment where anion resin was loaded with oxalic acid (reported in appendix 2) reinforced this belief.

Later in 1985, an attempt was made to analyse the foulants and to establish the mechanism of fouling. A sample of fouled anion resin was prepared under controlled conditions, and then three different methods of removing these foulants for analyses were tried. By use of the gas chromatography/mass spectrometry (GC/MS) a few possible foulants were revealed. Some of these foulants were known to have insoluble calcium salts, which tended to confirm the theory that the fouling on the weak anion resin was caused by insoluble salts forming within the pores.

Oxalic acid was a potential foulant but it was found to adsorb weakly on XAD-8. However, experiments conducted at Enstra in 1983 showed that lime regenerated weak anion resin was not rapidly fouled by D1/D2 effluent pre-treated by strong cation exchange and organic adsorption on XAD-8. Thus it would appear that XAD-8 nevertheless had sufficient capacity for

oxalic acid and other potential foulants to reduce their concentrations sufficiently to avoid fouling. Therefore experimental work with oxalic acid and XAD-8 remained of interest.

The work on foulant species identification provided a deeper insight into the nature of anion resin fouling. It was shown that high molecular weight carboxylic acids were at least part of the fouling problem. Several model compounds suitable for further study were identified, and a method for a more complete analysis of foulants was established. However, the work was found to be extremely time consuming and was discontinued in favour of the work discussed below. The details of the anion resin foulant analysis can be found in appendix 1.

1.5) Adsorption studies.

Experiments were begun with D1/D2 effluent to establish experimental procedures for measuring adsorption isotherms and adsorption kinetics. The isotherms obtained were similar to those of previous workers at UCT (Jackson, 1983; Harries, 1982 and Gordon, 1982), and the rate of adsorption was found to be an inverse function of the bead size. Later, the adsorption isotherm of cation exchanged D/C effluent was determined more accurately over a wide concentration range.

Regeneration of the XAD-8 loaded with bleaching effluent was not studied because it was believed that the ease of regeneration of this resin had been sufficiently demonstrated by Jackson (1983) and Kennedy (1973).

Initial studies of the adsorption of oxalic acid on XAD-8 showed a very high rate of adsorption. A spinning basket contactor was constructed to follow this rapid concentration change. For this purpose it was moderately successful and tests were also performed on phenol and cation exchanged D1/D2 effluent. The data was fitted to a rate equation based on the rate of diffusion through the film surrounding the adsorbent particles and on the solid phase diffusion within the particle.

The spinning basket reactor was found unsatisfactory for isotherm measurements, because of the unpredictable increase in ultraviolet (UV) absorption that occurred. Isotherms therefore had to be measured in separate experiments using sealed Xactics bottles. Isotherms measurements

where made for cation exchanged D1/D2 effluent, phenol, oxalic, benzoic, isophthalic, stearic, palmitic and malonic acids. These model compounds were selected for study on the basis of their potential as foulants and their popularity with previous researchers.

When it was possible to produce results with little scatter, it was found that the isotherms fitted the Dubinin isotherm well. The isotherm for the cation exchanged D1/D2 effluent fitted the Freundlich isotherm best and this was thought to be due to its multi-component nature. The Dubinin isotherm was considered to be a very powerful equation because it could predict the effect of changing temperature and pH. It was derived from the Polanyi theory of adsorption and had a limited ability to predict the adsorption of untested compounds.

1.6) Mathematical modeling of adsorption in counter-current contactors

A design method for contactors was developed from a simple and quick graphical method to a single component computer model. Computer models for a simple empirical rate equation and then a sophisticated diffusion rate equation were developed. This diffusion model had the advantage of being deductive and was able to predict the effect of changing particle size and liquid flow rate. The model could account for a variety of complicating factors in the contactor such as changing temperature and composition and it could model the regeneration column as well as the load column. If the adsorbent was changed, the only change required to the program was a new set of isotherm and rate constants.

It was proposed that SAPPI build a pilot plant to test the ion exchange /adsorption process described above. The computer program was used to design a suitable adsorption stage. This was done by substituting the isotherm and rate constants measured for the cation exchanged D1/D2 effluent into the program and testing a variety of design options.

1.7) Structure of XAD-8

A course on the use of the electron microscope was completed in 1985. The microscope was used to the study the pore size and other structural features of XAD-8. It gave some insights into ways of improving adsorption kinetics.

Chapter 2

Literature survey and theory

In this chapter the development of the theory is briefly traced through the literature. The intention is to give the reader an understanding of and a background to the theory used later in this thesis.

2.1) Anion resin fouling

Research at UCT by Hendry (1984) showed that organics from the paper bleaching effluent were taken up by the anion resin and occupied up to a third of the resin's capacity. They were easily removed during regeneration with sodium hydroxide. Regeneration with calcium hydroxide produced crystals of calcium chloride, which had a resale value. However, calcium hydroxide caused the anion resin to foul and lose its capacity. It was found that treatment of the fouled resin with sodium hydroxide only partially restored the resin capacity. Other methods for reversing the fouling were not tested. Tilsley (1979) found that treatment with sodium chloride, hydrochloric acid or sodium hypochlorite was effective for removing foulants from anion resins. It was reported by Betz (1976) that anion resins were reversibly fouled by organic acids and the stronger the acid the greater the fouling effect. However, the probable mechanism of the fouling observed by Hendry was the formation of insoluble calcium salts during regeneration. These salts could therefore not migrate out of the resin pores and accumulated causing fouling. The higher solubility of the sodium salts which could migrate out of the resin probably explained the partial reversal of the fouling when the resin was treated with sodium hydroxide.

The most feasible way to overcome the fouling problem was thought to be the removal of the organics from the effluent after cation exchange treatment using an adsorbent. The organics could then be recovered. Tests by Jackson (1983) and Kennedy (1973) showed that if XAD-8 was used for this removal, the organics could be recovered at a very high concentration. The regenerant stream could be incinerated for the recovery of its calorific value and the sodium hydroxide.

The experimental work on the analysis of anion resin foulants is reported in Appendix 1. The remainder of this section looks at the literature and the theory behind the analysis of the anion resin foulants in paper bleaching effluents.

2.1.1) Compounds previously found in bleaching effluents

The question which arose was which organics in the cation product solution fouled the anion resin, and how well would the adsorption step remove them. Identifying the compounds in the effluent that precipitate with calcium was considered a first step in answering this question.

A number of long chain carboxylic or fatty acids were found in bleaching effluents by Voss and Rapsomatiotis (1985), Easty et al (1978), Fox (1976), Brownlee and Strachan (1976) and Rogers (1973). They have essentially insoluble calcium salts (Raltson, 1948) and were therefore potential foulants. Oxalic acid was found in bleaching effluents (Dence and Annegren, 1979; Ota et al, 1973; Pfister and Sjostrom, 1979), and being a strong acid, it would readily load onto anion resins. Calcium oxalate is very insoluble (Weast, 1980; Linke, 1958). The solubility data that could be found for calcium salts has been tabulated in Appendix 6.

2.1.2) Analysis of anion resin foulants

A review of the literature showed that the most powerful method available for identifying organic compounds was to separate the mixture by gas liquid chromatography (GC) followed by Mass Spectroscopy (MS) to identify each component. Although high performance liquid chromatography (HPLC) followed by MS was becoming an attractive alternative, such a facility was not available.

2.1.2.1) Gas liquid chromatography

GC is performed in a glass or alloy steel column. The column is filled with a finely divided inert solid onto which a liquid adsorbent is coated. A carefully regulated stream of inert gas (usually helium or nitrogen) is passed through the column. A sample of the solution for analysis is injected into the front of column, and a portion of it vaporizes into the inert gas stream. The gas stream carries the vapour

down the column until the vapour is adsorbed by the column packing. A dynamic equilibrium is established between the components of the sample being adsorbed by the packing and being carried down the column as a vapour. Components with a low vapour pressure and/or a high affinity for the packing are only moved slowly down the column. Volatile components with a low affinity for the packing move rapidly down the column and exit first through a detector. Ideally therefore, the detector produces a series of peaks as each component emerges from the column.

To increase the rate at which the sample moves through the column, it is heated in an oven with an accurate temperature control. To increase the resolution between the different components, it is common to increase the temperature of the oven at a known rate during the run. Increasing the length of the column also helps the resolution but increases the time it takes for the sample to pass through the column. For very high resolution between peaks, glass capillary columns are used. These consist of a long (>10 m) capillary tube of glass whose walls are coated with the liquid adsorbent.

There were a range of possible detectors for measuring the concentration of the vapour in the inert gas stream leaving the column. Two types were readily available:

i) the flame ionization detector (FID) works by burning the vapour with hydrogen and air or oxygen. The burning process produces ions that make the flame conductive. A D.C. potential is applied to plates on either side of the flame, and the current that flows is an indication of the flow rate of ions through the detector. The flow rate of ions is proportional to the flow rate of the compounds in the carrier gas passing through the detector. The process is sensitive and has a linear response over a very wide concentration range;

ii) the mass spectrometer can provide information about the composition of the vapour as well as its concentration. The vapour leaving the GC column goes into a carrier-gas separator where the volume of carrier gas is reduced to a level that the

mass spectrometer can handle. The vapour is bombarded with a stream of electrons which ionizes the molecules and also splits them into smaller fragments.

The ions are then accelerated through a magnetic field which deflects them according to their mass. A detector at the other end measures the current received from the ions hitting it and releasing their charge. The detector current therefore indicates the concentration of ions and the deflection of the ions indicates their mass per charge ratio (m/e). The strength of the magnetic field is regulated to control the mass of the ions that hit the detector. By cycling the strength of the magnetic field, the spectrum of ions is scanned about once every five seconds.

An ionizing energy of 70 ev was typically used to ionize the sample (McLafferty, 1980; Budzikiewicz et al, 1967). This value was chosen because it had been found to leave most of the ions with a single charge. It also split the molecules into a number of fragments that gave the most information about the nature of the original or parent molecule. Some bonds in the molecule broke more easily than others during the ionization process. The mass and relative abundance of the ions produced was therefore characteristic of the molecule. Tables of the relative abundance of the ions produced from different molecules using 70 ev were available. eg. Mass spectrometry data centre (1974).

2.1.2.2) Derivatization for GC

It is believed that most of the compounds in the effluent that cause fouling of anion resins are carboxylic acids. Carboxylic acids are polar and often strongly adsorbed onto the liquid adsorbent of the GC column. Also they often have such low vapour pressures that they cannot pass through the column. Some of them also decomposed at the temperatures used for GC. The method used to solve this problem is to convert them to a more stable derivative with a lower vapour pressure and less polarity. A large number of suitable derivatives have been used. Probably the most popular derivatives are methyl esters. eg. Hornstein et al (1960). Zinkel and Engler (1977) tested several esters and found that

tertiary-butyl esters performed well. Trimethylsilyl esters were also popular, but Zinkel et al (1968) found that care needs to be taken because they are easily hydrolysed. The following examples show why methyl esters are useful derivatives: stearic acid decomposes at 360 °C and has a vapour pressure of 15 mmHg at 232 °C; methyl stearate has a vapour pressure of 747 mmHg at 442 °C and 15 mmHg at 215 °C. Isophthalic acid melts at 348 °C but the methyl ester boils at 282 °C. Oxalic acid sublimes at 157 °C and dimethyl oxalate boils at 164.5 °C.

2.2) Ultraviolet spectroscopy

The theory of UV spectroscopy was considered in some detail here because it was the predominant method of quantitative analysis used in this project.

2.2.1) The Beer-Lambert law.

The basis of quantitative analysis by ultraviolet absorbence is the Beer-Lambert law which is:

$$A = e.C.L = \log_{10}(I_0/I), \qquad (2.1)$$

where
- e = UV extinction coefficient,
- A = UV absorbence,
- I = Intensity of light transmitted through cuvette,
- I_0 = Original intensity of light,
- C = Concentration, [mole/l]
- L = Path length.

It is derived by combining the Lambert law with the Beer law. The Lambert law states that the ratio of intensities of incident to transmitted light is independent of the intensity of the light. The intensity of the transmitted light therefore decreases with the exponential of the path length. The Beer law came from the observation that doubling the concentration of a solution had the same effect as doubling the path length. True deviations from the Beer-Lambert law are rare and most apparent deviations are due to other effects (Beaven et al, 1961).

When there are two species in solution, their combined absorbence is the sum of the absorbences due to each species on its own. Therefore:

$$A = e_1C_1L + e_2C_2L.$$

The extinction coefficient (e) is a function of wavelength, and the e vs. wavelength curve is a valuable indication of the chemical structure of the compound being examined.

2.2.2) Absorption bands

The energy of the photons of UV radiation, and sometimes visible radiation, is sufficient to promote transitions between electronic energy levels. Figure 2.1 shows a simplified example of the electronic energy levels in an typical organic molecule (Rao, 1975).

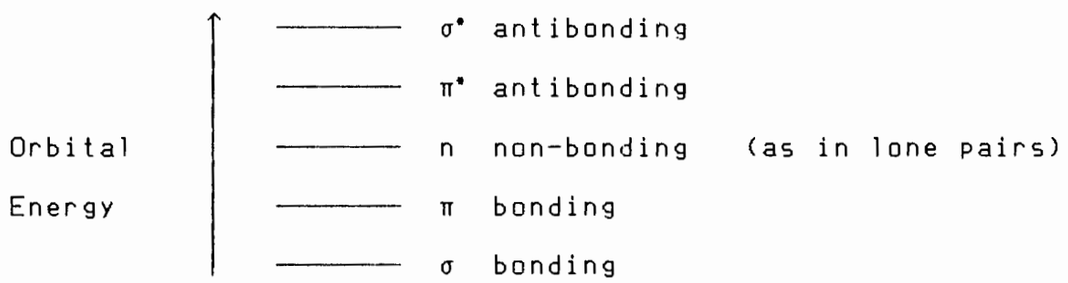

Figure 2.1. Electronic energy levels in a molecule

If a photon has just the right amount of energy to promote a π bonding electron to a π anti-bonding orbital then it has a probability of being absorbed. The possible transitions are $\sigma \rightarrow \sigma^*$, $\pi \rightarrow \pi^*$, $n \rightarrow \pi^*$ or σ^*, $\sigma \rightarrow \pi^*$, or $\pi \rightarrow \sigma^*$. The last two examples have a low enough probability to be ignored because the low probability means that the extinction coefficient will be low. The wavelengths that cause $\sigma \rightarrow \sigma^*$ transitions are usually below 200 nm and these wavelengths can only be measured by instruments that create a vacuum for the light path. Such transitions are therefore of limited practical interest. Functional groups in a molecule that cause absorption in the visible or near ultra violet wavelengths are called chromophores. A chromophore is usually associated with an unsaturated group.

Phenol has two UV peaks that are of practical interest. The first at about 215 nm is due to a $\pi \rightarrow \pi^*$ transition and has an extinction coefficient of about 6000 when in aqueous solution. The second peak at 270 nm is due to a theoretically forbidden $\pi \rightarrow \pi^*$ transition (Scott, 1964). This weak transition occurs because of the distortion of the molecular symmetry by molecular vibrations. Ketones have peaks at 190 nm due to non-bonding electrons (lone pair) on the oxygen being promoted to σ anti-bonding orbitals. However, with carboxylic acids the C =O bond is conjugated with the C - O - H bond and this causes a rise in the extinction coefficient and a slight increase in the wavelength of the peak. Oxalic acid has a strong peak at about 200 nm because the two acid groups are close enough to conjugate. Malonic acid has a much weaker peak at a shorter wavelength because the extra carbon atom between the carbonyl groups eliminates nearly all of the conjugation.

The fine structure of the spectrum is masked by the random kinetic energy of the molecules due to their temperature. When a molecule is in solution, the fine structure is additionally masked by the solvent-solute interaction forces. The spectrum is smoothed, the effect being greater in polar solvents. The peaks may also experience a shift in wavelength depending on the type of transition that is being observed. When ionization occurs the spectrum undergoes marked changes, the change being sensitive to pH.

Hydrogen bonding is a factor when working with carboxylic acids and phenols. The main result of hydrogen bonding is a concentration dependent shift in the absorption peak (Rao, 1975).

2.2.3) pH effects on UV absorbence

The spectrum of each ion in solution is different from that of other ions and of the undissociated molecule. Albert (1962) explains in detail how the extinction coefficient of each ion and the parent molecule is experimentally determined and how this information can be used to find the dissociation constant of the acid or base being investigated.

2.2.4) Effect of temperature

Increased temperature causes expansion of the UV cuvette and the solution in it. The linear thermal expansion of quartz is 5.5E-7 m/m °C. A 10 °C rise in temperature will therefore increase the path length 0.00055% which is negligible. However, water will expand by 0.26% when the temperature rises from 20 to 30 °C. This has the same effect as reducing the concentration by 0.26%. Although this change is small, the UV meter is capable of detecting such a change and regulation to within 4 °C (0.1%) is needed.

Other temperature effects are due to the changing pH caused by the temperature dependence of the dissociation constants. The dissociation constant of water rises from 6.809E-15 at 20 °C to 1.469E-14 at 30 °C (pK_w 14.1669 to 13.833). The dissociation constants of nearly all carboxylic acids also increases with temperature (Harned, 1950). The relative concentrations of ions in solution will therefore change with temperature and if the different ions have different extinction coefficients, the absorbence of light will also change.

2.2.5) Effect of the finite spectral band width

The finite size of the spectral bandwidth means that if readings are taken where the absorbence changes with wavelength, the absorbence at the shortest wavelength measured will be different from that at the longest wavelength measured. The instrument measures the average light intensity but the average absorbence is desired. The nature of the Beer-Lambert law (equation 2.1) means that a small but often significant error results (Beaven et al, 1961).

2.2.6) Stray light and turbidity

Stray light is light passing through the cuvette to the detector with a wavelength different from that indicated by the instrument. Its effect is to flatten the peaks of absorbence because although most of the light at the indicated wavelength is being absorbed by the sample, stray light is passing through to the detector. The effect is worst at the extremes of the wavelengths that the detector can handle because its sensitivity

is low at these wavelengths (Beaven et al, 1961). The instrument used suffered from this problem slightly and extensive servicing by the agent did not correct the fault.

Turbidity in the sample also creates false readings. Suspended solids diffuse light of all wavelengths so the effect will be most noticeable when the extinction coefficient is small. In some cases the absorption peaks can become minima because of destructive interference at wavelengths transmitted by the non-turbid solution. The amount of absorbence caused by turbidity depends on the refractive index of the solids and the solution, the shape of the solids, the nature of their surface and several other factors.

2.3) Adsorption isotherms

Having identified a number of potential anion resin foulants, the next task was to find out how well they would be adsorbed onto XAD-8. The section below gave a background of liquid phase adsorption theory and how it was developed. There was more in this section than was required for the reader only interested in modeling adsorption columns. Equations 2.3 (Freundlich) and 2.14 (Dubinin) were used in the models developed later, and the informed reader may refer directly to these equations. The literature on multicomponent adsorption was reviewed but the theory was not applied; mainly because the composition of the bleach effluents was not known.

Adsorption is the process by which an adsorbate is attracted to a solid surface so that the concentration of the adsorbate on the solid's surface is higher than it is in the surrounding fluid. Adsorption can be divided into two main classes, being chemisorption and physisorption. Chemisorption involves a chemical modification during the adsorption process. Physisorption involves no chemical modification of the adsorbate or the adsorbent, and is characterised by a lower heat of adsorption (usually positive in both cases). Physisorption is therefore easier to reverse in the regeneration process and regeneration is often the most costly step in the adsorption process. Only physisorption is considered in this report.

An adsorption isotherm is a measure of the amount of adsorbate (also called the solute when in the liquid phase) adsorbed by the adsorbent at a certain liquid concentration at a fixed temperature. There are many isotherm equations proposed in the literature and only the more useful and common examples are outlined below.

Many publications referenced in this chapter referred to work performed on activated carbon. This was because much less work had been performed on polymeric adsorbents. Although it could have been argued that adsorption on resins and activated carbon was different, this difference was on a quantitative level and not a qualitative one.

2.3.1) Single component isotherms

a) Henry's law:

the simplest isotherm is derived from Henry's law which states: 'the amount of gas adsorbed by a given volume of liquid at a given temperature is directly proportional to the pressure of the gas'. To a certain extent the argument can be applied to the adsorption of solutes onto solid adsorbents. The equation is:

$$q = H \times C_e, \qquad (2.2)$$

where q = Solute adsorbed per unit weight dry adsorbent,
C_e = Equilibrium fluid concentration,
(For the rest of this section C means C_e)
H = Henry's constant.

For most practical examples, it is only capable of modeling adsorption over a small concentration range. For dissolved solids or liquids adsorbing onto solid adsorbents, it generally applies better at low concentrations.

b) Langmuir isotherm:

Langmuir was among the first researchers to develop a theoretical adsorption isotherm (1918). He developed a model based on the assumption that the adsorbate forms a monolayer on the surface of the adsorbent.

The formula is:

$$q = \frac{Q\ k\ C}{(1 + k\ C)}, \qquad (2.3)$$

where k = Langmuir constant,
Q = Maximum value of q.

The theory is more applicable to gaseous adsorption on solids where mono-layer adsorption appears to be a fairly realistic assumption. It is generally accepted that in the liquid phase, multilayer adsorption starts at low concentrations. Cornel and Sontheimer (1986) found that the adsorption capacity of polymeric resins was not directly related to surface area as measured by nitrogen adsorption. It was not directly related to the pore volume measured by mercury porosimetry and pycnometry either. They concluded that the solute adsorbed into 'latent pores' which caused the observed swelling of the resin.

c) Freundlich isotherm:

Freundlich proposed his isotherm in 1926. It is a simple two-parameter equation that models the adsorption of solutes onto solid adsorbents, but is only accurate over small concentration ranges. To extend the range of application, different coefficients can be used for different concentration ranges. It has the form:

$$q = k_f\ C^{n_f}, \qquad (2.4)$$

where k_f = Freundlich constant,
n_f = Freundlich exponent.

Freundlich developed it empirically but it was later derived theoretically by Baly (1937). A feature of it that limited its popular acceptance was that it did not approach Henry's law at low concentrations.

d) BET isotherm:

Brunauer et al (1938) developed the BET isotherm which assumes:

i) the rate of adsorption is proportional to the 'pressure' of the adsorbate, and that the rate of desorption is proportional to the number of molecules with enough energy to overcome the surface forces. A dynamic equilibrium is reached between adsorption and desorption;

ii) an immobile adsorption on an energetically uniform surface;

iii) no interaction between adsorbed molecules;

iv) adsorption occurs by adsorbate molecules first forming a monolayer on the adsorbent surface, but forming multilayers as soon as the monolayer becomes crowded.

Details of the isotherm can be found in Coulson and Richardson (1979).

e) Miscellaneous three-parameter isotherms:

Jossens et al (1978) have compared a number of three-parameter isotherms that were suitable for extending to multicomponent adsorption modeling. All equations approached Henry's law at low concentrations. They were:

i) Toth equation:

$$q = q_{max} \, C \, (b + C^a)^{-1/a}, \qquad (2.5)$$

where a,b = constants,
q_{max} = a fictitious maximum that becomes the third fitted parameter;

ii) the Redlich-Peterson equation:

$$q = a \, C \, (1 + b \, C^k)^{-1}, \qquad (2.6)$$

where k = constant.

Note that this equation simplified to the Langmuir isotherm when k = 1;

iii) the three-parameter Newman equation:

$$q = [(a\ C)^{-1} + k(b\ C^k)^{-1}] \times [(a\ C)^{-1} + (b\ C^k)^{-1}]^{-2}; \qquad (2.7)$$

iv) the Jossens equation:

$$C = \frac{q}{a} \exp^{(kq^b)}. \qquad (2.8)$$

This equation expresses C as a function of q which was found to be a useful feature by Weber and Van Vliet (1979).

Jossens et al (1978) found, on comparing the four equations quoted above, that the Toth and Jossens equations best fitted the adsorption of organics on activated carbon. Their comparison was done using isotherm data of eight different compounds (including phenol) on activated carbon.

f) Weber-Van Vliet isotherm;

the Weber-Van Vliet equation (1979) is the most complex isotherm considered in this report. It is a four-parameter model, and the dependent variable is the liquid concentration instead of the adsorbed concentration. The changing of dependent variables makes the isotherm simpler to incorporate into the numerical models used to solve the kinetic equations. The isotherm is empirical and fits the data well. It has the form:

$$C = a_1 q^{(a_2 q^{a_3} + a_4)}, \qquad (2.9)$$

where a_{1-4} = isotherm coefficients.

g) Polanyi theory;

Polanyi did theoretical work on adsorption, starting in 1914. His work was mainly on the nature of the forces that caused adsorption and many

subsequent workers found that his theory explained the observed behaviour of adsorbents better than other theories they tested. A number of papers were published on methods of using the theory to calculate the adsorption of untested compounds using generally known properties such as density, melting point, refractive index and solubility. Because of this potential to predict isotherms, the theory was considered in some detail below. The theory also accounted for the effect of temperature and multicomponent adsorption.

Like Langmuir, Polanyi's theory was developed for gases but it was adapted to a more general adsorption of binary liquids by Hansen and Fackler (1957). It was further applied by Manes and Hofer (1969) to cover adsorption of solutes from solution. Schenz and Manes (1975) also explained aspects of the theory.

Most of Polanyi's papers were in German, but an English review of his theories was found in Polanyi (1932). He identified 4 forces that affected adsorption:

i) electrostatic forces are important when the solid surface is ionized as with adsorption on an ionic crystal such as potassium chloride. (Also with ion exchange);

ii) valence forces are the forces that occur when the adsorbate is chemically modified during adsorption. (This is now called chemisorption);

iii) dispersion forces (now known as London forces) are the same forces described by the constant 'a' in the van der Waals equation. This is substantiated by the fact that the condensibility and adsorption potential of gases are closely related. London forces result from the polarization of molecules, and are related to the ionization potential and polarizability of the molecules. They are also largely temperature independent and independent of whether the neighbouring adsorption site is occupied or not. The forces are also independent of whether the adsorbate is adsorbed or not. Dubinin (1960) made a more detailed study of adsorption dominated by dispersion forces (also called physisorption);

iv) capillary condensation is caused by surface tension holding the adsorbed liquid in the pores.

Polanyi developed his theory by considering the attraction of a gas to the adsorbent surface under the control of London forces. He introduced a concept called the adsorption potential (ϵ). ϵ was:

i) independent of temperature because it was due to temperature independent London forces;

ii) decreased with increased distance from the adsorbent's surface. The rate of decrease was not specified, and attempts to do so by Halsey (1948) and Hill (1949) met with limited success.

The adsorption potential was a measure of how strongly the adsorbent attracted adsorbates. Polanyi assumed that adsorption of gases below their critical temperature was similar to condensation of gases and derived the relation shown in equation 2.10. This relation said that adsorption would occur when ϵ was greater than the desorption driving force.

$$\epsilon > RT \ln \frac{P_o}{P}, \qquad (2.10)$$

where ϵ = adsorption potential,
R = gas constant = 0.0083144,
T = temperature, [K]
P_o = saturated vapour pressure of gas (at T),
P = partial pressure of gas.

It can be seen that as the temperature rises, the adsorption potential required to maintain equilibrium rises. This means that molecules that were in such a position that $\epsilon = RT\ln P_o/P$ are now in a position such that $\epsilon < RT\ln P_o/P$ and therefore desorb. It has been shown to account for the effect of temperature over a wide range (Treybal, 1980; Coulson and Richardson, 1979; Dubinin, 1960). Physisorption is an exothermic process and therefore this decrease in adsorption with temperature increase is expected on thermodynamic considerations.

If an imaginary surface is constructed of equal ϵ, then this surface encloses a volume Ø between itself and the adsorbent surface. As the value of ϵ used for the equipotential surface decreases, the volume Ø increases. The nature of the function describing this increase of Ø with a decrease of ϵ is dependent only on the adsorbent, and has to be measured experimentally. $\epsilon = f(Ø)$. This function is called the characteristic curve. The exact nature of the characteristic curve that fits a particular adsorbent depends on pore size distribution, surface active agents etc. For instance in fine pores, the adsorbate can be close to two surfaces and will be strongly adsorbed, but the available volume is small.

The major strength of the Polanyi theory is that once the characteristic curve has been determined using one compound on an adsorbent, the isotherms of all other compounds on that adsorbent can be predicted. The method of doing this can be explained by considering n molecules being adsorbed into the adsorption volume (Ø):

$$Ø = n \times \nabla, \qquad (2.11)$$

where ∇ = adsorption volume occupied per mole of adsorbate,
n = number of molecules adsorbed.

Grant and Manes (1966) showed that ∇ could be estimated with fair accuracy from the bulk liquid density. (Remembering that they were considering the adsorption of gases). Knowing ∇ and n, the adsorption volume could be calculated. Knowing the adsorption volume allowed the Polanyi potential to be calculated using the characteristic curve. Using the Polanyi potential, the partial pressure of the gas in equilibrium with the gas adsorbed within the adsorption volume could be found. Thus it was possible to estimate the isotherm of a gas using its saturated vapour pressure and its liquid density.

To apply the theory to solute adsorption from a liquid solution, the desorption of the liquid from the adsorbent had to be taken into

account. Manes and Hofer (1969) assumed that:

$$\epsilon_{s,l} = R\,T\,\ln(C_{s,sat} / C_s) = \epsilon_s - \epsilon_l\,\nabla_s / \nabla_l, \qquad (2.12)$$

where $C_{s,sat}$ = concentration of saturated solution,
ϵ_s = Polanyi potential of pure solute,
ϵ_l = Polanyi potential of pure solvent,
$\epsilon_{s,l}$ = Polanyi potential of adsorbate adsorbing from solvent.

This equation indicated two important phenomena that have been observed experimentally:

i) very soluble solutes were not adsorbed well and vice versa;

ii) solutes dissolved in solvents that were adsorbed strongly themselves were not adsorbed well.

A problem with this equation was that it could not be used for miscible solutes. Hasanain and Hines (1981) solved this by assuming that no water was adsorbed onto the XAD-2 that they used. Their expression for the Polanyi potential became:

$$\epsilon_{s,l} = RT\,\ln(1/X),$$

where X = mole fraction of solute.

Equation 2.12 suggested that it was possible to predict solute adsorption from the gas phase adsorption data of the solute and solvent measured separately. Manes and Hofer (1969) found that this was the case for the system they studied except at high adsorbent loadings. At high loadings the solute did not adsorb to the extent expected from the gas phase data, which suggested that the solute could not completely displace the solvent from the adsorption space. Hansen and Fackler (1953) noted a similar result when adsorbing aqueous alcohol solutions onto activated carbon and they had to customize their model by using a factor for the molar volume.

Another modification introduced by Manes and Hofer was one to account for the polarizability of the adsorbate. From equation 4, they derived the following equation:

$$\Upsilon_{s,1} = \Upsilon_s - \Upsilon_1 , \qquad (2.13)$$

where $\Upsilon = \epsilon / \nabla \beta$,

β = scale factor for reference substance (one used for measuring characteristic curve).

They estimated this scale factor using the following equation:

$$\Upsilon_{s,1} = \frac{p_s - p_1}{p_r} , \qquad (2.14)$$

where $p_i = \frac{n_i^2 - 1}{n_i^2 + 2}$,

n_i = refractive index of compound i,
subscript r refers to the reference substance,
subscript s refers to solute,
subscript 1 refers to solvent.

Wohleber and Manes (1971) found this correction did not work for water and that an empirical correction had to be used. They found that for water Υ_1 generally came to 0.28 when using heptane as the reference substance.

Some interesting observations came from other work in extending the Polanyi theory. Chiou and Manes (1974) discovered that although there was a general decrease of adsorption with increased temperature, there was a step increase in adsorption at a temperature within 1 °C of the bulk melting point of the solute. This suggested two things:

i) adsorbed solids did not pack as well onto the adsorbent surfaces as adsorbed liquids. This was probably due to the adsorbed solid trapping more solvent within the adsorption volume than the adsorbed liquid;

ii) since there was no change of the melting point in the adsorbed phase it was concluded that the adsorbed solute was in a similar physical condition to when it was in a pure form. The heat of adsorption is of the same order as the heat of solution and it would appear that adsorption was rather like precipitation of the solute, except it occurred in the pores of the adsorbent.

It was also noted that steric effects could reduce adsorption. Chiou and Manes (1973) found that octahedral metal acetylacetonates did not adsorb as well as the planar acetylacetonates. This effect was observed on activated carbon and on carbon black. It was therefore concluded that the effect was due to the inability of the octahedral molecule to get close to the surface and not due to molecular sieving effects.

h) The Dubinin interpretation of the Polanyi theory:

Many isotherm equations are reported in the literature and more could easily be proposed. An important attribute of an isotherm for incorporation into a multicomponent adsorption model is simplicity. This is because the equilibrium concentrations have to be calculated frequently when analysing dynamic systems and the time for each calculation needs to be minimized. Another important attribute is generality: can the isotherm be used to model adsorption of a wide range of adsorbates onto a wide range of adsorbents over a large concentration range? Finally the isotherm must be as accurate as possible.

These three criterion were considered carefully by Weber and Van Vliet (1981a and 1981b). They chose the Dubinin isotherm which was derived using the Polanyi theory.

The full Dubinin isotherm is:

$$\emptyset = \emptyset_o \exp(-\epsilon^k / B), \qquad (2.15)$$

where $\emptyset_o$ = maximum adsorption volume,
B = affinity coefficient,
k = exponent for ϵ.

Dubinin suggested a theoretical value of 2 for k. If this value was used, his isotherm became a two-parameter equation:

$$\emptyset = \emptyset_o \exp(-\epsilon^2/B). \qquad (2.15a)$$

If the definitions of the adsorption potential and the adsorption volume are substituted into equation 2.15 it becomes:

$$q = \rho \emptyset_o \exp \frac{(RT \ln(C_{sat}/C))^k}{-B}, \qquad (2.15b)$$

where ρ = density of adsorbate (measured in the bulk phase).

It can be seen that $\emptyset = \emptyset_o$ when $C = C_{sat}$. Therefore $\emptyset_o$ represents the maximum volume of adsorbate that the adsorbent can adsorb. The solubility of the adsorbate is a measure of its affinity for the solvent, and the parameter B is a measure of its affinity for the adsorbent.

2.3.2) Multicomponent isotherms

The isotherm constants measured for the D1/D2 effluent depend on the experimental method used. Crittenden and Weber (1978a) note similar effects. To explain these effects and to predict the removal of individual compounds from the effluent, it is necessary to have a multicomponent model of the adsorption process. Some of the multi-component isotherms mentioned in the literature are reviewed below.

a) Langmuir type isotherm;

this is a simple and therefore popular formula, but not generally accurate for solid solute adsorption on solids. The two component version was first proposed by Butler and Ockrent (1930). Jain (1973) extended it to account for the fact that some solutes cannot reach the whole surface because of steric hindrance in small pores. It is not discussed further because Yen and Singer (1984) showed that the ideal adsorption theory was significantly more accurate for modeling

adsorption of phenols on activated carbon. The isotherm is:

$$q_i = \frac{Q_i \; b_i \; C_i}{1 + \sum_{j=1}^{n} b_j \; C_j}, \qquad (2.16)$$

where q_i = grams solute i adsorbed per gram adsorbent,
C_i = liquid concentration of solute i,
Q_i = maximum value of q_i in single solute system (corresponds to complete monolayer coverage),
b_i = constants obtained from single solute isotherms,
n = number of components.

b) Yon-Turnoch isotherm;

this model was originally proposed by Yon and Turnoch (1971), but Fritz and Schlünder (1974) also developed a similar equation with which they were accredited by Mansour et al (1984). The origin of the two forms was slightly different. Yon and Turnock derived it theoretically for multi-component adsorption on molecular sieves, while Fritz and Schlunder simply found an empirical fit to their multicomponent data for phenol on activated carbon. The only difference in the equation was that the constant A_{ij} was split into two constants by Yon and Turnoch.

It is a popular general purpose model since it includes the Freundlich, Langmuir, Jaüger (1959), and Radke (1972a), isotherms as special cases. Its main disadvantage is that the constants are unique to each set of compounds considered. Their determination therefore requires a large amount of experimental work. It is presented below as reported by Fritz and Schlunder (1974).

$$C_i = \frac{a_{io} \; C_i^{b_{io}}}{a_i + \sum_{j=1}^{n} A_{ij} \; C_i^{b_{io}}}, \qquad (2.17)$$

where a_{io} = adsorption constant from single component data,
a_i = constant for component i,
A_{ij} = adsorption constant relating solutes i and j,
b_{io} = adsorption exponent from single component data,
b_{ij} = adsorption exponent relating solutes i and j.

c) Ideal adsorbed solution theory:

the IAS theory was originally proposed by Myers and Prausnitz and modified for liquid solutions by Radke and Prausnitz (1972b), and was based on the thermodynamic equivalence of the spreading pressure of each solute at equilibrium. It had the disadvantage that it used thermodynamic arguments that were appropriate to dilute solutions. Also its accuracy depended heavily on low concentration data, and it required the solution of (5n + 1) simultaneous equations (n = number of compounds).

Fritz (1981) extended the IAS model to use the Freundlich isotherm instead of the Langmuir isotherm used by Radke. Yen and Singer (1984) extended the theory further to use a modified three-parameter Freundlich isotherm. Digiano et al (1978) proposed a simplified version that was useful when considering more than two components. Jossens et al (1978) found it accurate for bi-component data except when the difference in pK of the components was large. They concluded that pH had an important effect, but were unable to predict it. They developed IAS models using both the Toth and the Jossens isotherms.

The IAS theory as presented by Yen and Singer (1984) is illustrated below:

$$\int_0^{q_1^*} \frac{d \log C_1}{d \log q_1}\, dq_1 = \int_0^{q_2^*} \frac{d \log C_2}{d \log q_2}\, dq_2 = \int_0^{q_n^*} \frac{d \log C_n}{d \log q_n}\, dq_n , \qquad (2.18)$$

$$C_{m\,i} = X_i\, C_i^* , \qquad (2.19)$$

$$\sum_{i=1}^{n} X_i = 1 , \qquad (2.20)$$

$$q_i = f(C_i) , \qquad (2.21)$$

$$\frac{1}{q_T} = \sum_{i=1}^{n} \frac{X_i}{q_i^*} , \qquad (2.22)$$

$$q_{m\,i} = X_i\, q_T , \qquad (2.23)$$

$$q_{m\,i} = \frac{(C_{m\,i}^{\circ} - C_{m\,i})}{m} , \qquad (2.24)$$

where C_i^* = solution-phase concentration corresponding to q_i^*,
$C_{m\,i}^{\circ}$ = initial concentration of species i,
C_m, q_m = concentration of species in the mixture,

q_T = total quantity of material adsorbed from mixture,
X = adsorbed mole fraction of solute in system,
m = dosage of adsorbent.

Equation 2.18 represents the equivalence of the spreading pressures of the solutes and equation 2.21 represents the isotherm relationship for the individual solutes. Equations 2.19 and 2.23 assume that the solute forms an ideal solution in the dissolved and adsorbed phases respectively. Equations 2.20, 2.22 and 2.24 are material balances.

d) Sheindorf model;

this model was proposed by Sheindorf et al (1981) and was based on the Freundlich isotherm since this isotherm was the simplest that adequately described solid solute adsorption on activated carbon.

It assumed that each component had an exponential distribution of adsorption site energies, and that the adsorption of each sorbate at each energy level was given by the competitive Langmuir isotherm (Sheindorf et al, 1982). A disadvantage was that the coefficient A_{ij} had to be determined experimentally for each pair of compounds. It had the form:

$$q_i = K_{fi} C_i \left(\sum_{j=1}^{n} A_{ij} C_j \right)^{n_{fi}-1}, \qquad (2.25)$$

where K_{fi} = Freundlich isotherm constant for the ith component,
n_{fi} = Freundlich isotherm constant (compound i),
A_{ij} = coefficient accounting for interaction between components i and j.

e) Okazaki model;

this model was similar to the last in that the Langmuir isotherm was assumed to hold at each energy level. The distribution of energy levels was, however, assumed to be a simple inverse relation. While Sheindorf integrated the energy level function from an energy level of $-\infty$ to $+\infty$, Okazaki used limits of integration between k_{max} and k_{min}. He thus created a new single component isotherm. This theory also had the

disadvantage of requiring a lot of experimental data. The multicomponent model was:

$$q_i = \frac{Q_i C_i}{\ln\left(\frac{k_{i,max}}{k_{i,min}}\right)} \int_{k_{i,min}}^{k_{i,max}} \frac{dK_i}{1 + \sum_{j=1}^{n} \left(\frac{K_i}{k_{i,max}}\right)^{K_{i,j}} k_{j,max} C_j}, \qquad (2.26)$$

where $K_{i,max}$ = maximum adsorption energy for compound i,
$K_{i,min}$ = minimum adsorption energy for compound i,
Q_i = ultimate uptake capacity of compound i.

f) Polanyi theory:

Rosene and Manes (1976) showed how the Polanyi theory could be adapted to the competitive adsorption of solids from aqueous solution. Their work followed on from that of Shenz and Manes (1975) who considered binary liquid solutes, and Grant and Manes (1966) who considered binary gas mixtures.

The adsorption driving force per mole of single adsorbate is:

$$-\Delta G_i = \epsilon_i - RT \ln(C_{sat}/C)_i, \qquad (2.27)$$

where ϵ_i = adsorption potential of solute i from the solvent (previously $\epsilon_{s,i}$),
G = Gibbs free energy,
C = concentration of solute (not in equilibrium).

It is assumed that there is no interaction in the adsorbed state between the solids competing for adsorption sites. Therefore, for the adsorption of dn_i moles of solid i and the displacement of dn_j moles of solid j, we have:

$$\nabla_i \, dn_i + \nabla_j \, dn_j = 0.$$

$$\Rightarrow \quad dn_j = -(\nabla_i/\nabla_j) dn_i. \qquad (2.28)$$

For the jth component to displace the ith component, there must be a decrease in the Gibb's free energy, so:

$$dG = \Delta G_i \, dn_i + \Delta G_j \, dn_j \leq 0. \qquad (2.29)$$

Substituting equations 2.27 and 2.28 in 2.29 we get:

$$\frac{dG}{dn_i} = -\frac{\epsilon_i}{\nabla_i} + \frac{RT}{\nabla_i} \ln \frac{C_{i\,sat}}{C_i} + \frac{\epsilon_j}{\nabla_j} - \frac{RT}{\nabla_j} \ln \frac{C_{j\,sat}}{C_j} \leq 0 \qquad (2.30)$$

as the criterion for displacement of component j by component i. This equation was applied to two solids by Rosene and Manes (1976) and to three by Rosene and Manes (1977a). Rosene and Manes (1977b) also used it to predict the effect of pH. The above authors found that solids did not pack into the adsorption volume as well as liquids. A correction factor therefore had to be applied to the molecular volumes (∇) in such cases.

Greenbank and Manes (1981) performed a valuable comparison between the IAS and the Polanyi theories. Their data did not show either theory to be consistently superior to the other.

2.3.3) Species grouping:

When modeling a system with a large number of components, the possibility of grouping the components to simplify the model was very attractive. Calligaris and Tien (1982), and Mehrotra and Tien (1984) showed that the IAS theory could model multicomponent adsorption. They then did a theoretical study to find a way of grouping the species into pseudo-species. They found that in batch equilibrium systems the error introduced into the calculation was less that 8% for each pseudo-species if each component had an adsorption affinity within 1 order of magnitude of the others. They used the Freundlich isotherm and the coefficients for the pseudo-species were obtained by averaging the coefficients for each species in the group. If the initial concentrations (C_o) were widely different they used a weighting factor based on C_o. When modeling fixed-bed dynamic systems, they found that the isotherm and the diffusion rates had to be similar. Similar work was performed by Crittenden et al (1985) except they determined their pseudo-isotherms experimentally.

Later work by Ramaswami and Tien (1986) showed that the Freundlich coefficient could be ignored as a criterion for grouping species. The

grouping criteria were that the Freundlich exponent should be within 20% and the particle mass-transfer coefficients should be within the same order of magnitude. They found that the predicted adsorption of pseudo-species grouped according to the new criteria agreed with experimental results as well or better than predictions using no grouping.

2.3.4) Accounting for the effect of resin voidage on isotherms

Most authors have worked with adsorption systems where they added the adsorbate solution to dry adsorbent, or the volume of solvent held in the resin was negligible compared to the total volume. Therefore they were able to ignore the porosity of their adsorbent when calculating isotherms. However, in this study work was performed with poorly adsorbed compounds. This meant that the volume of resin had to be large compared to the volume of bulk solution. Since the resin had to be introduced into the experiment wet, it carried with it a significant volume of water which had to be accounted for.

2.3.4.1) Definition of voidages

Voidage is defined as the fraction of voids in a system. The word porosity has a very similar meaning but refers more specifically to the fractions of pores in a porous particle.

A formula for the voidage of a bed of resin on a volume basis is:

$$\epsilon = \frac{V_l}{(V_l + V_r + V_p)}, \qquad (2.31)$$

where V_l = volume of solution (not including that in adsorbent pores),
V_r = volume of resin (not including pore volume, ie. the volume of the adsorbent skeleton),
V_p = volume of solution in adsorbent pores.

Other useful definitions of voidage used are:

voidage of the adsorbent particle;

$$\epsilon_p = \frac{V_p}{V_p + V_r}, \qquad (2.32)$$

ii) The deductive approach picks out the relevant mechanisms of adsorption and combines them into a rate equation. The

voidage on a porous particle basis;

$$\epsilon_v = \frac{V_l + V_p}{V_l + V_p + V_r}, \qquad (2.33)$$

voidage of a settled bed;

$$\epsilon_s = \frac{V_l}{V_l + V_p + V_r}, \qquad (2.34)$$

where V_l = Volume of solution in bed,

and voidage of a fluidized bed;

$$\epsilon_f = \frac{V_l}{V_l + V_p + V_r}. \qquad (2.35)$$

2.3.5) Theoretical analysis of adsorption versus temperature.

The Dubinin isotherm and the solubility and density correlations for phenol were used to make a theoretical study of how temperature affects adsorption. The results from this study only apply strictly to phenol, but it is likely that similar effects would be observed with other compounds. Figure 2.2 shows that if the Polanyi theory applies, the effect of temperature is quite marked especially at low concentrations. These results suggest that some attention should be given to cooling solutions that are to be loaded on the adsorbent and heating solutions for regenerating the adsorbent.

2.4) Adsorption kinetics

Coulson and Richardson (1979) split models for adsorption kinetics and adsorber design into three classes.

i) The inductive approach choses a rate mechanism and the rate equation for this mechanism is developed. There are numerous examples in the literature such as Helfferich (1962), Weber and Crittenden (1975) and Hendricks and Kuratti (1982). The equations are generally simple, and one example is discussed later.

ii) The deductive approach picks out the relevant mechanisms of adsorption and combines them into a rate equation. The

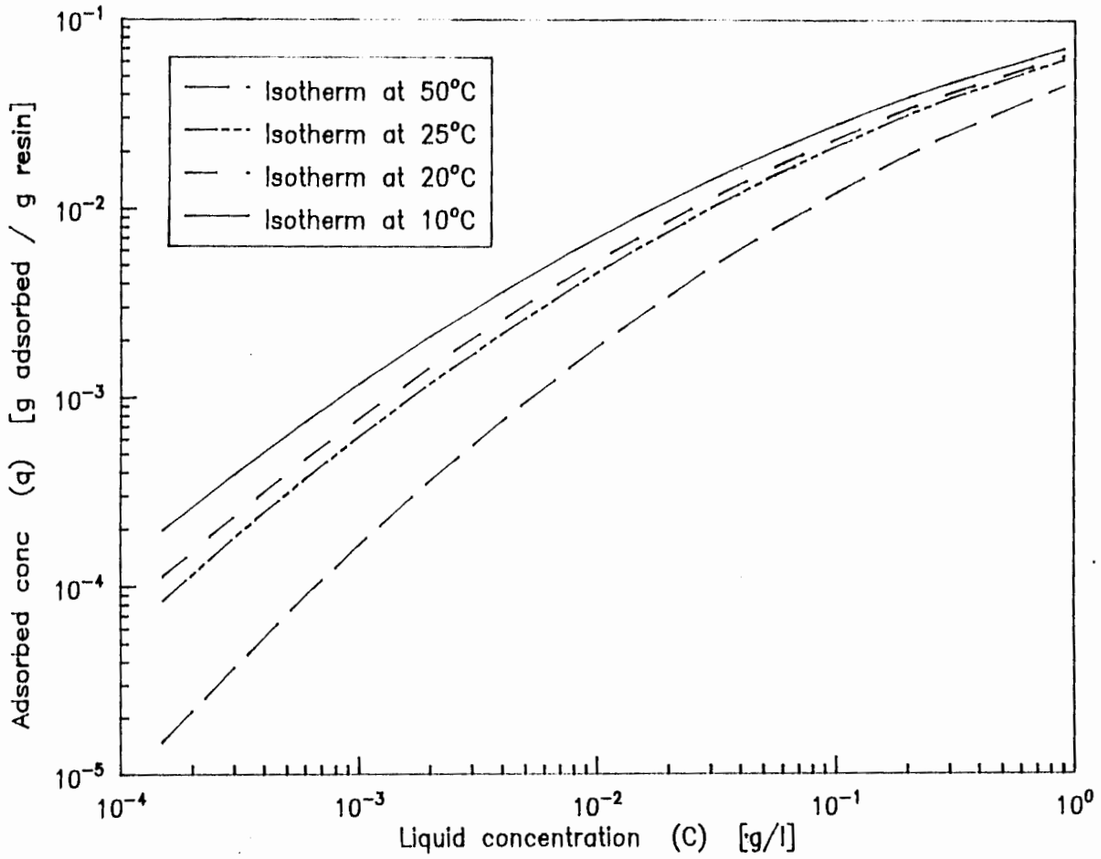

Figure 2.2 Theoretical adsorption data for phenol on XAD-8 at different temperatures.

resultant equations are usually complicated and require numerical solutions. Again there are numerous examples in the literature and some of them are discussed later.

iii) The staged separations method divides the system into a number of equilibrium stages. The size of an equilibrium stage needs to be determined and then the performance of the whole system can be determined graphically. This method is used extensively for evaluating chromatography columns, but is not suitable for modeling the type of adsorption contactor of interest in this application. An alternative method is to estimate the stage efficiency (or percentage approach to equilibrium) of each stage. The design can again be done graphically and the method is explained below.

Some extensive literature reviews of a wide range of kinetic models can be found in McKay (1984), Mansour et al (1982) and Weber and Chakravorti (1974).

2.4.1) A simple empirical kinetics model

The simplest way to model adsorption kinetics is to assume a first order reversible reaction.

$$\frac{dC}{dt} = K\,(C - C_e),$$

where C = concentration of bulk solution,
C_e = concentration of solution in equilibrium with solid phase,
K = rate constant,
t = time.

It was found that this equation did not fit the experimental data well. One of the problems encountered was that the volume of liquid held in the pores of XAD-8 was too large to be ignored as was usually done when considering adsorption. No simple empirical kinetics model accounting for the pore volume could be found in the literature so one was developed. The approach taken was to separate the liquid in the pores from the bulk solution. Two connected rate equations resulted; one for adsorption of the adsorbate from the pore solution; and the second for diffusion of adsorbate from the bulk to the pore solution. Simple linear rate equations were used to describe these steps.

The rate of change of the solid phase concentration was given by:

$$\frac{dq}{dt} = K_q(q_e - q), \qquad (2.35)$$

where q_e = equilibrium resin concentration in equilibrium with pore solution,
K_q = rate constant,

and the rate of change of pore concentration was:

$$\frac{dC_p}{dt} = K_p(C - C_p), \qquad (2.36)$$

where C_p = pore solution concentration,
K_p = rate constant.

C_s and q_s were related by the isotherm equation, and a material balance was used to relate change in C_s to change in C.

2.4.2) Diffusion model of kinetics

When an adsorbent particle was placed in an adsorbate solution, diffusion of adsorbate from the bulk solution to the inner pores of the adsorbent began. The adsorption process could be broken down into several stages:

i) there was a boundary layer of solution surrounding the particle, and adsorbate diffused across this boundary. This process was called film diffusion here, but some authors used other terms such as 'external mass transfer';

ii) the adsorbate diffused down the pores of the particle. The mechanism was the same as diffusion through the bulk solvent and was called pore diffusion;

iii) thirdly the adsorbate diffused along the surfaces of the pores. The mechanism was assumed to be a process of the adsorbate leaving its adsorption site and hopping to a new vacant site. It was called surface diffusion. Pore and surface diffusion worked in parallel and were often lumped together in a solid phase diffusion term (also called internal mass transfer);

iv) the final source of resistance to adsorption was the time it took for the adsorbate to be adsorbed after it reached its adsorption site. The rate of adsorption was generally accepted as negligible.

Most of the literature reviewed assumed that Fick's law of diffusion applied in all cases. Adsorption in the liquid phase was assumed to be isothermal. The concentrations were usually assumed to be low enough for the diffusion of the bulk solvent in the opposite direction to the

solute to be ignored. In such cases Fick's law took the form:

$$N_a = D \frac{dC}{dx}, \qquad (2.37)$$

where N_a = flux due to diffusion per unit area,
D = diffusion coefficient,
x = distance.

The rate equations governing each stage in the adsorption process are briefly presented below.

2.4.2.1) Film diffusion

A film with a sharp concentration gradient formed around the adsorbent particle when it was put in a fluid. The thickness of the film could not be measured accurately but was of the order of 10^{-5} m (Helfferich, 1962). It was assumed that diffusion across the film was fast compared with the concentration changes at the film boundaries. It was also assumed that diffusion occurred only in the radial direction. Using these assumptions the flux through the film was described by a modification of equation 2.37.

$$N_a = D \frac{C - C_s}{\delta}, \qquad (2.37a)$$

where C_s = liquid phase concentration on outside surface of adsorbent,
δ = film thickness.

Since δ could not be directly measured, it was combined with D into a single film diffusion coefficient K_s.

K_s was defined in the equation:

$$K_s (C - C_s) = \frac{\rho_s}{R_p^2} \frac{\partial}{\partial t} \int_0^{R_p} q\, r^2 \, dr, \qquad (2.38)$$

where ρ_s = density of dry adsorbent = $\frac{\text{mass dry resin}}{(V_r + V_p)}$,
R_p = average radius of adsorbent particles,
r = distance from particle centre.

The left side of the equation represented the diffusion through the film and the right hand side represented the accumulation within the adsorbent particles.

A number of relationships had been proposed for estimating K_f. Cornel et al (1986) found the relation proposed by Gnielinski to be the best of the four that they evaluated. However they did not take into account the roughness factor of adsorbent particles that Van Vliet et al (1980) used. Van Vliet (1987) found a close correlation between surface roughness of spherical adsorbent particles and the film diffusion coefficient. He found that the roughness factor could be estimated using the fractal dimension of the particle's cross section. To measure the fractal dimension of a particle, it was bisected and carefully polished before taking an electron micrograph of the cross section. The perimeter of the cross section was then measured using stride steps of decreasing length. The shorter the stride, the greater the perimeter, and plotting perimeter vs. log of stride length produced an almost linear plot. The negative of this slope was defined as the fractal dimension of the particle.

2.4.2.2) Pore diffusion

The concentration gradient in the solution in the pores caused diffusion through the pores. The pores were not straight so an empirical tortuosity factor had to be included in the diffusion coefficient (D_p). D_p was therefore unique for each adsorbent as well as for each adsorbate. The equation as presented by Liapis and Rippin (1977), and by Neretnieks (1976a) was:

$$\frac{\partial q}{\partial t} + \epsilon_p \frac{\partial C_p}{\partial t} = \frac{\epsilon_p}{r^2} \frac{\partial}{\partial r} \left(D_p \, r^2 \frac{\partial C_p}{\partial r} \right), \qquad (2.39)$$

where ϵ_p = voidage of adsorbent, (eqn. 2.32)

C_p = concentration of solution in adsorbent pores.

The pore diffusion coefficient should be given roughly by:

$$D_p = D \, \epsilon_p / \gamma,$$

where γ = tortuosity factor.

Cornel et al (1986) found that although the tortuosity factor could not be less than unity, the experimental values for D_p were up to 5 times larger than $D\,\epsilon_p$. Their conclusion was that pore diffusion was much less important than surface diffusion. Komiyama and Smith (1974), Fritz et al (1981) and Neretnieks (1976c) also found that pore diffusion only accounted for a small proportion of the solid phase diffusion resistance. This suggested that pore diffusion could be ignored in most cases of adsorption.

2.4.2.3) Surface diffusion

Surface diffusion results from the fact that adsorption is a dynamic process. Adsorbed molecules are free to leave the surface and migrate to an area of lower concentration.

The surface diffusion coefficient (D_s) controls diffusion as follows:

$$\frac{\partial q}{\partial t} + \epsilon_p \frac{\partial C_p}{\partial t} = \frac{1}{r^2} \frac{\partial}{\partial r} \left(D_s\, r^2 \frac{\partial q}{\partial r} \right). \qquad (2.40)$$

Komiyama and Smith (1974) found that benzaldehyde was adsorbed more that 100 times as well onto XAD-4 when dissolved in water than when in a mixture of 57.2% methanol in water. This was expected according to the Polanyi theory because the polystyrene matrix of XAD-4 was much more strongly attracted to methanol than to water. The adsorption potential was therefore lower when the adsorbate was dissolved in methanol. They found that the solid phase diffusivity was increased 10 fold when the benzaldehyde was dissolved in the water methanol mixture which suggested that the solid phase diffusivity was inversely related to the adsorption potential. When the adsorption potential was low, it was easy for the adsorbate to leave its adsorption site and hop to an area of lower concentration. Finally they found that solid phase diffusion was independent of the surface area. This also supported the theory that the predominant mechanism of solid phase diffusion was surface diffusivity.

The surface diffusion coefficient was found to be temperature and concentration dependent. This dependence was well illustrated by experiments performed by Suzuki and Fujii (1982). They mounted activated carbon in a plate separating two mixed chambers. They were able to study the diffusion of solute as it moved linearly through a fixed

length of carbon at a fixed temperature and concentration. Their results showed that the surface diffusion coefficient was proportional to the temperature and the exponent of the adsorbed concentration. The increased concentration meant that the adsorption potential of the most recently adsorbed molecules was lower and they could therefore migrate more easily to a new site. The temperature dependence resulted from the increased mobility of the adsorbate with increased temperature.

Neretnieks (1976c) tested the adsorption of 5 phenolic compounds and benzoic acid on activated carbon. He found that surface diffusion predominated over pore diffusion in all cases. The sensitivity of surface diffusion to concentration was different for each compound. All except benzoic acid showed an increase with increased concentration. He also found that the models for pore and surface diffusion became similar when the surface diffusion was concentration dependent.

The equation used to describe concentration dependence was:

$$D_q = D_{q0} \exp(\alpha(q/q_0)), \qquad (2.41)$$

where α = concentration dependence factor,
D_{q0} = surface diffusion at zero concentration,
q_0 = maximum solid phase concentration.

2.4.2.4) The choice of a complete diffusion model

The three basic equations 2.38 - 2.40 were often accepted as being all that was required to accurately model adsorption. Neretnieks (1976a) combined the pore and surface diffusivity and solved the resultant equation using the film diffusion term as a boundary condition. Liapis and Rippin (1977) had a similar approach but unlike Neretnieks, they used concentration dependent pore and surface diffusion coefficients. They also extended the model to multicomponent adsorption. Mansour et al (1984) used a similar set of equations and included the rate of adsorption at the adsorbent surface. They found that the rate of adsorption had little effect unless it was very slow which was not usually the case. Lee (1978) derived an analytical solution for biporous adsorption kinetics. The biporous adsorbent approach was common for gaseous

adsorption on catalyst particles, but the additional complication was not often justified with liquid phase adsorption.

The first model chosen was the surface diffusion model using the film diffusion as a boundary condition. It effectively lumped the pore and surface diffusion coefficients into a single solid phase diffusion coefficient (D_s) which was assumed to be constant. No attempt was made to derive D_s from D_q and D_p since they all had to be determined experimentally anyway. The model also assumed that the pore volume was small enough to be ignored. There were 4 reasons for choosing this model:

i) a number of workers (some already mentioned) had shown that surface diffusion and film diffusion were the most important rate limiting steps in most cases;

ii) the model was used to determine the rate constants in the only other literature found that studied the kinetics of adsorption on XAD-8: Van Vliet et al, (1980); Van Vliet and Weber, (1981); Weber and Van Vliet (1981);

iii) no model had been shown to completely describe adsorption kinetics. Since the final choice of equation could not be a perfect description of the adsorption process, a compromise had to be reached between ease of use and accuracy. The authors just mentioned and Crittenden and Weber (1978b) claimed the model was both accurate and easy to use;

iv) Crittenden and Weber (1978a) and Crittenden and Weber (1978c) described its derivation and the derivation of numerical analogs for the solution of the equations in some detail. Their work was therefore used as a check for the first version of the kinetics modeling program.

A computer program was coded and tested against the data of Van Vliet et al (1980). When the program was functioning correctly, it was used to analyse experimental data. It was found that the assumption of no pore volume and constant solid phase diffusion was unacceptable for the applications of interest here. These assumptions were therefore removed

and the program was modified to use the new equations. These equations are formally derived below.

2.4.2.5) Derivation of the chosen model from first principles

Equations 2.38 to 2.40 were presented without explaining their derivation. The model finally chosen was derived using the standard procedure of taking a mass balance on a differential volume of the system being considered (Crank, 1970; Bird et al, 1960).

Ficks law was assumed to apply, but the diffusion was dependent on the solid phase concentration. Equation 2.37 therefore had to be adapted to account for the different units and became:

$$N_s = \rho_s D_s \frac{dq}{dr}. \qquad (2.37b)$$

A spherical shell within a single particle was considered. The inside surface of the shell was a distance r from the centre of the particle. The shell had a thickness of Δr, so the outside surface was at a distance $r + \Delta r$ from the particle centre. A mass balance on this shell said that what accumulated within it was the difference between what diffused in and what diffused out.

Diff. in through outside of shell.	Diff. out through inside of shell.	Accumulation within shell

$$4\pi(r+\Delta r)^2 N_s|_{r+\Delta r} = 4\pi r^2 N_s|_r + \left(\frac{\partial q}{\partial t}\rho_s + \frac{\partial C_p}{\partial t}\epsilon_p\right)4\pi\left(r + \frac{\Delta r}{2}\right)^2 \Delta r. \qquad (2.42)$$

Substituting equation 2.37b in 2.42, and dividing by $4\pi\Delta r$ gave:

$$\frac{(r+\Delta r)^2 D_s \left.\frac{\partial q}{\partial r}\right|_{r+\Delta r} - r^2 D_s \left.\frac{\partial q}{\partial r}\right|_r}{\Delta r} = \left(\rho_s \frac{\partial q}{\partial t} + \epsilon_p \frac{\partial C_p}{\partial t}\right)\left(r + \frac{\Delta r}{2}\right)^2.$$

Taking the limit $\Delta r \rightarrow 0$ and re-arranging produced:

$$\frac{\partial q}{\partial t} + \frac{\epsilon_p}{\rho_s}\frac{\partial C_p}{\partial t} = \frac{1}{r^2}\frac{\partial}{\partial r}\left(D_s r^2 \frac{\partial q}{\partial r}\right). \qquad (2.43)$$

If the diffusion coefficient D_s was independent of concentration and the adsorption isotherm such that $q >> C_p/\rho_p$, then equation 2.43 could be simplified to:

$$\frac{\partial q}{\partial t} = \frac{D_s}{r^2} \frac{\partial}{\partial r}\left(r^2 \frac{\partial q}{\partial r} \right). \qquad (2.43a)$$

Introducing the following dimensionless groups into equation 2.43a resulted in the equations as presented by Crittenden (1978a):

$\bar{c} = C/C_o$,
C_o = influent or original liquid concentration,
$\bar{r} = r/R_p$,
$\bar{q} = q/q_e$,
$\bar{C}_p = C_p/q_e$,
q_e = equilibrium solid-phase conc evaluated at influent or original liquid conc,
$\bar{t} = \frac{D_s t}{R_p^2}$ = dimensionless time:

$$\frac{1}{\bar{r}^2} \frac{\partial}{\partial \bar{r}}\left(\bar{r}^2 \frac{\partial \bar{q}}{\partial \bar{r}} \right) = \frac{\partial \bar{q}}{\partial \bar{t}}. \qquad (2.44)$$

Introducing dimensionless groups to equation 2.43 was more difficult. Assuming D_s was concentration dependent meant that it changed with radial position ($\bar{r}$) because concentration changed with radial position. Therefore $\bar{t}$ also changed with radial position. The technique finally chosen to overcome this problem was related to the numerical technique used to solve the equation. To solve the equation numerically, the particle radius was divided into a series of steps: a finite number of fixed radial positions were chosen and the conditions at each radial position were evaluated. One of the conditions to be evaluated was then $\bar{t}$ which was unique to each radial position. $\bar{t}$ therefore carried a subsript (i) indicating that it only applied for radial position i. $\bar{t}_i$ was determined using D_s calculated from the surface concentration at that particular radial position. The resultant equation could therefore only be solved by numerical techniques. The dimensionless form of equation 2.28a was then:

$$\frac{1}{\bar{r}^2} \frac{\partial}{\partial \bar{r}}\left(\bar{r}^2 \frac{\partial \bar{q}}{\partial \bar{r}} \right) = \left(\frac{\partial \bar{q}}{\partial \bar{t}_i} + \frac{\epsilon_p}{\rho_s} \frac{\partial \bar{C}_p}{\partial \bar{t}_i} \right). \qquad (2.44a)$$

Equations 2.44 and 2.44a just derived only applied within the particle. To determine what happened at the centre and the surface of the particle, special boundary conditions had to be evaluated. Considering first the outside surface of the particle, a mass balance was performed on the adsorbate diffusing through this boundary:

$$\left(\frac{\partial q_{s,v}}{\partial t}\rho_s + \frac{C_{p,s,v}}{\partial t}\epsilon_p\right)\frac{4}{3}\pi R_p^3 = D_{s,M}\left.\frac{\partial q}{\partial r}\right|_{r=R_p}\rho_s\ 4\ \pi R_p^2,$$

where $q_{s,v}$ = average of surface concentration,
$C_{p,s,v}$ = average of pores solution concentration,
$D_{s,M}$ = solid phase diffusion evaluated at the surface.

Dividing by the surface area resulted in a form of the equation convenient for defining the film diffusion coefficient.

$$\left(\frac{\partial q_{s,v}}{\partial t}\rho_s + \frac{C_{p,s,v}}{\partial t}\epsilon_p\right)\frac{R_p}{3} = \rho_s D_{s,M}\left.\frac{\partial q}{\partial r}\right|_{r=R_p} = k_s (C-C_s).$$

The boundary condition at the particle surface could then be written as:

$$k_s (C-C_s) = \rho_s D_{s,M}\left.\frac{\partial q}{\partial r}\right|_{r=R_p}, \qquad (2.45)$$

or if the $q_{s,v}$ was evaluated as follows:

$$q_{s,v} = \frac{\rho_s \int_0^R 4\pi r^2 q\, dr}{\rho_s\ 4/3\ \pi\ R_p^3} = \frac{3}{R_p^3}\int_0^{R_p} r^2 q\, dr, \qquad (2.46)$$

and $C_{p,s,v}$ evaluated as:

$$C_{p,s,v} = \frac{3}{R_p^3}\int_0^{R_p} r^2 C_p\, dr, \qquad (2.47)$$

then the boundary condition could also be written as:

$$K_s (C - C_s) = \frac{1}{R_p^2}\frac{\partial}{\partial t}\int_0^{R_p} r^2\left(q\rho_s + C_p\epsilon_p\right) dr. \qquad (2.48)$$

If $q >> C_p/\rho_s$ then equation 2.48 could be simplified to:

$$K_s (C - C_s) = \frac{\rho_s}{R_p^2}\frac{\partial}{\partial t}\int_0^{R_p} r^2 q\, dr. \qquad (2.48a)$$

The boundary conditions were made dimensionless by substituting the following dimensionless groups in equations 2.47 and 2.48:

$$Sh_b = \frac{k_s R_p}{D_s Dg_b}, \qquad (2.49)$$

where Sh_b = Sherwood number for batch systems,

$$Dg_b = \frac{\rho_s q_e}{C_0} = \text{solute distribution parameter.} \qquad (2.50)$$

For systems with variable diffusion coefficients, the solid phase diffusion was evaluated at the surface. Therefore equation 2.49 became:

$$Sh_b = \frac{k_s R_p}{D_{s,M} Dg_b}. \qquad (2.49a)$$

The results of the substitutions were:

$$Sh_b (\bar{c} - \bar{c}_s) = \left.\frac{\partial q}{\partial r}\right|_{r=1}, \qquad (2.51)$$

and

$$Sh_b (\bar{c} - \bar{c}_s) = \frac{\partial}{\partial \bar{t}} \int_0^1 r^2 \left(q + \bar{c}_p \frac{\varepsilon_p}{\rho_s}\right) dr. \qquad (2.52)$$

On neglecting the pore solution, equation 2.52 became:

$$Sh_b (\bar{c} - \bar{c}_s) = \frac{\partial}{\partial \bar{t}} \int_0^1 r^2 q \, dr. \qquad (2.52a)$$

The boundary condition at the particle centre resulted from symmetry:

$$\frac{\partial q}{\partial r} = 0. \qquad (2.53)$$

Finally the initial condition for the solid phase had to be given. For a fully regenerated adsorbent it was:

$$q(r)_{\bar{t}=0} = 0. \qquad (2.54)$$

2.4.2.6) Diffusion kinetics in batch contactors

A material balance was performed on the bulk liquid in a batch reactor.

Accumulation in solid phase	Accumulation in pore solution	Removal from liquid phase

$$V_b(1-\epsilon)\,\rho_s\,\frac{\partial q_{a\,v}}{\partial t} + V_b(1-\epsilon)\epsilon_p\,\frac{\partial C_{p\,a\,v}}{\partial t} = -V_b\,\epsilon\,\frac{\partial C}{\partial t},$$

where V_b = total volume of the batch system,
ϵ = voidage of batch system (equation 2.29).

Dividing by V_b and ϵ resulted in:

$$\frac{(1-\epsilon)}{\epsilon}\,\frac{\partial}{\partial t}\left(q_{a\,v}\,\rho_s + C_{p\,a\,v}\,\epsilon_p\right) = -\frac{\partial C}{\partial t}.$$

Substituting in the definitions of q_{av} and C_{pav} (equations 2.46 and 2.46), and the dimensionless groups gave the final form:

$$\frac{\partial \bar{c}}{\partial \bar{t}} = -D_{e\,b}\,\frac{(1-\epsilon)}{\epsilon}\,3\,\frac{\partial}{\partial \bar{t}}\int_0^1\left(\bar{q} + \bar{c}_p\,\frac{\epsilon_p}{\rho_s}\right)r^2\,dr. \qquad (2.55)$$

Neglecting the pore solution this became:

$$\frac{\partial \bar{c}}{\partial \bar{t}} = -D_{e\,b}\,\frac{(1-\epsilon)}{\epsilon}\,3\,\frac{\partial}{\partial \bar{t}}\int_0^1 \bar{q}\,r^2\,dr. \qquad (2.55a)$$

The initial condition for the bulk material balance was:

$$\bar{c}_{(\bar{t}\,=\,0)} = 1. \qquad (2.56)$$

The solution of these equations by finite differences is explained in Chapter 5.

2.4.2.7) Diffusion kinetics in fluidized beds

In a fluidized bed, the pore diffusion equations described in section 2.4.2.5 were still applicable but the bulk material balance was different from the batch contactor. The first problem to consider was how to model the fluidized bed.

The fluidized bed would give the best possible performance if it behaved

as a packed bed. In actual practice, its approach to packed bed performance would increase as the percentage fluidization decreased. The worst possible performance would be that of a continuous stirred tank reactor (CSTR). Although the mixing of the adsorbent in a fluidized bed would increase to a limited extent with increased percentage fluidization, the liquid would never be perfectly mixed. Anderson (1986) modeled a fluidized bed by assuming plug-flow of the liquid and that the adsorbent was perfectly mixed. He assumed that the rate of adsorption was characterized by an average concentration. Another approach would be to assume a packed bed of adsorbent and a perfectly mixed liquid. Dodds et al (1973) assumed the CSTR model as a first step with a view to improving the model later. Gomez-Viillard et al (1981) and Buijs and Wesselingh (1980) also used the CSTR model and found that the prediction agreed with their experimental results.

The approach taken here, also, was to assume the worst possible case and to model the fluidized bed as a CSTR. A material balance was performed on each contactor stage as follows:

Flow into contactor stage	Flow out of contactor stage	Accumulation in bulk solution	Accumulation on adsorbent	Accumulation in pore solution

$$F\,C_{i-1} = F\,C_i + \epsilon_f\,V_f\,\frac{\partial C_i}{\partial t} + \rho_s\,(1-\epsilon_f)\,V_f\,\frac{\partial q_{s,v}}{\partial t} + \epsilon_p\,(1-\epsilon_f)\,V_f\,\frac{\partial C_{p,v}}{\partial t},$$

where F = flow rate into stage i,
C_{i-1} = concentration of solution entering stage i,
C_i = concentration of solution in stage i,
V_f = total volume of fluidized bed.

Dividing by F and re-arranging gave:

$$C_i = C_{i-1} - \left(\epsilon_f\frac{V_f}{F}\,\frac{\partial C_i}{\partial t} + \rho_s\,(1-\epsilon_f)\frac{V_f}{F}\,\frac{\partial q_{s,v}}{\partial t} + \epsilon_p\,(1-\epsilon_f)\frac{V_f}{F}\,\frac{\partial C_{p,v}}{\partial t}\right).$$

To convert this equation into dimensionless form, some new dimensionless groups had to be defined. They were:

$$\tau = V_f / F,$$
$$Tm = t/(\tau Dg_f),$$
$$Dg_f = \frac{\rho_s \; q_o \; (1-\epsilon_f)}{C_o \; \epsilon_f},$$
$$N_f = \frac{D_s \; t \; Dg_f}{R_p^2}.$$

Introducing these dimensionless groups gave:

$$\bar{c}_i = \bar{c}_{i-1} - \left(\frac{\epsilon_f}{Dg_f} \frac{\partial \bar{c}_i}{\partial Tm} + \epsilon_f \frac{\partial \bar{q}_{a,v}}{\partial Tm} + \frac{\epsilon_p \epsilon_f}{\rho_s} \frac{\partial \bar{c}_{p\,a,v}}{\partial Tm} \right). \qquad (2.57)$$

Because the dimensionless groups were changed, the solid phase diffusion equation (2.44a) also had to be changed slightly. The new form was:

$$\frac{N_{f\,i}}{r^2} \frac{\partial}{\partial r} \left(r^2 \frac{\partial q}{\partial r} \right) = \left(\frac{\partial q}{\partial Tm} + \frac{\epsilon_p}{\rho_s} \frac{\partial \bar{c}_p}{\partial Tm} \right). \qquad (2.44b)$$

The same problem occurred with equation 2.44b as with equation 2.44a; this time it was N_f that used the surface diffusion coefficient and therefore varied with radial position. Again, the problem was solved by indexing N_f and evaluating it at the concentration found at the relevant radial position.

The boundary condition equation (2.52) also had to be changed slightly to:

$$St_f (\bar{c} - \bar{c}_s) = \frac{\partial}{\partial Tm} \int_0^1 r^2 \left(q + C_p \frac{\epsilon_p}{\rho_s} \right) dr, \qquad (2.58)$$

where $St_f = \frac{K_s \; (1-\epsilon_f) \; \tau}{R_p \; \epsilon_f}$ = Stanton number for flow through systems.

2.4.3) Staged separation method

By assuming that the resin and liquid in each stage came to equilibrium, it was possible to graphically model the performance of a CCC using a McCabe-Thiele type diagram. Although the method was not accurate it

showed clearly the best possible performance that a column could achieve given the isotherm of the adsorbent to be used.

The adsorption isotherm and operating lines were drawn on a graph. The operating line represented the relative flow rates of the adsorbent and the liquid stream. Although these flow rates were not truly continuous, the average flow rates were easily determined. The operating line equation was:

$$q = \frac{F}{F_s} (C - C_{n,p}) + q_{n,p+1}, \qquad (2.59)$$

where F_s = flow rate of adsorbent,
$q_{n,p+1}$ = concentration of clean adsorbent,
$C_{n,p}$ = concentration of processed effluent.

By stepping between the operating line and the isotherm, it was possible to determine the minimum number of stages required for a particular column performance. By finding a method to estimate the fractional approach to equilibrium in each stage, it would be possible to reach a more realistic estimate of the number of stages required. The method was applied to data for the cation exchanged D1/D2 effluent in Chapter 6.

2.5) Regeneration of adsorbents

The regeneration of the adsorbent is just as important as the loading of it. All adsorbents are too expensive to throw away when fully loaded. Also the compounds adsorbed on them often have a value. Efficient regeneration is also required if pollution is to be minimized.

Ortlieb et al (1981) found that assuming a fully regenerated resin gave an optimistic design for a contactor; the amount of regeneration actually achieved needed to be estimated. Kennedy (1973) and Jackson (1983) studied the regeneration of several adsorbents using sodium hydroxide and found that XAD-8 was the easiest to regenerate. Work by Jackson and this author showed that activated carbons were so difficult to regenerate with sodium hydroxide that the cost of regeneration could over-shadow

all other costs. Martin and Ng (1985) tested a wide range of regenerants for activated carbon loaded with carboxylic acids. The regeneration efficiency was low for all compounds they tested. However, XAD-8 was so easily regenerated that the regenerant stream could be burned in a furnace without any pre-treatment. Although Harries (1982) found that XAD-8 lost some of its capacity after 12 loading and regeneration cycles, no other workers with XAD-8 have reported this effect and it was assumed that the XAD-8 regained its full capacity after regeneration.

2.6) Counter-Current Contactors

Counter-current contacting has the advantage that the diffusion driving force is always kept as large as is possible. This improves the kinetic and overall conversion performance of the contactor compared to a batch contactor. A simple packed bed contactor has the disadvantage that the adsorbent at the end of the bed is not fully utilized. Some popular methods for achieving the best performance from an adsorbent are examined below.

2.6.1) A summary of counter-current contactor designs

i) Packed bed systems; the simplest concept was to have two or more packed beds in series. When breakthrough occurred in the last column, it was switched out of the loading circuit and into the regeneration circuit. A freshly regenerated packed bed was put into the beginning of the loading circuit. Such a merry-go-round system needed a sophisticated valve system for switching the streams. The process was briefly described by Coulson and Richardson (1979).

Another system developed was the Chem-Seps process. Resin in the packed state was transported around a circuit using pulses of liquid. It had the disadvantage of damaging the resin and causing a 25 to 35% loss of resin per annum.

The Asahi process used water lifts to transport the resin into hoppers above the load and regeneration columns. When the hoppers were filled, a ball valve was opened so that the resin

could drop into the column below. This system and the Chem-Seps system were described by Slater (1981).

Packed beds allow the resin to be loaded to its full capacity because the fluid closely approximates plug flow and the exhausted and virgin resin particles never mix. Also the flow of liquid past the resin particles is fast which means the film diffusion is fast, but this comes with the disadvantage of a large pressure drop across the bed. However, the main problem is that they are rapidly clogged by fine solid particles in the liquid and the necessary filtering is often very expensive; in such cases a fluidized or mixed bed is required. Fluidized and mixed beds require a larger volume because the mixing of the resin and liquid decreases the overall adsorption driving force.

ii) Stirred contactors; the CSIRO (Australia) developed a system where the loading was performed in a stirred contactor. Resin was withdrawn from the bottom with a peristaltic pump and put into a fluidized regeneration column. The stirring of the load contactor meant the system was only suitable for systems with very favourable equilibria: Slater, (1981).

iii) Fluidized beds; the Himsley and Cloete-Streat systems consist of a series of fluidized beds, usually placed vertically on top of each other. The Porter and CANMET Slater systems use a horizontal arrangement of fluidized beds. The Himsley system achieves resin transfer between two stages by occasionally pumping liquid from the higher stage to the lower stage. The normal flow from the lower to the higher stage is therefore reversed and resin transfer occurs. The Cloete-Streat system achieves transfer by occasionally stopping the up-flow for all stages and then reversing the flow for a short period. The Porter system uses a series of contactors, each lower than its neighbour. Fluid flows by gravity from the top of the first stage to the bottom of the next. Resin is transported by air lift pumps. The CANMET Slater system attempts to prevent damaged to the resin by transporting it using a vacuum. The resin is sucked from the bottom of the one contactor into the hoppers above the next

contactor. When the hopper is full it is vented (back to atmospheric pressure) and the valve at the bottom is opened to empty the resin into the contactor below. All these systems are described by Slater (1981).

2.6.2) The Cloete-Streat contactor

Choosing the best contacting system involved a number of considerations. Attrition of the resin needed to be minimized. The merry-go-round system of packed beds would be the best in this regard because the resin was never moved. Its use was not considered because it used packed beds and the treatment of effluents containing solids was of interest. A survey of three Cloete-Streat type and one Porter type contactor used for uranium recovery showed that about 1% of resin was lost per month (Cloete, 1984). This suggested that the complicated vacuum resin transfer system of the CANMET Slater design was not justified.

Another consideration was the amount of liquid used to transport the resin. This was of particular concern in the regeneration column where the flow of liquid was small compared to the flow of resin. The liquid used to transport the resin out of the bottom of the column was wasted, so the quantity used had to be small. The Cloete-Streat column performed well in this regard because it allowed the resin bed to settle first and the bed was pulled down in the packed state.

Dodds et al (1973), Ortlieb et al (1981), and Gomez-Vaillard and Kershenbaum (1981), found that the fraction of the resin bed transferred during each cycle had a noticeable effect on the overall performance of a Cloete-Streat column. They found that the efficiency increased to a maximum at the stage where 100% of the stage was transferred at each cycle. The Cloete-Streat column had the advantage of being able to transfer all of the resin in a stage without wasting column capacity by leaving one of the stages empty.

The Himsley system had a complicated system for transferring resin. It was assumed that the simplest design would be the least expensive, and the vertical arrangement of the Cloete-Streat column seemed to be the simplest to construct for a given number of stages. This column therefore appeared to be the one of choice.

2.7) Settling in fluidized beds

2.7.1) Settling of spherical particles in a bed

The theory in this section is based on the presentation by Coulson and Richardson (1978).

The free falling velocity U_0 in a fluidized bed for $0.2 < Re < 500$ is given by:

$$U_0 = \frac{d^2(\rho_s - \rho_f)g}{18\mu(1 + 0.15Re^{0.687})}, \qquad (2.60)$$

where d = particle or bead diameter,
μ = viscosity of fluid,
g = gravitational constant,
ρ_f = density of fluid,
ρ_s = effective density of beads,
Re = renolds number.

The falling velocity corrected for column diameter - or sedimentation velocity at infinite dilution - (U_i) is:

$$U_i = 10(\log(U_0) - d/D_t), \qquad (2.61)$$

where D_t = Column diameter,

and the voidage of the bed is given by:

$$\epsilon_f = (U_c/U_i)^{1/N}, \qquad (2.62)$$

where U_c = superficial velocity of fluid,

and $$N = (4.4 + 18\, d/D_t)Re^{-0.1}, \qquad (2.63)$$

for $1 < Re < 200$.

Chapter 3

Experimental methods and materials

This chapter first explains the choice of analytical method for measuring the concentrations of the solutions that were contacted with the adsorbent. Secondly, the properties and use of XAD-8 is examined. This was the resin previously chosen for adsorbing organics from the bleach effleunts. It was later learned that Rohm and Haas had discontinued manufacturing it. They are making another resin which is to replace it, and the details given below only require slight adaption when applied to the new resin (possibly XAD-1180). Next, the development of a method for cleaning the raw XAD-8 is examined. Finally the laboratory procedures used to measure the isotherms and the kinetics of adsorption are presented.

3.1) Quantitative analytical methods

3.1.1) Choice of analytical method

A method of measuring the concentrations of the solutions contacted with the XAD-8 was required. The ideal method would be quick, convenient, accurate, specific to the species of interest, and either readily available or cheap enough to fit into the available budget. Some time was spent studying the alternatives. The following five methods were available and suitable for the quantitative analytical work:

i) spectrophotometric analysis in the ultraviolet range (UV absorbence) is a very quick and versatile method of concentration measurement. Readings could be taken on a batch basis or continuously using the plotting facility included with the machine. The accuracy is as good as ± 0.1% if all interferences are removed. Unfortunately, the method is very sensitive to the presence of contaminants. Temperature effects also cause errors. When measuring concentrations of multicomponent mixtures, compounds with large extinction coefficients tend to dominate the readings. It is therefore important to state the wavelength used for the absorption measurements:

ii) electrical conductivity is also a quick method of concentration measurement, but it can only be used for conductive solutions. It is extremely sensitive to contaminants in the solutions. It was used to measure the concentration of oxalic and malonic acid solutions;

iii) gas chromatography with a flame ionization detector (FID) suffered from none of the disadvantages just mentioned, and could be even more accurate. Its use was ruled out because the analyses would have been slow to perform, and setting up the equipment and experimental procedure would have been too expensive and time consuming;

iv) the use of high performance liquid chromatography (HPLC) was considered to be the most attractive alternative. Limited use was made of this method, but it was very slow because the equipment was not on site;

v) the chemical oxygen (COD) demand test was popular for measuring the total quantity of organic compounds in complex aqueous solutions. The problem with this test was that is was very time consuming.

3.1.2) Ultraviolet absorbence

3.1.2.1) The instrument used

The instrument available in the department was a Varian Superscan 3. This was a double-beam scanning UV-Visible spectrophotometer with digital read-out of photometric data and a built-in chart recorder. The wavelength range was 190 to 900 nanometers (nm) and the measurements could be made in units of absorbence, percentage transmission or fractional concentration. The instrument also had base-line programming and a time-base facility. ie. it could plot absorbence at a fixed wavelength vs. time on the chart recorder. It could also plot absorbence vs. wavelength. The wavelength readout was a 4 digit digital display with a 0.1 nm resolution. The accuracy was claimed to be better than 0.2 nm. The percentage transmission range was claimed to be 000.0 to 144% and the absorbence range -0.140 to 3.000 absorbence units.

It was found that although the instrument would give absorbence readings of up to 4.000, readings above 1.5 were non-linear and readings above 2.0 tended to be meaningless. The machine developed several faults that had to be fixed, so a lot of time had to be spent on maintaining the optimum performance from the it.

A number of cuvettes were available for holding the solutions of interest. Since most readings were taken at wavelengths below 300 nm, exclusive use was made of quartz cuvettes. Two cuvettes were required; one for the reference beam; and the other for the measuring beam. The reference cuvette always contained distilled water. Distilled water was used in the sample cuvette to zero the instrument. Open cuvettes with 1.000 and 4.000 cm path lengths and flow-through cuvettes with 0.3, 1.000 and 4.000 cm paths lengths were available. Holders with a water jacket for maintaining a fixed temperature were available for the 1 cm cuvettes.

The instrument had a variable spectral bandwidth (the difference between the highest and lowest wavelength in the beam). A wide spectral bandwidth gives a stronger light beam and it was found that this improved the stability of the readings when doing accurate work. A spectral bandwidth of 3.0 was used unless an absorbence vs. wavelength scan was being done, in which case a 1.4 nm bandwidth was used to obtain better peak definition.

3.1.2.2) Contamination and UV

When using UV absorbence, it was necessary to clean everything that touched the solution of interest very carefully and then to rinse everything thoroughly with some of the solution. It was found that many plastics released substances that absorbed light at the short wavelengths used for measuring the concentration of non-aromatic carboxylic acids such as oxalic and malonic acid. Several ideas on possible sources of error were obtained by the thorough work performed and reported by Junk et al (1974). The steps found necessary for the minimization of these interferences are explained below:

i) the cleanliness of the UV cuvettes was checked by swopping them around while both contained distilled water. A change in absorbence of more than about 0.02 in matched cuvettes indicated that one or both were dirty and both were cleaned. They were

cleaned by soaking them for about 10 minutes in a methanolic potassium hydroxide solution and then rinsing them in methanol followed by tap water. They were then dried with a clean tissue on the outside, and the inside when feasible. Before being used they were rinsed with distilled water and they were stored in distilled water for short periods of disuse. When using unmatched cuvettes (for instance there were no matching cuvettes for the flow-through cuvettes), the UV absorbence of the cuvettes could differ by more than 0.03 even when clean. This difference was noted for future checks on cleanliness;

ii) all apparatus was checked to see if it changed the UV absorbence of solutions it came into contact with. It was found that distilled water shaken in the volumetric flasks or the plastic Xactics bottles showed an increase in UV absorbence at 200nm. If this increase was more than about 0.01 the container was washed again or discarded.

When a solution was introduced into a pipette or volumetric flask, the absorbence often decreased slightly. To eliminate this effect, containers were rinsed with the solution that they were going to carry. For instance, to dilute a stock solution of phenol by 10 : 1, 0.1 l of the stock would be drawn up in a clean pipette and poured into a clean 1 l volumetric flask. The flask would be filled with distilled water and the solution thoroughly shaken. A UV reading would be taken and the solution discarded and a new solution made using the freshly rinsed pipette and flask. If the new UV reading was more than about 5% higher (or occasionally lower), more checks would be performed to eliminate the source of error;

iii) a spinning basket contactor was used to study the kinetics of adsorption. A pump was needed to circulate the solution from the contactor through the flow-through cuvette. The first pump used was a peristaltic one and it was found that it introduced contamination into the system. Changing the plastic tubing in the system did not help. It was replaced with a Hughes long stroke micro pump. This unit contained no plastic parts (except the teflon seal) and was connected to the UV spectrophotometer

by thin bore stainless steel tubing. Testing it against the peristaltic pump showed that it introduced three times less contamination into the system as measured by UV absorbence at 225 nm.

3.1.2.3) Choosing a wavelength

As already mentioned, the UV absorbence of solutions needed to be in the range 0 to 1.5 if accurate results were required. For optimum accuracy, readings between 0.8 and 1.5 were desired. There were three ways of achieving UV absorbences in this range;

i) adjust the concentration of the solution with distilled water;

ii) change the path length of light by using different cuvettes;

iii) change the wavelength at which the readings were taken.

The first method was time consuming because of the necessary precautions needed - such as meticulous cleaning of pipettes, flasks etc. The second method was limited by the range of path lengths available and the need to zero the UV spectrophotometer each time different cuvettes were used. Therefore the third method was used whenever possible. It was possible to find a suitable wavelength in all cases except that of concentrated phenol. Phenol at 0.1 N had too great an absorbence at all wavelengths below 287 nm. The problem was that the absorbence changed rapidly with wavelength in this region. The UV extinction coefficient at 287 nm was 15.8 and at 289 nm it was 6.7. This made the absorbence readings less reliable, and it was necessary to dilute some of the phenol solutions to double-check readings in this region. When very dilute solutions were being measured the 4 cm cuvette was used, but it had the disadvantages of being difficult to clean and requiring a large solution sample. (12 cm^3 as opposed to 3 cm^3 for the 1 cm cuvette normally used).

Figure 3.1 shows the shape of the UV absorbence vs. wavelength curves for oxalic acid, phenol and malonic acid. The vertical axis was plotted on a log scale. The curves plotted are for pure solutions measured at an appropriate concentration and are not necessarily accurate under different conditions. A peak at about 200 nm was common for the carboxylic acid group and the peak at 270 nm was characteristic of the

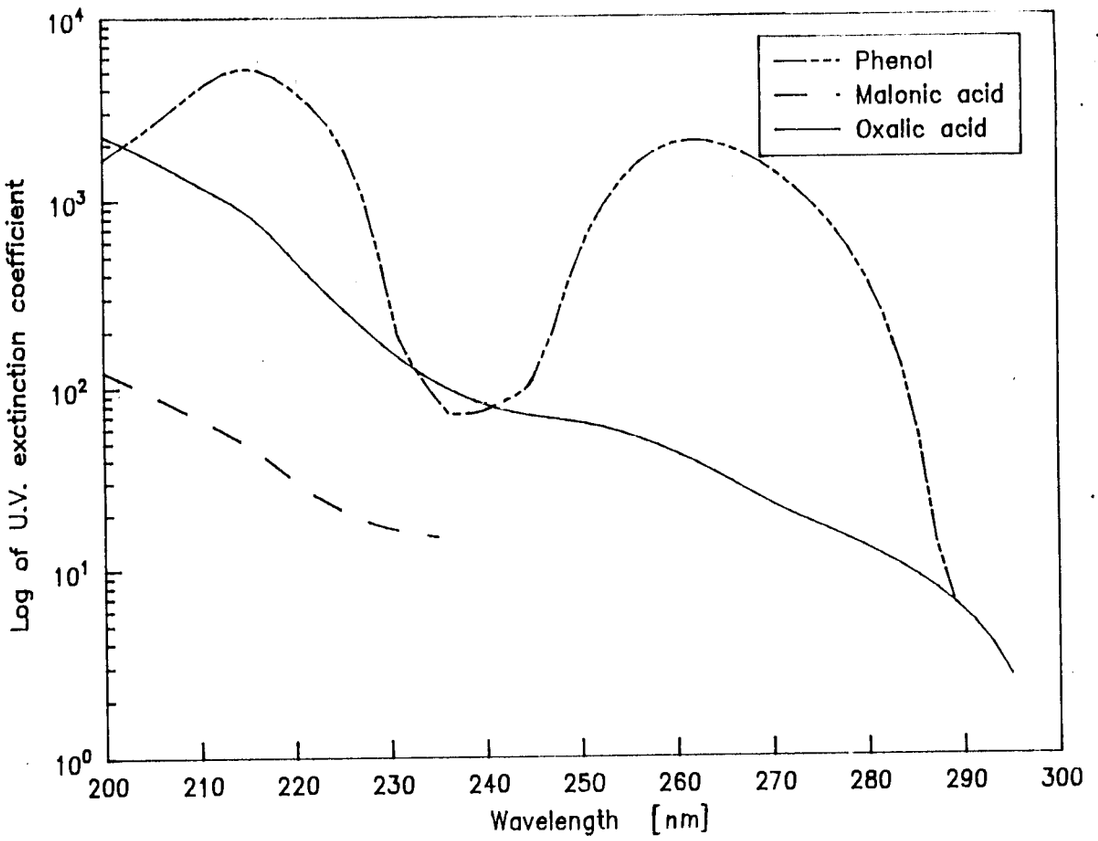

Figure 3.1 U.V. absorption versus wavelength for aqueous solutions of pure compounds.

benzene ring (aromatic group). The position of the oxalic acid peak was found to be sensitive to the concentration, shifting to a shorter wavelength in more dilute solutions. This effect was probably due to hydrogen bonding, the strength of the hydrogen bonds being concentration dependent. Another possible cause was that each ionic species had a unique absorbence curve, and changing the concentration of the acid changed the dissociation of the acid.

It was found that even for absorbence readings between 0 and 1.5, the solutions did not have a linear concentration vs absorbence relationship. This was probably due to the finite spectral bandwidth as explained in Chapter 2. The changing dissociation of acids may have also had an influence as explained below. The deviation from linearity actually encountered was up to 2%; if a 1 M solution had an absorbence of 1.000 at a certain wavelength, a 0.5 M solution generally had an absorbence of 0.501 to 0.51. To correct for this, a series of three or four standards were made for each decade range of concentration. The resultant UV

absorbence vs. concentration curves were fitted to quadratic equations. The equations were used to interpret UV absorbence readings made in the range they covered.

3.1.2.4) pH and its influence on UV absorption

If a compound ionizes, each ionic species has a unique UV absorbence spectrum. For instance oxalic acid ionizes as shown below.

$$C_2H_4O_4 + H_2O \rightarrow C_2H_3O_4^- + H_3O^+$$

$$C_2H_3O_4^- + H_2O \rightarrow C_2H_2O_4^{--} + H_3O^+$$

The dissociation constants for this ionization at 25 °C are (Rappoport, 1967):

$$K_1 = \frac{[H_3O^+][C_2H_3O_4^-]}{[C_2H_4O_4]} = 5.37E\text{-}2 \quad (pK_1 = 1.27),$$

$$K_2 = \frac{[H_3O^+][C_2H_2O_4^{--}]}{[C_2H_3O_4^-]} = 5.25E\text{-}5 \quad (pK_2 = 4.28).$$

An experiment was done to determine the UV extinction coefficients of the two oxalate ions and the associated acid. At a pH of 1.27, there were approximately equal amounts of associated acid ($C_2H_4O_4$) and single-charged ion ($C_2H_3O_4^-$). To suppress at least 99% of the ionization, a pH of -0.73 would be needed. No buffer was available for such pH values, so a 0.0008 M solution of oxalic acid was prepared in a 1 M solution of hydrochloric acid. The pH was 0.18 which meant there was less than 10% ionization. The UV absorbences of the mixture and the 1 M hydrochloric acid were measured and the difference used to calculate the extinction coefficient of the associated oxalic acid. It was found to be 131 at 225 nm.

Measuring the extinction coefficient of the single-charged ion required a pH of about 2.7 or 2.8 since $pK_2 = 4.28$ at 25°C. Again, no suitable buffer was available so hydrochloric acid was used to achieve a pH of 2.78. The extinction coefficient was 2150 at 225 nm. Finally the UV absorbence was measured on a solution with a pH of 9.95 to determine the

extinction coefficient of the double-charged ion. A substantial correction had to be made for the UV absorbence of the sodium hydroxide solution used to achieve this pH. The result was 1475.

The results for the extinction coefficients of each absorbing species were:

Absorbing species	$(C_2H_4O_4)$	$(C_2H_3O_4^-)$	$(C_2H_2O_4^{--})$
Extinction coefficient	130	2150	1475.

The differences were significant which meant that the UV absorbence would be very sensitive to the percentage dissociation especially at a pH of 1 to 2.

3.1.2.5) Effect of temperature on UV readings

The UV absorbence of a single chemical species does not usually change significantly with temperature (Rao, 1975; Beaven et al, 1961). The problem was that the concentration of ionic species was pH and temperature sensitive and each ionic species had a unique UV absorbence curve. The experimental significance of this was that care was needed to ensure that all readings were taken on solutions at the same temperature and pH as the calibration standard. Constant temperature was achieved by storing the standard and unknown solutions in the same room and then making all UV readings within a short period (less than 30 minutes).

The effect of a change of temperature on the concentration of each ionic species of oxalic acid is illustrated with a numerical example. Harned and Owen (1950) showed that K_2 is temperature sensitive, their results being:

K2 × 10^5	5.91	5.82	5.70	5.55	5.40	5.18	4.92	4.67	4.41	3.83
Temp	0	5	10	15	20	25	30	35	40	50

At a pH of 4 K_1 has little effect because $[H_3O^+] = 1E-4$.

Therefore $[C_2H_3O_4^-]/[C_2H_4O_4] = 537$.

ie. $[C_2H_4O_4]$ is small compared to $[C_2H_3O_4^-]$ and can be neglected at all temperatures.

However $[C_2H_2O_4^{--}]/[C_2H_3O_4^-] = 0.518$ at 25 °C.

Therefore for a 0.001 N solution $[C_2H_3O_4^-] = 0.000659$,

and $[C_2H_2O_4^{--}] = 0.000341$.

The absorbence of the solution is the sum of the absorbences due to each ion, so at 25 °C it is:

Absorbence = 2150 × 0.000659 N × 1 cm + 1475 × 0.000341 N × 1 cm
= 1.92.

At 0 °C $[C_2H_3O_4^-] = 0.000629$ and $[C_2H_2O_4^{--}] = 0.000371$,

and the UV absorbence is 1.90.

At 50 °C it is 1.96.

The difference in UV extinction coefficient at 225 nm between $[C_2H_3O_4^-]$ and $[C_2H_4O_4]$ is much greater and if K_1 is sensitive to temperature then the absorbence will be much more sensitive to temperature in the pH range 1 to 2. When performing such calculations it must be remembered that pH tends to change with temperature, and that the dissociation constant for water changes. The relative concentrations of the ions is therefore not so simple to calculate. The full details of these complications were not pursued because concentrations were calculated by comparing UV readings with known standards at the same temperature.

Ideally, the two dissociation constants would have been determined at a range of temperatures. This would have enabled the calculation of the relative concentrations of each ionic species and this, with a knowledge of the extinction coefficient of each species, would have enabled the

calculation of the total oxalate concentration. This would have been very time consuming though, so a simpler experiment was performed to find the effect of temperature on UV absorbence. A solution of oxalic acid was prepared and put into a cuvette in the temperature controlled cuvette holder. Water at a known temperature was allowed to flow through the holder for 30 minutes to ensure that the solution inside was at a fixed temperature. A series of readings were taken at different concentrations and temperatures. The results are in table 3.1.

Table 3.1

Change of UV absorbence of oxalic acid with temperature

Conc. of oxalic [M]	Temperature [°C]	λ [nm]	Absorbence	pH	% change per °C
0.0005	18.2	200	1.187	3.2	-0.01
	29.4		1.185		
	45		1.183		
0.005	16.9	225	1.389	2.4	0.28
	26.9		1.429		
	36.6		1.471		
	46.3		1.504		
0.05	17.6	275	0.840	1.6	0.24
	30.3		0.860		
	42.3		0.890		
0.005	26	225	1.365	2.4	(1.2)
	27		1.381		up
	29		1.419		(0.25)
	31		1.451		down
	29		1.450		
	26		1.433		

The results show that absorbence at 225 nm (pH 2.4) and 275 nm (pH 1.6) increases significantly with temperature. At 200 nm and a pH of 3.2, there appears to be a decrease. The most interesting set of results was the last one. The first three sets of results were made in a sealed cuvette, but the last set was made in an open cuvette. The solution in the open cuvette showed a much sharper rise, but it did not go back to where it started when the temperature was dropped again. On the rising slope, its absorbence increased 1.2% per °C but on the dropping slope it dropped 0.25% per °C. The rise in absorbence at 26 °C was 5% in about 3 hours. In another experiment where the temperature was held at 26 °C for 3.5 hours, the absorbence only rose 0.65%. Although evaporation accounted for a proportion of this rise, it was expected that a component of air was dissolving in the solution and causing most of the rise. In the spinning basket, the rise had been much more dramatic, so tests were done in it.

The motor for spinning the basket tended to become warm and would heat up the solution in the contactor. To check whether this temperature rise was significant, the temperature before and after a run was checked. The rise was found to be 2 to 3 °C per hour which was considered unimportant for 30-minute runs.

3.1.2.6) Effect of aerating solutions:

It was observed that the UV absorbence of oxalic acid solutions that were not in an air-tight container always showed an increase in absorbence with time, even when there was no change of pH or temperature and no significant evaporation. The only cause that could be imagined was that some component of the air was absorbing into the solution. To measure the magnitude of aeration effect in the spinning basket, an experiment was performed: 0.2 l of a 0.005 M oxalic acid solution was put into the contactor. The empty basket was placed in the oxalic acid and the solution was pumped through the UV cuvette, but the basket was not spun. After 30 minutes the motor was turned on and left on for another 30 minutes; see table 3.2.

Table 3.2

Effect of aeration on UV absorbence

Time	pH	Absorbance	Temp	Comments
15h46	1.92	1.374	22.7	
16h06	1.91	1.376	22.8	
16h16	1.90	1.376	22.8	Basket spinning
16h21	1.90	1.393	22.8	
16h46	1.89	1.424	23.0	

The effect of spinning the basket was very marked, suggesting that the agitation of the solution in air was a major source of error. Extensive modifications to the apparatus were not undertaken to solve this problem.

3.1.3) Electrical conductivity

The instrument used was a Philips digital conductivity meter PW9506. The instrument had a range of 0.0000 to 199.9 milliSiemens per centimeter in four decade ranges.

The relation between conductivity and concentration was not quite linear (because of changing dissociation with concentration and the conductivity of the distilled water used). A series of solutions of different concentrations were prepared and their conductivities measured. The conductivity vs. concentration data was fitted to a quadratic equation and this equation was used to interpret conductivity readings. Curves were created for malonic and oxalic acids. All other single compound solutions used did not have high enough conductivities to allow accurate results. With the bleaching effluents, there was no way of isolating the contribution of the hydrochloric acid and other inorganic ions from that of the organic ions.

3.1.4) High performance liquid chromatography

The instrument used was the one kept by SAPPI R&D, Enstra. It was a Dionex 2110i with a conductivity detector. The column used was an AS 4 with a membrane suppressor. The suppressor reagent was 0.025 l of 4 N

sulphuric acid in 4 l. A 50 µl sample loop was used.

To obtain accurate results, the samples for HPLC analyses were diluted to about 0.001 M. ie. if the original solution contacted with the resin was 0.01 M the original, and all subsequent samples, would be diluted 10 times with distilled water.

3.2) Properities and preparation of XAD-8

3.2.1) The chemical composition of XAD-8

XAD-7 and XAD-8 are macroporous polymethacrylic resins manufactured by Rohm and Haas. The basic monomer from which XAD-8 is manufactured is methacrylic acid which has the structure:

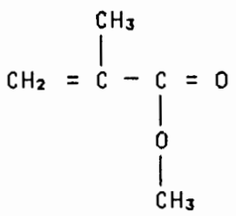

This monomer is polymerized with another monomer called a crosslinker. The crosslinker has two double bonds so that it can react at two sites. It has the function of linking the polymethacrylate chains together to make the polymer insoluble, hard and tough. The structure of XAD-8 is represented below (Kunin, 1980).

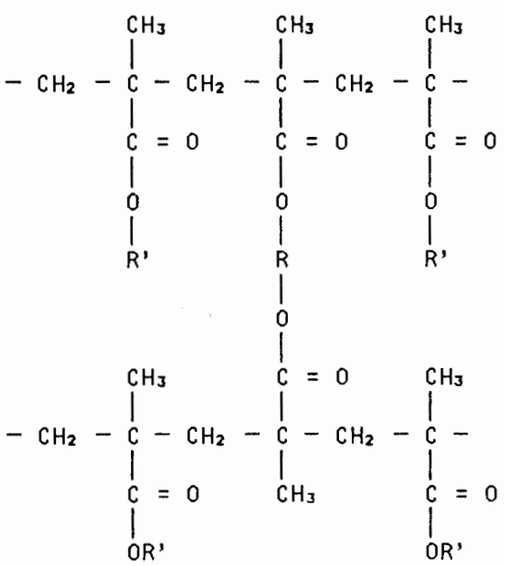

The nature of the groups R and R' are not divulged since they have an important effect of the adsorption and physical properties of the resin. Divinylbenzene was the most popular choice of crosslinker (Helfferich, 1962); Aiken et al (1979) state that XAD-8 is nonaromatic and therefore more resistant to fouling. Although they may not have taken the crosslinker into consideration when making this statement, it is more likely that one or more of the several available aliphatic crosslinkers are used. Aiken et al also state that XAD-8 has a very low ion-exchange capacity of about 0.01 mequiv per gram. They do not say how the resin gets this capacity.

The methacrylic polymers are more polar than the styrene polymers with a dipole moment of 1.8 debyes as opposed to 0.3 debyes. This means that they are more hydrophilic than the styrene polymers, but they still have a strong hydrophobic nature. Being more polar, they have a greater affinity for polar molecules such as carboxylic acids. (Kunin, 1980).

Junk et al (1974) found that napthalene, ethylbenzene and benzoic acid were released from new XAD resin. Scott et al (1984) found that diethenylbenzene, dodecane, ethenylethylbenzene, 1-methyl-1 H-indene, methylnapthalenes and undecane were released from XAD resins. These compounds obviously were used at some stage in the manufacture of the resins.

3.2.2) The physical properties of XAD-8

XAD-8 is composed of tough white beads that can withstand high pressure and temperature. Their average particle diameter when wetted by water is 0.46 mm. Figure 3.2 shows the size distribution of the beads determined by washing the beads through a series of sieves with water. The average pore diameter is 2.25E-8 m, the surface area is 160 m^2/g and the true wet density is 1090 kg/m^3 (Rohm and Haas, 1981).

Van Vliet et al (1980) collected and measured a number of physical

properties for various resins including XAD-8. Their results were:

B.E.T surface area	=	140 m^2/g,
skeletal density	=	1230 g dry resin/l solid matrix,
particle density	=	445 g dry resin/l particle,
particle porosity	=	0.638,
average percent dry resin	=	41.1 %.

An idea of the pore structure was obtained by taking micrographs of XAD-8. A selection of these micrographs can be seen in figure 3.3. The micrographs have to be taken of the dried resin, and since the resin swells by 25% when wetted, any physical measurements taken from the micrographs will be low.

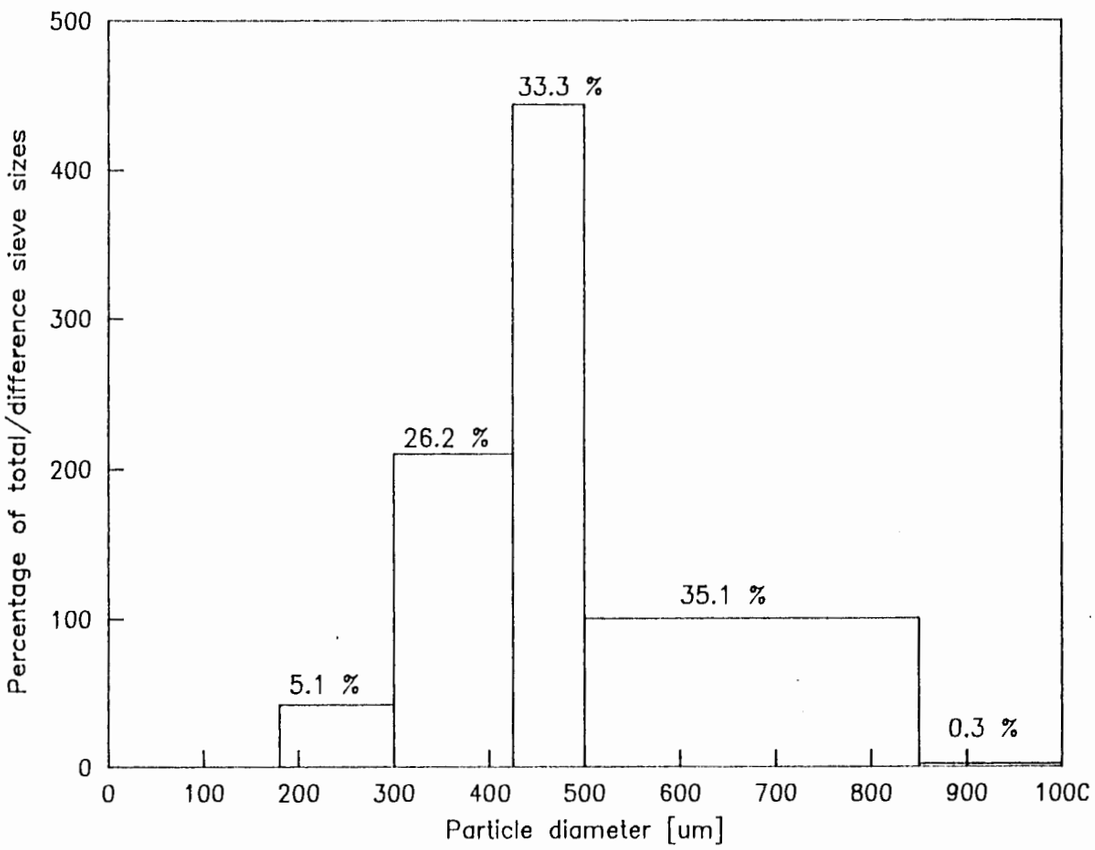

Figure 3.2 Size distribution of XAD-8 particles

Broken XAD-8 bead

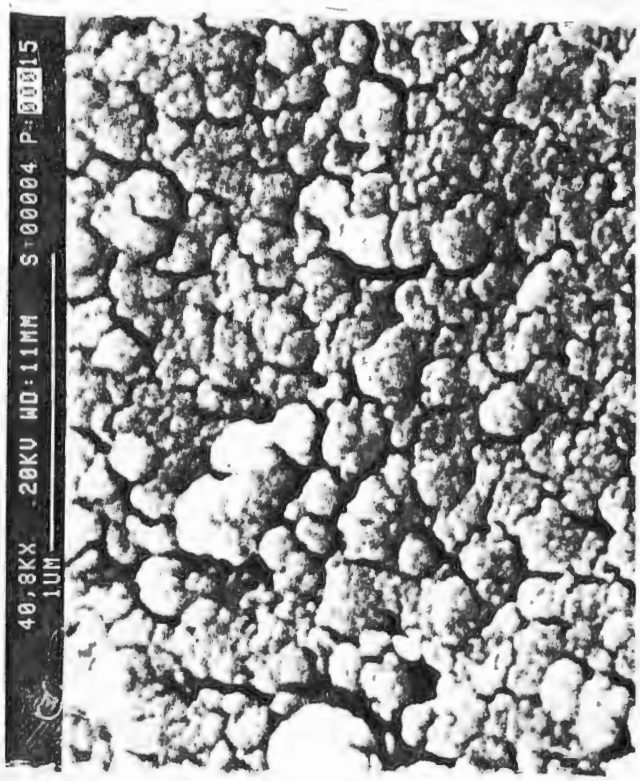

Close-up of undamaged resin surface

Damaged section of XAD-8 surface

Close-up of damaged surface

Figure 3.3 Electron micrographs of XAD-8 resin beads

3.2.3) Finding a method to clean XAD-8

Several different methods for cleaning XAD-8 have been reported. Van Vliet et al (1980), washed it successively with deionized distilled water and methanol and then rinsed it thoroughly with water. Thurman et al (1978) washed the resin for 5 days with 0.1 N sodium hydroxide followed by 24 hours of Soxhlet extractions each with methanol, acetonitrile and diethyl ether. The resin was then stored under methanol until ready for use. Before use it was rinsed with 200 column volumes of water, then 0.1 N sodium hydroxide or 0.1 N hydrochloric acid to adjust the pH to that of the solution to be tested.

Thurman et al (1978) used a very similar method to Junk et al (1974). Junk et al tested 3 methods of cleaning XAD-2 resin. They found degassing at 225 °C under 10-7 torr, and heat desorption at 200 °C in an inert gas stream, to be inferior to their method of Soxhlet extraction. They stated that contaminants such as napthalene, ethylbenzene and benzoic acid were trapped interstitially within the bead during manufacture. They claimed that during the cooling and venting process required with their first two methods, new surfaces were exposed causing severe contamination. They found that the resin must also always be kept wet to prevent the occurrence of contaminants in the blank.

The manufacturer (Rohm & Haas, 1981) recommends the following preparation method:

i) slurry the resin in a beaker with demineralised water to remove the sodium chloride and sodium carbonate used to control bacteria;

ii) after two water washes, slurry the resin in an organic solvent such as methanol, acetone or isopropanol. This swells the resin allowing the release of low molecular weight impurities;

iii) the resin should be stored and transported in the organic solvent. During transport the solvent level must not drop below the level of the top of the resin bed;

iv) wash with water in upflow for 10 minutes to remove fine particles and air bubbles.

They stressed that it was important that the resin remains submerged in solvent at all times after being wetted with methanol.

Junk et al claimed their method was accurate and reliable for concentrations down to 10 ppb or less, and the method took 2 years to develop. Van Vliet et al stated that their method was adequate for concentrations down to 200 ppb. Since the UV meter used in this work could only resolve down to 100 ppb of oxalic acid, it was initially thought that a similar method to Van Vliet et al's would be sufficient. Such a method was tried but the isotherms measured using resin prepared by this method showed a lot of scatter. This discovery led to an extensive series of experiments. In all, five different cleaning methods were tried and are reported below:

i) an adaptation of Van Vliet et al's method was tried first: new resin was put into a Millipore filter holder and washed with water then twice with methanol. It was then washed with sodium hydroxide followed by hydrochloric acid and water until the conductivity of the water did not change. Conductivity was used because it was found that any solution introduced into the Millipore filter holder dissolved something in the plastic that absorbed light at the wavelengths of interest (around 200 nm).

   The cleaned resin was transferred to Xactics (number 122) bottles. These bottles were made of food grade polyvinyl chloride (PVC) and had polypropylene snap-on lids, and were found not to release measurable quantities of UV absorbing compounds into aqueous solutions. The bottles with the resin and various solutions inside were put on a wheel that rotated at 4 to 5 revolutions per minute. The UV absorbence of the solutions in the bottles showed a slow but significant rise due to the release of contaminants;

ii) the second method tried was to investigate the possibility of driving the contaminants from the resin by heating it in air. Fresh resin was dried for 48 hours at 110 °C. Seventy grams was

weighed into a polycarbonate Millipore holder, and washed with methanol then water three times. It was then transferred to a perspex column and washed with sodium hydroxide, hydrochloric acid, sodium hydroxide, oxalic acid and finally water. The UV absorbence of the water never dropped below about 0.05 (200nm, 4 cm cell), even after contacting the resin with steam.
It was later found that the perspex column was releasing substances that were absorbing the light. Since this was the second time that plastic containers had caused problems, it was concluded that minimal use of plastics would have to be made in all experimental work. Beaven et al (1961) reported that plasticizers and other compounds that absorb light are often extracted from plastics. Curran and Tomson (1983) quantified the release of substances into water from a number of plastics. They found that Teflon was the best followed by PVC and Polyethylene. They concluded that plastics made soft or flexible with plasticizers would cause problems. All future work was therefore performed in vessels that had been carefully checked for the release of contaminants. A glass column was acquired and used to hold the resin being rinsed with water. Also the Millipore filter holder was replaced with a sintered glass Buchner funnel. Although this Buchner funnel was much better than the Millipore filter holder, it still released measurable amounts of contaminants even after extensive cleaning with acids, bases and organic solvents.

It was found that this method could produce resin that did not release significant contamination while in the glass column in which it was being cleaned. However, as soon as the resin was removed from the column, it started releasing contaminants again;

iii) the next method tried was to Soxhlet extract dried resin with methanol, acetone and steam for about 5 hours each. The resin could not be transferred from the Soxhlet extraction apparatus into the Xactics bottles, so it was transferred first to the glass Buchner funnel.

An attempt to wash the resin in the Buchner funnel with water failed because the steam had dried the resin and water cannot wet dry resin. An attempt was made to wet it with acetone but a large proportion of beads still floated indicating they were not fully wetted. (Acetone was used to see if it would wash out of the resin faster than methanol which took large quantities of water to wash out: no substantial difference was found.) Adding methanol to the acetone wetted resin caused the release of air indicating that methanol was more strongly attracted to the resin surface than acetone. The resin was then washed with over 6 litres of distilled water while in the Buchner funnel, using a squeeze bottle to agitate the resin. The resin was put into weighed Xactics bottles with a test solution, and the bottles placed on the rotating wheel. The UV absorbence of the solutions still indicated an unacceptable release of contaminants;

iv) the fourth method tried was to determine if very long periods of treatment would help. It was found that diethyl ether wets the resin better than acetone or methanol, so ether was used to wet and clean the resin. The resin treated by method ii was soaked in ether for 40 hours, and then washed continuously with distilled water, treated with activated carbon, for 2 weeks. (Junk et al (1974) also used such water.) Activated carbon treated distilled water was used because it was found that this water had a lower UV absorbence at 200 nm that untreated distilled water. The water did, however, have a higher conductivity than untreated water, especially when the carbon was fresh.

When the UV absorbence of the water flowing into the column was the same as that coming out, the resin was transferred to the Buchner funnel so that it could be washed again and transferred to the Xactics bottles. The UV absorbence again rose when the resin was contacted with water or oxalic acid in the Xactics bottles;

v) the final method tried was the use of ultrasound to drive the contaminants into solution more quickly. The 0.3 l of the resin

from method iv was put into a one litre volumetric flask. The UV absorbence was 0.041 and rose to over 3.1 after 10 minutes in the ultrasonic bath. The resin was moved to the glass column and washed with 2 litres of water and then exposed to another 10 minutes of ultrasound while in the flask. Again the UV absorbence increased markedly from 0.175 to over 3.1.

The glass column was set up in the ultrasonic bath and exposed to ultrasound intermittently (about 10 minutes on and 10 off) while a continuous stream of distilled water was passed through the column at 5 l/hour. Over a period of one hour the UV absorbence dropped from 0.4 to 0.1. It remained at 0.1 for the next hour of treatment. The ultrasound was then left off and water was passed through the column for a further 10 hours at 2 l/hour. The UV absorbence dropped to 0.011 below that of distilled water pumped into the column. (All UV readings at 200nm in 4 cm cell).

It was observed while performing the above experiments that the Soxhlet extraction and the ultrasound were the methods that removed the most dirt from the resin. It was proposed that the new resin should be Soxhlet extracted first, then soaked in ether or methanol before being treated by low intensity ultrasound with a concurrent distilled water wash.

3.2.4) Evaluation of ultrasound cleaning

Very little literature could be found on the use of ultrasound for modifying the behaviour of adsorbents. Wang and Cheng (1982) found that ultrasound increased the rate of adsorption of 4-(2-pyridylazo) resorcinol on XAD-2 compared to an unstirred sample, but not as much as mechanical agitation did. Vasil'ev and Kabeiya (1976) found that ulrasound increased the rate of ion-exchange by a factor of at least two, and and that the resins could be washed more quickly and with less water when subjected to ultrasound.

Ultrasound caused a continuous release of contaminants from the resin, no matter which cleaning technique was used previously. Soxhlet extraction seemed to be able to remove contaminants loosely held on the

resin, but any physical agitation of the resin caused the release of more tightly held contaminants. These contaminants were so tightly held that the process of trying to remove all of them by ultrasound caused destruction of the beads. A balance had to be found between destroying too many beads and cleaning them adequately. The ultrasound bath used first (method v) had a power of about 4000 Watts. It was found that it caused a large proportion of the beads to float and it gradually destroyed them.

To minimize this loss of resin, a smaller ultrasound bath with an output of about 300 Watts was used for subsequent work. This bath was much better, but still destroyed some beads and made some float. It was used because it could be left on continuously and did not have to be constantly attended to.

To try to quantify the rate of release of UV absorbing substances from the ultrasound treated resin, an experiment was performed over 32 days. About 15 g (0.045 l) of resin cleaned by method 5 was put into a 0.2 l flask. Water was added and the flask was subjected to ultrasound continuously in the small ultrasound bath. Periodically, about 0.14 l of the water was withdrawn and replaced with fresh distilled water. The UV absorbence of the withdrawn water was tested. Figure 3.4 shows the results. The rate figures were derived from the UV absorbence of the solution and the time since the previous sample. No attempt was made to assign units to this result.

The resin released contaminants continuously with no sign of the rate of release decreasing. The first 3 days of treatment were under high power mode, and the treatment from day 12 to day 16 was under medium power mode. The rest was under low power mode. Figure 3.4 shows that the rate of release was a function of the sound intensity. It was also found that the average rate dropped if the period between samples was increased. The conclusion was that it was impossible to completely clean the XAD-8 without destroying it. The resin was therefore cleaned as far as practically possible and then corrections were made to account for the remaining contamination.

Examination of the ultrasonically cleaned beads under a light microscope did not reveal any damage to whole beads. That is, no beads with cracks

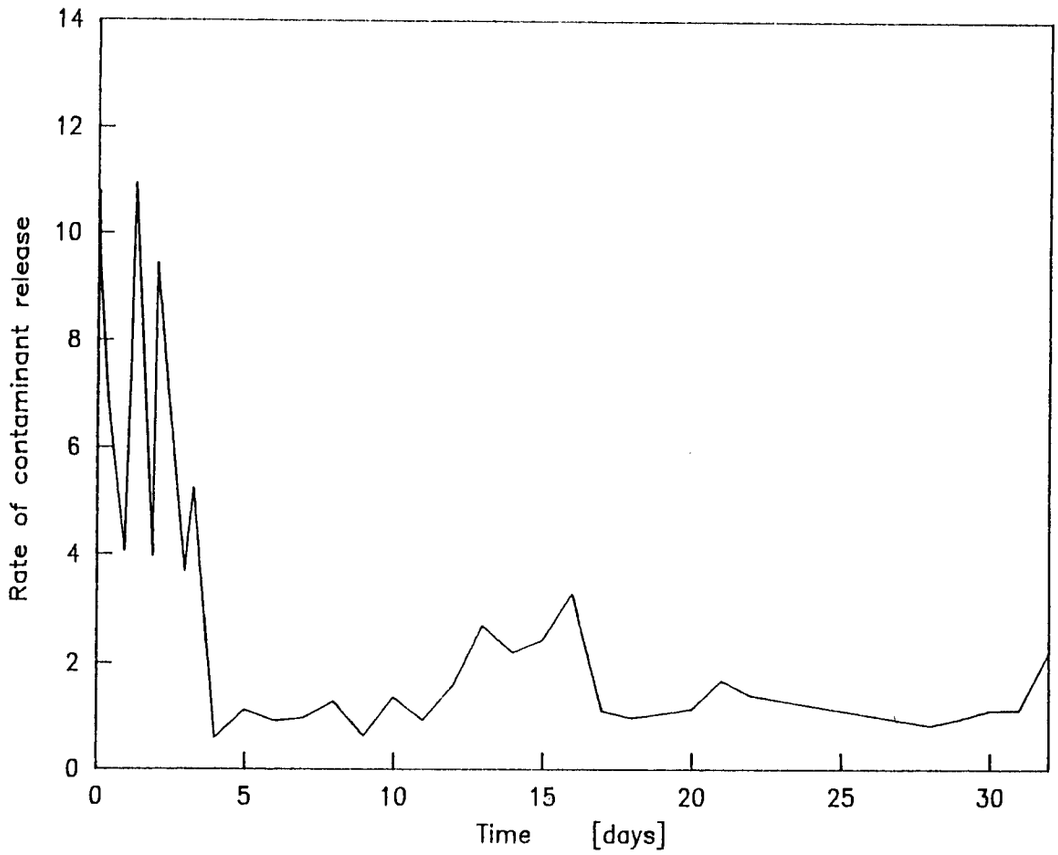

Figure 3.4 Rate of release of contaminants from XAD-8 subjected to ultrasound

or chips were seen but small chunks of beads that had been totally destroyed made the solution look like milk. It would therefore appear that once a bead had developed a crack from the ultrasound treatment, it rapidly disintegrated into small pieces.

3.2.5) The chosen cleaning method

The cleaning method that was found to work best was to pump about 10 bed volumes of 0.1 N sodium hydroxide solution through a fluidized bed of the resin. The bed was held in the low power ultrasound bath and the flow rate was about 5 bed volumes per day. The resin used had been previously Soxhlet extracted with ether and methanol and then soaked in ether followed by methanol. The bed was then washed by pumping distilled water through it while still subjecting it to ultrasound. After about 2 days of washing at 50 bed volumes per day, the conductivity of the effluent from the bed was the same as the influent. (Within the sensitivity of the conductivity meter). This indicated that all the

sodium hydroxide had been washed out, but the UV absorbence was still high. A periodic water wash was continued for at least 4 more days in which time about 100 more bed volumes of distilled water were used. The final 20 bed volumes of wash were fast to fluidize the bed and remove all the fine particles (the ultrasound was turned off). After all this, the UV absorbence at 200 nm was still about 0.02 (resolution of instrument = 0.001).

It must be stressed that this cleaning method took a long time and could have been speeded up if the resin had only been needed for work with concentrated solutions.

3.2.6) Accounting for contamination

For the purpose of calculating the isotherms, it was assumed that the resin released contamination into the solution at a rate directly proportional to the mass of resin present. ie. the release of dirt was assumed to be limited by the kinetics of the process only. There was assumed to be no equilibrium concentration limitation. Also if the compounds of interest in the original solution affected the release of contaminants, there was no way of accounting for it.

The experimental isotherm results were processed using Lotus 123 spread-sheets. The values from these spread-sheets and sample detailed calculations may be found in Appendix 3.

3.2.7) Method for measuring water retained by resin

As explained above, the cleaned resin should never be allowed to come into direct contact with air. If this happened some of the resin dried and when attempts were made to wet it again with water, air bubbles were trapped in the resin. These bubbles caused the resin to float and restricted the surface available for adsorption. Since the resin had to be weighed out wet, some way was needed to account for the water carried with the it.

Determining the pore volume (V_p) was difficult because the amount of water carried by the resin depended on how it had been drained or dewatered. Water was not only held in the pores of the resin but also

on the surface, particularly where two beads touched. Sucking water from the resin bed in a Buchner funnel removed most of the external water and some of the pore water. Centrifuging the resin also removed a lot, but not all, of the water from the pores. The amount of water held by the centrifuged resin depended on the speed and duration of the centrifuging but typically it was about 1.4 g water per g resin.

Using volume to measure XAD-8 was also inaccurate. Resin wetted by methanol had a volume 10% greater than resin wetted by water. Dried resin had a volume 25% less than water wetted resin. The volume also depended on how well the bed was packed because the height of a loosely packed bed could be decreased 5% by vibrating the container. The only universal basis on which to measure resin quantities was therefore dry mass.

The most accurate way found to account for the water carried with the resin was to take a sample of the wet resin just before it was to be used, and to dry it. The mass of the dried sample was compared with its wet mass to find the amount of water carried by the resin. The heat and time required to completely dry the resin was checked. Resin was dried at 60 °C for one day, followed by 125 °C for another day, followed by 225 °C for a third day. The resin mass on the last day was 2.204 g. Assuming this was completely dry resin, the resin from the 125 °C oven contained 0.010 g water per g resin and the resin from the 60 °C oven contained 0.019 g per g. The resin from the Buchner funnel carried 2.335 g per g, so it was concluded that the drying conditions introduced a negligible error. An oven where the resin was safe from spillage and contamination was available at 110 °C, so this oven was used for drying. Boening et al (1980) used the same method and found that 9 hours at this temperature was sufficient, but at least 24 hours was allowed.

3.3) Preparation of solutions

Stock solutions of each adsorbate tested were made up in one or two litre volumetric flasks. The concentrations chosen were 0.5 M for oxalic acid, 0.1 M for phenol, 0.087 M for malonic acid, 0.0025 g/l for stearic acid, 0.006 g/l for palmitic acid, 0.0437 g/l for isophthalic acid and 2.0 g/l for benzoic acid. In all cases, except malonic acid and phenol, these were the highest convenient concentrations that could be achieved without

there being a danger of solute precipitating. The benzoic, isophthalic, stearic and palmitic acids were obtained from Sigma, St Louis, U.S.A. The oxalic acid came from Merck, Darmstadt and the phenol came from Saarchem Pty. Ltd., Muldersdrift, R.S.A. All chemicals were assayed to at least 99% purity by the manufacturer.

The desired mass of solid solute was weighed out in a carefully cleaned beaker and washed into a carefully cleaned volumetric flask. The solutions of oxalic and malonic acid were tested by titrating them against sodium hydroxide solution. The results agreed within 0.1%.

To get the benzoic and isophthalic acids to dissolve, the flasks were gently corked before they had been completely filled with distilled water, and heated gently. The flasks were then allowed to cool before being filled to the mark with distilled water. With stearic and palmitic acids, the flasks had to be heated to 80 °C and maintained at this temperature with mixing for several hours. The process was repeated on two subsequent days to ensure that all the acid had dissolved.

Solutions of desired concentrations were made by diluting the stock solutions using carefully cleaned pipettes and volumetric flasks. If a dilution of more than 1000 : 1 was needed, it was done in 2 stages.

3.4) Measurement of adsorption isotherms

3.4.1) Standard method for isotherm measurement

Checks were made at all stages to see if the procedure was introducing contamination. The preparation of the solutions required about 2 litres of water, the quality of which had to be consistent. A 2 litre glass bottle was filled with glass distilled water, and only this water was used for preparing all solutions. This water was also used for rinsing all apparatus used for transferring the water, and for zeroing the UV meter. The quality of the water (judged by its UV absorbence at 200 nm) was also checked against previous samples of water; only very small variations were ever noted.

Resin cleaned as explained in section 3.2.5 was put into a sintered glass Buchner funnel and rinsed yet again by sucking distilled water through

the resin bed. When the UV absorbence of the rinse water reached a minimum (about 0.02 at 200 nm in 4 cm cell), the excess water was sucked off until the water level almost reached the top of the resin bed. Resin was then transferred by spatula to weighed Xactics bottles. The cleanliness of the Xactics bottles was checked first by adding about 0.05 l of water to them and thoroughly shaking them for several minutes. The water was then tested to see if the bottle was clean enough. The bottles were finally dried with an air jet and weighed.

When all the resin was transferred to the bottles, they were closed and shaken to mix the resin. A portion of the resin from each bottle was then transferred to a weighed beaker for drying and the subsequent calculation of retained water. This retained water diluted solutions added to the bottles later so its quantity had to be known for the necessary corrections to be made. The bottles with the wet resin were re-weighed to find the mass of resin within, and the dry mass was calculated using the result obtained from the sample that had been dried.

Typically, seven bottles were used in all. 0.2 l of the distilled water was put in the first (no resin). Another contained 0.2 l of the adsorbate solution (again, no resin). The third 'control bottle' contained resin and water. The other 4 contained a solution of the adsorbate and varying amounts of resin. Four bottles contained 0.02 l of solution (one of which contained no resin), and the bottle with the most resin contained only 0.1 l of solution. This left 0.1 l of solution for rinsing any apparatus used to transfer the solution.

The bottles were placed on the rotating wheel for 24 hours. The UV absorbence, conductivity and pH of the solution in each bottle was then measured. The pH and conductivity were measured by introducing a clean probe into the bottle. The UV absorbence was measured by withdrawing 0.003 l samples from the bottle with a syringe. The syringe was rinsed twice with the solution. The rinse solution from the syringe was used to rinse the cuvette. It was found that pouring the solution straight from the bottle into the cuvette caused loss of resin in some cases so the method was not often used.

It was determined that about 99% of the solution was removed when the cuvette was emptied. This was done by pouring solutions of known but

different concentration into the cuvettes and testing the absorbence. Therefore, 2 rinses with the solution of interest should have left very little contamination in the cuvette. A similar procedure done with the 0.005 l syringes showed that about 97% of the solution was removed when they were emptied. Extra care was needed when changing from solutions of high concentration to solutions of low concentration and several distilled water rinses were done first.

Samples from the bottle containing only adsorbate solution were used to calibrate the UV meter. This calibration was occasionally checked against the solution remaining in the volumetric flask in which the solution was originally prepared. No difference was ever found indicating that the Xactics bottles were not introducing an error.

The UV reading of the solution from the bottle with distilled water and resin was used to calculate the correction factor for the readings from the other 4 bottles containing adsorbate. Appendix 3 gives an example calculation of how the control result was used to correct the other results.

3.4.2) Modified method for bleaching effluents

To achieve the low effluent concentrations desired, a slightly different experimental technique was used for measuring isotherms of bleaching effluents. A method that would represent the behaviour of a counter-current contactor was also desired. It was believed that diluting the effluent with distilled water would change the nature of the isotherm. This was because the adsorbent adsorbed the components in the effluent selectively. Adsorption therefore reduced the concentration of the easily adsorbed components, while the more hydrophilic components (such as chloride and sulphates and highly soluble organic species) remained almost untouched. Diluting the effluent with water reduced the concentration of everything unselectively. Some other way therefore had to be found to achieve representative results at low equilibrium concentrations.

Resin was put into 6 bottles. One was filled with effluent, and the other 5 were filled with water. After 24 hours the water was removed from the second bottle and replaced with effluent from the first bottle.

Fresh effluent was put into the first bottle again. The process was continued until on the 6th day, the last bottle was filled with effluent contacted in the previous 5 bottles. The effluent in the 6th bottle had therefore been contacted with the resin in all 6 bottles so its concentration was very low. This experimental method mimicked several features of a counter-current contactor.

3.4.3) Time required to reach equilibrium

24 hours was generally allowed for the XAD-8 to come to equilibrium with the solution it was contacted with. To check that this time was sufficient, a control was performed where D1/D2 effluent was contacted with resin for 11 days. The pH rose very slowly during the experiment from 3.8 to 5.0. The concentration of the organics in solution rose slightly after the initial drop. The concentration of the organics dropped to a minimum of 0.6 of the original after 6 to 8 hours. It then started to rise slowly over the next 10 days to 0.7 of the original.

The rise in the pH was not understood, but the result of its rise was desorption of organics from the resin because of the dissociation of molecules adsorbed at the lower pH. It was probable that only a portion of this absorbence rise was due to rising pH and that the remainder was due to the release of contaminants from the resin. It therefore appeared that the contact period used for isotherm measurements on XAD-8 had to be an optimum between several factors. The kinetics of effluent adsorption was slower than that of any other solution tested, so 8 hours would be enough time to reach equilibrium in all cases. Prolonged contact also had to be avoided to prevent the release of contaminants or changing pH becoming an unnecessarily large factor. Experimental convenience therefore dictated that 20 to 24 hours of contact would be used.

3.5) Measurement of adsorption kinetics

The resin used to measure kinetics was sieved first so that the effect of particle size could be isolated. Unless otherwise stated, the fraction between 425 and 500 μm was used. (Resin used for isotherm measurements only was not sieved).

3.5.1) Measuring kinetics in sealed bottles

The rate of adsorption of the bleaching effluents on XAD-8 was measured by taking samples from Xactics bottles. The procedure was started in the same way as the isotherm determination; by putting a weighed amount of clean resin into Xactics bottles. It was found that it took about 10 seconds to pour the effluent into the bottles. The pouring was therefore started 5 seconds before the minute. The bottle was immediately sealed and agitated by hand for about 100 seconds. The bottle was opened again and a 2ml sample was withdrawn. The sample took about 5 seconds to withdraw, so the withdrawal was started 2 seconds before the minute. It was judged that 2 minutes was the shortest time period worth using considering that the error in the procedure was as much as 10 seconds. Subsequent samples were taken after increasingly long time periods. The pH and conductivity of the initial and final solutions was measured.

3.5.2) The perspex spinning basket contactor

While performing kinetic experiments on oxalic acid, using the bottle method, it was found that the system had gone about 90% of the way to equilibrium before the first sample was taken (after 2 minutes). The bottle method was therefore unsatisfactory for such work. To follow the fast adsorption kinetics, a spinning basket contactor was built based on the design given by Helfferich (1962). It had the following advantages over the use of bottles:

i) the reactor vessel was directly connected to a flow-through sample cuvette in the UV meter by a pump. This allowed a continuous sample of the solution to be tested with the minimum of delay, and by using the recorder on the UV instrument, the accuracy with respect to time was within 3 seconds;

ii) the resin was immersed and withdrawn from the solution with the minimum of delay. The problem of pouring the solution into the bottles did not occur, and the starting time for the adsorption run was accurately defined;

iii) the solution could be quickly changed, enabling a series of runs to be completed in a shorter time;

iv) it was possible to immerse the whole unit in a water bath to study the effect of temperature and to eliminate temperature drifts during the experiment. There was not enough time to use this feature.

The main problems with the apparatus were:

i) it was impossible to remove all the liquid from the vessel and the pump. This therefore introduced a small experimental error;

ii) it took a long time to replace or clean the adsorbent in the basket after a set of runs;

iii) the speed of the basket could not be accurately controlled. This together with possible uneven flow rates in different parts of the bed of resin within the basket meant that the determination of the film diffusion coefficient was not accurate.

The reactor consisted of a basket made of perspex and a 180 μm stainless steel gauze. The basket was opened and filled with dried resin. The resin was dried to allow accurate measurement of its mass, and because it was easier to load the basket with dry resin. The resin was washed with methanol and sodium hydroxide and rinsed with distilled water. No amount of rinsing could get the rinse water to come clean as measured by UV absorbence. Attempts to measure the kinetics of oxalic acid adsorption in the perspex reactor failed to give usable results. It was suspected that the methanol used for cleaning the resin was absorbed into the perspex and was slowly released into the oxalic acid solution. Also the methanol caused visible damage to the perspex.

It was decided that perspex was not a suitable material of construction and a search was made for a better material. The material of choice had to be machinable. This eliminated glass because it would have been impossible to blow a basket. The use of teflon was also considered but found to be too expensive. No other plastic had the required physical strength or chemical inertness. The range of available metal alloys was surveyed, and it was decided to build the next contactor out of 316 alloy steel.

To minimize the adsorption of various organics onto stainless steel chromatography columns, it is common practice to silylate them (Campbell, 1985). The silylating reagent reacts with the active groups on the surface, and puts a trimethylsilyl group on the surface instead. The technique was investigated but the silyl group could react with water, so the process could not be used in this application (Jennings, 1980). Other methods of minimizing adsorption investigated were to coat the metal surfaces with glass, or a plastic with a low surface energy such as PVC, polyethylene or PTFE (teflon). No-one could be found to do this cladding. It was decided that the steel would have to be treated by simply washing it with the solution to be tested and then with distilled water.

3.5.3) The 316 alloy steel spinning basket contactor

The second contactor was built out of 316 alloy steel; figure 3.5 shows the design. The UV absorbence of solutions in it sometimes rose slowly for some undetermined reason. Also, some solutes were found to adsorb noticeably on the metal surfaces. For instance 0.1 l of a 0.02 N solution of phenol was put into the cleaned and dried alloy contactor, and measurements of the concentration by UV at 240 nm indicated that nearly 10% of the phenol was adsorbed after 5 minutes. To eliminate this effect, the vessel and the pumping circuit through the UV cuvettes was rinsed with the solution of interest. The basket itself could not be rinsed since the resin in it would have adsorbed solute from the rinse solution.

The best experimental procedure found for this apparatus was as follows: resin was cleaned using the same method described in section 3.2.5. The resin was then put into the pre-weighed basket which was sealed again and weighed. A sample of resin was put into a beaker for drying and subsequent determination of water content. Distilled water was placed in the vessel and pumped through the UV cuvette until the reading was steady. The spinning basket was then put into the water and the UV absorbence at 200 nm was monitored. It was found that about 3 such rinses were required before the UV reading rose less than 0.01 in 5 minutes of contact. The vessel and pumping circuit was then rinsed with the solution of interest. After as much of the rinse solution as possible had been removed, 0.25 l of the solution was measured into the vessel.

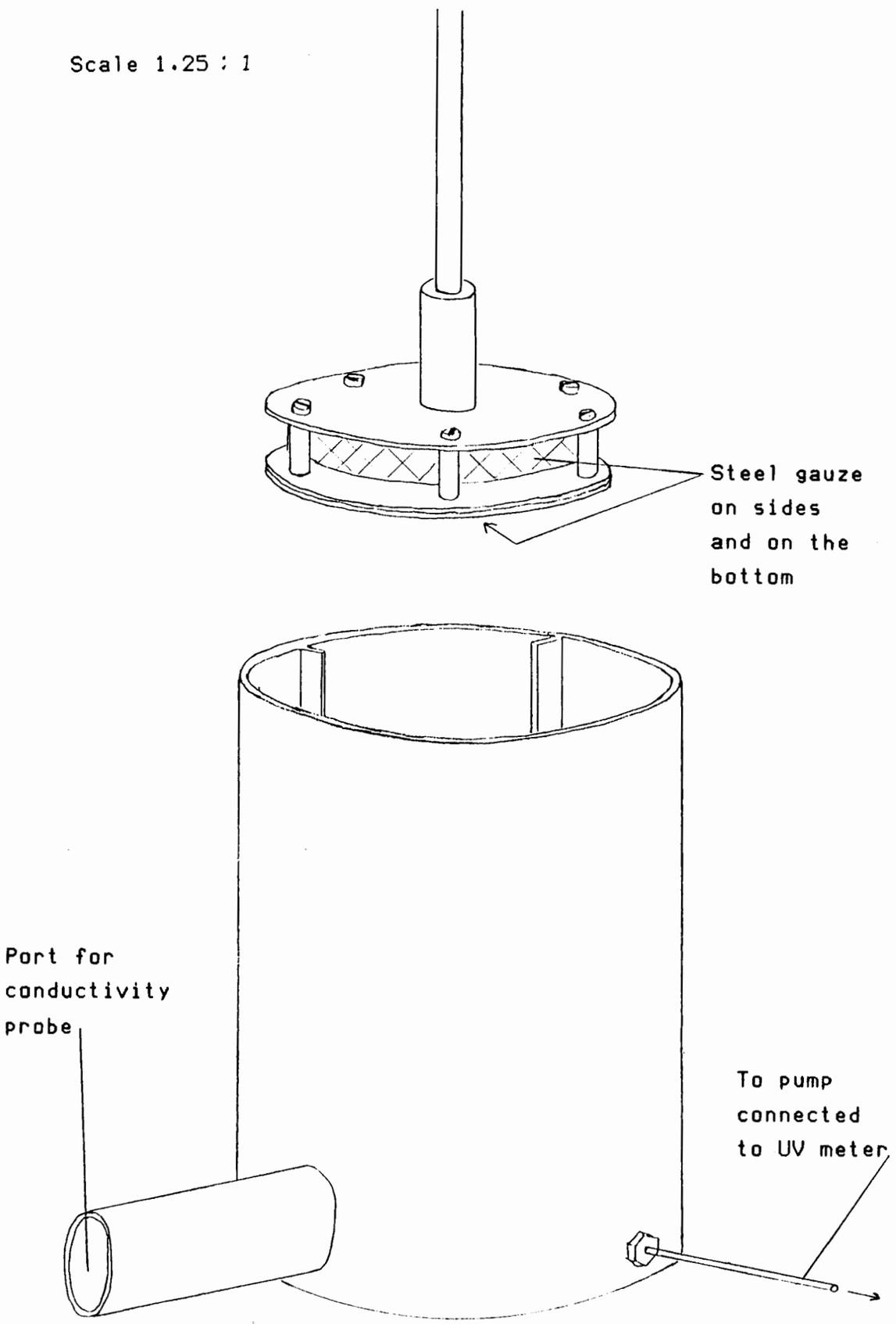

Figure 3.5 The alloy steel spinning basket contactor.

The basket was re-weighed to determine the amount of water retained by the resin, and the pump was started to obtain a steady reading on the UV meter. The recorder on the UV meter was also started. About 15 seconds later, the basket's motor was started and after another 15 seconds the basket was lowered into the solution.

The motor for the spinning basket had a variable speed reduction on it. This unit was not very robust, so runs were limited to about 30 minutes. The optimum speed for the spinning basket was investigated and found to be about 300 r.p.m. Higher speeds caused solution to splash out of the vessel and also the centre of the vortex would drop below the top of the basket. By injecting sodium hyroxide solution into the vessel and measuring the conductivity, it was determined that mixing was adequate. The vessel had a port for a conductivity probe and the conductivity rose to its final level within 2 seconds and was steady after about 3 seconds. The same test on the UV meter showed a response time nearly 2 seconds longer due to the delay in pumping the solution to the cuvette. This delay was not a factor when measuring kinetics because the start time was taken at the point (defined within 0.5 seconds) where the recorder trace started to drop.

The problem of the unexplained rise in UV absorbence was never fully solved and restricted the usefulness of the apparatus. Readings were taken using fairly concentrated solutions because the errors introduced were less significant on concentrated solutions. Some samples from runs in the contactor were sent for analysis by HPLC.

Chapter 4

Isotherms of bleaching effluents and model organics on XAD-8.

To find the most suitable equation for modeling the experimental results, the different isotherm equations are compared. The results of the experiments with pure compounds are reported next and then the results for the bleaching effluents are presented. Where possible, isotherm results are compared with literature values. Finally the results of testing an activated carbon as an adsorbent are reported.

Van Vliet et al (1980) stated specifically that they used dry adsorbent mass as a basis for measuring isotherms. As was explained in Chapter 3, this was the most accurate basis to use and it was used throughout this report. The units chosen for the solid phase concentration were grams (not mg) of adsorbate per gram of resin (dry mass). This was to eliminate the need for conversion factors in the mass balances. The units used for solution concentration were grams solute per litre of solution unless otherwise stated. The advantage of these units was that the conversion factor for converting to SI units was unity. SI units were not used for reporting experimental results because most measurements were made using the smaller units of grams and litres rather than kilograms and metres cubed.

4.1) Comparison of isotherm equations

A few comparisons were performed to help evaluate the different isotherm eqautions discussed in section 2.3.1. The Weber-Van Vliet equation was used as the standard, and some of the others were compared against it. The phenol isotherm was chosen because Van Vliet et al (1980) measured its isotherm accurately over a wide concentration range, and their results agreed well with those of this author measured over an even wider range. Another reason was that it was the least acidic (and ionic) of the compounds studied in this report which meant it was the least affected by pH.

Table 4.1 shows the data. The first column is a range of suitable adsorbed concentration values. The second column is the liquid phase

concentration calculated from the first column using the Weber-Van Vliet isotherm. The remaining columns are concentration values calculated from the first or second column as appropriate, using the indicated isotherm equation.

Table 4.1

Comparison of isotherm equations against the Weber-Van Vliet isotherm for phenol on XAD-8

Adsorbed q [mg/g]	Weber-VV Conc [g/l]	Henry q	Freundlic q	Toth q	Red-Pet q	Jossen Conc	Dubinin q
0.011	0.0324	0.0130	0.0226	0.0142	0.0142	0.0222	0.0081
0.02	0.0536	0.0215	0.0340	0.0235	0.0236	0.0406	0.0159
0.05	0.1183	0.0473	0.0643	0.0518	0.0519	0.1032	0.0436
0.1	0.2195	0.0878	0.1058	0.0959	0.0961	0.2106	0.0921
0.2	0.4162	0.1665	0.1773	0.1813	0.1817	0.4329	0.1923
0.5	1.0137	0.4055	0.3636	0.4382	0.4384	1.1432	0.5029
1	2.075	0.8300	0.6479	0.8857	0.8844	2.4318	1.0339
2	4.4544	1.7818	1.1999	1.8518	1.8440	5.3063	2.1163
5	13.421	5.3683	2.9207	5.1169	5.0688	15.767	5.4142
10	33.793	13.517	6.1514	10.966	10.849	38.304	10.906
20	93.727	37.491	14.006	21.549	21.635	100.85	21.577
50	434.98	173.99	48.307	38.969	42.711	434.81	50.275
100	1656.8	662.73	142.06	47.487	59.525	1606.5	88.019
200	7623.3	3049.3	486.58	50.943	76.429	7649.1	136.37
Average % error		190.11	47.87	20.26	17.74	12.9	11.55

The equations used with their coefficients were:

Weber-Van Vliet $C = 2.075\ q^{(0.2313\ q^{0.2131}\ +\ 0.834)}$

Henry $q = 0.4\ C$

Freundlich $q = 0.36\ C^{0.81}$

Toth $q = 52.19\ C\ (78.89 + C^{0.9319})^{(-1/0.9319)}$

Redlich-Peterson $q = \dfrac{0.4399\ C}{(1 + 0.016896\ C^{0.87695})}$

Jossen $C = 1.9696\ q\ \exp(0.2108\ q^{0.49905})$

Dubinin $q = 1071*0.1642*\exp\dfrac{0.0083144*296*\ln(79.9/C))^2}{-128.81}$

The average percentage error was calculated using the equation:

$$\text{average \% error} = \sum_n \left(\frac{|q_{calculated} - q_{expected}|}{q_{expected}}\right) \frac{100\%}{n}$$

Where n = Number of data points

$q_{calculated}$ = q calculated using isotherm under test

$q_{expected}$ = q calculated using Weber-Van Vliet isotherm

q was replaced by C for the Jossen equation

The results are presented graphically in figures 4.1 to 4.3. The figures show the areas of weakness for each isotherm equation. It can be seen that the Dubinin equation is the most accurate equation compared to the Weber - Van Vliet equation. It is fairly simple and it can be written with q or C as the dependent variable. This feature is very useful when modeling the kinetics using the diffusion model as will be seen in Chapter 5. It is not easy to re-arrange variables on the Weber - Van Vliet and Jossen isotherms which are the first and third most accurate isotherms considered here.

The re-arranged form of the full Dubinin isotherm is:

$$C = \exp\left[\ln C_{sat} - \frac{1}{RT}\left(-B \ln\left(\frac{q}{\rho \emptyset_o}\right)\right)^{\frac{1}{k}}\right]. \qquad (2.13b)$$

Another important reason for choosing the Dubinin isotherm is that it predicts the change of adsorption capacity with temperature.

The final reason for choosing the Dubinin isotherm is that being a direct interpretation of the Polanyi theory, it is easy to adapt it to the multicomponent models derived using the Polanyi thoery.

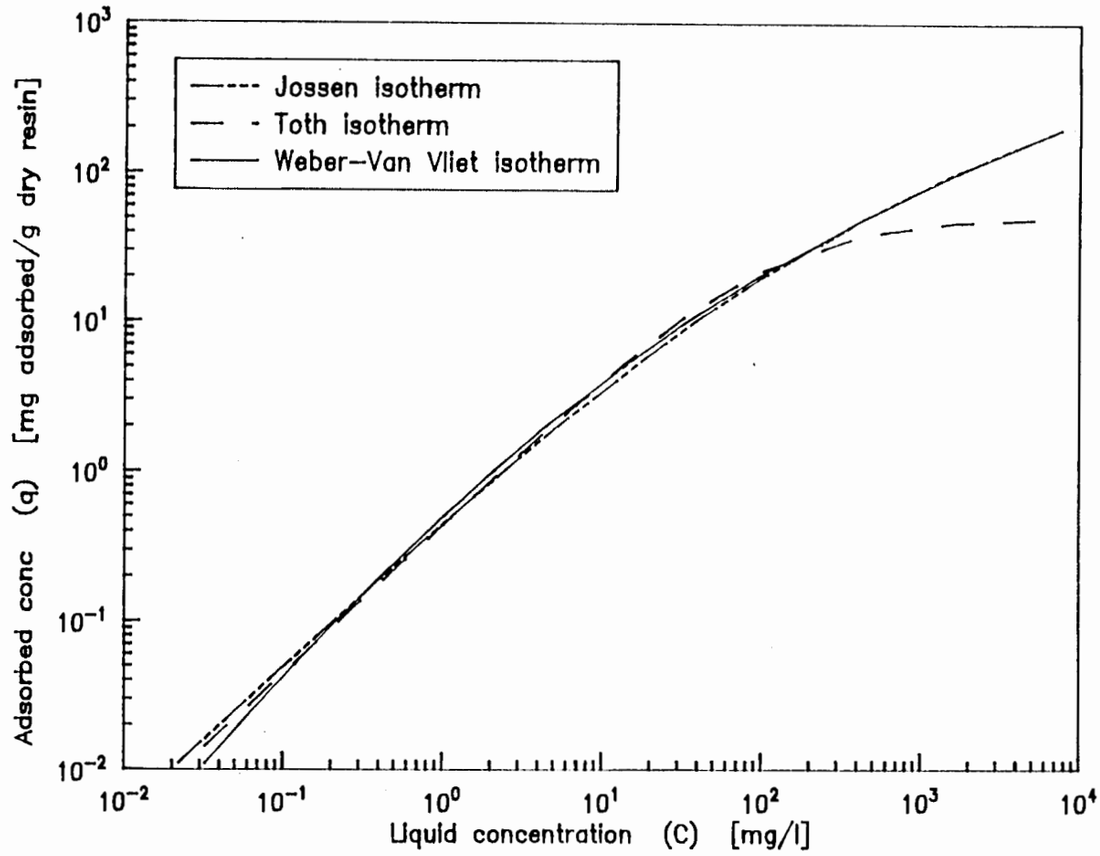

Figure 4.1 Comparison of isotherm equations due to Weber–Van Vliet, Toth and Jossen

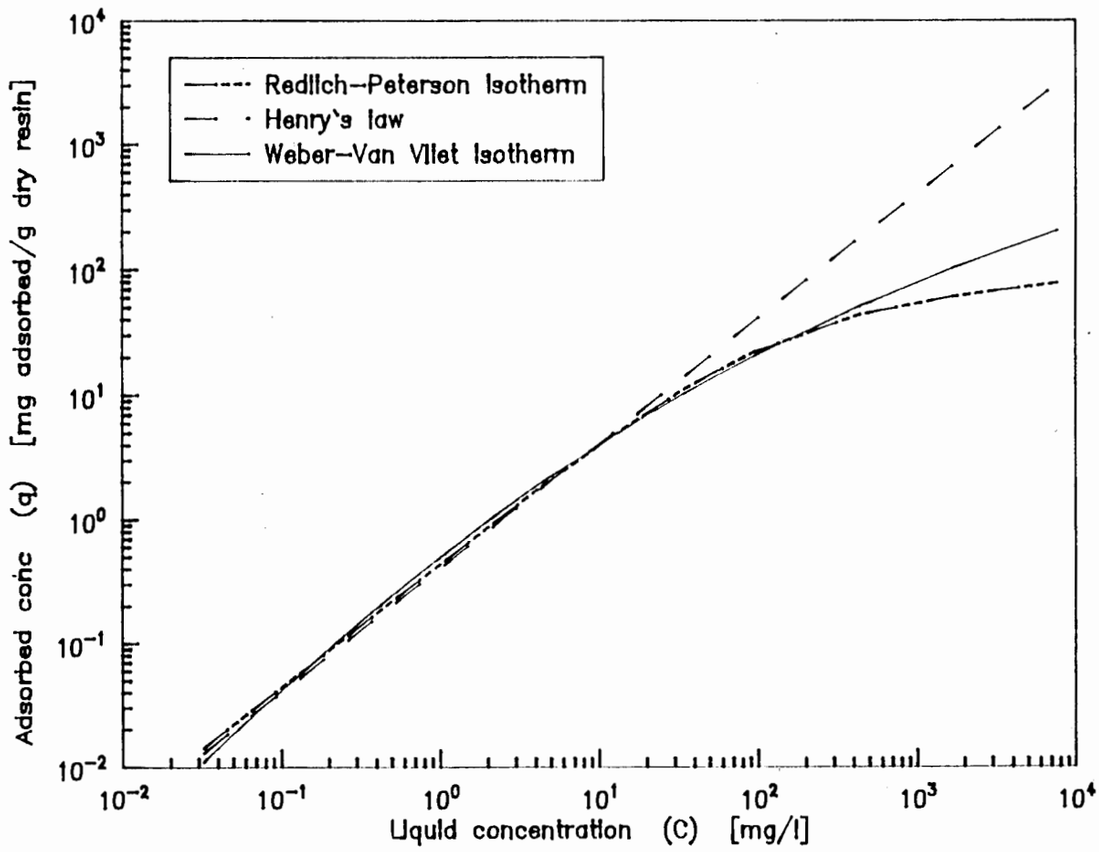

Figure 4.2 Comparison of isotherm equations due to Weber–Van Vliet, Henry and Redlich–Peterson

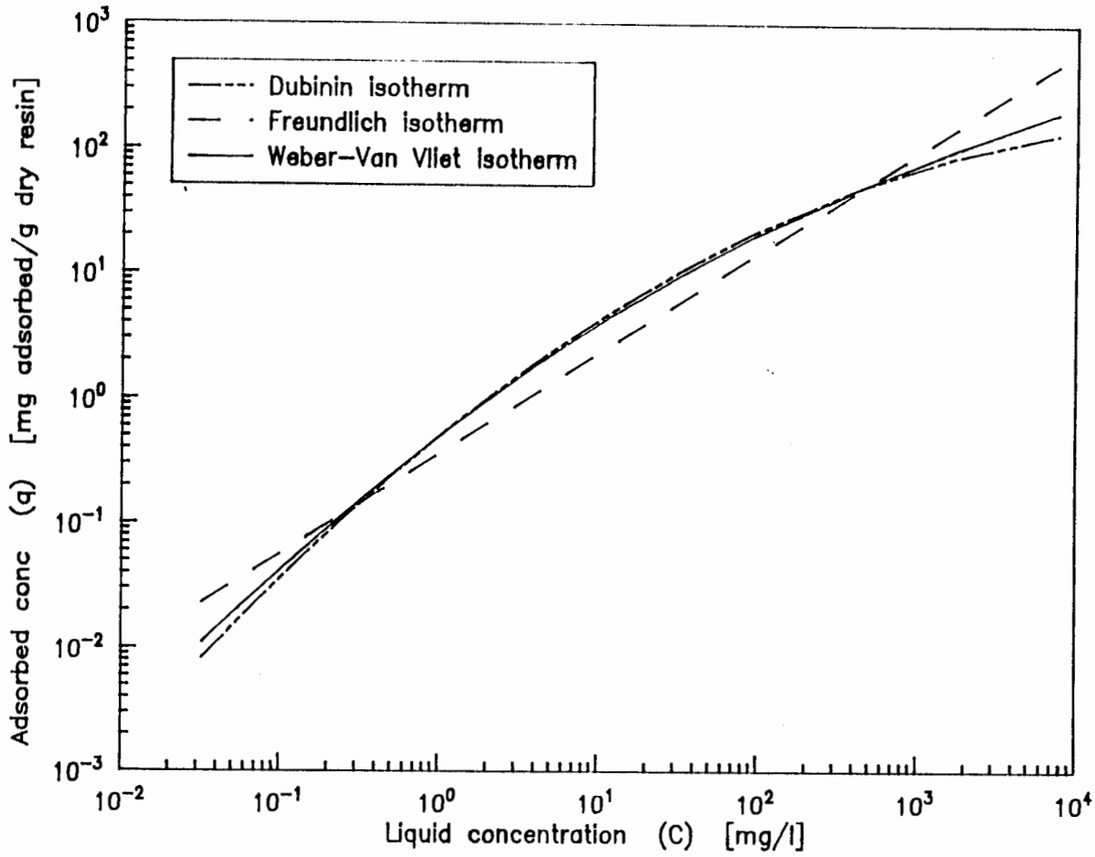

Figure 4.3 Comparison of isotherm equations due to Weber–Van Vliet, Freundlich and Dubinin

4.2) Isotherms results on XAD-8

The preferred units for liquid phase concentration were grams per litre and for solid phase concentration they were grams of adsorbate per gram of dry adsorbent. A problem arose when presenting the isotherm results for the bleaching effluents because the quality of the effluent was not constant. The multicomponent nature of the bleaching effluent meant that an isotherm measured on an effluent with a high concentration would not be the same as one measured on an effluent with a low concentration. It was assumed that the proportions of the different organic components would be less variable. Therefore presenting concentrations as a fraction of the original concentration was expected to be a more reproducible system.

The liquid phase concentration of the bleaching effluents was expressed as the dimensionless group C/C_o or $\bar{C}$. To convert from $\bar{C}$ to C, it was simply necessary to multiply by the original concentration (C_o). The result was then in the units used to express C_o. The dimensionless group

for expressing the solid phase concentration was q/q_e or $\bar{q}$, where q_e was the solid phase concentration in equilibrium with C_o. However, q_e could not be determined until the isotherm relation was known. It was also not so simple to convert between $\bar{q}$ and q, so another set of units was used that only required the multiplication by C_o to convert to the units of grams adsorbed per gram dry adsorbent. The units were [l C/C_o g resin]. These units represent the fraction of the organics originally carried in a litre of effluent adsorbed per gram of dry adsorbent.

The isotherm results are summarised in table 4.2. Columns 2 to 4 show the Dubinin isotherm coefficients that best fitted the isotherm data. Columns 5 to 7 show the physical property data and the last two columns show the coefficients for the freundlich isotherm.

Table 4.2

Isotherm results

Adsorbate	Affinity coeff. [KJ/ mole]^k	Adsorp volume $\times 10^6$ [g/l]	Isotherm coeff.	Temp [°C]	Solubility [g/l]	Density [g/l]	Freundlich	
							coeff	exp
Oxalic acid	78.08	4.365	-	18	75.1	1650	-	-
	0.3710	556.6	0.451	18	75.1	1650		
Malonic acid	81.62	49.88	-	20	768	1630	-	-
	144.2	11.49	-	20	768	1630		
Phenol	142.36	139.1	-	20	76.2	1073	-	-
Isophthalic acid	23.98	8.183	-	20	0.13	1590	-	-
Benzoic acid	38.59	98.12	-	20	3.1	1266	-	-
D1/D2 effluent	-	-	-	-	-	-	0.45	5.5
Cation X effluent	10.29	21.42	-	18	C_o	1000	1.055	3.04

4.2.1) Oxalic acid isotherm

Figure 4.4 shows the experimental results and the curves for the Dubinin isotherms that fitted the data. The 2-parameter Dubinin equation was fitted to the data measured using UV. This equation did not fit well and so the 3-parameter equation was tried as well. Both curves are shown in figure 4.4. The pH of the solutions varied from 5 for the low concentration solutions to 1.5 for the concentrated solutions which may explain the scatter in the results.

To apply the Dubinin equation, values were needed for the density and aqueous solubility of solid oxalic acid. The solubility versus temperature data was fitted to an equation similar to the equation used by Washburn. The equation fitted to the solubility data between 10 and 40 °C (Seidal, 1940) was:

$$C_{sat} = \frac{556.7}{\exp(2770.4/T - 7.387) - 1}.$$

The isotherm was measured at 18 °C, so the solubility was 75.1 g/l.

Perry (1973) gives the density of oxalic acid as 1653 kg/m^3 at 19 °C and Washburn et al (1928) gives it as 1.6145 at 17 °C. It was taken as 1650 at all temperatures. The solubility and density data for oxalic acid and other compounds is given in Appendix 6.

The isotherm constants for the 2-parameter equation were:

$B = 78.08$ [(KJ/mole)^2],
$\emptyset_0 = 4.365E\text{-}6$ [g/l],

and for the 3-parameter equation:

$B = 0.3710$ [(KJ/mole)$^{0.451}$],
$\emptyset_0 = 5.566E\text{-}4$,
$k = 0.451$.

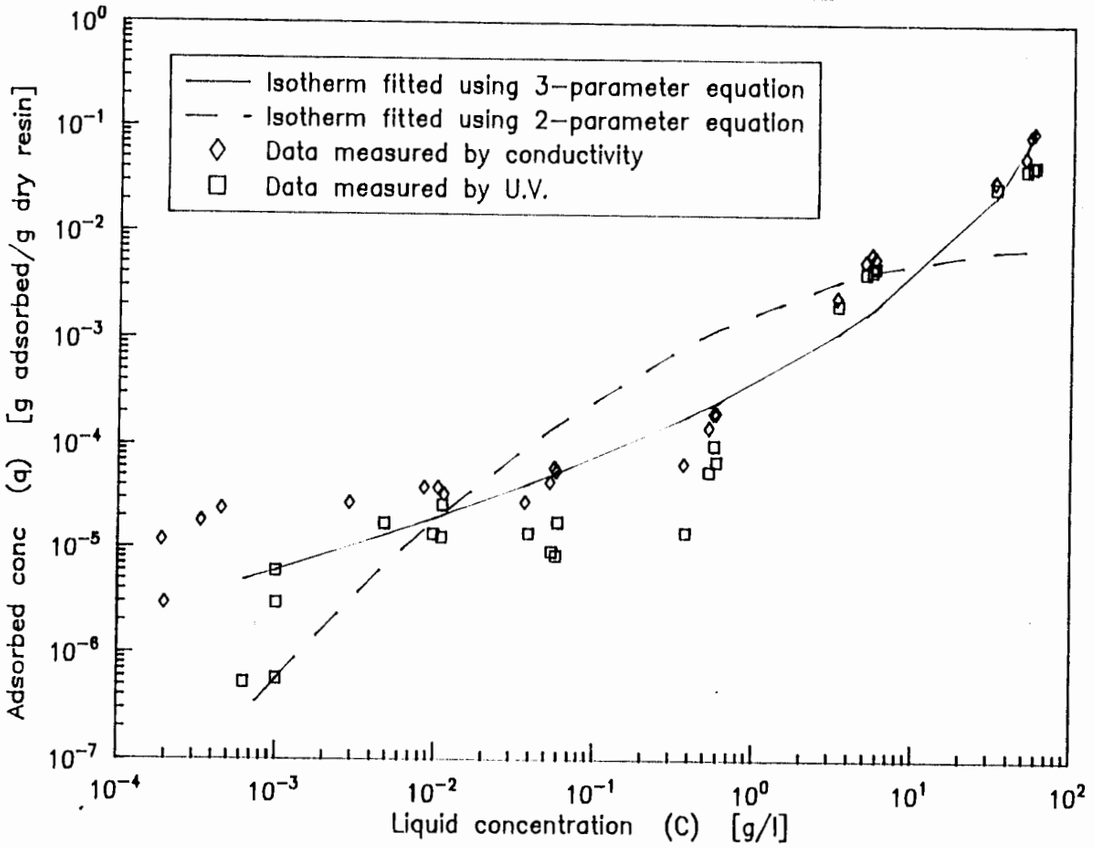

Figure 4.4 Adsorption of oxalic acid. The two isotherm curves use versions of the Dubinin equation

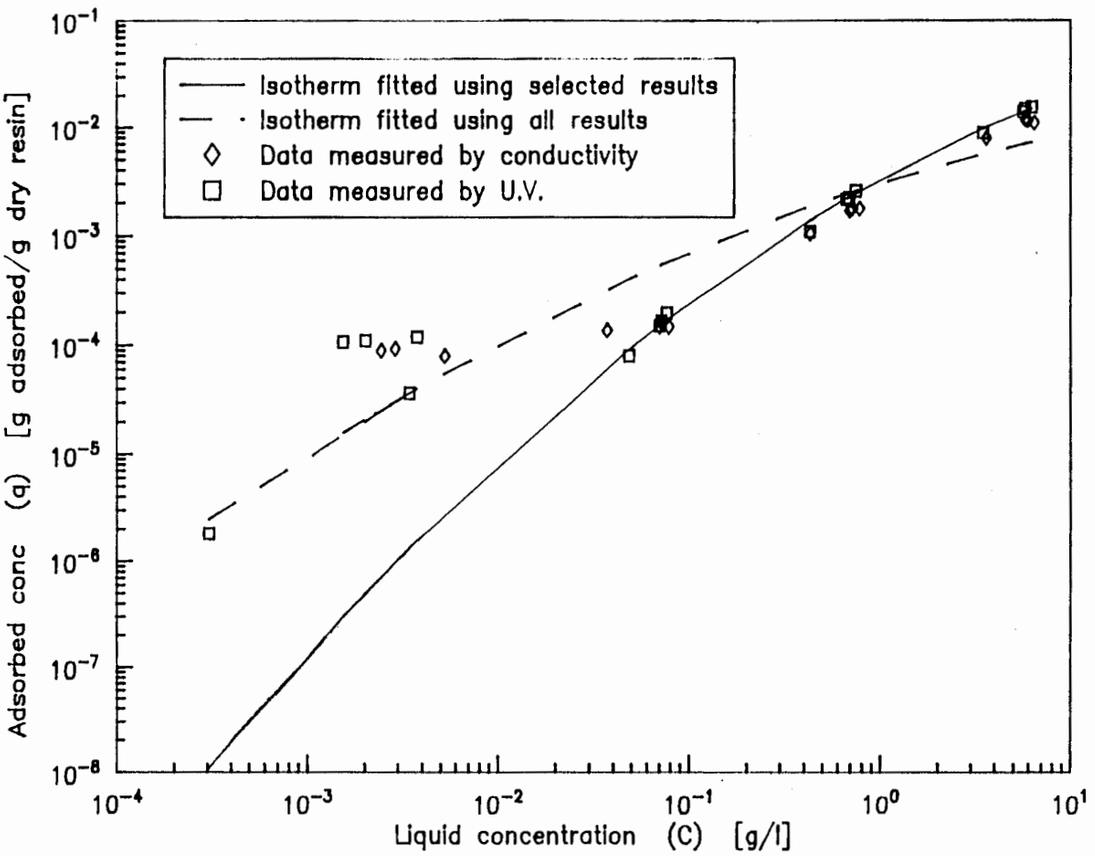

Figure 4.5 Adsorption data for malonic acid on XAD-8. The two isotherm curves use the Dubinin equation

The 3-parameter oxalic acid isotherm at 18 °C (291K) was therefore expressed as:

$$q = 1650 * 5.566E-4 * \exp\frac{(0.0083144 * 291 * \ln(75.1/C))^{0.451}}{-0.371}.$$

All detailed experimental results are in Appendix 3.

4.2.2) Sodium oxalic

The ease of regenerating XAD-8 loaded with oxalic acid using sodium hydroxide was of interest. An attempt was made to measure the isotherm of oxalic acid in the form of sodium oxalate at a pH of over 10. The sodium hydroxide used to adjust the pH absorbed light at the same wavelength as the oxalate. This was due to the hydroxide ions (Beaven 1961), so the pH had to be re-adjusted to about 2 with hydrochloric acid before meaningful results could be obtained. An extra experimental error was introduced by the pH adjustments and the results showed eight negative results among the total of 16. This suggested that the capacity of XAD-8 for sodium oxalate was so low that extremely accurate results would be needed to obtain any quantitative conclusions.

4.2.3) Malonic acid

Figure 4.5 shows the results. It was found that the results measured at liquid concentrations above 0.01 g/l showed little scatter and fitted the 2-parameter Dubinin isotherm very well. The pH of the solutions dropped from 6 to 2 as the concentration rose.

The isotherm was measured at 20 °C and the coefficients obtained by fitting the results where C > 0.01 were:

C_{sat} = 768,
ρ = 1630, (Perry, 1973)
B = 81.62,
$\emptyset_o$ = 4.988E-5.

Below 0.01 g/l the results showed scatter due to the contaminants from the resin. Fitting the Dubinin isotherm to all the positive results gave the result:

$$B = 144.2,$$
$$\emptyset_o = 1.149E\text{-}5.$$

Both curves are plotted on figure 4.5.

The correlation for the solubility of malonic acid between 10 and 50 °C (Washburn et al, 1928) was found to be:

$$C_{sat} = \frac{2553}{\exp(482.8/T - 0.1829) - 1}.$$

4.2.4) Phenol

Phenol was studied so that the method of isotherm determination could be checked by comparing results with literature results: the agreement was good. Figure 4.6 shows the results. Solubility between 10 and 50 °C fitted the equation:

$$C_{sat} = \frac{1.9419}{\exp(14.86/T - 0.02555) - 1}.$$

Washburn et al (1928) reported its density to be:

$$\rho = 1092 - 0.8188\ T - 0.0067\ T^2.$$

The coefficients for the isotherm measured at 20 °C using the Dubinin isotherm were:

$$C_{sat} = 76.2,$$
$$\rho = 1073,$$
$$B = 142.36,$$
$$\emptyset_o = 1.3909E\text{-}4.$$

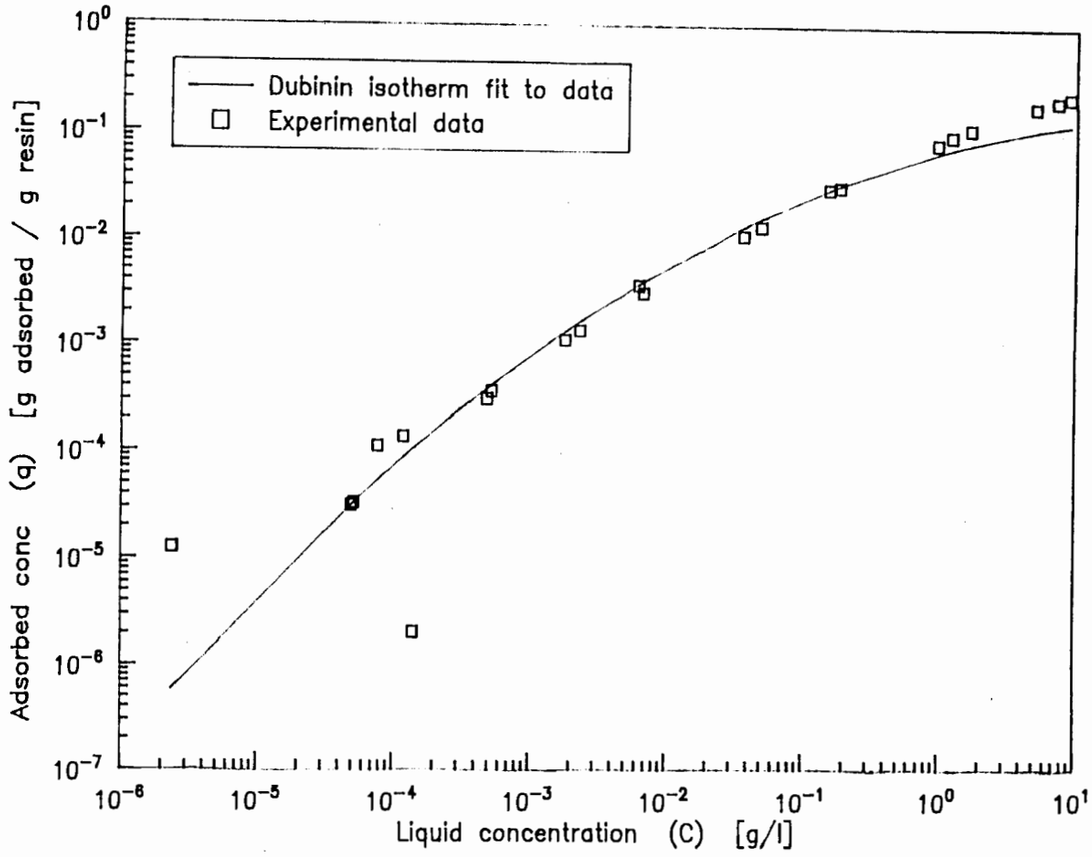

Figure 4.6 Adsorption data for phenol on XAD–8 fitted to Dubinin isotherm.

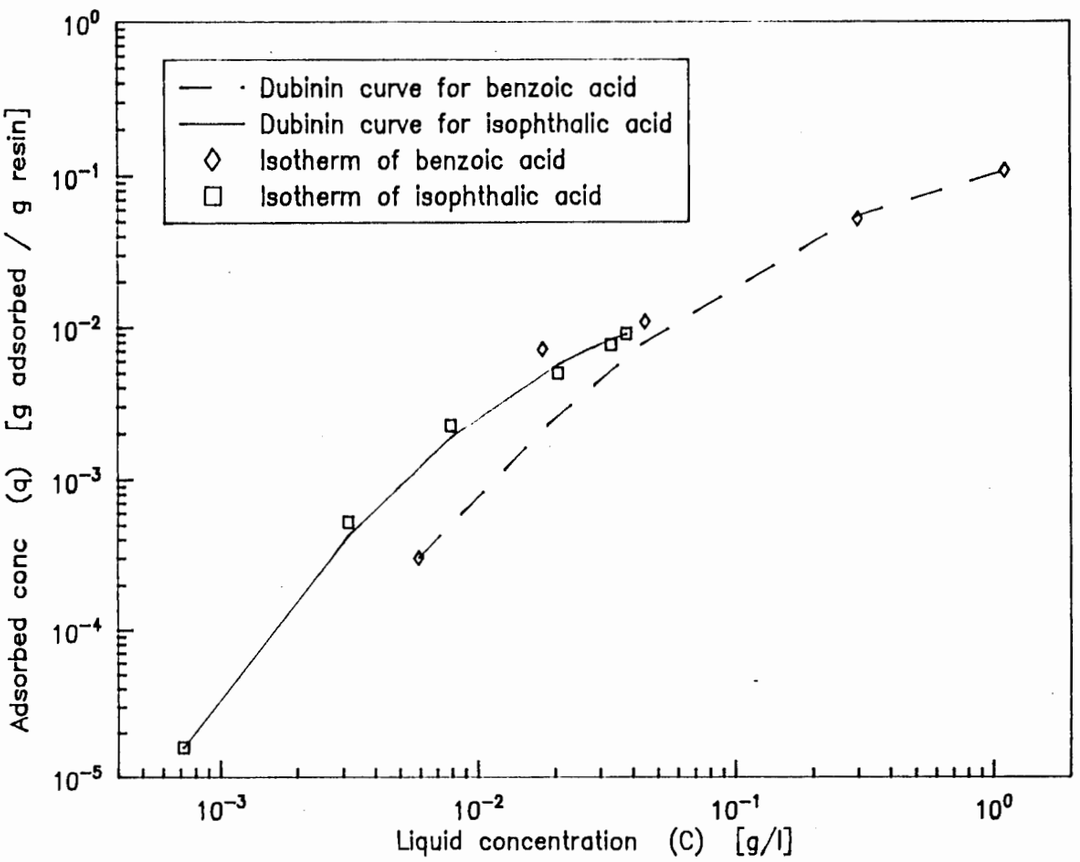

Figure 4.7 Adsorption data for benzoic and isophthalic acids on XAD–8 fitted to Dubinin isotherm.

The pH of all solutions was between 5 and 6. The scatter in the results for phenol started at a concentration more than 20 times lower than that for malonic acid. This was because the UV extinction coefficient of phenol at 215nm was 13 times as high as malonic acid's at 200nm. Also the contaminants had a lower extinction coefficient at 215 nm than 200 nm.

4.2.5) Stearic acid

Stearic acid has a solubility of about 0.0029 g/l at 20 °C (Raltson, 1942). The UV absorbence at this concentration was not high enough to be distinguished from that of the contaminants leached out of the resin. No isotherm could therefore be obtained for stearic acid using UV absorbence for analysis. The results of the experiment can be found in Appendix 3.

4.2.6) Palmitic acid

The comments about stearic acid apply to palmitic acid as well because its solubility is also very low at 0.0072 g/l (Raltson, 1942).

4.2.7) Isophthalic acid

The isotherm curve obtained for isophthalic acid is shown in figure 4.7. The coefficients used for the Dubinin isotherm were:

$T = 20,$
$C_{sat} = 0.13,$ (Stephen and Stephen, 1963)
$\rho = 1590,$
$B = 23.98,$
$\emptyset_0 = 8.183E-6.$

4.2.8) Benzoic acid

The benzoic acid isotherm is also shown in figure 4.7. The Dubinin equation was found to fit the data well using the coefficients:

T = 20,
C_{sat} = 3.1, (Seidal, 1940)
ρ = 1266,
B = 38.59,
$\emptyset_o$ = 9.812E-5.

The pH of all isophthalic and benzoic acid solutions was between 3.0 and 4.0.

4.2.9) Pure D1/D2 effluent

Isotherms for untreated fresh D1/D2 effluent were measured on XAD-8. The Freundlich isotherm was fitted to the data and the result was:

$$q = 0.45\ C^{3.5}.$$

Figure 4.8 shows the data. The results show scatter because they were obtained before the importance of cleaning the XAD-8 had been fully realised.

4.2.10) Cation exchanged D1/D2 effluent

To model the counter-current contactor envisaged for the organics removal, accurate isotherm data was needed for the cation exchanged effluent. A fresh sample of effluent was obtained and the whole isotherm was measured before the sample was two weeks old. The results are shown in figure 4.9.

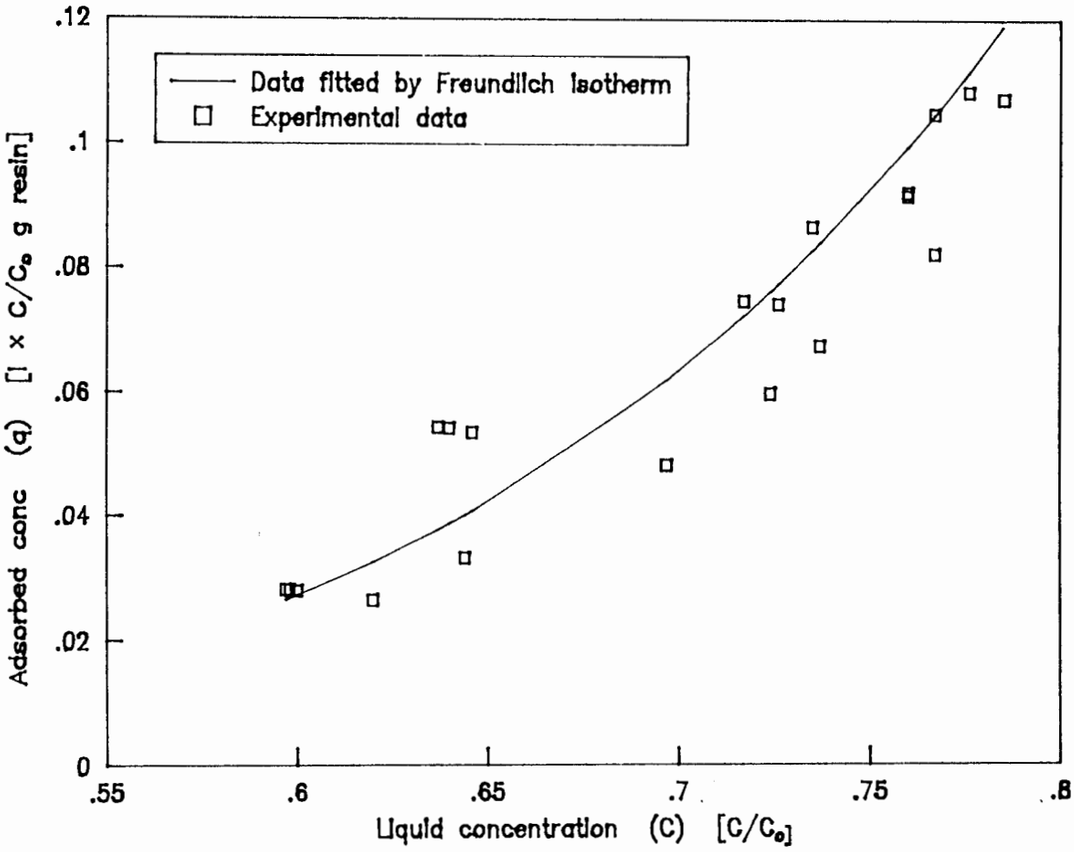

Figure 4.8 Adsorption data for untreated D1/D2 effluent on XAD-8.

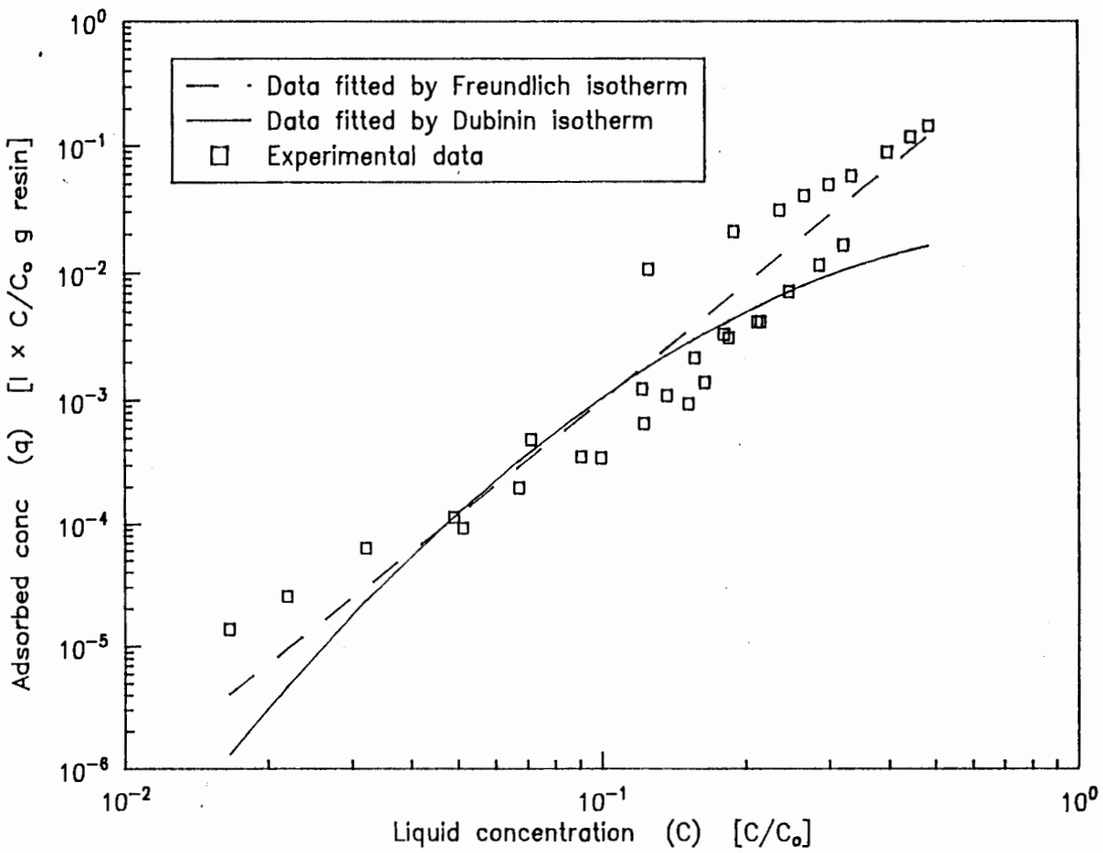

Figure 4.9 Adsorption data for cation exchanged D1/D2 effluent on XAD-8.

The results were scattered because of the variation in experimental technique required to cover the wide concentration range. The results from the first bottle, where effluent fresh from the cation exchange column was placed, are all on a smooth curve at the top right hand corner of the graph just above the Freundlich isotherm curve. The rest of the data, from bottles that received effluent from previous bottles, was more scattered. This shows that some components of the effluent are adsorbed much more easily than others. A multicomponent model is obviously needed for adequate explanation of effluent adsorption.

The 2-parameter Dubinin isotherm was fitted to the data, but did not give a good fit. Since the solubility of the effluent (C_{sat}) was not known, it was assumed that the effluent was saturated. The density of the solids in the effluent was not known either, so 1000 kg/m^3 was assumed. With these assumptions the Dubinin coefficients were:

$$T = 18,$$
$$B = 10.29,$$
$$\emptyset_o = 2.142E-5.$$

The Freundlich equation was found to give a better fit:

$$q = 1.055\ C^{3.04}.$$

Both fitted isotherms are shown in figure 4.9.

4.3) Comparison of isotherms with literature values

The only literature isotherms found for pure compounds on XAD-8 were measured by Van Vliet et al (1980 and 1981). Figure 4.10 shows a comparison of their isotherm (measured at 23 °C) and that measured by this author at 20 °C. Van Vliet at al buffered their solutions with 0.005 N sodium bicarbonate to a pH of about 8.4. Buffering was not used here because all the buffers tested were found to absorb at the UV wavelengths of interest. Also the pH of interest was between 1 and 2 and no buffers were known for this range. Finally it was suspected that the buffer would adsorb on the resin and affect the results.

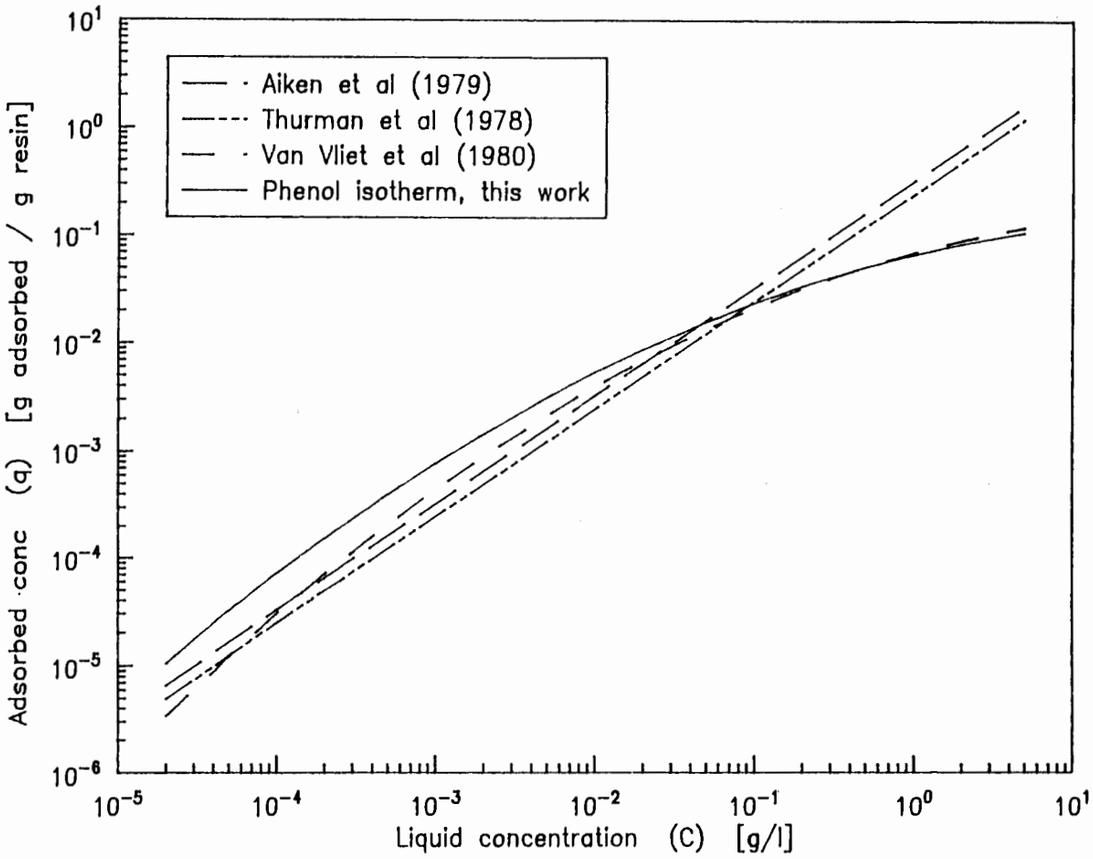

Figure 4.10 Comparison of adsorption of phenol on XAD-8 with results due to Van Vliet, Thurman and Aiken

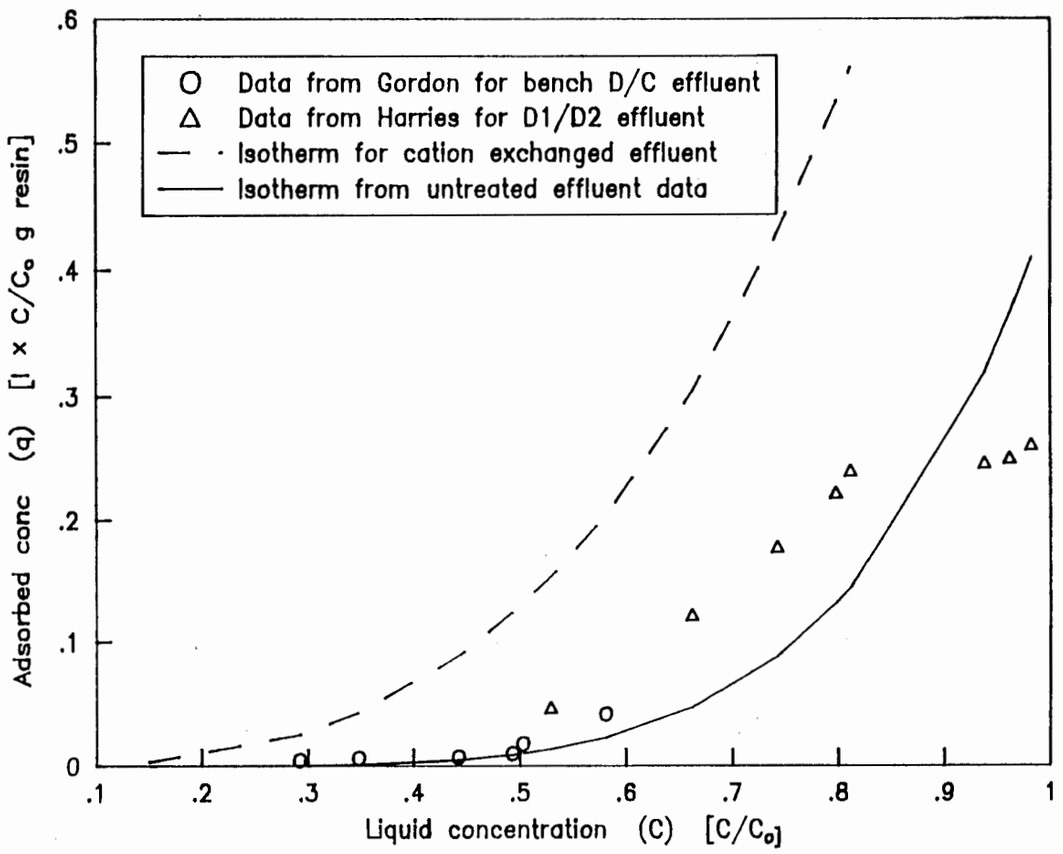

Figure 4.11 Comparison of isotherm results from Gordon (1982) and Harries (1982) with results obtained here

Boening et al (1980) measured the isotherm of humic acid on charged (ion exchange) and uncharged (including XAD-8) resins. He used pH values of 5.5, 7.0 and 8.0 which were; "typical of those found in water treatment plants". The problem was that the humic acid was probably dissociated at these pH values and all uncharged adsorbents tested had a very low capacity for it. However, Aiken et al (1979) tested the adsorbence of fulvic acid (a subclass of humic acid which is a complex mixture of natural acids) and found that XAD-8 had a 50 times greater capacity for it at a pH of 1.5 compared to a pH of 7.0. It would therefore appear that contrary to Boening et al's conclusions, XAD-8 would be a suitable adsorbent for humic substances if an economic method of achieving a sufficiently low pH values was available. Its low capacity at a high pH means it would be easily regenerated by the addition of a base. Aiken et al found that 98% of the adsorbed fulvic acid was removed by 0.1 N sodium hydroxide, compared to 70% for XAD resins made from styrene divinylbenzene.

Gordon (1982) measured the isotherm of bench produced D/C effluent and Harries (1982) measured the adsorption of D1/D2 effluent. Their results were compared in figure 4.11. Gordon used COD to measure the effluent concentrations. His results were made dimensionless by dividing them by the COD of the original effluent. The results due to Harries were measured using the dissolved organic carbon (DOC) method and were also converted to dimensionless units. The results from both authors were similar to those measured by this author on untreated effluent. The figure shows clearly how the lower pH of the cation exchanged effluent (2 as opposed to 4) produced a much more favorable adsorption isotherm.

Thurman et al (1978) and Aiken et al (1979) measured 'capacity factors' or Henry's law constants for various compounds on XAD-8, but not full isotherms. Aiken et al measured the adsorption of phenol and benzoic acid on several resins including XAD-8, but they did not state the concentration of the equilibrium solution. Their distribution coefficient for phenol was 325. Assuming they used dry resin mass as a basis, this converts to a Henry's law constant (as defined in equation 2.2) of 0.325. ie. $q = 0.325\ C$.

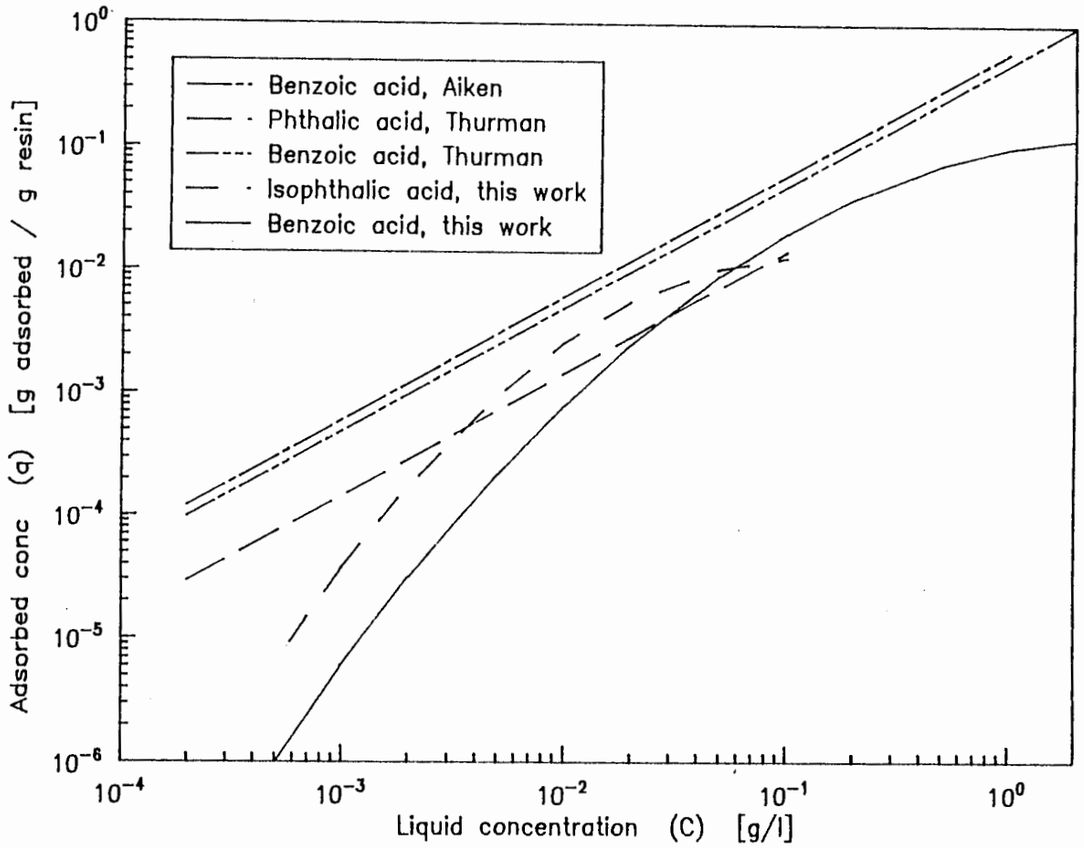

Figure 4.12 Comparison of adsorption of benzoic and isophthalic acids on XAD-8 with literature values.

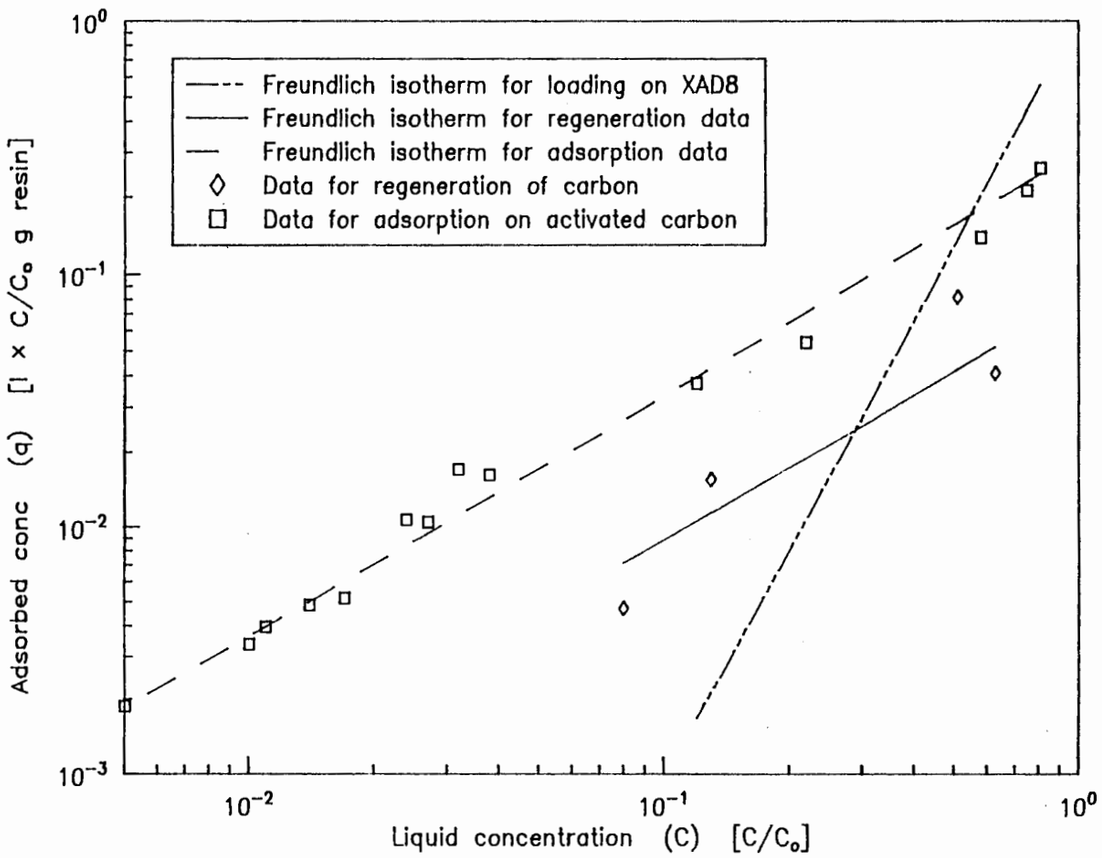

Figure 4.13 Adsorption and regeneration data for cation exchanged D/C effluent on activated carbon. Isotherm on XAD-8 is compared.

Chapter 5

Kinetics of adsorption

This chapter deals first with the method of calculation of the kinetic parameters from the kinetic experiments. Only the diffusion model is discussed in this chapter; the empirical model is discussed in Appendix 4. The second section of the chapter presents the results of fitting the equations to the experimental data.

5.1) Diffusion kinetics model

5.1.1) Reasons for pursuing a numerical rather than an analytical solution

i) The diffusion equations developed in Chapter 2 did not have an analytical solution unless a linear isotherm (Henry's law) was used. Mathews and Su (1983) found that the Freundlich isotherm was not accurate enough to give accurate kinetic results. A linearized isotherm would have produced even larger errors. It was also found that the column design was sensitive to the accuracy of the isotherm so the error introduced by a linearized isotherm would be unacceptable.

ii) Computer time was becoming less expensive and numerical solutions to nonlinear problems were becoming more practical.

iii) The analytical solutions were in the form of converging series, usually derived by taking Laplace or Fourier transforms; eg. (Crank, 1970). Analytical solutions, therefore, did not avoid the use of a computer.

iv) Numerical solutions allowed for the incorporation of complicating factors such as changing temperatures, input concentrations, and other adsorber conditions. Most importantly, they allowed the development of a multicomponent model.

5.1.2) Choice of a numerical technique

Many authors used numeric techniques to solve systems of equations describing adsorption; many used either:

i) backward differences only;

ii) Crank-Nicolson and backward differences;

iii) orthogonal collocation.

Mansour (1984) claimed that backwards difference methods were easier to adapt to multicomponent problems and that Crank-Nicolson methods experience problems with stability. (He was using a more complex model than most though). Weber and Liu (1980) claimed that orthogonal collocation was more efficient than backward differences methods, but Mansour claimed the opposite provided a variable time step was used.

The choice of method had to be made without actually testing the different alternatives because of the large amount of time required to code the necessary computer programs. Backward difference methods were more straightforward than orthogonal collocation, and the methods were explained in more detail in the literature. Von Rosenburg (1969), Crank (1970), Smith (1969) and Gerald (1984) present the backward differences and Crank-Nicolson methods particularly clearly. It was therefore decided that a finite differences method would be used since there was no guarantee of a more efficient solution from an orthogonal collocation method, which would have taken longer to perfect.

There remained a choice of the backward difference or Crank-Nicolson method to solve the particle diffusion equation (2.44). The Crank-Nicolson method was more efficient but less stable than the backward differences method. Crittenden and Weber (1978b) used the Crank-Nicolson method for the same problem without instability problems. They also presented the numerical analogs required. In addition they presented the backward differences analogs used to solve the material balance equations (2.55 and 2.57), so their method was chosen.

5.1.3) The simplified solid phase diffusion equation.

The simplified model, which neglected the pore solution and assumed a constant diffusion coefficient, was descritized into a numeric analog first.

The particle diffusion equation (2.44) is re-stated below and separated into a form suitable for discretization.

$$\frac{\partial q}{\partial t} = \frac{1}{r^2} \frac{\partial}{\partial r}\left(r^2 \frac{\partial q}{\partial r} \right) = \frac{2}{r^2}\left(\frac{\Delta q}{\Delta r} + \frac{\Delta^2 q}{\Delta r^2}\right). \qquad (2.44)$$

Taking backward differences gives:

$$\frac{q_i - q_i'}{\Delta t} = \frac{2}{r_i} \frac{q_{i+1} - q_{i-1}}{2\,\Delta r} + \frac{q_{i+1} - 2q_i + q_{i-1}}{(\Delta r)^2},$$

where q' = q at the previous time step,
i = Number of radial distance steps from particle centre

Re-arranging gives:

$$\frac{\Delta r^2}{\Delta t}(q_i - q_i') = \left[(1 + \frac{\Delta r}{r})q_{i+1} - 2\,q_i + (1 - \frac{\Delta r}{r})q_{i-1}\right].$$

The Crank-Nicolson method achieves second order correctness by averaging the analogs at the present and the previous time steps and the result is:

$$\frac{1}{2}\left[(1+\frac{\Delta r}{r})q_{i+1} - 2q_i + (1-\frac{\Delta r}{r})q_{i-1} + (1+\frac{\Delta r}{r})q_{i+1}' - 2q' + (1-\frac{\Delta r}{r})q_{i-1}'\right]$$

$$= \frac{\Delta r^2}{\Delta t}(q_i - q_i'), \qquad (5.1)$$

re-arranging:

$$\left(1 + \frac{\Delta r}{r}\right) q_{i+1} - 2\left(1 + \frac{\Delta r^2}{\Delta t}\right) q_i + \left(1 - \frac{\Delta r}{r}\right) q_{i-1}$$

$$= -\left(1 + \frac{\Delta r}{r}\right) q_{i+1}' + 2\left(1 - \frac{\Delta r^2}{\Delta t}\right) q_i' - \left(1 - \frac{\Delta r}{r}\right) q_{i-1}'. \qquad (5.2)$$

If i = 1 corresponds to the centre of the particle, and there are M - 1

radial steps, then i = M corresponds to the particle surface. The analog presented in equation 5.2 holds for all points except i = 1 and i = M; q at these points is determined using the boundary conditions.

Equation 2.53 is the boundary condition at the centre of the particle.

$$\frac{\partial q}{\partial r} = 0. \qquad (2.53)$$

The analog Crittenden and Weber (1978b) derived from this equation is:

$$3q_1 - 4q_2 + q_3 = -3q_1' + 4q_2' + q_3'.$$

They did not explain how they derived this analog, and it was suspected at it gave inaccurate results. Another analog was derived as follows: (Smith, 1969).

$$\frac{\partial q}{\partial t} = \frac{1}{r^2}\frac{\partial}{\partial r}\left(r^2 \frac{\partial q}{\partial r} \right) = \frac{\partial^2 q}{\partial r^2} + \frac{2}{r}\frac{\partial q}{\partial r}, \qquad (2.44)$$

but $\frac{2}{r}\frac{\partial q}{\partial r} = \frac{0}{0}$ at $r = 0$.

Smith used the Maclaurin expansion to show that equation 2.44 became:

$$\frac{\partial q}{\partial t} = 3\frac{\partial^2 q}{\partial r^2} \qquad \text{at } r = 0. \qquad (5.3)$$

Taking backward differences we get:

$$\frac{(q_1 - q_1')}{\Delta t} = \frac{3(q_2 - 2q_1 + q_0)}{(\Delta r)^2},$$

but $q_2 = q_0$ by equation 2.53. Therefore:

$$\frac{(q_1 - q_1')}{\Delta t} = \frac{6(q_2 - q_1)}{(\Delta r)^2}.$$

Applying the Crank-Nicolson analog, the final result after re-arranging is:

$$\left(\frac{(\Delta r)^2}{3\,\Delta t} + 1 \right) q_1 - q_2 = \left(\frac{(\Delta r)^2}{3\,\Delta t} - 1 \right) q_1' + q_2'. \qquad (5.4)$$

Crittenden and Weber used the boundary condition described by equation 2.52a to calculate the concentration at the surface of the particle. It is rewritten below.

$$Sh_b (\bar{c} - \bar{c}_s) = \frac{\partial}{\partial \bar{t}} \int_0^1 q \; r^2 \; dr. \qquad (2.52a)$$

If the right hand side is integrated using the trapezoidal rule then the numeric analog is:

$$\frac{\partial}{\partial \bar{t}} \left[\sum_{i=2}^{M} \left(\frac{1}{2} (q_i \; r^2_i + q_{i-1} \; r^2_{i-1}) \Delta r_i \right) \right].$$

The indexing starts with i = 1 and there are M-1 radial steps. Therefore $r_1 = 0$ and $r_M = 1$.

Re-arranging it becomes:

$$\frac{\partial}{\partial \bar{t}} \left[\sum_{i=2}^{M-1} \left(r_i^2 \; q_i \right) + \frac{1}{2} q_M \right] \Delta r.$$

Discretizing this PDE produces:

$$\frac{\Delta r}{\Delta \bar{t}} \left[\left[\sum_{i=2}^{M-1} \left(r_i^2 \; q_i \right) + \frac{1}{2} q_M \right] - \left[\sum_{i=2}^{M-1} \left(r_i^2 \; q_i' \right) + \frac{1}{2} q_M' \right] \right]. \qquad (5.5)$$

Finally the analog for the boundary condition is obtained by replacing the right hand side of equation 2.52a with equation 5.5 and re-arranging:

$$\sum_{i=2}^{M-1} \left(r_i^2 \; q_i \right) + \frac{1}{2} q_M = \sum_{i=2}^{M-1} \left(r_i^2 \; q_i' \right) + \frac{1}{2} q_M' + \frac{\Delta \bar{t}}{\Delta r} Sh (\bar{c} - \bar{c}_s). \qquad (5.6)$$

The computation needs to take into account the fact that $\bar{c}_s$ is a function of q_M (the concentration at the particle surface), the function being the isotherm relationship used. The isotherms used here are the Dubinin or Freundlich isotherms. The Dubinin isotherm with C as the dependent

variable is given in equation 2.14b. The Freundlich isotherm inverts to:

$$C_* = \exp\left(\frac{\ln(q_M)-\ln(K_f)}{n_f}\right). \qquad (2.3a)$$

It was found that if diffusion through the surface film was much faster than the solid phase diffusion, the particle saturated at its surface. The analogs presented above had no way of knowing that the surface of the particle had reached equilibrium with the bulk solution. The method therefore predicted unrealistically high concentrations on the particle surface and went unstable because of the non-linear nature of the isotherm.

Using equation 2.51 instead of 2.52a to describe the boundary conditions at the particle surface was tried. This approach predicted a very slow approach to equilibrium because it held the concentration at the particle surface unrealistically low.

Another experiment was performed where the isotherm equation was directly incorporated into the numeric analog - by substituting equation 2.14b into equation 5.6. A square M+1 by M+1 matrix was created and solved to find the M q values, and $\bar{C}$, simultaneously. It was found that the method had no advantages over the more straightforward method of calculating $\bar{C}$ using equation 2.14b and substituting the value in equation 5.6.

The only way found to achieve numerical stability was to use the equations derived above until the particle surface reached equilibrium with the bulk solution. A test for this was included in the program. From that point on, film diffusion was ignored. This meant that equation 2.52a was no longer valid for the boundary condition at the particle exterior. Instead, the isotherm relation was used to predict the surface concentration using the bulk concentration: after q_M had over-shot the concentration where it was at equilibrium with the bulk solution C, it was assumed to be in equilibrium with C. The analog of equation 5.2 was

used up to i = M-2. For i = M-1, q_M was fixed so the analog became:

$$-2\left(1 + \frac{\Delta r^2}{\Delta t}\right) q_{M-1} + \left(1 - \frac{\Delta r}{r}\right) q_{M-2} =$$
$$-2\left(1 + \frac{\Delta r}{r}\right) q'_M + 2\left(1 - \frac{\Delta r^2}{\Delta t}\right) q'_{M-1} - \left(1 - \frac{\Delta r}{r}\right) q'_{M-2}. \quad (5.2a)$$

Changes were also required in the equations used for the liquid phase mass balance; they were explained below. A numeric example was also given below.

5.1.4) The liquid phase mass balance equation

To find the new liquid phase concentration, equation 2.55a had to be solved.

$$\frac{\partial \bar{c}}{\partial t} = - Dg_b \frac{(1-\epsilon)}{\epsilon} 3 \frac{\partial}{\partial t} \int_0^1 q\, r^2\, dr. \quad (2.55a)$$

The integral on the right hand side of the above equation had already been determined using equation 5.5. To save repeating the calculations, equation 2.52a was substituted into equation 2.55a. The result was:

$$\frac{\partial \bar{c}}{\partial t} = - Dg_b \left(\frac{1-\epsilon}{\epsilon}\right) 3\, Sh_b\, (\bar{c}' - \bar{c}'_s).$$

The best way found to descritize this first order PDE was to use forward differences. Taking backward differences and also calculating $\bar{c}$ and $\bar{c}_s$ at the mid point between the present and the previous time steps was tried. It was found that forward differences gave the most stable analog and that there there was little difference in the accuracy of the 3 methods. Forward differences also provided a slightly quicker solution so it was the obvious choice. The equation was:

$$\frac{\bar{c} - \bar{c}'}{\Delta t} = - Dg_b \left(\frac{1-\epsilon}{\epsilon}\right) 3\, Sh_b\, (\bar{c}' - \bar{c}'_s).$$

Expressing this equation in terms of $\bar{c}$ gave:

$$\bar{c} = \bar{c}' - \Delta t\, Dg_b \left(\frac{1-\epsilon}{\epsilon}\right) 3\, Sh_b\, (\bar{c}' - \bar{c}'_s). \quad (5.7)$$

$\bar{C}_s$ was calculated from the isotherm relation using q_M which was calculated from the solid phase mass balance discussed above.

The above included the film diffusion rate equation which was ignored after the surface concentration went above the level where it was in equilibrium with the bulk solution concentration. Therefore, after this point, the bulk concentration could no longer be derived using the film diffusion coefficient and equation 2.55a was used directly. The numeric analog was:

$$\bar{C} = \bar{C}' - Dgb \left(\frac{1-\epsilon}{\epsilon}\right) 3 \Delta r \left[\sum_{I=2}^{M-1} \left(r_I^2 \ (q_I - q_I') \right) + q_M' \right]. \quad (5.8)$$

An example of the application of the above numeric analogs follows.

5.1.5) A test example of the numeric analog

To test the numeric analogs of the diffusion equations and the program written to use them, data from the literature was used as a test example. The data chosen was from Van Vliet et al (1980), figure 4. This example was chosen because:

i) it used the same mathematical model;

ii) it used a compound also used in this work: phenol.

5.1.5.1) Setting up the model

The adsorbent used in this example was a charred polymeric resin called ambersorb XE-340 with a particle diameter of 3 → 4.2E-4 m. The data was tabulated below.

Table 5.1

Data for example used to test kinetics program.

Property	Symbol	value	units
Average particle radius	R_p	1.7E-4	m
Volume solution	V	3	l
Mass adsorbent	Mr	1.684	g
System voidage	ϵ	0.999412	(1,684g carbon in 3l)
Particle density	ρ_s	995	g/l
Density of phenol	ρ	1071	g/l
Temperature	T	293	K
Affinity coefficient	B	359	$(kJ/mole)^2$
Maximum adsorption volume	$\emptyset_0$	1.39E-4	l/g
Surface diffusion coeff	D_s	4.84E-14	m^2/s
Film transfer coefficient	k_s	1.01E-5	m/s

Table 5.2

Experimental data

Time [sec]	Liquid concentration [g/l]
0	0.05
900	0.0468
2040	0.0444
3900	0.0417
14520	0.036
28860	0.032
86400	0.0252

All the above data was given to the program which proceeded with the solution as follows:

Using 8 radial steps, $\Delta r = 0.125$. $Sh_b = 32.476$, $Dg_b = 1156{,}6$ and $q_e = 0.06055$. Choosing $\Delta t = 90$ s, made $\Delta\bar{t} = 1.344E-4$.

Using the left hand side of equation equation 5.4, the first line of the 9 x 9 matrix shown in table 5.3 below was obtained. The right hand side of the equation made the first line of the 1 x 9 matrix on the right. The next 7 lines were obtained using equation 5.2. The last line came from equation 5.6. Solving these 9 simultaneous equations gave the value of q at the 9 radial positions.

Table 5.3

Simultaneous equations for finding q

(q_1)	(q_2)						(q_8)	(q_9)	
39.74	-1.0	0.0	0.0	0.0	0.0	0.0	0.0	0.0	0.0
0.0	-234.4	2.0	0.0	0.0	0.0	0.0	0.0	0.0	0.0
0.0	0.50	-234.4	1.50	0.0	0.0	0.0	0.0	0.0	0.0
0.0	0.0	0.6667	-234.4	1.3333	0.0	0.0	0.0	0.0	0.0
0.0	0.0	0.0	0.7500	-234.44	1.250	0.0	0.0	0.0	0.0
0.0	0.0	0.0	0.0	0.80	-234.44	1.20	0.0	0.0	0.0
0.0	0.0	0.0	0.0	0.0	0.8333	-234.44	1.1667	0.0	0.0
0.0	0.0	0.0	0.0	0.0	0.0	0.8571	-234.44	1.1429	0.0
0.0	1.0	4.0	9.0	16.0	25.0	36.0	49.0	32.0	2.235

The initial condition was that $q_i = 0$ at $t = 0$, $i = 1 \rightarrow M$. This meant that the the right hand matrix was all zeros except for the last line which represented the amount of adsorbate that had diffused through the external film during the first time step. The solution of these equations after the first time step therefore only required one division: 2.2355/32 = 0.06859 which was the value of q_M at $t = \Delta t$.

The next step was to find the new liquid concentration which was done using equation 5.7. The result was $q = 0.9911$. $\bar{c}_s$ was then calculated so that the film diffusion could be estimated on the next time step. $\bar{c}_s$ was the liquid phase concentration in equilibrium with q_M and was found using equation 2.14b.

The program marched forward in time until it found that $q_M > \bar{c}_s$. After this occurred, it was assumed that $q_M = \bar{c}_s$. This occurred after 11334 seconds in the example quoted above. At this point $C = 0.0367$, $q_9 = 0.944$ and $\bar{c} = 0.734$. After calculating $\bar{c}s$ from q_9 it came to 0.792, which was higher than $\bar{c}$, so the model was changed to ignore film diffusion.

5.1.5.2) Algorithms for solving the simultaneous equations

For the computer to solve the large number of simultaneous equations that occurred at each time step, it needed an efficient algorithm. The first one tried was based on Gauss elimination. The left hand matrix shown in table 5.3 was unchanged as long as the time step was unchanged. If the matrix was inverted, then q could be obtained simply by multiplying the inverse matrix with the matrix shown on the right of table 5.3. The problem with this method was that Gauss elimination did not invert the matrix perfectly because of rounding errors. Using double precision (80 bit) computations did not solve the problem.

The second method tried was Gauss-Seidal iteration. The method worked by making successive estimates of the matrix values one at a time. The new estimate of each point was calculated using the most recent available estimate of the values of the neighbouring points. Estimates were made of each value in the matrix iteratively until a pre-defined level of convergence was achieved. The analog was developed as follows:
re-arranging equation 5.2 it became:

$$q_i = \frac{r}{2}\left[(1 + \frac{\Delta r}{r})q_{i+1} - 2q_i + (1 - \frac{\Delta r}{r})q_{i-1}\right] + b_i ,$$

$$\text{where} \quad b_i = q_i' + \frac{r}{2}\left[(1 + \frac{\Delta r}{r})q_{i+1}' - 2q_i' + (1 - \frac{\Delta r}{r})q_{i-1}'\right],$$

$$r = \frac{\mathcal{D}t}{(\Delta r)^2}.$$

Re-arranging again and introducing the Gauss-Seidal algorithm gave:

$$q_i = \frac{r}{2(1+r)}\left[(1 + \frac{\Delta r}{r})q_{i+1}'' + (1 - \frac{\Delta r}{r})q_{i-1}\right] + \frac{b_i}{1 + r}, \qquad (5.9)$$

where q refers to q at the most recent Gauss-Seidal iteration,
q'' refers to the previous Gauss-Seidal iteration,
q' refers to the previous time step.

The computations were started in the middle of the particle, so q_1 was calculated first using the Gauss-Seidal algorithm applied to equation 5.4.

The analog in full was:

$$q_1 = \frac{q_2'' + \left(\frac{(\Delta r)^2}{3\,\Delta t} - 1\right) q_1' + q_2'}{\left(\frac{(\Delta r)^2}{3\,\Delta t} + 1\right)}, \qquad (5.10)$$

The program then moved to the outside of the particle using equation 5.9 until it reached the particle surface. There it used equation 5.11 (derived from equation 5.6) to find q_M

$$q_M = 2\left[\sum_{i=2}^{M-1}\left(r_i^2\, q_i'\right) + \frac{1}{2} q_M' - \sum_{i=2}^{M-1}\left(r_i^2\, q_i''\right) + \frac{\Delta t}{\Delta r} Sh(\bar{c}' - c_s')\right]. \qquad (5.11)$$

Finally the bulk concentration was found using equation 5.7 as before.

This method was found to be more stable than Gauss elimination. The program generally converged within 9 iterations which meant that it was more efficient that the Gauss elimination method when small radial steps were used (involving large matrices). It was also found that the program took longer to switch from the surface and film diffusion model to the surface diffusion only model. If a small enough time step was used on the above example the switch never occurred. The program's ability to switch was retained because it was found necessary when analysing systems with different diffusion coefficients. It also increased its ability to handle a wide range of conditions.

After switching to the surface diffusion only model, equations 5.10 and 5.9 were used as before. Equation 5.11 was not used and q_M was found from the equilibrium relationship using $\bar{c}$. $\bar{c}$ was found using equation 5.8.

To improve the efficiency of the Gauss-Seidal method, a system of successive over-relaxation (SOR) was commonly used. The relaxation coefficient recommended by Smith (1969) was tried but was found to introduce instability. Other relaxation coefficients were tried but none could make the program run faster than the straightforward Gauss-Seidal method. The example tried took at least 50 seconds central processing

unit (CPU) time using the SOR method and under 40 seconds using the Gauss-Seidal method.

5.1.5.3) Testing the accuracy of different step sizes

The smallest step size used was $\Delta r = 0.005$ with 3000 time steps between data points. The results were tabulated in table 5.4.

Table 5.4

Data predicted by program

Time [sec]	q read from graph	q predicted
0	0.05	0.05
900	0.0468	0.04680
2040	0.0444	0.04472
3900	0.0417	0.04251
14520	0.036	0.03619
28860	0.032	0.03198
86400	0.0252	0.02535

The results were well within the error introduced when reading the data off the graph. This solution took about 10 hours of CPU time. Larger steps were compared to check the accuracy against step size. The results were shown in table 5.5.

Table 5.5

Comparison of step sizes

$\Delta\Gamma$	Time steps	Average % error	CPU time [sec]
0.01	800	0.04	4200
0.0133	200	0.26	1560
0.025	100	0.65	355
0.04	400	1.50	557
0.04	50	1.73	106
0.04	5	5.9	34.8
0.1	20	11.1	15.5
0.125	10	16.8	6.6
0.2	8	28.3	3.6

The error was calculated using the formula:

$$\% \text{ error} = \frac{\left|(\text{Predicted } \bar{C}) - (\bar{C} \text{ calc. using } \Delta\Gamma = 0.005,\ 3000 \text{ time steps})\right|}{(1 - (\bar{C} \text{ calculated using } \Delta\Gamma = 0.005,\ 3000 \text{ time steps})) / 100\%}.$$

The data showed that an accurate answer required both the time steps and the radial distance steps to be small. It was common to aim for an Γ value of ½ or 1. Since $\Gamma = \Delta\bar{t}/(\Delta\Gamma)^2$ the time steps needed to be reduced four times when the radial steps were halved.

5.1.6 Accounting for concentration dependent surface diffusion and particle porosity

When the adsorbate was poorly adsorbed, as with oxalic acid on XAD-8, the particle porosity could no longer be neglected. Also, it was found that the surface diffusion coefficient often showed a strong concentration dependence. The program was therefore modified to account for porosity and variable diffusion rates. The relevant solid phase diffusion equation was:

$$\frac{\partial \bar{q}}{\partial \bar{t}_i} + \frac{\epsilon_p}{\rho_s}\frac{\partial \bar{c}_p}{\partial \bar{t}_i} = \frac{1}{r^2}\frac{\partial}{\partial r}\left(r^2 \frac{\partial \bar{q}}{\partial r} \right). \qquad (2.44a)$$

When desritizing, $\bar{t}_i$ was evaluated using D_s evaluated at the concentration on the adsorbent surface at radial position r_i. The backward difference result was:

$$\frac{q_i - q_i'}{\partial \bar{t}_i} + \frac{\bar{c}_p - \bar{c}_p'}{\partial \bar{t}_i}\frac{\varepsilon_p}{\rho_s} = \frac{1}{(\Delta r)^2}\left[\left(1-\frac{\Delta r}{r_i}\right)q_{i-1} - 2q_i + \left(1+\frac{\Delta r}{r_i}\right)q_{i+1}\right]. \quad (5.12)$$

The Crank-Nicolson analog converted the term on the right hand side to the average value of the present and the previous time steps. For the purposes of the Gauss-Seidal iteration, the values from the previous time step were grouped together as:

$$b_i = q_i' + \frac{r_i}{2}\left[\left(1 - \frac{\Delta r}{r_i}\right)q_{i-1}' - 2q_i' + \left(1 + \frac{\Delta r}{r_i}\right)q_{i+1}'\right],$$

where $r_i = \frac{\Delta \bar{t}_i}{(\Delta r)^2}$ ($\bar{t}_i$ evaluated at previous time step).

Substituting this group into the Crank-Nicolson analog derived from equation 5.12 and applying the Gauss-Seidal method gave:

$$q_i = \frac{1}{(1+r_i)}\left[\frac{r_i}{2}\left[\left(1-\frac{\Delta r}{r}\right)q_{i-1} + \left(1+\frac{\Delta r}{r}\right)q_{i+1}''\right] - \frac{\varepsilon_p}{\rho_s}(\bar{c}_{p,i}'' - \bar{c}_{p,i}') + b_i\right]. \quad (5.13)$$

The conditions at the particle centre were derived using equation 5.3 extended to account for the pore solution and variable surface diffusion.

$$\frac{\partial q_i}{\partial \bar{t}_i} + \frac{\varepsilon_p}{\rho_s}\frac{\partial \bar{c}_p}{\partial \bar{t}_i} = \frac{3}{r^2}\frac{\partial}{\partial r}\left(r^2 \frac{\partial q_i}{\partial r}\right) \qquad \text{at } r = 0. \quad (5.3a)$$

Applying the Crank-Nicolson and Gauss-Seidal methods to this equation it became:

$$q_i = \frac{q_i' + r_i(q_2' - q_i') - \frac{\varepsilon_p}{\rho_s}(\bar{c}_{p,i}'' - \bar{c}_{p,i}') + r_i q_2''}{(1 + r_i)}, \quad (5.15)$$

where $r_i = \frac{3\,\Delta \bar{t}_i}{(\Delta r)^2}$.

When film diffusion was controlling the boundary condition for

the particle surface was:

$$Sh_b(\bar{c} - \bar{c}_s) = \frac{\partial}{\partial \bar{t}} \int_0^1 r^2 \left(q + \bar{c}_p \frac{\epsilon_p}{\rho_s}\right) dr. \qquad (2.52)$$

The right hand side of this equation was descritized using the trapezoidal rule in the same manner as equation 2.52a. Re-arranging and applying the Gauss-Seidal method gave:

$$q_M = b_M + \frac{2Sh_b \Delta \bar{t}_M}{\Delta r}\left(\bar{c}' - \bar{c}'_{p,M}\frac{q_e}{C_o}\right) - 2\sum_{i=2}^{M-1}\left(q_i + \bar{c}_{p,i}\frac{\epsilon_p}{\rho_s}\right)r_i^2 - \bar{c}_{p,M}\frac{\epsilon_p}{\rho_s}, \qquad (5.15)$$

where $b_M = 2\sum_{i=2}^{M-1}\left(q_i' + \frac{\epsilon_p}{\rho_s}\bar{c}'_{p,i}\right)r_i^2 + \left(q_M' + \frac{\epsilon_p}{\rho_s}\bar{c}'_{p,M}\right).$

While film diffusion was important, the bulk liquid concentration was found using the result of substituting equation 2.52 in equation 2.55 which was:

$$\frac{\partial \bar{c}}{\partial \bar{t}} = -Dg_b\left(\frac{1-\epsilon}{\epsilon}\right) 3\, Sh_b\, (\bar{c} - \bar{c}_s).$$

This equation was descritized using forward differences. $\bar{c}_s$ was determined using the pore solution concentration at the particle surface.

$$\bar{c} = \bar{c}' - \Delta \bar{t}_M\, Dg_b\left(\frac{1-\epsilon}{\epsilon}\right) 3\, Sh_b\, (\bar{c}' - \bar{c}'_{p,M}\frac{q_e}{C_o}). \qquad (5.16)$$

When the film diffusion was negligible, the bulk concentration was found using equation 2.55.

$$\frac{\partial \bar{c}}{\partial \bar{t}} = -Dg_b\left(\frac{1-\epsilon}{\epsilon}\right) 3 \frac{\partial}{\partial \bar{t}} \int_0^1 \left(q + \bar{c}_p \frac{\epsilon_p}{\rho_s}\right) r^2\, dr. \qquad (2.55)$$

The numeric analog was:

$$\bar{c} = \bar{c}' - Dg_b\left(\frac{1-\epsilon}{\epsilon}\right)3\Delta r\left[\sum_{i=2}^{M-1}\left(q_i - q_i' + \frac{\epsilon_p}{\rho_s}(\bar{c}_{p,i} - \bar{c}'_{p,i})\right)r_i^2 + \frac{1}{2}\left(q_M'' - q_M' + \frac{\epsilon_p}{\rho_s}(\bar{c}''_{p,M} - \bar{c}'_{p,M})\right)\right]. \qquad (5.17)$$

The solid phase concentration on the particle's outside surface was found using the new value of $\bar{c}$ in the isotherm relation as before.

5.2) The computer program for determining rate constants

The compiler used for the computer programs was Turbo Pascal version 3. This compiler was chosen because of its rapid compilation of the source code and its efficient execution of the compiled code. Professional packages for solving partial differential equations were available for mainframe computers. They were not used because it would have been difficult to transport the programs to other computers. The programs were therefore written as a complete unit ready to run on an IBM PC compatible computer. The program for determining the adsorption rate constants is in Appendix 7.

The program starts by reading the experimental data from a file. It then converts the data to dimensionless units and calculates a number of commonly used combinations of figures. It divides the time between each set of experimental readings into a user defined number of sections. Using the user defined first guess of the rate coefficients it calculates the predicted concentrations. It compares these results with the experimental results and finds the error. It then finds the error using a new set of rate coefficients, thus starting the search for the coefficients that give the smallest error.

A number of checks had to be included to ensure that the model remained stable.

5.3) Experimental results

Table 5.6 summarizes the experimentally determined rate constants. The full results are in Appendix 4.

Table 5.6

Diffusion coefficient results

Adsorbate	Adsorbent	Film Diffusion Coeff.	Solid phase diffusion	Conc dependence factor	Average error
Phenol 0.001 M	XAD-8	2.12E-5	1.15E-12	-	1.5%
0.01 M		1.95E-5	4,80E-12	-	2.8%
0.1 M		7.60E-6	6.81E-11	-	11.4%
all concentrations		1.43E-5	7.8E-13	18.4	7.8%
Oxalic acid	XAD-8				
3-parameter isotherm		1.63E-3	9.27E-7	339	-
2-parameter isotherm		2.43E-3	6.8E-10	184	40%
Cation exchanged	XAD-8				
D1/D2 effluent		1.7E-5	5.9E-12	0.1	16%
D1/D2 effluent on:	XAD-8				
5 to 8.5E-4 m resin		7.6E-6	1.0E-12	-	-
3 to 4.25E-4 m resin		7.0E-6	2.0E-12	-	-
1.8 to 3E-4 m resin		5.0E-6	8.5E-13	-	-
Cation exchanged	carbon				
D/C effluent		2E-6	2.7E-14	-	-

5.3.1) Phenol

The need for a concentration dependent solid phase diffusion coefficient was illustrated by the results for phenol; its value increased 60 fold with a 100 fold increase in concentration. Figures 5.1 to 5.3 show the data and how the diffusion model fitted it.

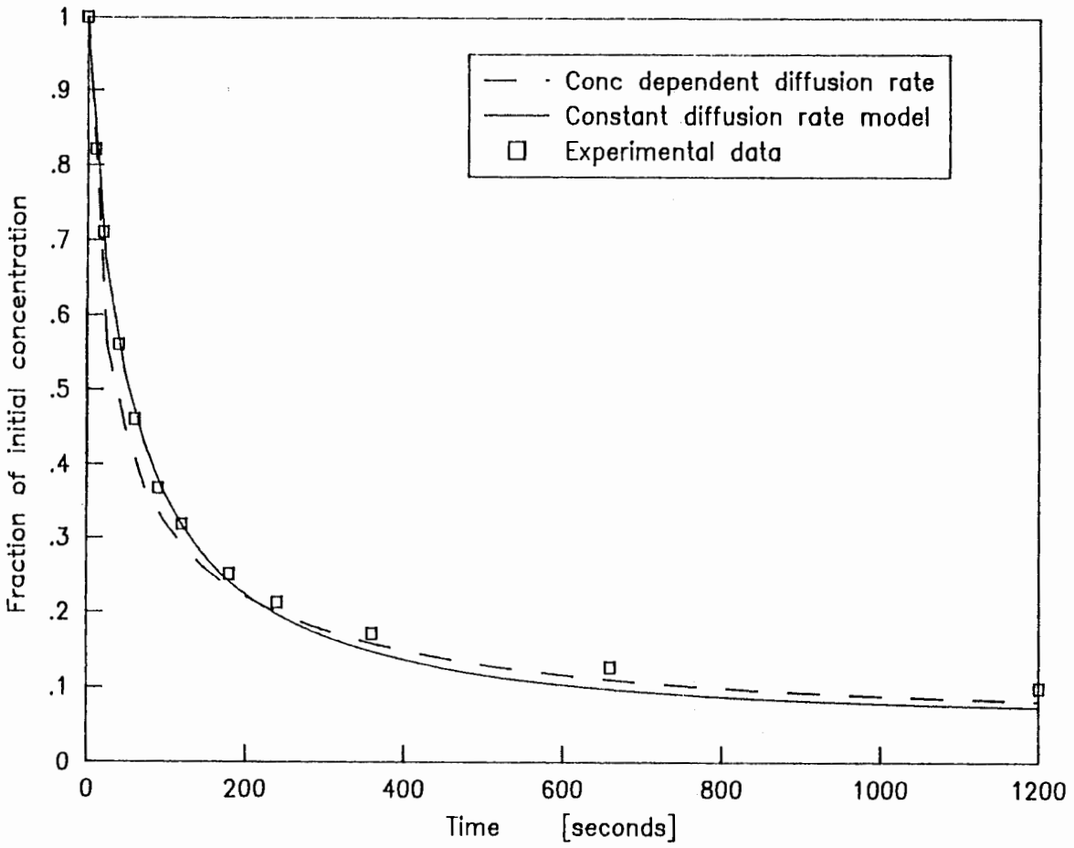

Figure 5.1 Rate of adsorption of phenol on XAD−8, initial concentration = 0.001 M

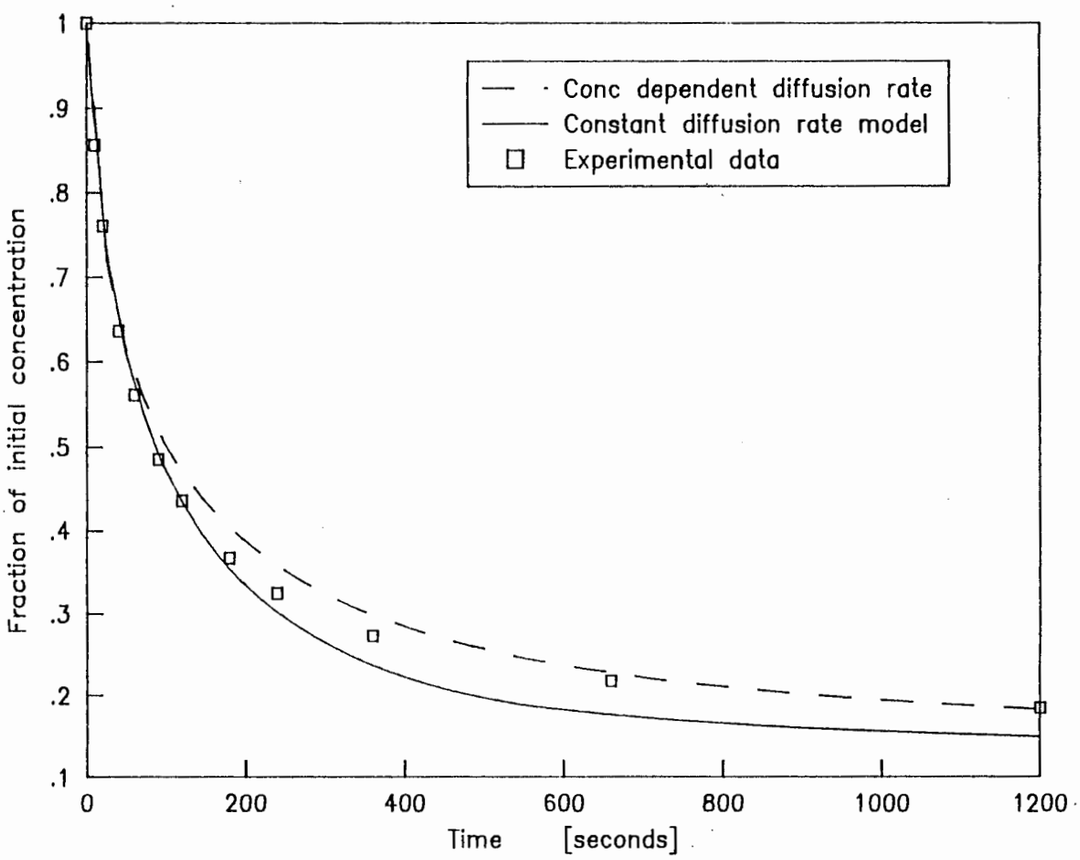

Figure 5.2 Rate of adsorption of phenol on XAD−8, initial concentration = 0.01 M

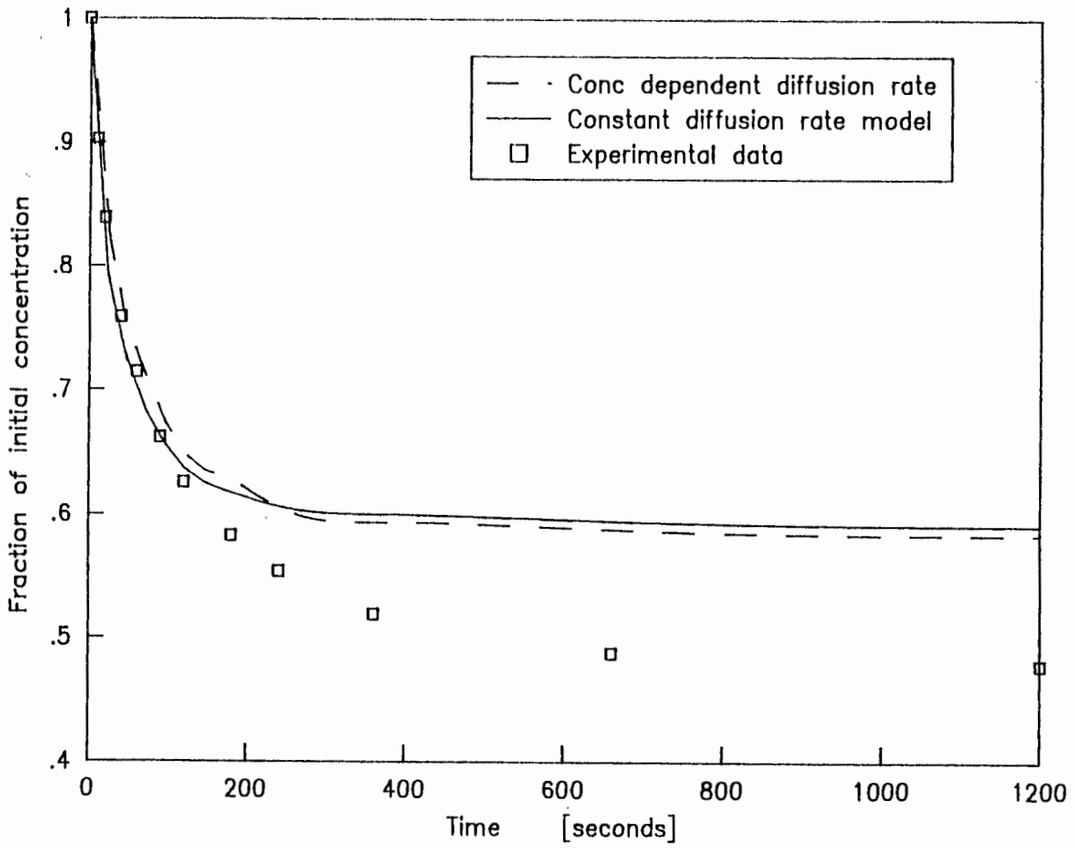

Figure 5.3 Rate of adsorption of phenol on XAD-8, initial concentration = 0.1 M

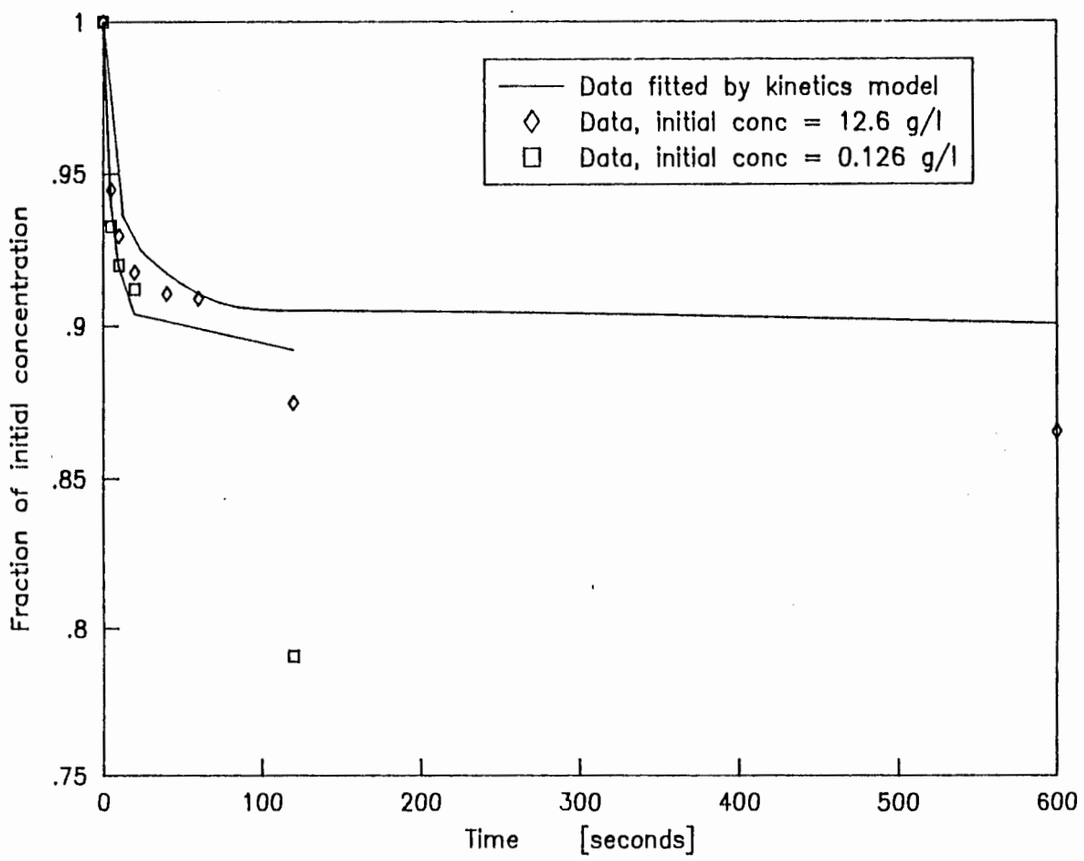

Figure 5.4 Rate of adsorption of oxalic acid on XAD-8, fitted by concentration dependent diffusion model

5.3.2) Oxalic acid

The rate of adsorption of oxalic acid was also tested over a 100 fold concentration range. Figure 5.4 shows the data for 2 of the experiments, and the curves show the best fit obtained with the diffusion model using the 3-parameter Dubinin isotherm. The isotherm predicted a poor adsorption in this concentration range (see figure 4.4), which explained the poor fit obtained. Also, the solution concentrations at 120 and 600 seconds were measured using HPLC; the absence of interference effects with this technique made these results lower than the earlier results obtained using UV absorbence. The rate coefficients that best fitted the data were therefore unrealistically high. Using the 2-parameter isotherm, the coefficients were lower but still surprisingly high. Figure 5.5 shows that a better fit was obtained.

5.3.3) Cation exchanged D1/D2 effluent

The experimental results of the four runs performed are shown in figures 5.6 to 5.9. These figures also show how the diffusion model fitted the data.

5.3.4) Effect of the resin particle diameter.

Figures 5.10 to 5.12 show the results for experiments where pure D1/D2 effluent was loaded onto XAD-8. Bearing in mind the scatter on the experimental results, the model seems to be able to simulate the effect of adsorbent particle size.

5.3.5) Activated carbon

The results of adsorbing cation exchanged D/C effluent on activated carbon showed very small diffusion coefficients. Figures 5.13 and 5.14 show the results. The figures also show the results using the empirical model. Only the first few points were fitted with this model because it went unstable after that point. Although the program for the diffusion model had to include a number of checks to keep it stable, it was clearly superior to the empirical model.

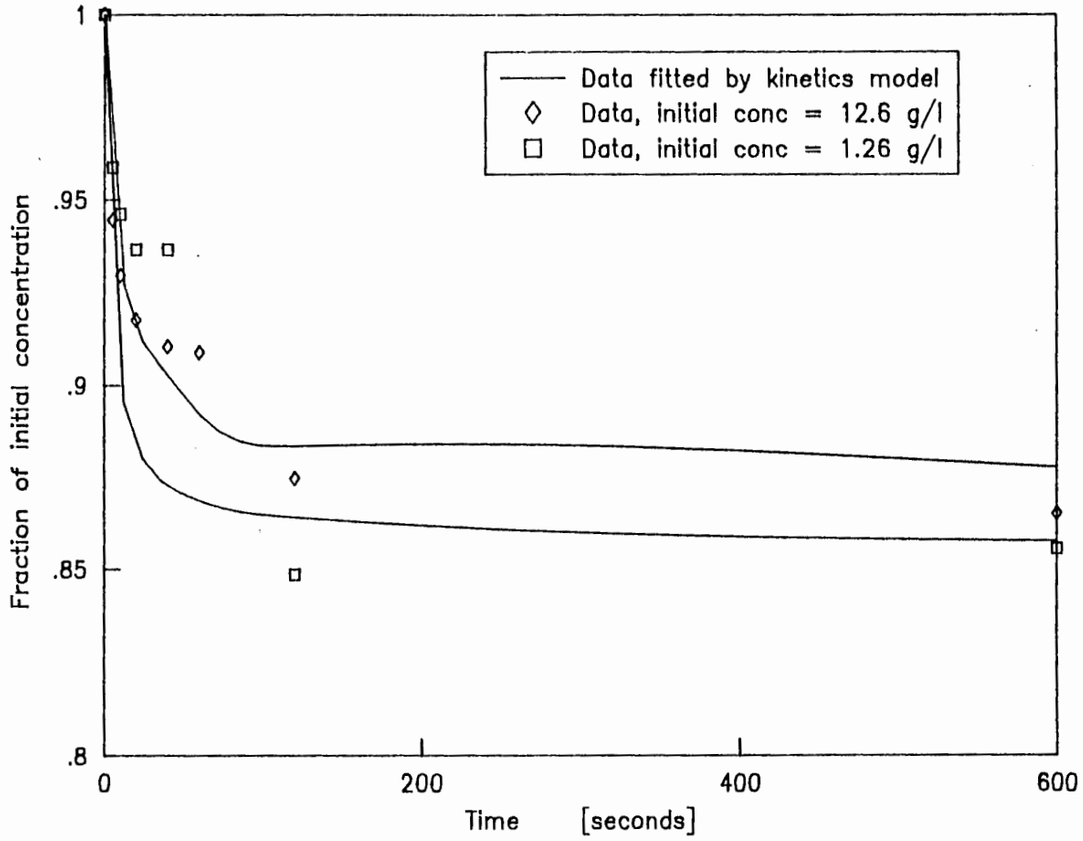

Figure 5.5 Rate of adsorption of oxalic acid on XAD−8, fitted by concentration dependent diffusion model

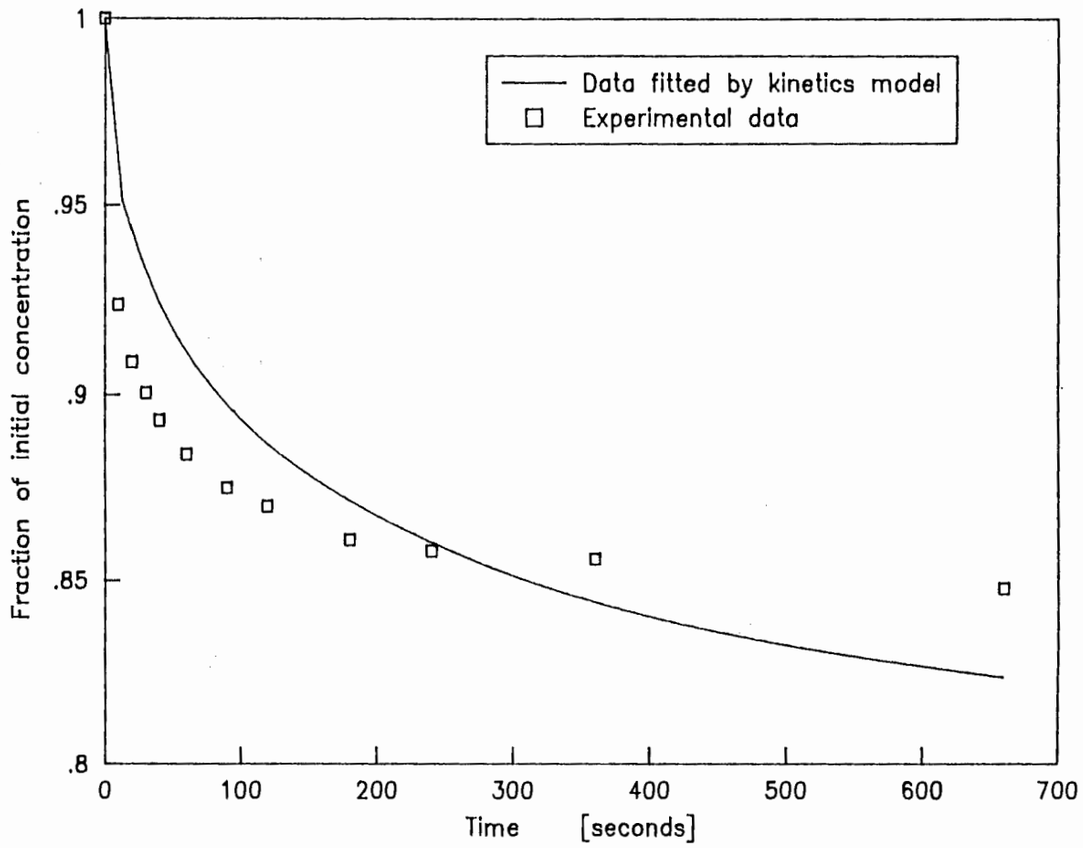

Figure 5.6 Rate of adsorption of cation exchanged D1/D2 effluent on XAD−8. Initial concentration = 0.0984

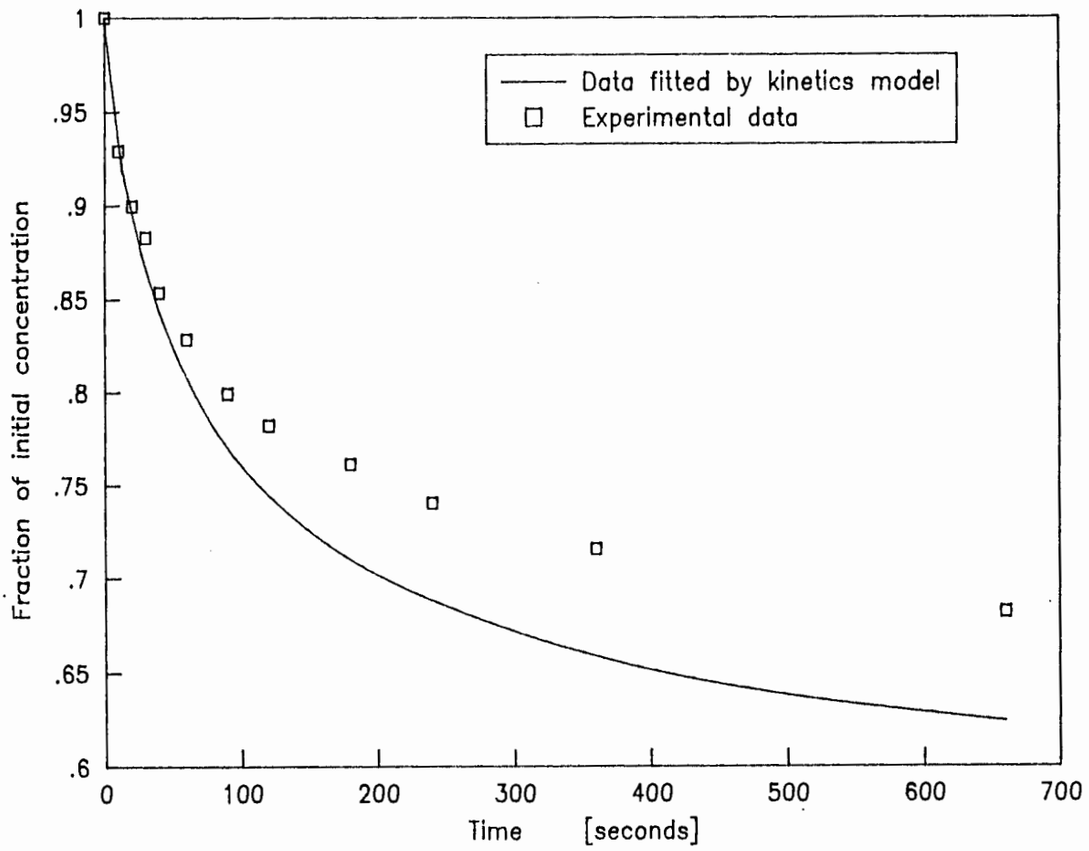

Figure 5.7 Rate of adsorption of cation exchanged D1/D2 effluent on XAD-8. Initial concentration = 0.239

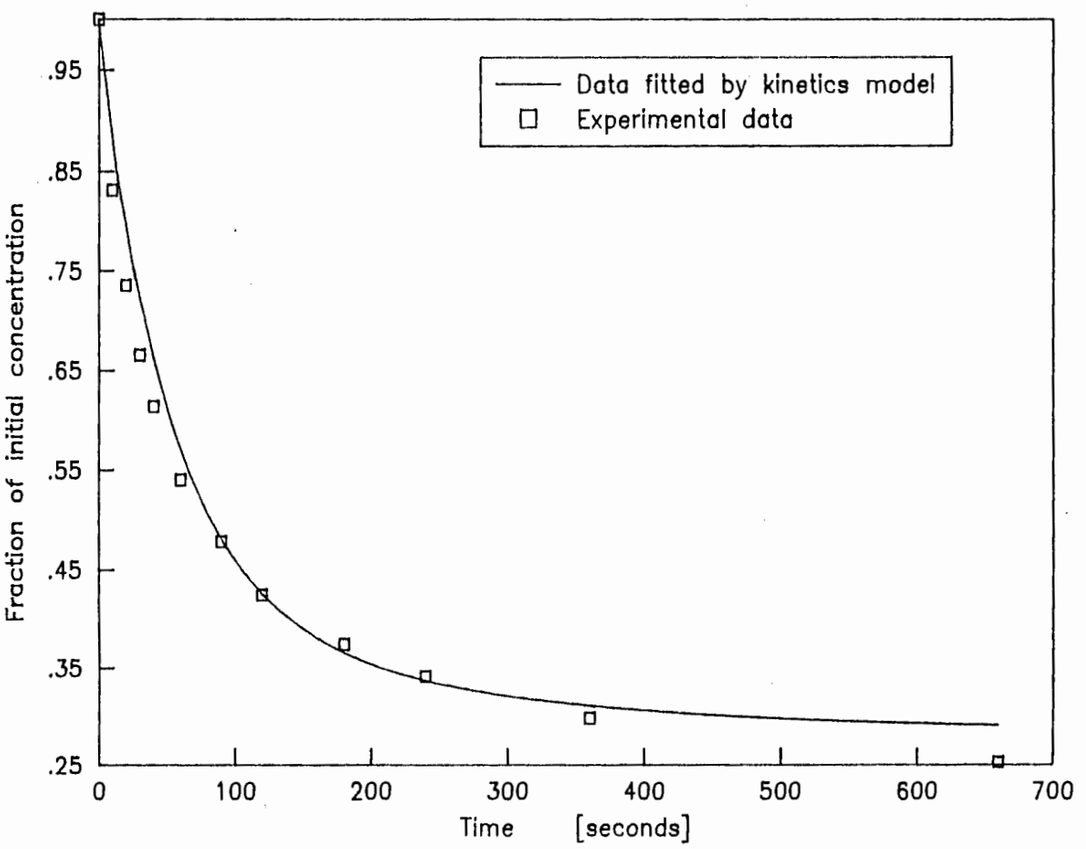

Figure 5.8 Rate of adsorption of cation exchanged D1/D2 effluent on XAD-8. Initial concentration = 1.0

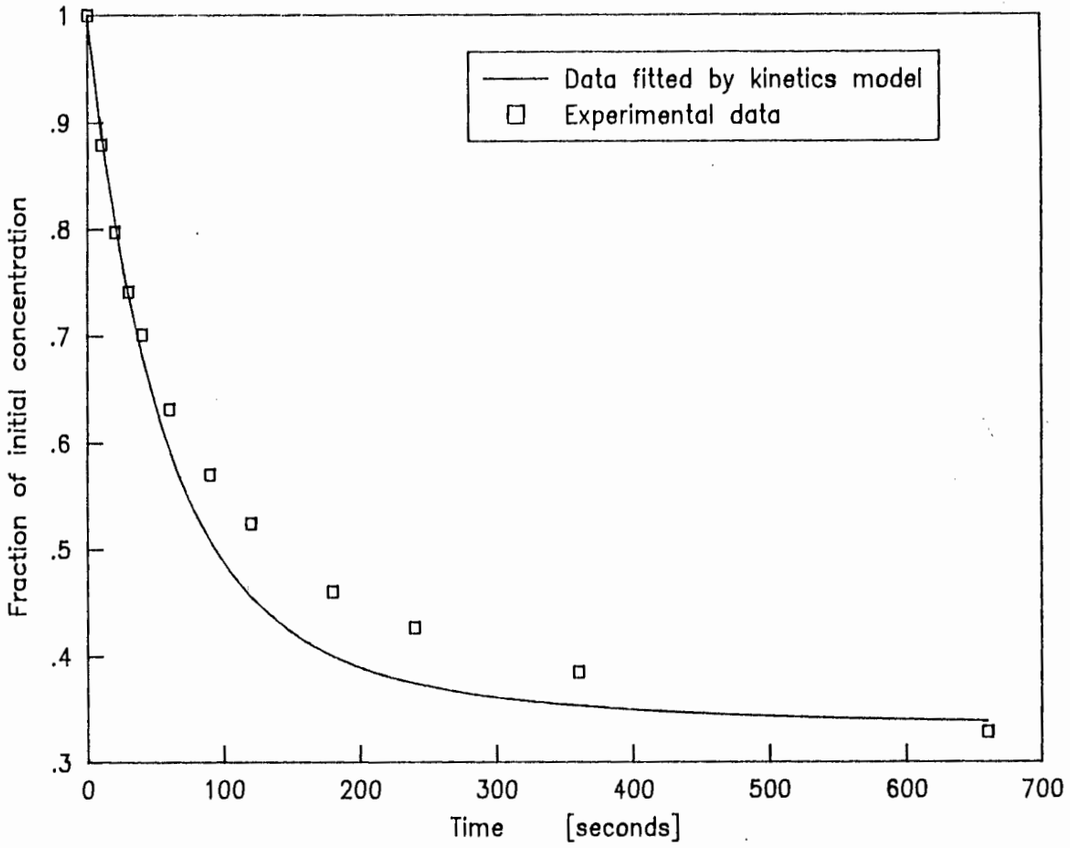

Figure 5.9 Rate of adsorption of cation exchanged D1/D2 effluent on XAD-8. Initial concentration = 1.0

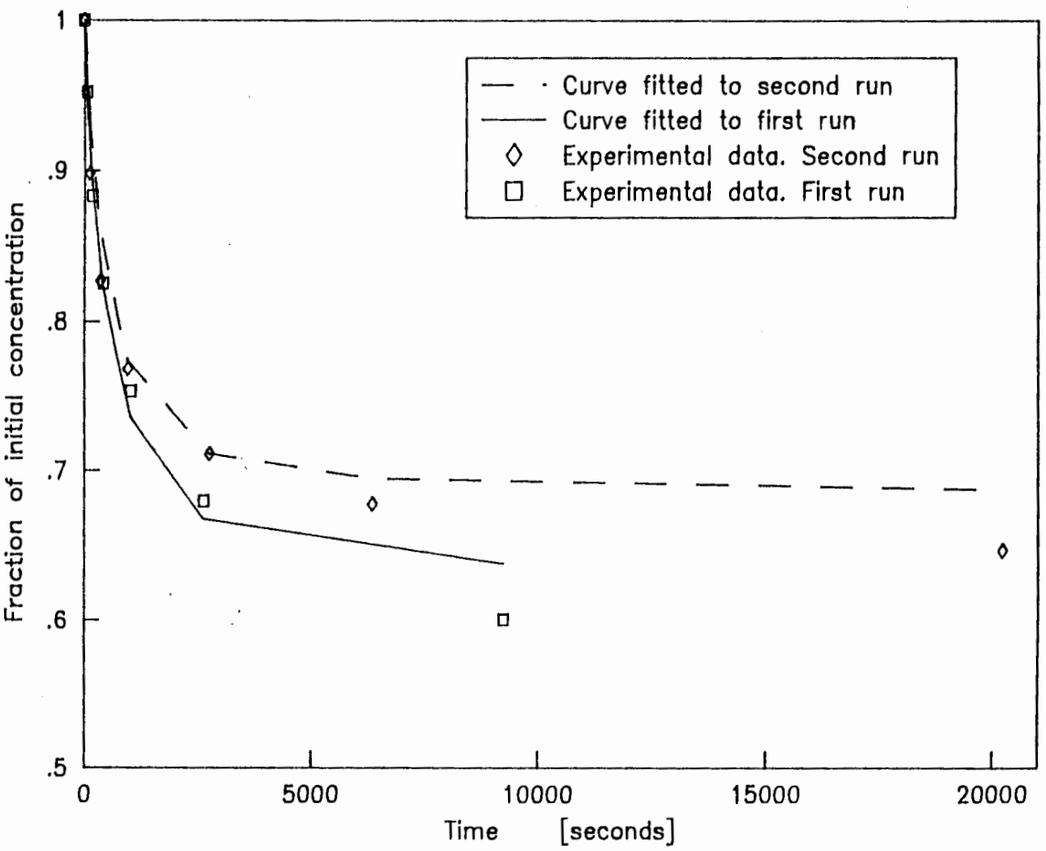

Figure 5.10 Rate of adsorption of D1/D2 effluent on 5 to 8.5E-4 m size fraction of XAD-8.

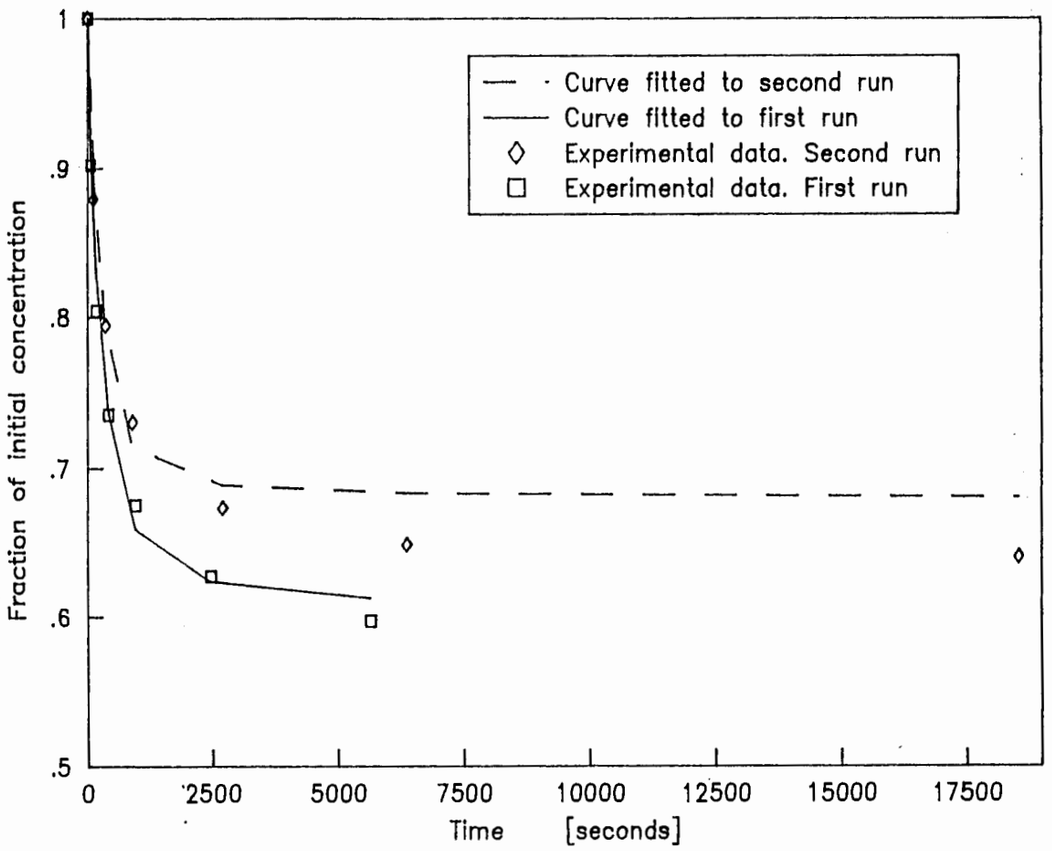

Figure 5.11 Rate of adsorption of D1/D2 effluent on 3 to 4.25E−4 m size fraction of XAD−8.

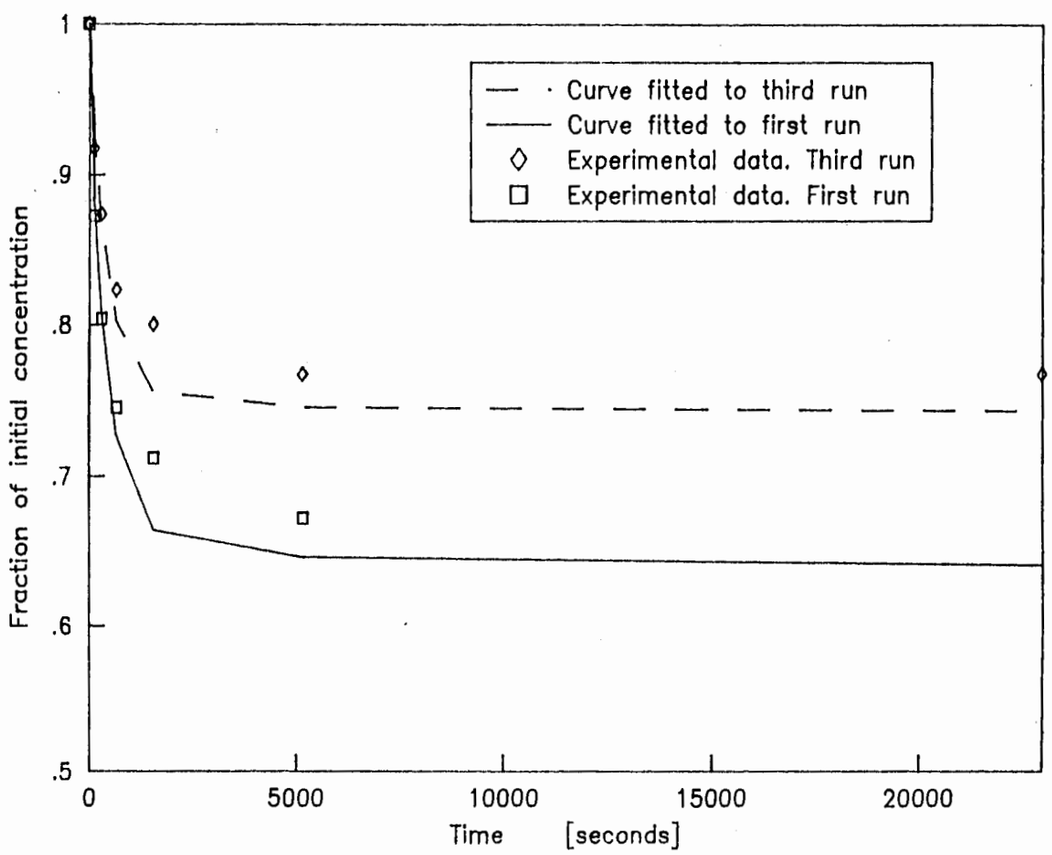

Figure 5.12 Rate of adsorption of D1/D2 effluent on 1.8 to 3E−4 m size fraction of XAD−8.

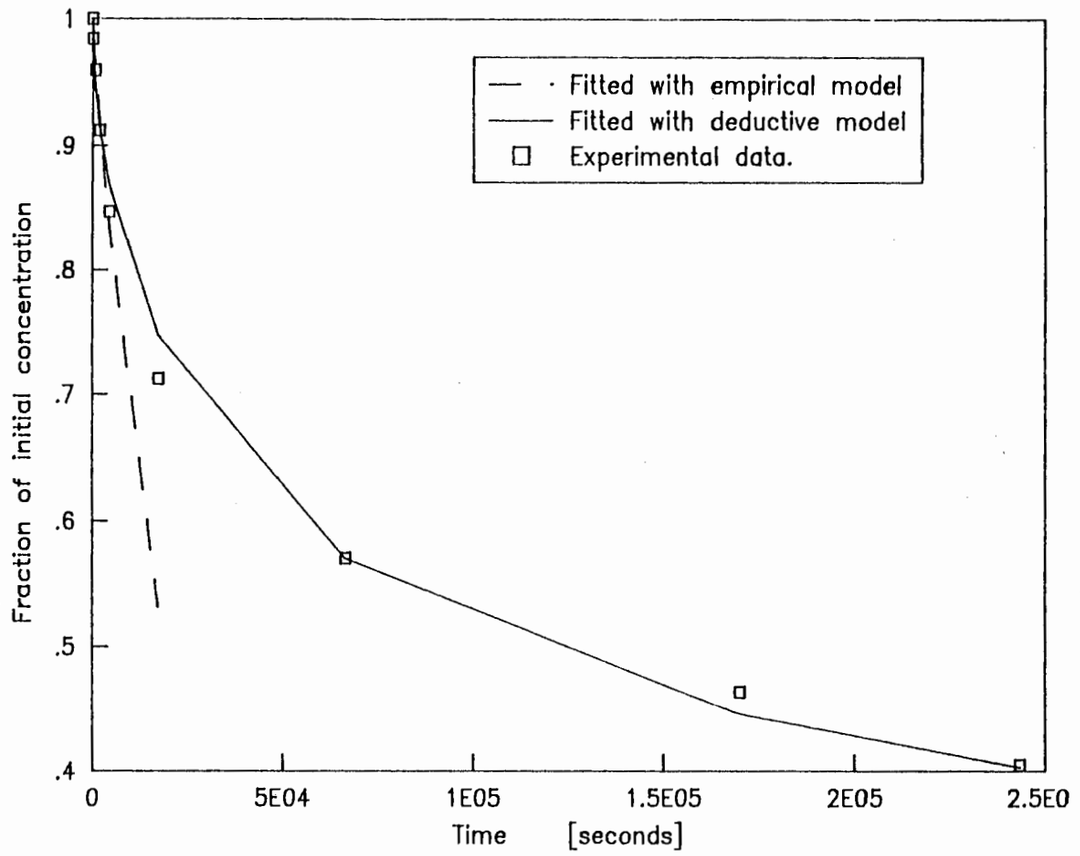

Figure 5.13 Rate of adsorption of cation exchanged D/C effluent on activated carbon, run 1.

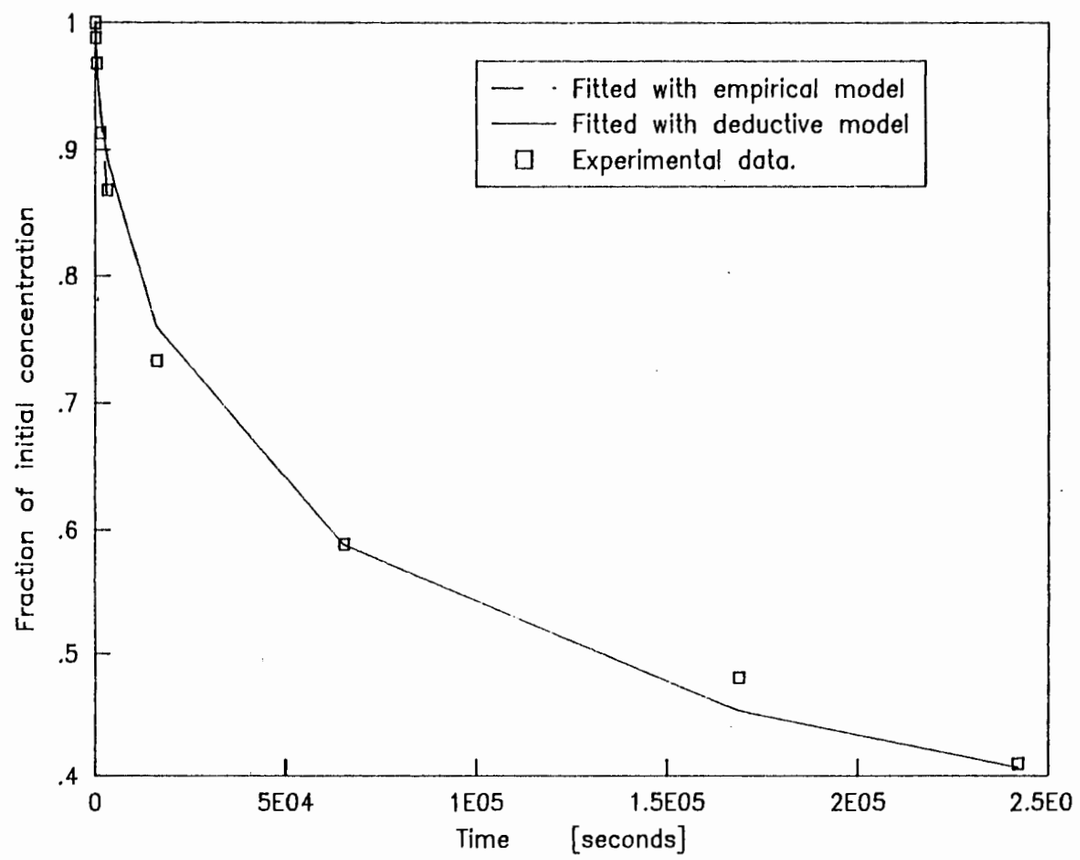

Figure 5.14 Rate of adsorption of cation exchanged D/C effluent on activated carbon, run 2.

Chapter 6

Design of counter-current contactors

The proposed method for removing organics from the pulping effluents was to use adsorbents in a counter-current contactor (CCC). The reasons for using a CCC and the reasons for choosing the Cloete-Streat design were mentioned in Chapter 2.

Three methods for modeling CCC columns were discussed in Chapter 2. The first method presented below was a graphical one which did not directly use adsorption rate data. It could therefore make no account for the column size, type of adsorbent, temperature or a number of other variables. The main advantages of the graphical method were its simplicity and its ability to show what the best possible contactor performance could be using the appropriate isotherm. The second method made use of an empirical rate equation. The third was a deductive model that was developed by assuming a mechanism of adsorption and then solving the equations that described this mechanism. This model was shown to be superior to the empirical model in Chapter 5. The empirical model was not considered in this chapter.

The first thing the CCC modeling program must do is to predict the amount of resin contained in each stage of the column. Each stage contains enough resin for the fluidized bed to fill approximately 95% of the stage. If the fluidized bed occupies a larger volume, resin gets carried up to the next stage. The space between the top of the bed and the top of the stage depends on factors such as the flow patterns out of the top of the stage and the size distribution of the adsorbent. Variations in the flow rate will also increase the space at the top of the stage. Having estimated the amount of resin held in each stage, the program then uses the experimentally determined rate constants and isotherms to estimate the concentration profiles in the column. The numerical analogs required for solving the kinetic equations are very similar to those required for the batch contacting system. Finally, the program is used to illustrate the potential performance of a number of column sizes.

6.1) Graphical method of column design

The theory of the graphical design method was explained in Chapter 2. The equation of the operating line was:

$$q = \frac{F}{F_s} (C - C_{n,p}) + q_{n,p+1} . \qquad (2.59)$$

Figure 6.1 shows the graphical design of a column which is set to pull the resin beds down when the out-flow concentration reaches 20% of the in-flow concentration. The operating line has a slope of 0.2075 and stepping off between this line and the isotherm shows that eight equilibrium stages are required. The isotherm is for the adsorption of cation exchanged D1/D2 bleach effluent on XAD-8. If the effluent flow rate is 0.29 l/s then the resin flow rate is 1.398 g/s. Substituting the following values in equation 2.59 produces the concentration of the adsorbent leaving the bottom of the column (stage 1) during a pull-down:

$F = 0.29$ l/s,
$F_s = 1.398$ g/s,
$C_0 = 1.0$ C/C_0,
$C_8 = 0.20$ C/C_0,
$q_9 = 0.0$ lC/C_0 g. (Resin entering the top stage (8) assumed to be perfectly regenerated).

Then $q_1 = 0.166$ lC/C_0 g. (Concentration of fully loaded resin)

Figure 6.2 shows the equivalent situation for an activated carbon column but with a carbon flow rate of 1.3775 g/s. The graphical method indicates that only 5 equilibrium stages are required to remove 95% of the organics from the effluent stream. The method does not show how difficult it is to achieve something approaching an equilibrium stage using activated carbon.

Looking at the isotherm for the adsorption of cation exchanged D1/D2 effluent on XAD-8, it can be seen that the required adsorbent flow rate depends mostly upon the required percentage removal of organics. The isotherm for adsorption of cation exchanged D/C effluent on activated carbon is much more favourably shaped for adsorption. The required

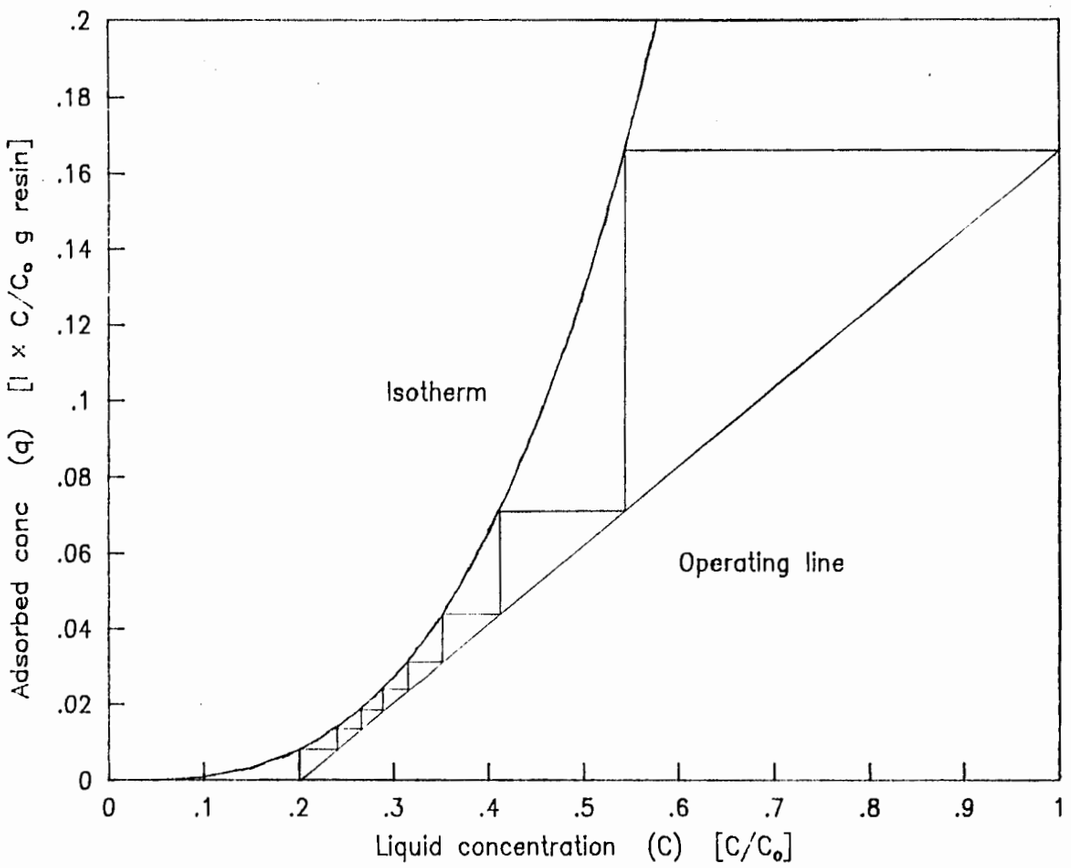

Figure 6.1 Graphical design of XAD–8 column for the removal of 80% of the organics from D1/D2 effluent.

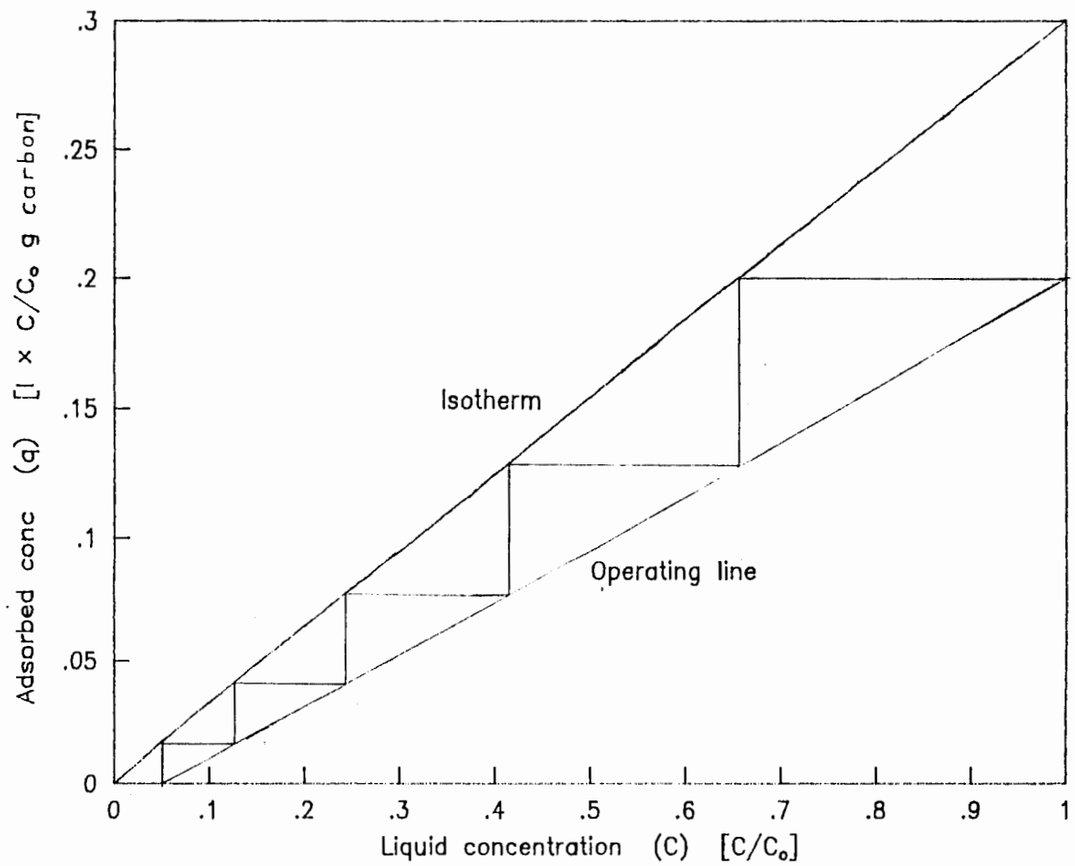

Figure 6.2 Graphical design of activated carbon column for the removal of 95% of the organics from D1/D2 effluent.

flow rate of activated carbon depends mostly on the number of stages. Packed beds behave like a large number of stages in series and their use may have to be considered when using activated carbon.

6.2) Settling in fluidized beds

6.2.1) Density of XAD-8 beads

The effective density of XAD-8 has been quoted as 1050 g/l by Rohm and Haas (1972), but later literature quoted the value as 1090 (Rohm and Haas, 1981). It was therefore decided to investigate the problem in more detail.

i) Matrix density: the manufacturer quotes the resin matrix of XAD-8 as having a density of 1230 g/l (Rohm and Haas, 1981; Van Vliet et al, 1980; Rohm and Hass, 1978). An experiment was done to find the density of the resin being used. Resin was put into a solution of sodium hydroxide, the concentration of which was adjusted until the resin was suspended in the solution with no tendency to float or sink. The density of the solution was then measured in a 0.05 l density bottle as 1203 g/l and a repeat of the experiment using another sample of resin in a 0.05 l volumetric flask gave a reading of 1197. The average was 1200 g/l ± 10 g/l at 20 °C.

ii) Particle porosity: the effective density depends on the matrix density, and the adsorbent porosity (voidage of adsorbent particle).

Van Vliet et al (1980) measured the particle porosity (ϵ_p) as 0.638 and the manufacturer (Rohm and Haas, 1978) quoted a value of 0.52. Experiments were done to find out which figure was more accurate.

Van Vliet measured the porosity by centrifuging the resin and measuring the amount of water retained. However, centrifuged resin agglomerated unlike dried resin. This suggested that water was retained on the surface of the beads as well as in the pores.

An estimate of the porosity was made using the opposite approach. Resin was dried and put into a weighed density bottle and re-weighed. The bottle was then filled with distilled water and weighed again. The hydrophobic nature of the resin stopped the water from entering the pores, but also made it difficult to remove the air trapped between the beads. After removing all the air that would come out of the bottle, the porosity was estimated by calculating the volume of air trapped in the resin. The result for ϵ_p was 0.47.

iii) Settling velocity: the final and most practical test was to find out what bead porosity gave the correct prediction of the fluidizing properties of the resin. The bed expansion of a fluidized bed of XAD-8 was tested in a 0.025 m ID column with 70.0 g of resin (dry mass) in it. Table 6.1 shows the results, assuming an average particle diameter of 4.6E-4 m ± 1E-5 m. (The particle diameter was previously estimated using a series of sieves; see Figure 4.1).

Table 6.1

Fluidizing XAD-8

Flow Rate $l/s \times 10^4$	Bed height [m]	Bed expansion %	Predicted bed height using porosities of: 0.56	0.57
0	0.45	0		
3.03	0.606	34.7	0.604	0.608
4.44	0.696	54.7	0.687	0.693
5.85	0.75	66.7	0.770	0.778
7.09	0.84	86.7	0.845	0.855

The predicted bed heights in the last 2 columns of the table were calculated using the theory explained above. If a porosity of 0.56 was used, the bed heights were more accurately predicted than if a porosity of 0.57 was used. This illustrated how

6.2.3) Example calculation

A pilot plant is proposed to treat 25 m^3/day or 0.29 l/s of effluent. This flow rate was chosen because it was the minimum flow rate required for the satisfactory operation of the ion exchange columns: the resin tends to bridge in smaller diameter columns used for lower flow rates. The XAD-8 adsorbent is less dense than the ion exchange resins and the particle size is smaller, so a larger column diameter has to be used. Much more than 100% fluidization is not generally desired because the smaller particles get carried out of the stages. Also the adsorbent hold-up becomes small. Much less than 100% fluidization requires a very large column diameter. The column diameter for the XAD-8 load column is therefore restricted to between 0.4 and 0.5 m: 0.4 m was assumed in this report. The properties of pure water were used for the calculations because those of the effluent were variable.

The column modeling program started by calculating the cross sectional area of the column which was 0.1257 m^2. The superficial velocity U_c was then calculated at 0.00231 m/s or 13.8 cm/min. The effective density of the beads was calculated to be 1087 g/l. The free falling velocity U_o was found from equation 2.60. Equation 2.60 needed a Renolds number which depended on U_o, so an initial guess for U_o was made at 0.008 m/s; Re = 3.75. The program iterated using the method of successive substitution until the correct values of U_o and Re were found. This took 5 iterations.

$$U_o = \frac{(4.6E\text{-}4)^2 * 9.81 * (1097 - 1000)}{18 * 9.8E\text{-}4 * (1 + 0.15 * Re^{0.687})}$$

$$= 0.00768$$

when Re = 3.60

U_t was the falling velocity corrected for the column (equation 2.61), and was very similar to U_o at 0.00766 m/s.

The voidage (ϵ_f) was calculated from equation 2.62 using the value of N calculated from equation 2.63:

$\epsilon_f = 0.735,$

$N = 3.89.$

The solid phase diffusion equation was:

$$\frac{N_{f\,i}}{r^2}\frac{\partial}{\partial r}\left(r^2\,\frac{\partial q}{\partial r}\right) = \left(\frac{\partial q}{\partial T_a} + \frac{\epsilon_p}{\rho_s}\frac{\partial \bar{c}_p}{\partial T_a}\right), \qquad (2.44b)$$

which was descritized to:

$$q_i = \frac{1}{(1+\Gamma_i)}\left[\frac{\Gamma_i}{2}\left[\left(1-\frac{\Delta r}{r}\right)q_{i-1} + \left(1+\frac{\Delta r}{r}\right)q''_{i+1}\right] - \frac{\epsilon_p}{\rho_s}(\bar{c}''_{p\,i}-\bar{c}'_{p\,i}) + b_i\right], \qquad (5.13)$$

where $b_i = q'_i + \frac{\Gamma_i}{2}\left[\left(1-\frac{\Delta r}{r_i}\right)q'_{i-1} - 2q'_i + \left(1+\frac{\Delta r}{r_i}\right)q'_{i+1}\right]$,

just as for the bulk contactor model except Γ_i was defined as:

$$\Gamma_i = \frac{\Delta T_a\, N_{f\,i}}{(\Delta r)^2}.$$

The conditions at the centre of the particle were given by equation 5.3a again, but with the dimensionless groups applicable for flow through systems.

$$\frac{\partial q}{\partial T_a} + \frac{\epsilon_p}{\rho_s}\frac{\partial \bar{c}_p}{\partial T_a} = \frac{3}{r^2}\frac{\partial}{\partial r}\left(r^2\,\frac{\partial q}{\partial r}\right) \qquad \text{at } r = 0. \qquad (6.3)$$

The numeric analog was therefore equation 5.15.

$$q_i = \frac{q'_i + \Gamma_i\,(q'_2 - q'_i) - \frac{\epsilon_p}{\rho_s}(\bar{c}''_{p\,i} - \bar{c}'_{p\,i}) + \Gamma_i\,q''_2}{(1+\Gamma_i)}. \qquad (5.15)$$

The only difference was that Γ_i was defined as:

$$\Gamma_i = \frac{3\,\Delta T_a\, N_{f\,i}}{(\Delta r)^2}.$$

The boundary condition at the particle surface was:

$$St_f\,(\bar{c} - \frac{q_e}{C_0}\,\bar{c}_{p\,m}) = \frac{\partial}{\partial T_a}\int_0^1 r^2\left(q + C_p\,\frac{\epsilon_p}{\rho_s}\right)dr, \qquad (2.58)$$

where $St_f = \frac{K_s\,(1-\epsilon_f)\,\tau}{(R_p\,\epsilon_f)}$ = Stanton number for flow through systems.

Its numerical analog was:

$$q_M = b_M + \frac{2St_f \Delta T_s}{\Delta r}\left(c' - c'_{p,M}\frac{q_s}{C_0}\right) - 2\sum_{i=2}^{M-1}\left(q_i + c_{p,i}\frac{\epsilon_p}{\rho_s}\right) r_i^2 - c''_{p,M}\frac{\epsilon_p}{\rho_s}, \tag{6.5}$$

where $b_M = 2\sum_{i=2}^{M-1}\left(q'_i + \frac{\epsilon_p}{\rho_s} c'_{p,i}\right) r_i^2 + \left(q'_M + \frac{\epsilon_p}{\rho_s} c'_{p,M}\right).$

The bulk material balance for the column was:

$$c_i = c_{i-1} - \left(\frac{\epsilon'}{Dg_f}\frac{\partial c_i}{\partial T_s} + \epsilon'\frac{\partial q_{s,v}}{\partial T_s} + \frac{\epsilon_p \epsilon'}{\rho_s}\frac{\partial c_{p,s,v}}{\partial T_s}\right). \tag{2.42}$$

The definitions of $q_{s,v}$ and $c_{p,s,v}$ (dimensionless forms of equations 2.46 and 2.47) were substituted into this equation to give:

$$c_i = c_{i-1} - \frac{\epsilon'}{Dg_f}\frac{\partial c_i}{\partial T_s} - 3\epsilon'\frac{\partial}{\partial T_s}\int_0^1 r^2\left(q + C_p\frac{\epsilon_p}{\rho_s}\right) dr. \tag{6.6}$$

Substituting equation 2.58 into equation 6.6 and descritizing produced:

$$c_i = c_{i-1} - \frac{\epsilon'(c_i - c'_i)}{Dg_f\ \Delta T_s} - 3\epsilon_f St_f (c_i - c_{p,M}\frac{q_s}{C_0}).$$

Applying the Gauss-Seidal algorithm this became:

$$c_i = \left[c'_{i-1} + \frac{\epsilon' c'_i}{Dg_f\ \Delta T_s} - 3\epsilon' St_f\left(c'_i - c'_{p,M}\frac{q_s}{C_0}\right)\right]\frac{Dg_f\ \Delta T_s}{\epsilon' + Dg_f\ \Delta T_s}. \tag{6.7}$$

When the film diffusion was negligible equation 6.6 was used directly. The numeric analog was:

$$c_i = \left[c''_{i-1} - \frac{3\epsilon_f \Delta r}{\Delta T_s}\left[\sum_{i=2}^{M-1}\left(q_i - q'_i + \frac{\epsilon_p}{\rho_s}(c_{p,i} - c'_{p,i})\right) r_i^2 + \frac{1}{2}\left(q''_M - q'_M + \frac{\epsilon_p}{\rho_s}(c''_{p,M} - c'_{p,M})\right)\right]\right.$$

$$\left. + \frac{\epsilon_f c_i}{Dg_f \Delta T_s}\right]\frac{\Delta T_s\, Dg_f}{\Delta T_s\, Dg_f + \epsilon'}. \tag{6.8}$$

q_M was then determined using the isotherm relation on the value of c_i just determined.

6.4) The column modeling program

The program for calculating the performance of the column is shown in Appendix 8. The program is coded in Turbo Pascal for an IBM AT, but a version was coded for a Sperry Univac 1100 mainframe computer because it was taking too long to run on the IBM AT.

To help the reader follow the logic of the program, the pascal commands are written in capitals. The program variables only make selective use of capitals. The units used by the program are Kg and m^3 instead of g and l used previously. This is because of the larger scale of the pilot plant being modeled.

The program first calculates the bed expansion expected in the column given the flow rate, column diameter and data for the resin. It then proceeds to calculate the concentration profiles in each stage of the column. It starts at the bottom stage (number 1) and works to the top. It then increments the time and works up through the column again. When the concentration of processed effluent from the top of the column exceeds a pre-set value, it simulates a pull-down in the column.

6.5) Results using the column modeling program

6.5.1) XAD-8 as adsorbent

The experimental data provided no correlation between Renolds number and the film diffusion coefficient. All diffusion coefficients were therefore used directly from experimental results: K_f = 1.7E-5, D_{s0} = 5.9E-12, α = 0.1. These values were entered into the column modeling program and table 6.3 shows some of the results. The third column shows the concentration at which the program was set to simulate a pull-down and the fith column is the time it took to reach this concentration after initially being loaded with clean resin. The forth column shows the solid phase concentration of the resin leaving the bottom of the column after steady state had been achieved. The sixth column also reflects steady state results. The final column was included to illustrate a limitation on the time between pull-downs. When resin leaves the column, it carries effluent from the first stage with it. Because XAD-8 must be kept wet, it was assumed that the volume of effluent removed with the

resin was just sufficient to cover the settled bed. This volume of effluent goes to the regeneration column and is not recovered, so the seventh column reflects the significance of this carry over.

Table 6.3

Predicted counter-current column performance

Number of stages	Average out-put conc. C/C_o	Final out-put conc. C/C_o	Loaded resin conc. q/q_o	Time to first pull-down [min]	Average time between pull-downs [min]	Percentage of in-flow volume recovered
4	0.0851	0.10	0.0222	47.5	24.1	90.6
6	0.0863	0.10	0.0347	98.6	37.3	93.9
10	0.0872	0.10	0.0439	211.9	46.5	95.1
4	0.1250	0.15	0.0548	100.6	61.0	96.3
6	0.1272	0.15	0.0760	181.5	85.3	97.3
10	0.1278	0.15	0.1027	354.8	92.7	97.6
4	0.1489	0.18	0.0804	180.8	91.7	97.5
6	0.1531	0.18	0.1213	348.7	134.8	98.3
10	0.1545	0.18	0.1492	719.2	156.2	98.5

Figure 6.3 shows how the time between pull-downs varies with average output concentration for columns with 4, 6 and 10 stages. This is an important figure because it shows what performance the column modeling program predicts for the proposed pilot plant.

Figures 6.4 and 6.5 show graphically how the program predicted the concentrations in each of the 6 stages used to remove 88% of the organic compounds. Figure 6.4 uses the values averaged over the period between pull-downs. It therefore accurately reflects the average out-flow concentration but the resin leaving the bottom of the column has a concentration higher than the 0.0514 indicated. Figure 6.5 reflects the values just before a pull-down. It therefore accurately reflects the concentration of the resin leaving the column, but does not reflect the true quality of the out-flow.

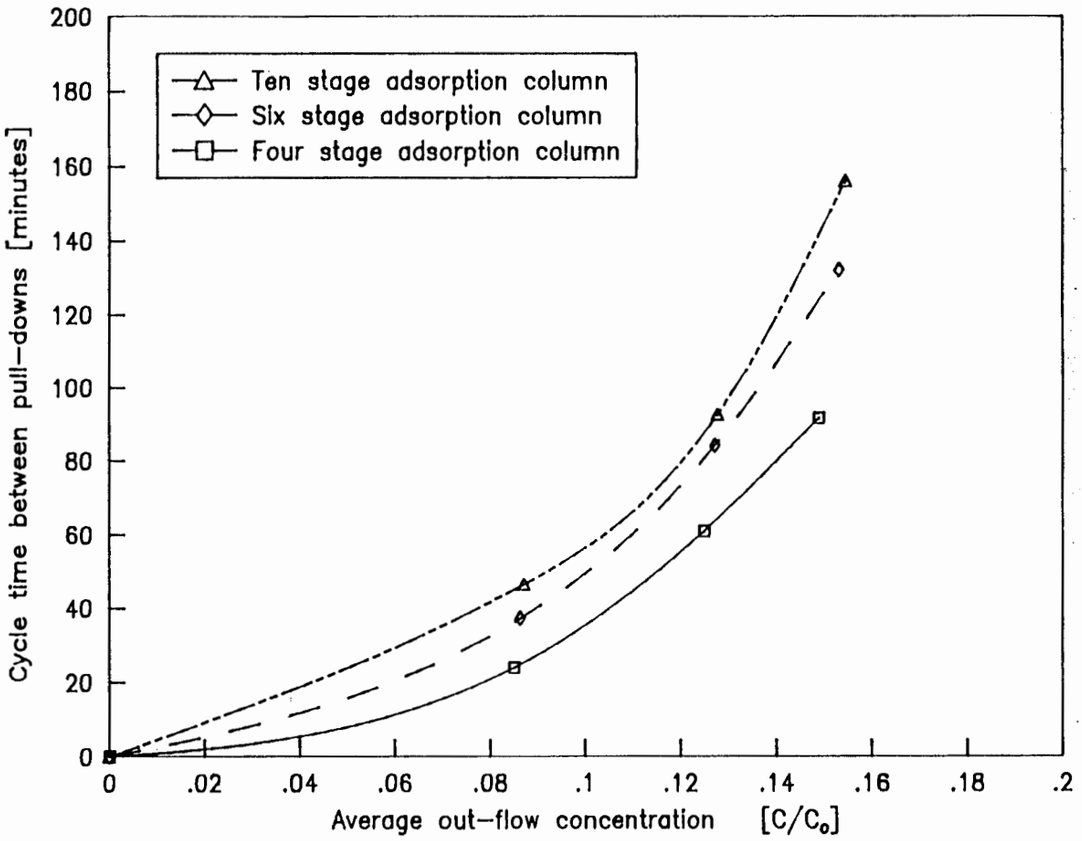

Figure 6.3 Cycle time between pull-downs vs. average out-flow concentration for XAD-8 columns with 4, 6 and 10 stages

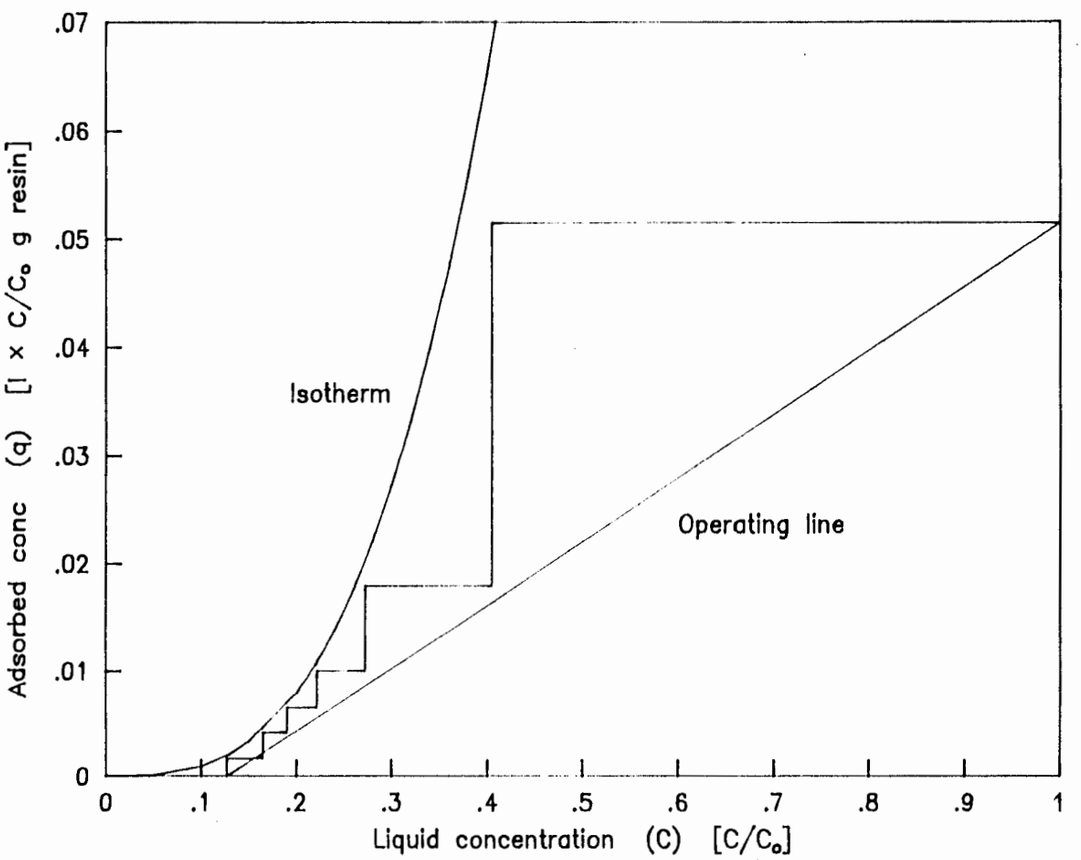

Figure 6.4 Results from column modeling program averaged between pull-downs. 6 stages & 85.3 minutes between pull-downs.

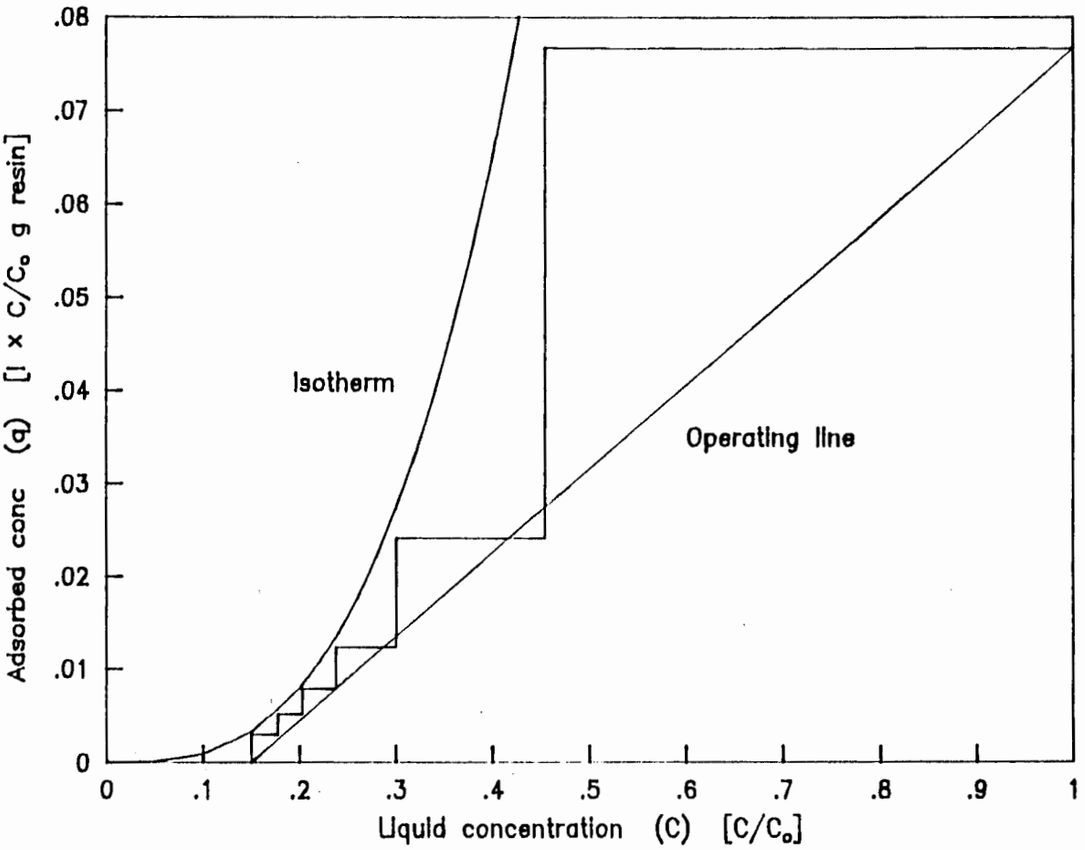

Figure 6.5 Results from column modeling program just before pull-down. Six stages and 85.3 minutes between pull-downs.

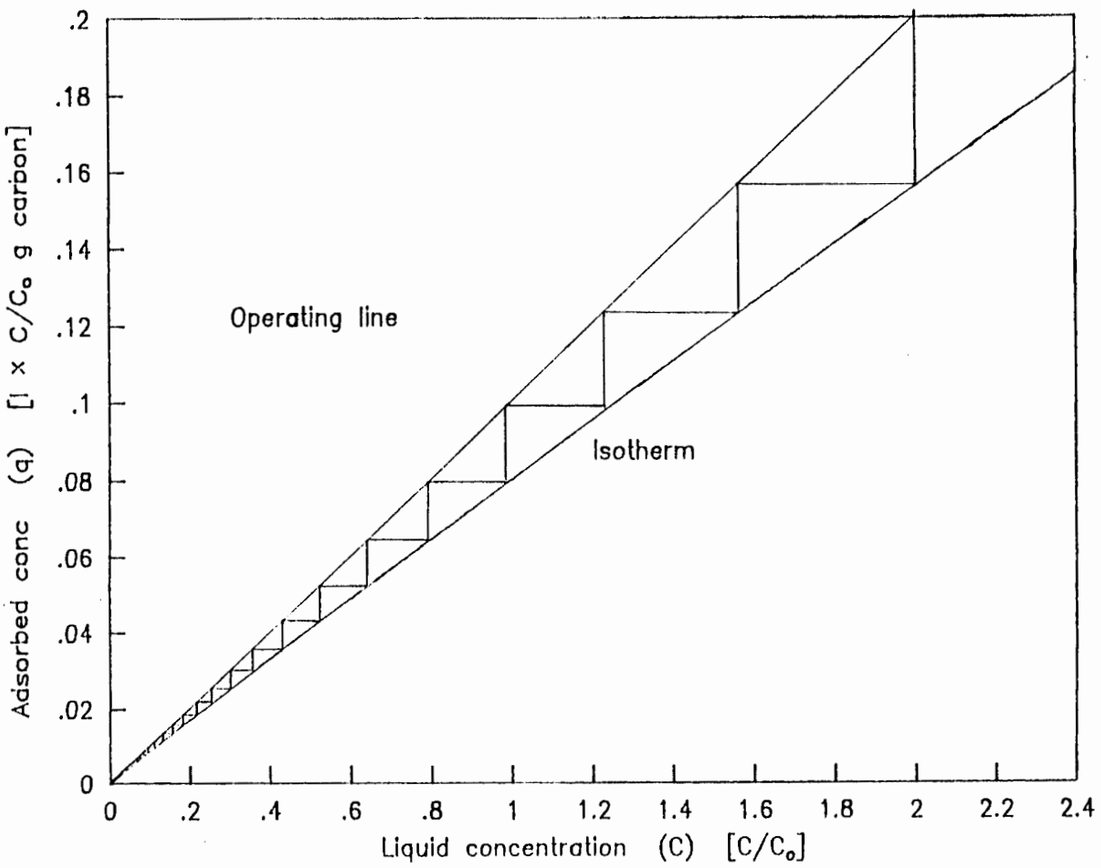

Figure 6.6 Graphical design of regeneration column for activated carbon loaded with 0.2 l x C/C$_o$ g carbon.

The results also show that columns using XAD-8 do not require many stages. The rapid adsorption kinetics mean that a completely mixed stage comes very close to equilibrium. Because of the shape of the isotherm, there is a very definite pinch-point. Therefore at a fixed resin flow rate, the benefit of adding more stages is small. More detailed results are given in Appendix 8 after the program.

6.5.2) Activated carbon as adsorbent

The activated carbon tested had a larger particle diameter and a higher matrix density than XAD-8. It therefore settled much faster and there was more freedom of choice of column diameter. However, the column design program required stages to be over 10 m high: smaller stages did not come anywhere near equilibrium because of the slow rate of adsorption. It was therefore decided that the carbon particle size would have to be reduced to a point where a reasonable amount of fluidization (10 to 100 percent) would occur in a 0.4 m column: the same size as the proposed XAD-8 column. An average diameter of 0.0002 m was found to give 116% fluidization, and the carbon hold-up was 32.7 Kg per 1 m high stage. The program predicted that a ten stage column would take 1270 minutes before the out-flow concentration would reach 0.05. The problems became apparent when the pull-downs started, because the average time between pull-downs was 40 minutes. This was not nearly enough time for the carbon to load efficiently. Therefore, a CCC using carbon would need at least 20 stages.

6.6) Regeneration of the adsorbents

Any economic evaluation of an adsorption process needs to take careful account of the regeneration step. The manufacturer (Rohm and Haas, 1972) and Kennedy (1973) claim that a bed of XAD-8 loaded with bleach effluent can be fully regenerated with less than 4 bed volumes of weak wash. (Weak wash is a weak sodium hydroxide solution used in the wood pulping process). They estimate that the quantity of weak wash need only be increased 10% to accommodate the XAD-8 regeneration step. The weak wash is then burnt in the recovery furnace. The concentration of organics in the weak wash is so high that the latent heat of vapourization of the water is less than the heat recovered from burning its organic load. The sodium hydroxide is recovered by the electrostatic precipitators on the

furnace. This together with the fact that no change in performance was reported after 400 load-regenerate cycles means that the net operating cost of their adsorption process is very low.

Since the regeneration isotherm for the effluent on XAD-8 was not measured, an accurate design of the regeneration stage could not be performed. However, based on the results presented by Rohm and Haas (1972) and Kennedy (1973), it could be assumed that 1.5 bed volumes of 0.1 N sodium hydroxide would be more than sufficient to regenerate the resin. The settled bed volume of the pilot plant load stage was to be 53.6 l. For the proposed plant with 6 stages and 132 minutes between pull-downs, the required regenerant flow rate would be 0.0102 l/s or 0.88 m^3/day. Assuming complete regeneration of the resin, the alkaline regenerant stream would carry an organic load 25 times that of the original bleach effluent.

Tests from this work showed that the rate of desorption was at least as fast as the rate of adsorption. Since the regeneration isotherm probably has the same shape as the loading isotherm, it should be favourably shaped for regeneration. It is therefore proposed that the pilot plant be built with only three stages for contacting the resin with sodium hydroxide and three stages for rinsing. A column diameter of 0.18 m would give about 11% fluidization which is about the minimum that can be used without danger of the bed plugging. To hold all the resin from the load column, the regeneration column would need stages 2.47 m high. To allow for the expected higher density and viscosity of the solution in this column, a stage height of at least 2.5 m should be allowed.

The regeneration isotherm for activated carbon was measured. Figure 6.6 shows the graphical design of a regeneration column for the carbon loaded as indicated by Figure 6.2. Figure 6.6 shows that the regenerant stream has a concentration of twice the original effluent's (as opposed to 25 times for XAD-8). On this bases, sodium hydroxide can be eliminated as an alternative for regenerating activated carbon.

Chapter 7

Conclusions.

7.1) Anion resin foulants

Several compounds were identified as anion resin foulants. Their presence in SAPPI's bleaching effluents and their potential for fouling anion resins was established from the results of a single test. To establish their role beyond doubt, further tests would be required. The compounds were:

oxalic acid,
anthraquinone,
palmitic (hexadecanoic) acid,
14-methylhexadecanoic acid,
9,12-octadecadienoic acid,
stearic (octadecanoic) acid,
isophthalic acid.

Compounds less positively identified as foulants were:

numerous long chained carboxylic (fatty) acids,
dulcitol, sorbitol or other monosaccharides,
2,4-tertiary butyl-6-methyl phenol and other phenol derivatives,
derivatives of anthraquinone.

Many of these compounds were known to have calcium salts with very low solubilities in water. This suggested that the formation of insoluble calcium salts within the anion resin was an important cause of fouling. Most of the compounds mentioned above with the exception of oxalic acid and the monosaccharides had a low solubility in water. Since the capacity of XAD-8 for a particular compound had been shown to be inversely related to its solubility, XAD-8 would probably remove most foulants very effectively (Przyjazny, 1985; Thurman et al, 1978).

Oxalic acid and the monosaccharides will probably prove to be the most difficult anion resin foulants to adsorb. Since the presence of monosaccharides in the bleaching effluent and their fouling potential

for anion resins was not well established, oxalic acid was the compound of most interest. A separate test for its potential to foul anion resins showed that it did cause fouling. Oxalic acid is a strong acid with $pKa_1 = 1.27$. This means that any adsorption step that removes oxalic acid is likely to cause a substantial rise in the pH of the solution. This might create problems with the weak anion exchange step for the removal of chlorides.

7.2) Testing the anion resin fouling capacity of compounds

An experiment was performed using the life testing apparatus at Enstra to confirm if oxalic acid is a significant foulant for anion resins. The A378 anion resin used showed a 20% drop in capacity after oxalic acid had been removed from it once by regeneration with calcium hydroxide. This showed that oxalic acid is a foulant, and that its concentration should be carefully monitored in the pilot plant (for testing the proposed system of ion exchange/adsorption for bleach effluent treatment).

7.3) Isotherm equations

Of the many isotherm equations considered, the Dubinin isotherm seemed to be the best for most applications. It was shown to accurately fit the single compound adsorption data from this work and others. It could predict the effect of changing temperature and pH and it also had a limited ability to predict untested isotherms. Being derived from the Polanyi theory of adsorption, it could be easily adapted to model multicomponent isotherms using the theories of multicomponent adsorption based on the Polanyi theory. Finally the equation could be written as a function of the liquid or the solid phase concentration. This was a very valuable feature for the adsorption kinetics modeling program. When modeling the adsorption of a multicomponent effluent as a single component, the Freundlich equation was found to be more suitable.

7.4) Measurement of isotherms

A number of isotherms were measured using U.V. absorbence to determine the solution concentrations. This analytical method was found to be very sensitive to interference from compounds slowly released from XAD-8.

There were several other sources of interference, but careful experimental technique reduced them to an acceptable level. U.V. absorbence was not ideally suited for multicomponent concentration measurement because compounds with large extinction coefficients dominated the results. A more versatile analytical method was urgently required and HPLC was recommended.

XAD-8 was found to be very difficult to clean by this worker and others. The use of soxhlet extraction and ultrasound to clean XAD-8 was found to be very effective.

The experimental method used to measure the isotherm of the bleaching effluent was designed to reflect the situation in a C.C.C. The results showed that a multicomponent model was needed to satisfactorily model the adsorption of complex mixtures. Balzli et al (1978) came to the same conclusion.

7.5) Adsorption kinetics

A diffusion rate model for adsorption kinetics was developed and found to fit the data better than an empirical adsorption model developed earlier. The diffusion model was therefore used extensively despite the fact that it used a large amount of computer time.

The solid phase diffusion coefficient for phenol and oxalic acid was found to be concentration dependent. The equation used to describe this dependence was not completely satisfactory because the model did not fit the data well when it covered a wide concentration range. The coefficient for the cation exchanged D1/D2 effluent appeared to be only slightly concentration dependent.

The speed of the spinning basket used to measure adsorption rates could not be accurately controlled. Therefore the velocity of fluid flowing past the resin could not be determined and the correlation between the film diffusion coefficient and the fluid flow rate could note be measured. Also it was suspected that the fluid flow rate was not uniform in the bed of resin in the basket.

7.6) Design of counter-current contactors

Each stage of the C C C was modeled as a mixed tank. This was a worst case model and the actual performance would be better. It was found that columns using XAD-8 came very close to equilibrium in each stage. It was therefore possible to design such a column using the convenient graphical method illustrated in Chapter 6. Both this graphical design method and the numerical model results showed that the required flow rate of XAD-8 was mainly dependent on the quality required of the processed effluent. Adding more stages to columns using XAD-8 helped but to a limited extent.

Columns using activated carbon did not appear to be feasible. The diffusion in the carbon was so slow that very large columns would be required to achieve the ideal residence time (about 2 to 4 days).

A multicomponent model of the column was not developed because the numerical efficiency of the single component kinetics model had to be improved first.

Chapter 8

Recommendations

8.1) Anion resin fouling

The anion resin fouling problem needs to be studied using a pilot plant. The suggested approach is as follows:

i) Place an XAD-8 adsorption step between the cation and the anion exchange steps. The XAD-8 should remove about 85% of the organics.

ii) If the XAD-8 treated effluent still causes fouling, try cleaning the fouled anion exchange resin periodically. Tilsey (1979) found that treating fouled anion resin with sodium chloride, hydrochloric acid or sodium hypochlorite (1% free chlorine) could relieve the problem. Calcium oxalate may make up a large proportion of the compounds fouling the resin, and it dissolves in hydrochloric acid. Therefore, soaking the resin in hydrochloric acid and regenerating with sodium hydroxide is likely to be effective. The use of ultrasound to aid the removal of foulants could also be tested.

iii) A styrene-divinylbenzene anion resin was originally proposed for the pilot plant. If fouling of this resin cannot be prevented by the above two steps, then a methacrylic anion resin should be tried. These resins are more expensive, but they are less easily fouled and they have faster kinetics. They may therefore prove to be more economical.

iv) The use of activated carbon for organic removal should be the last resort because regenerating the carbon is costly and a large inventory is required. The carbon could be used to polish the effluent treated by XAD-8, or it could be used by itself. Without a multicomponent model, the better system could not be predicted.

Oxalic acid is probably the critical anion resin foulant. Its presence in the processed effluent leaving the adsorption stage and entering the anion exchange stage must be monitored. A convenient and specific test for it must therefore be found. The use of HPLC is recommended, possibly using techniques described by Libert (1981).

If the pilot plant data shows that compounds besides oxalic acid are important foulants, then attention needs to be given to their analysis. The use of glass capillary GC columns and high resolution mass spectrometry has been shown to be very effective for the analysis of complex mixtures of organic acids (Lewis et al, 1979), and is recommended. Zinkel and Engler (1977) found that glass was better than stainless steel for GC columns used for analysing sensitive carboxylic acids. They also found that tertiary-butyl derivatives where the most suitable of those they tested. Having identified the foulants, their fouling capacity could be tested using the technique described in Appendix 2.

8.2) Choice of adsorbent for recovering organic compounds

It is recommended that XAD-8 (or a similar adsorbent such as XAD-1180) be used in the pilot plant to protect the anion resin. Figure 4.17 shows that XAD-8 has a very high capacity for organic compounds in the bleaching effluent at high liquid concentrations. Activated carbon performs much better at low concentrations. It is therefore suggested that the use of activated carbon only be considered if data from the pilot plant shows that more than 85 to 90% organics removal is required.

Efficient regeneration is the key to the adsorption step. XAD-8 has been shown to be very efficiently regenerated by sodium hydroxide. Activated carbon on the other hand is so inefficiently regenerated by caustic that

the flow in the regeneration stage would have to be no less than one third of that of the effluent being processed.

Grinding the adsorbents to increase the rate of adsorption has been considered. It is not recommended for XAD-8 because the adsorption rate is already high enough. With activated carbon, the required particle size would be so small that the powder would be difficult to control.

8.3) Future experimental work

Cooling the effluent entering the adsorption stage and heating the wash water entering the regeneration stage may prove to be economically worth-while. Therefore experimental confirmation of the effect of temperature on effluent adsorption could be useful.

The suggested apparatus for further adsorption studies is a micro-column about 0.02 m long and 0.02 m diameter. A number of recent workers have adopted this method (Van Vliet, 1987; Cornel et al, 1986; Aguwa et al, 1984; Mateka and Eliasek, 1982; Weber and Liu, 1980). It is sensitive to the values of both the film and the solid phase diffusion coefficients, so the effect of the superficial flow rate could be studied. The resin would be cleaned, loaded and regenerated without having to move it out of the column. This has been shown to decrease the release of contaminants (Olufsen, 1980; Junk et al, 1974). The column could be put in an ultrasound bath where it could be heated and subjected to ultrasound at the same time to get it very clean in a reasonable time. This reduction of the contamination problem would allow the measurement of the isotherms of sparingly soluble compounds that could not be measured in this work. Analysing the results would be numerically intensive, but the equations would be very similar to the column modeling equations presented here. A problem would be the time required for the regeneration of the resin. A system for regenerating several columns at once would be needed.

8.4) The column modeling program

Computer programs for finding the diffusion coefficients from experimental data and for designing adsorption contactors have been coded. They require a lot of computer time and attention needs to be given to making them more efficient. Once this has been done they could be extended to model multicomponent adsorption.

The programs were not used to model desorption, but could easily be adapted to do so. Ortlieb et al (1981) found that the desorption step had to be modeled at the same time as the adsorption step for an accurate simulation of a CCC A complete column modeling program would therefore model both columns at the same time.

8.5) Construction of a pilot adsorption plant

At the time of writing, the first part of the pilot plant (cation exchange section) was nearing completion. The second part (adsorption section) was still to be designed. The following suggestions were made for this design. The column should use XAD-8 in 6 stages, 0.4 m in diameter and 1 m high. If 85% organics removal is required, a pull-down is required every 132 minutes. The suggested regeneration column has 6 stages, 0.18 m ID and 2.5 m high. 3 stages would be used for regeneration and 3 for rinsing the resin. The final column design must bear in mind the need to keep the XAD-8 wet at all times.

If the use of activated carbon is found to be essential, some methods for reducing costs could be considered. Van Vliet and Venter (1984) reported the use of infrared to thermally regenerate activated carbon. Picht et al (1982) used supercritical carbon dioxide to regenerate several adsorbents. Mathews and Fan (1983) found that semifluidized beds closely approached the performance of a packed bed, but retained the advantages of a fluidized bed. A series of semifluidized beds of activated carbon may give the required adsorption performance.

REFERENCES

Aiken G.R., (1979), "Comparison of XAD macroporous resins for the concentration of fulvic acid from aqueous solution", Analytical chemistry, 51, no. 11, pp 1799 - 1803.

Albert A. and Serjeant E.P., (1962), "Ionization constants of acids and bases", Methuen & co., London.

Augwa A.A. et al, (1984), "Estimation of effective intraparticle diffusion coefficients with differential reactor columns", J. Water P. C., 56, no 5, pp 442 - 448.

Beaven G.H., Johnson E.A., Willis H.A. & Miller R.G.J., (1961), "Molecular spectroscopy", Heywood & co., London.

Betz, (1976), "Handbook of industrial water conditioning", 7th ed.

Bird R.B., Stewart W.E. and Lightfoot E.N., (1960), "Transport phenonena", John Wiley and sons, New York.

Boening P.H., Beckmann D.D. and Snoeyink V.L., (1980), "Activated carbon versus resin adsorption of humic substances", J. Am. Water, 72, no 1, pp 54 - 59.

Brownlee B. and Strachan W.M., (1976), "Persistent organic compounds from a pulp mill in a near-shore freshwater environment", in Keith L.H., "Identification and analysis of organic pollutants in water", Ann Arbor science, chapt 35, pp 661 - 667.

Buijs A. and Wesselingh J.A., (1981), "Batch fluidized ion-exchange column for streams containing suspended particles", Journal of Chromatography, 201, pp 319 - 327.

Butler J.A.V. and Ockrent C., (1930), "Studies in Electrocapillarity III.", Journal Physical Chemistry, 34, 2841.

Calligaris M. and Tien C., (1982), "Species grouping in multicomponent adsorption calculations", The Canadian Journal of Chemical Engineering, 60, pp 772 - 780.

Campbell Dr., (1985), Hewlett packard, Cape Town, personal communication.

Chiou C.C.T. and Manes M., (1973), "Application of the Polanyi adsorption potential theory to adsorption from solution on activated carbon. 4. Steric factors as illustrated by the adsorption of planar and octahedral acetylacetonates", Journal Physical Chemistry, 77, no 6, pp 809 - 813.

Chiou C.C.T. and Manes M., (1974), "Application of the Polanyi adsorption potential theory to adsorption from solution on activated carbon. 5. Adsorption from water of some solids and their melts, and a comparison of bulk and adsorbate melting points", Journal Physical Chemistry, 78, no 6, pp 662 - 626.

Cloete F.L.D., (1984), "Comparative engineering and process features of operating continuous ion exchange plants in Southern Africa", in "Ion exchange technology" by Naden D. and Streat M., Ellis Horwood ltd. Chichester.

Cornel P. and Sontheimer H., (1986), "Sorption of dissolved organics from aqueous solution by polystyrene resins. I. Resin characterization and sorption equilibrium", Chemical Engineering Science, 41, No 7, pp 1791 - 1800.

Cornel P., Sontheimer H., Summers R.S. and Roberts P.V., (1986), "Sorption of dissolved organics from aqueous solution by polystyrene resins. II. External and internal mass transfer", Chemical Engineering Science, 41, No 7, pp 1801 - 1810.

Coulson J.M. and Richardson J.F., (1978), "Chemical Engineering", Vol 3, 3rd ed., Pergamon Press.

Coulson J.M. and Richardson J.F., (1979), "Chemical Engineering", Vol 3, 2nd ed., Pergamon Press.

Crank J., (1970), "The mathematics of diffusion", 2nd ed., Oxford University Press, London.

Crittenden J.C. and Weber Jr.,W.J., (1978a) "Predictive model for design of fixed-bed adsorbers: Parameter estimation and model development", Journal of Environmental Engineering, EE2, pp 185 - 187.

Crittenden J.C. and Weber Jr.,W.J., (1978b) "Predictive model for design of fixed-bed adsorbers: Single-component model verification", Journal of Environmental Engineering, EE3, pp 433 - 443.

Crittenden J.C. and Weber Jr.,W.J., (1978c) "Model for design of multi-component adsorption systems", Journal of Environmental Engineering, EE6, pp 1175 - 1195.

Crittenden J.C., Luft P. and Hand D.W., (1985), "Prediction of multicomponent adsorption in background mixtures of unknown composition", Water Research, 19, no 12, pp 1537 - 1548.

Curran C.M. and Tomson M.B., (1983), "Leaching of trace organics into water from five common plastics", Ground Water Monitor Review, 3, no 3, pp 68 - 71.

de Koning A.J., (1974), "Analysis of egg lipids", Journal of Chemical Education", 51, no 1, pp 48 - 50.

de Koning A.J., (1985), personal communication.

Dence and Annegren, (1979), "Chlorination", in Singh R.P. "The bleaching of Pulp", 3rd ed., Tappi Press.

Digiano F.A., Baldauf G., Frick B. and Sontheimer H., (1978), "A simplified competitive equilibrium adsorption model", Chemical Engineering Science, 33, pp 1667 - 1673.

Dressler M., (1979), "Extraction of trace amounts of organic compounds from water with porous organic polymers", Journal of Chromatography, 165, pp 167 - 206.

Dubinin M.M., (1960), "The potential theory of adsorption of gases and vapours for adsorbents with energetically nonuniform surfaces", Chemical Reviews, 60, no 2, pp 235 - 241.

Easty D.B., Borchardt L.G. and Wabers B.A., (1978), "Wood derived toxic compounds: Removal from mill effluents by waste treatment processes", Tappi, 61, no 10, pp 57 - 60.

Fritz W., and Schlunder E.U., (1974), "Simultaneous adsorption equilibria of organic solutes in dilute aqueous solution on activated carbon", Chemical Engineering Science, 29, pp 1279 - 1282.

Fox M.E., (1976), "Fate of selected organic compounds in the discharge of kraft paper mills into lake Superior", in Keith L.H., "Identification and analysis of organic pollutants in water", Ann Arbor Science, Chapt 34, pp 641- 659.

Gerald C.F. and Wheatley P.O., (1984), "Applied numerical methods", 3rd ed., Addison-Wesley Publishing co., Reading.

Gomez-Vaillard R., Kershenbaum L.S. and Streat M., (1981), "The performance of continuous, cyclic ion-exchange reactors", Chemical Engineering Science., 36, pp 307 - 317.

Gomez-Vaillard R. and Kershenbaum L.S., (1981), "The performance of continuous, cyclic ion-exchange reactors. II. reactions with intraparticle diffusion controlled kinetics", Chemical Engineering Science, 36, pp 319 - 326.

Gordon D., (1982), "Removal of organics from bleaching plant effluents using activated carbon and polymeric adsorbents", Project report, Department of Chemical Engineering, UCT.

Grant R.J. and Manes M., (1966) "Adsorption of binary hydrocarbon gas mixtures on activated carbon", Industrial and Engineering Chemistry Fundamentals, 5, pp 490 - 498.

Greenbank M., and Manes M, (1981), "Application of the Polanyi adsorption potential theory to adsorption from solution on activated carbon. 11. Adsorption of organic liquid mixtures from water solution", Journal of Physical Chemistry, 85, no 21, pp 3050 - 3059.

Halsey G., (1948), "Physical adsorption on non-uniform surfaces", The Journal of Chemical Physics., 16, no 16, pp 931 - 937.

Hansen R.S. and Fackler Jr., W.V., (1953), "A generalization of the Polanyi theory of adsorption from solution", Journal of Physical Chemistry, 57, no 7, pp 634 - 637.

Harned H.S., and Owen B.B., (1950), "The physical chemistry of electrolytic solutions", 2nd ed., Reinhold publishing co.

Harries R.C., (1982), "Studies on organic removal from bleach plant effluent using adsorbent materials", Report for SAPPI Ltd.

Hasanain M.A. and Hines A.L., (1981), "Application of the adsorption potential theory to adsorption of carboxylic acids from aqueous solutions onto a macroreticular resin", Ind. Eng. P.D.D., 20, no 4, pp 621 - 625.

Hill T.L., (1949), "Physical adsorption and the free volume model for liquids", Journal of Chemical Physics, 17, p 590.

Helfferich F., (1962), "Ion exchange", McGraw-Hill, New York.

Hendricks D.W and Kuratti L.G., (1982), "Derivation of an empirical sorption rate equation by analysis of experimental data", Water Research, 16, pp 829 - 837.

Hendry B.A., (1984), "Removal of organics from paper pulp bleaching effluent", Department of Chemical Engineering, UCT.

Hornstein I., et al, (1960), "Determination of free fatty acids in fat", Analytical Chemistry, 32, no 4, April, pp 540 - 542.

Jain J.S, Snoeyink V.L., (1973), "Adsorption from bisolute systems on active carbon", J. Water P.C., 45, no 12, pp 2463 - 2479.

Jackson D., (1983), "Study of organic removal from paper bleaching effluent using a range of adsorbent materials", project report for Department of Chemical Engineering, UCT.

Jennings W., (1980), "Gas chromatography with glass capillary columns", 2nd ed., Academic Press, pp 309 - 314.

Jossens L., Prausnitz J.M., Fritz W., Schlunder E.U. and Myers, (1978), "Thermodynamics of multisolute adsorption from dilute aqueous solutions", Chemical Engineering Science, 33, no 8, pp 1097 - 1106.

Junk G.A. et al, (1974), "Use of macroreticular resins in the analysis of water for trace organic contaminants", Journal of Chromatography, 99, pp 745-762.

Kennedy (1973), "Macroreticular polymeric adsorbents", Ind. Eng. P.R.D. 12, no 1, pp 56 - 61.

Komiyama H. and Smith J.M., (1974), "Surface diffusion in liquid-filled pores", AIChE J., 20, no 6, pp 1110 - 1117.

Kunin R., (1980), "Porous polymers as adsorbents - a review of current practice", Amber-hi-lites, no 163.

Lee L.P., (1978), "The kinetics of sorption in a biporous adsorbent particle", AIChE J., 24, no 3, pp 531 - 533.

Levenspiel, O., (1979), "The Chemical Reactor Omnibook", Corvallis.

Lewis S. et al, (1979), "High resolution gas chromatographic/real-time high resolution mass spectrometric identification of organic acids in human urine", Analytical Chemistry, 51, no 8, pp 1275 - 1285.

Liapis A.I. and Rippin D.W.T., (1977), "A general model for the simulation of multicomponent adsorption from a finite bath", Chemical Engineering Science, 32, pp 619 - 627.

Libert B., (1981), "Rapid determination of oxalic acid by reversed-phase high-performance liquid chromatography", Journal of Chromatography, 210, pp 540 - 543.

Linke W.F., (1958), "Solubilities of inorganic and metal-organic compounds", Vol 1, 4th ed., Van Nostrand Co., Princeton.

McKay G., (1984), "Mass transfer processes during the adsorption of solutes in aqueous solutions in batch and fixed bed adsorbers", Chem. Eng. R., 62, pp 235 - 246.

Manes M. and Hofer L.J.E., (1969), "Application of the Polanyi adsoprtion potential theory to adsoprtion from solution on activated carbon", Journal of Physical Chemistry, 73, no 3, pp 584 - 590.

Mansour A.R., Von Rosenberg D.U. and Sylvester N.D., (1982), "Numerical solution of liquid-phase multicomponent adsorption in fixed beds", AIChE J., 28, no 5, pp 765 - 772.

Mansour A.R., Shahalam A.B., Von Rosenberg D.U. and Sylvester N.D., (1984), "A general nonequilibrium multicomponent adsorption model: numerical solution", Separation Science and Technology, 19 no 8&9, pp 479 - 496.

Martin R.J. and Ng W.J., (1985), "Chemical regeneration of exhausted activated carbon", Water Research, 19, no 12, pp 1527 - 1535.

Mass spectrometry data centre, (1974), "Eight peak index of mass spectra", 2nd ed.

Mateka Z. and Eliasek J., (1982), "Liquid-size diffusion controlled cation exchange kinetics", Desalination, 42, no 3, pp 315 - 320.

Mathews A.P. and Fan L.T., (1983), "Comparison of performance of packed and semifluidized beds for adsorption of trace organics", AIChE symposium series, 230, no 79, pp 79 - 85.

Mathews A.P. and Su C.A., (1983), "Prediction of competitive adsorption kinetics for two priority pollutants", Environmental Progress, 2, no 4, pp 257 - 261.

Mehrotra A.K. and Tien C., (1984), "Further work in species grouping in multicomponent adsorption calculation", Can. J. Ch. En., 62, pp 632 - 643.

Neretnieks I., (1976a), "Adsorption in finite bath and coutercurrent flow with systems having a nonlinear isotherm", Chemical Engineering Science, 31, pp 107 - 114.

Neretnieks I., (1976b), "Adsorption in finite bath and coutercurrent flow with systems having a concentration dependent coefficient of diffusion", Chemical Engineering Science, 31, pp 465 - 471.

Neretnieks I., (1976c), "Analysis of some adsorption experiments with activated carbon", Chemical Engineering Science, 31, pp 1029 - 1035.

Ortlieb H.-J., Bunke G. and Gelbin D., (1981), "Separation efficiency in the cyclic steady state for periodic countercurrent adsorption", Chemical Engineering Science, 36, pp 1009 - 1016.

Ota M., Durst W.B. and Dence C.W., (1973), "Low molecular weight compounds in spent chlorination liquor", Tappi, 56, no 6, pp 139 - 143.

Perry R.H. and Chilton C.H., (1973), "Chemical Engineers Handbook", 5th ed., McGraw-Hill.

Pfister K. and Sjostrom E., (1979), "Characterization of spent bleaching liquors. 6. Composition of material dissolved during chlorination and alkali extraction", Paperi ja Puu - Papper och Tra, no 10, pp 619 - 622.

Picht R.D. et al, (1982), "Regeneration of adsorbents by a supercritical fluid", AIChE symposium series, 78, no 219, pp 136 - 149.

Polanyi M., (1932), "Theories of the adsorption of gases. A general survey and some additional remarks.", Transactions Faraday Society, 28, pp 316 - 333.

Przyjazny A., (1985), "Evaluation of the suitability of selected porous polymers for preconcentration of organosulphur compounds from water", Journal of Chromatography, 346, pp 61 - 67.

Radke C.J. and Prausnitz J.M., (1972a), "Adsorption of organic solutes from aqueous solutions on activated carbon", Ind. Eng. F., 11, p 445 - 451.

Radke C.J. and Prausnitz J.M., (1972b), "Thermodynamics of multi-solute adsorption from dilute liquid solutions", AIChE J., 18, no 4, pp 761 - 768.

Raltson A.W., and Hoerr C.W., (1942), "The solubilities of the normal saturated fatty acids", Journal of Organic Chemistry, 7, no 6, pp 546 - 555.

Ramaswami S. and Tien C., (1986), "Simplification of multicomponent fixed-bed adsorption calculations by species grouping", Ind. Eng. P.D.D., 25, pp 133 - 139.

Rao C.N.R., (1975), "Ultraviolet and visible spectroscopy", Butterworths, 3rd ed.

Rappoport Z., (1967), "Handbook of tables for organic compound identification", 3rd ed., The Chemical Rubber Company.

Rogers I.H., (1973), "Isolation and chemical identification of toxic components from kraft mill wastes", Pulp and Paper Magazine of Canada, 74, pp 111 - 116.

Rohm and Haas, (1972), "Decolorization of kraft pulp bleaching effluents using Amberlite XAD-8 polymeric adsorbent", Philadelphia.

Rohm and Haas, (1978), "Amberlite and Amberlyst ion exchange resins and adsorbents, summary chart of properties and applications", Philadelphia.

Rohm and Haas, (1981), "Laboratory column procedures for testing Amberlite polymeric adsorbents", Philadelphia.

Rosene M.R., and Manes M., (1976), "Application of the Polanyi adsorption potential theory to adsorption from solution on activated carbon. 7. Competitive adsorption of solids from water solution", Journal of Physical Chemistry, 80, no 9, pp 953 - 959.

Rosene M.R., and Manes M., (1977a), "Application of the Polanyi adsorption potential theory to adsorption from solution on activated carbon: 9. Competitive adsorption of ternary solid solutes from water solution", Journal of Physical Chemistry, 81, no 17, pp 1646 - 1650.

Rosene M.R., and Manes M., (1977b), "Application of the Polanyi adsorption potential theory to adsorption from solution on activated carbon: 10. pH effects and "hydrolytic" adsorption in aqueous mixtures of organic acids and their salts", Journal of Physical Chemistry, 81, no 17, pp 1651 - 1657.

Scott A.I., (1964), "Interpretation of the ultraviolet spectra of natural products", Pergamon Press.

Scott S.P., Sutherland N. and Vincent R.J., (1984), "The application of pre-concentration and GC/MS techniques to the analysis of water samples", Analytical Proceedings, 21, pp 179 - 184.

Seidell A., (1940), "Solubility of inorganic and metal organic compounds", 3rd ed., 1 D. Van Nostrand, New York.

Seidell A., (1941), "Solubility of organic compounds", 3rd ed., 2 D. Van Nostrand, New York.

Sheindorf C., Rebhun M. and Sheintuch M., (1981) "A Freundlich type multicomponent isotherm", Journal Colloidal Interface Science, 79, p 136.

Sheindorf C., Rebhun M. and Sheintuch M., (1982) "Organic pollutants adsorption from multicomponent systems modeled by freundlich type isotherm", Water Research, 16, pp 357 - 362.

Shenz T.W. and Manes M., (1975), "Application of the Polanyi adsorption potential theory to adsorption from solution on activated carbon. 6. Adsorption of some binary organic liquid mixtures", Journal of Physical Chemistry, 79, pp 604 - 609.

Smith G.D., (1969), "Numerical solution of partial differential equations", Oxford University press, London.

Stephen H. and Stephen T., (1963), "Solubilities of inorganic and organic compounds", 1, Pergamon.

Stoffel W., Chu F., Ahrens E. H., (1959), "Analysis of long-chain fatty acids by gas-liquid chromatography", Analytical Chemistry, 31, no 2, pp 307 - 308.

Suzuki M. and Fujii T., (1982), "Concentration dependence of surface diffusion coefficient of propionic acid in activated carbon particles", AIChE J., 28, no 3, pp 380 - 385.

Svehla S., (1980), "Comprehensive analytical chemistry", Vol 10, Elsevier scientific publishing Co.,Oxford.

Thurman E.M., Malcolm R.L. and Aiken G.R., (1978), "Prediction of capacity factors for aqueous organic solutes adsorbed on a porous acrylic resin", Analytical Chemistry, 50, no. 6, pp 775 - 779.

Van der klashorst G.H., (1984), "The low molecular weight phenolic compounds present in an industrial hardwood soda/AQ spent liquor" Part II, Hout 366, National Timber Research Institute, CSIR.

Van der Merwe Dr., (1985), SMM instrumentation, Cape Town, personal communication.

Van Vliet B.M., (1980), "Modelling and prediction of specific compound adsorption by activated carbon and synthetic adsorbents", Water Research, 14, pp 1719-1728.

Van Vliet B.M., (1987), NIWR, CSIR, Pretoria, personal communication.

Van Vliet B.M. and Venter L., (1984), "Infrared thermal regeneration of spent activated carbon from water reclamation", Water Science Technology, 17, pp 1029 - 1042.

Van Vliet B.M. and Weber W.J., (1981), "Comparitive performance of synthetic adsorbents and activated carbon for specific compound removal from wastewaters", J. Water P. C., 53, no 11, pp 1585 - 1598.

Van Vliet B.M., Weber W.J. and Hozumi H., (1980), "Modeling and prediction of specific compound adsorption by activated carbon and synthetic adsorbents", Water Research, 14, pp 1719 - 1728.

Vasil'ev V.V. and Kabeiya F., (1976), "Use of ultrasound in ion-exchange chromatography reactions under static conditions", Russian Ultrsonics, 6, no 3, pp 113 - 114.

Von Rosenberg D. U., (1969), "Methods for the numerical solution of partial differential equations", American Elsevier Publishing co., New York.

Voss R.H. and Rapsomatiotis A., (1985), "An improved solvent extraction based procedure for the gas chromatographic analysis of resin and fatty acids in the pulp mill effluents", Journal of Chromatography, 346, pp 205 - 214.

Wang Z. and Cheng K.L., (1982), "Effect of ultrasound and mechanical agitation on adsorption of 4-(2-pyridylazo) resorcinol by Amberlite XAD-2", Ultrasonics, 20, no 5, pp 215 - 216.

Washburn E.W., et al, (1928), "International critical tables of numerical data, physics, chemistry and technology", 1st ed., McGraw-Hill, New York.

Weast R.C., (1980), "Handbook of Chemistry and Physics", Chemical Rubber co., 60th ed.

Weber T.W. and Chakravorti R.K., (1974), "Pore and solid diffusion models for fixed-bed adsorbers", AIChE Journal, 20, no 2, pp 228 - 238.

Weber Jr.W.J, and Crittenden J.C., (1975) "MADAM1 - A numeric method for design of adsorption systems", J. Water P.C., 47, no 5, pp 924 - 940.

Weber Jr.W.J. and Keinath T.M., (1967), "Mass transfer of perdurable pollutants from dilute aqueous solution in fluidized adsorbers", AIChE symposium series, 63, no 74, pp 79 - 89.

Weber Jr.W.J. and Liu K.T., (1980), "Determination of mass transport parameters for fixed-bed adsorbers", Chemical Engineering Communications, 6, pp 49 - 60.

Weber W.J.Jr. and Van Vliet B.M., (1979), "A general isotherm explicit in terms of solution concentration", Technical memorandum EWRE-010379, Environment and Water resources engineering laboratory, University of Michigan, Ann Arbor.

Weber W.J.Jr. and Van Vliet B.M., (1981a), "Synthetic adsorbents and activated carbons for water treatment: overview and experimental comparisons", J. Am. Water, 73, no 8, pp 420 - 426.

Weber W.J.Jr. and Van Vliet B.M., (1981b), "Synthetic adsorbents and activated carbons for water treatment: statistical analyses and interpretations", J. Am. Water, 73, no 8, pp 426 - 431.

Wohleber D.A., Manes M., (1971), "Application of the Polanyi potential theory to adsorption from solution on activated carbon. 2. Adsorption of partially miscible organic liquids from water solution", The Journal of Physical Chemistry, 75, no 1, pp 61 - 64.

Yen C-U and Singer P.C, (1984), "Competitive adsorption of phenols on activated carbon", Journal of Environmental Engineering, 100, no 5, pp 976 - 989.

Yon C.M. and Turnock P.H., (1971), "Multicomponent adsorption equilibria on molecular sieves", AIChE symposium series, 67, no 117, pp 75 - 83.

Zinkel D.F. and Engler C.C., (1977), "Gas-liquid chromatography of resin acid esters", Journal of Chromatography, 136, pp 245 - 252.

Zinkel D.F., Lathrop M.B. and Zank L.C., (1968), "Preparation and gas chromatography of trimethylsilyl derivatives of resin acids and the corresponding alcohols", Journal of Gas Chromatography, 6, pp 158 - 160.

Analysis of anion resin foulants

A promising proposal for treating paper pulp bleaching effluents involved removing the anions (mainly chloride) from the effluent with a weak anion exchange resin. The anion exchange resin would then be regenerated with lime to produce calcium chloride. The problem was that organic compounds also loaded onto the ion exchange resin, and lime could not completely remove them. This appendix gave a summary of the methods used to identify some of these organic compounds that caused the fouling problem.

A1.1 Organic compounds previously found in bleaching effluents

Finding the compounds in the effluent that precipitated with calcium was considered to be a first step towards identifying the foulants. Dence and Annergren (1979) reviewed the literature on the composition of bleaching effluents and listed a number of compounds previously identified. Other authors also listed compounds found in bleach effluents, but finding the solubility of these compounds and that of their calcium salts was not easy. The solubility of a number of compounds was listed in Appendix 6. The solubilities of the following carboxylic acids, previously reported in bleach effluents, and their calcium salts were found:

formic acid,
acetic acid,
oxalic acid,
malonic acid,
succinic acid and
palmitic acid.

In all cases, the solubility of the calcium salt was lower than that of the sodium salt or the free acid. All these acids might therefore cause fouling. Oxalic acid had the calcium salt with the lowest solubility at 0.007 g/l at 20°C. It was also the strongest organic acid found in the effluents so it had the greatest potential for anion resin fouling. Other possible foulants were the class of compounds called fatty acids (long chained carboxylic acids) . Raltson (1948) found that their calcium salts were effectively insoluble.

A1.2) Chemical tests for possible foulant species

Practical work was started by adding 0.13 g of calcium hydroxide to 0.55 l of effluent which increased the pH from 3.5 to 8.3. The precipitate formed was filtered off on 0.80 µm Millipore filter paper. To learn more about this precipitate, its solubility in different solvents was tested. The solvents tested were:

methanol,
ethanol,
ethyl acetate,
carbon tetrachloride,
chloroform,
acetone,
glacial acetic acid,
cyclohexanol,
cyclohexane,
decanol,
ethandiol and
formic acid.

Formic acid caused a few small bubbles to form but no other changes were noted. The precipitate was dissolved by strong mineral acids, presumably because the acid reacted with the calcium organic salt to form the calcium mineral salt and the organic acid. Although these tests revealed little about the composition of the precipitate, they suggested a way of reversing at least a portion of the fouling of the anion exchange resin. The fouling of the anion resin was shown to be partially reversible when sodium hydroxide was used to regenerate it instead of calcium hydroxide. If the regenerated resin were to be loaded with a strong acid and then regenerated again with sodium hydroxide, the fouling may be completely eliminated.

Because oxalic acid had been identified as a potential foulant, an attempt was made to confirm its presence in the calcium precipitate filtered from the neutralized effluent. Solubility tests performed on pure calcium oxalate found it to behave in a similar way to the precipitate from the effluent. The only difference was that it did not form bubbles when added to formic acid.

A more specific chemical test for oxalic acid involved heating the solid carefully with diphenylamine to form aniline blue (Svehla, 1980). This was a dark green solid that dissolved in ethanol to give a blue solution. The precipitate was subjected to this test and gave a light green solution. The technique was tested on pure oxalic acid and pure calcium oxalate. The test worked on oxalic acid, but not on calcium oxalate. It was found that hydrochloric acid had to be added to the calcium oxalate and then the water had to be boiled from the solution before the test would work. Adding hydrochloric acid to the calcium oxalate formed calcium chloride and oxalic acid. The calcium chloride did not appear to affect the test. The precipitate from the effluent was dissolved in hydrochloric acid, and the excess solids were filtered off. The solution was boiled to dryness and tested for oxalate as described above. A formation of a dark green solid that turned blue on the addition of ethanol confirmed the presence of oxalic acid in the Enstra D1/D2 effluent.

An estimate of the oxalate concentration was made by two methods.

i) Ultraviolet absorption spectra of the effluent before and after adding calcium hydroxide were measured. 0.13 g of calcium hydroxide was added to 0.55 l of effluent. Oxalic acid was added to another sample of effluent as an internal standard. Enough oxalic acid was added to increase its concentration in the effluent by 0.0001 M. The U.V. spectra showed a decrease in absorption for the calcium treated effluent and an increase for the oxalic acid treated effluent. In both cases, the absorbence started to deviate measurably from that of the untreated effluent at wavelengths below 230 nm, and the deviation increased with decreased wavelength, the pattern of deviation being similar in both cases. The increase in U.V. absorbence of the oxalic acid treated effluent was about 1.1 times the decrease shown by the calcium hydroxide treated effluent.

These spectra helped confirm the postulation that the calcium-precipitable compounds in the effluent were carboxylic acids. The nature of the spectra also suggested that most of the

precipitated compounds did not have any unsaturated or aromatic groups. If these compounds had a similar U.V. extinction coefficient to oxalic acid then their total concentration was about 9E-5 M.

ii) The mass of precipitate from 0.55 l of effluent was measured at about 0.038 g ±40%. If this was all calcium oxalate, it would represent a concentration of 5.4E-4 M in the effluent. The two techniques indicated that the oxalic acid concentration in the effluent was probably below 5E-4 M. The significance of this was that the presence of only 3E-6 M of calcium would be required to exceed the solubility product of calcium oxalate (in a neutral solution).

A1.3) Mass spectroscopy tests

Mass spectroscopy was carried out to collect more information about the composition of the calcium precipitate from the effluent. The basic operation of the mass spectrometer was explained in Chapter 2.

The calcium precipitate was dried in preparation for mass spectrometry. The mass spectrometer vaporised the volatile substances in the sample by heating it to 220 °C and then increasing the temperature to 290 °C over a period of 14 minutes. The compounds possibly present in the sample were determined by comparing the results with published tables of typical fragmentation patterns.

The fact that the sample was probably a complex mixture of compounds meant that a positive identification was unlikely. Also the mass spectra obtained from the sample at 220 °C was not very different from the spectra obtained at 290 °C. The instrument therefore had not separated the components well and the peaks on the mass spectra probably represented ions from many different sources. However, the spectra did show a distribution of mass per electron charge (m/e) peaks that indicated the presence of 2,4-tertiary butyl-6-methyl phenol and hydrochloric acid. This could have been a coincidence so little significance was attached to this result. However, it did encourage the further analysis of possibly anion resin foulants using the GC/MS method.

A sample of pure calcium oxalate was heated to redness (+500 °C) in a test tube and no change was noted. Its presence would therefore be difficult to detect by mass spectrometry. The absence of peaks in the spectra indicating the presence of calcium oxalate therefore did not prove its absence in the sample.

A1.4) Liquid chromatography/mass spectroscopy of foulants

The simple tests described above did not reveal much information about the fouling of anion resins. A more direct technique for identifying the foulants in the effluent was to extract them from anion resin that had been fouled by loading it with effluent and regenerating it with calcium hydroxide. The process was repeated several times to increase the concentration of foulants on the resin.

A1.4.1) Fouling the anion resin for analysis

Two samples of fouled anion resin were prepared. The aim of the experimental work was simply to foul a sample of anion resin with compounds from the bleaching effluent. Therefore, little experimental effort was spent on monitoring the progress on the experiment. However, it was possible to draw some conclusions from the measurements that were taken.

Method 1: 0.0188 l of A368 was placed into a packed bed, and effluent from a 1 litre flask was recirculated through the bed continuously for at least a day. The U.V. absorbence and pH were measured at the beginning and end of each contact. The flask was then re-filled with effluent, and the process repeated about 10 times. ie. the resin was contacted with 10 litres of effluent. The flask was then filled with a nearly saturated solution of calcium hydroxide (1 g/l) which was recirculated for at least a day. The pH and U.V. absorbence were again measured at the beginning and end of each run. To ensure that the resin was fully regenerated, it was contacted with another solution of 0.2 g/l calcium hydroxide. Finally the resin was given a single wash by placing distilled water in

the flask and recirculating it for at least a day. Absorbence and pH were measured as before.

The whole cycle was repeated 5 times. During the loading period of the second cycle, the packed column became so persistently clogged with solids that the resin had to be transferred to a fluidized column. The movement of resin in the fluidized column prevents the solids forming a permanent plug between the beads.

The U.V. absorbence data was used to estimate the changes of organic concentrations in each contact. A mass balance produced the results of total loading and regeneration reflected in table 1. The units of the results are the fractional change in U.V. absorbence at 270 nm multiplied by the total volume of solution.

The change in pH during each contact was used to estimated the change in ionic concentration. This calculation was not accurate because the organic anions in the solution had an effect on the pH. However, the results were accurate enough to show how the resin capacity dropped as it was fouled.

The results using this technique are reported in table 1 below.

Method 2: Because method 1 was rather slow, the volume of resin was reduced from 0.0188 l to 0.0062 l and the volume of solution increased from 1 to 2 l. This increased ratio of effluent to resin meant that the effluent did not need to be changed as often (twice as opposed to 10 times) to get the same amount of anion loading on the resin. A flask with a magnetic stirrer was used to avoid difficulties with a fixed bed. Unfortunately this resulted in serious abrasion of the resin by the magnetic stirrer and some of it was lost as a fine powder each time the solution was decanted.

The results using this second technique are reported in table 2.

A1.4.2) Results of fouling anion resin.

Table A1.1

Anion resin fouling by column contact

Cycle	Loading		Regeneration	
	change in UV absorbence	Cl- removed [meq.]	change in UV absorbence	Ca+ used [meq.]
1	3.9	1.88	2.9	14.7
2	4.1	2.81	3.4	10.3
3	4.7	2.15	4.8	9.7
4	4.3	0.83	3.1	12.7
5	3.6	0.23	5.6	26.1
Total	20.6	7.90	19.8	73.5

TABLE A1.2

Anion resin fouling by stirred vessel contact

Cycle	Loading		Regeneration	
	change in UV absorbence	Cl- removed [meq.]	change in UV absorbence	Ca+ used [meq.]
1	2.2	1.07	2.6	5.74
2	1.1	1.33	0.93	3.1
3	1.1	0.94	0.80	3.0
4	0.63	0.35	0.74	4.25
5	0.86	0.58	0.61	0.87
6	0.68	0.27	0.78	3.6
7	1.1	0.24	0.33	3.3
Total	7.67	4.78	6.79	23.86

A1.4.3) Discussion of anion resin fouling

The equivalents of calcium hydroxide used for regeneration, were always much higher than the equivalents of chloride removed. This suggested that calcium hydroxide was neutralised by the organics during regeneration.

The change in U.V. absorbence during the loading was generally slightly larger than the change during regeneration. If the U.V. extinction coefficient was the same under loading and regeneration conditions, then this indicated that some of the organics were remaining on the resin.

Although the kinetics of the exchange were not carefully monitored, there was a large decrease in the rate of ion exchange with each load-regenerate cycle particularly after the first.

A1.4.4) Preparation of anion resin foulants for GC separation

The two batches of resin were combined and portions of about 3 g were used to test three different techniques for extracting the foulants from the resin.

The analysis of the foulants was planned on the assumption that they were carboxylic acids. These acids could not be injected directly onto the gas chromatograph (GC) column because they were either not volatile enough to be carried through to the detector, they were unstable or they adsorbed too strongly to the GC adsorbent. Esters of the acids were more volatile and chemically stable and were less polar and therefore less likely to foul the column. Hornstein et al (1960) analysed carboxylic acids by converting them to their methyl esters directly on an anion resin. It was therefore decided that the foulants would be derivatized on the resin rather than removing them with a solvent first.

Method 1: Methylation by the method of de Koning (1974)

This method required the saponifacation of the acids on the resin with 0.4 g solid sodium hydroxide dissolved in 0.02 l methanol. After 20 minutes, 0.02 l of 20% boron trifluoride in methanol was added and the mixture refluxed for 10 minutes. 0.030 l of hexane was added through the condenser and refluxing was continued for 1 minute. Saturated sodium chloride solution was added until the organic layer filled the neck of the flask where it could be removed with a Pasteur pipette. A sodium chloride solution was used because organic compounds are generally less soluble in such solutions than they are in water. The hexane was then dried over sodium sulphate and evaporated to about 0.0005 l. A control experiment on the original resin was also performed.

Extracting with diethyl ether instead of hexane was tried. The results were not conclusive because there were too many peaks all over-lapping.

Method 2: Butylation by the method of de Koning (1985)

Butylation was chosen because butyl esters are less volatile than methyl esters and the results from methods 1 and 3 indicated that the solvent peak was hiding some of the foulant peaks. By butylating the foulants it was hoped that their peaks would be shifted away from the solvent peak. The method involved adding about 3 g of resin (previously dried in a desiccator for one week) to 0.02 l butanol, 0.01 l benzene and 0.001 l concentrated sulphuric acid. The mixture was refluxed for 90 minutes and then transferred to a separating funnel. 0.05 l of petroleum ether was added, and the mixture was washed with 3 aliquots of 0.02 l water. The petroleum ether layer was dried over sodium sulphate and evaporated to reduce the volume to about 0.001 l. The results from analysing the GC peaks with the mass spectrometer (GC/MS) were inconclusive so no control was done. It was later discovered that the instrument had lost its calibration.

Method 3: This derivatization method was adapted from the methods reported by Stoffel et al (1959) and Ota et al (1973), and involved refluxing the resin with anhydrous hydrochloric acid in methanol.

About 3 g of the fouled resin was put in a refluxing beaker with 0.005 l concentrated hydrochloric acid, 0.04 l methanol and an excess of anhydrous calcium chloride (dried at 130 °C for 3 days) to keep the solution anhydrous. The mixture was refluxed for three hours and then poured through filter paper. The beaker contents were washed out with 0.05 l of water. The filtered solution was extracted with 2 aliquots of 0.02 l of diethyl ether, and finally the ether layer was washed with a sodium bicarbonate solution followed by water. Carbon tetrachloride, hexane and benzene were also tested as extractants, but the pale colour of the resultant solutions, and the absence of peaks from the GC columns showed that these solvents were inferior to ether. A control was not performed because the results obtained from the GC/MS run were not conclusive.

A1.4.5) The gas chromatography method

Samples of the organic layers prepared as explained above were injected onto a 3 m long by 0.003 m ID glass GC column packed with SP 2330 on 100/120 mesh chromosorb WHP-SP (Van Der Merwe, 1985). The GC/MS system was not readily available so the GC/FID system was used to select the samples worthy of more detailed study and to determine the best chromatographic conditions. The GC/FID results also helped with the comparison of the foulant layer from method 1 and its control. Two columns were therefore made. One to connect to the flame ionization detector and the other to connect to the mass spectrometer. The most important experimental variables were the volume of sample injected onto the column, and the temperature profile used during the run. The best results were obtained by injecting 4 µl of sample into a port held at 190 °C. The column was initially at 90 °C and its temperature was increased at 8 °C/min up to 250 °C where it was held for the further 20 minutes required for all the peaks to appear. GC/FID runs were

performed on the different solutions from all 3 derivatization methods to help decide which solutions to send for GC/MS analysis and what conditions to use on this column.

Figure A1.1 shows the FID response obtained from passing the hexane layer through the column. The foulants were derivatized using method 1. Figure A1.2 shows the response for the control sample. The numbers above the peaks indicate retention time in minutes. Comparing the two figures shows that the control has three peaks that are larger than the corresponding peaks on the fouled resin sample. These are at retention times of 4, 14.4 and 19.5 minutes. In all other cases, the peaks from the fouled resin sample are the same as or higher than their corresponding control peaks. Only the three peaks at 16.75, 17.49 and 32.91 minutes are markedly less prominent in the control sample.

A1.4.6) Results from the GC/MS runs

The mass spectrometer was used as a detector for the GC column to enable the identification of the foulants.

The most conclusive results came from the sample that was methylated with boron trifluoride and extracted with hexane. A control was performed for this method and the results are discussed first.

Method 1; Figures A1.3 and A1.4 show the total ion current profiles for the fouled resin and its control. The total ion current is the current received by the detector from the ions of all masses that strike it. It is therefore an accurate representation of the quantity of solute leaving the GC column at a given time. Figures A1.3 and A1.4 are therefore directly equivalent to figures A1.1 and A1.2 respectively. They show clearly how the carrier-gas separator between the gas chromatography column and the mass spectrometer reduces the resolution of the GC/MS system.

The reduced resolution means that it is difficult to identify the different peaks using the total ion current profile. However, one of the powers of mass spectroscopy is the ability to perform a constant m/e or 'selective ion monitoring' (SIM) profile. What this means is

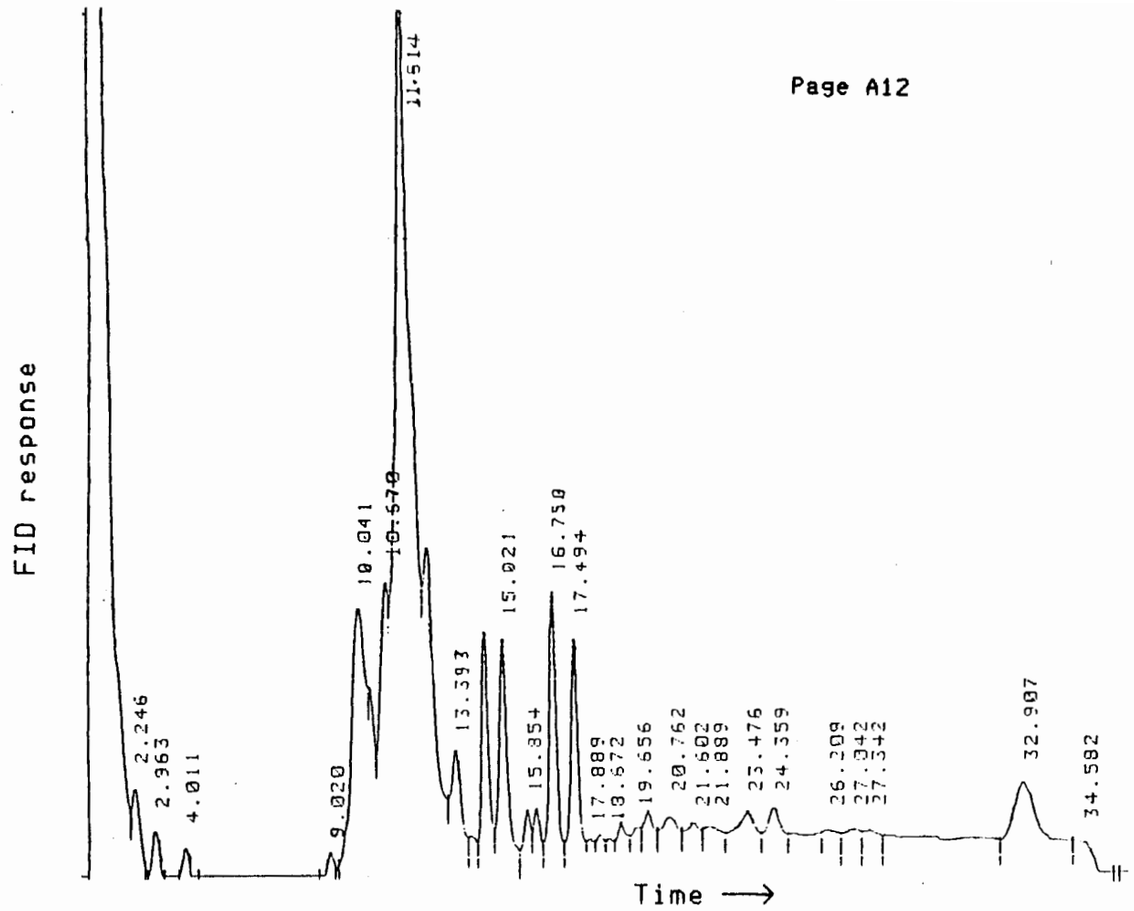

Figure A1.1. GC/FID response for hexane layer with anion resin foulants.

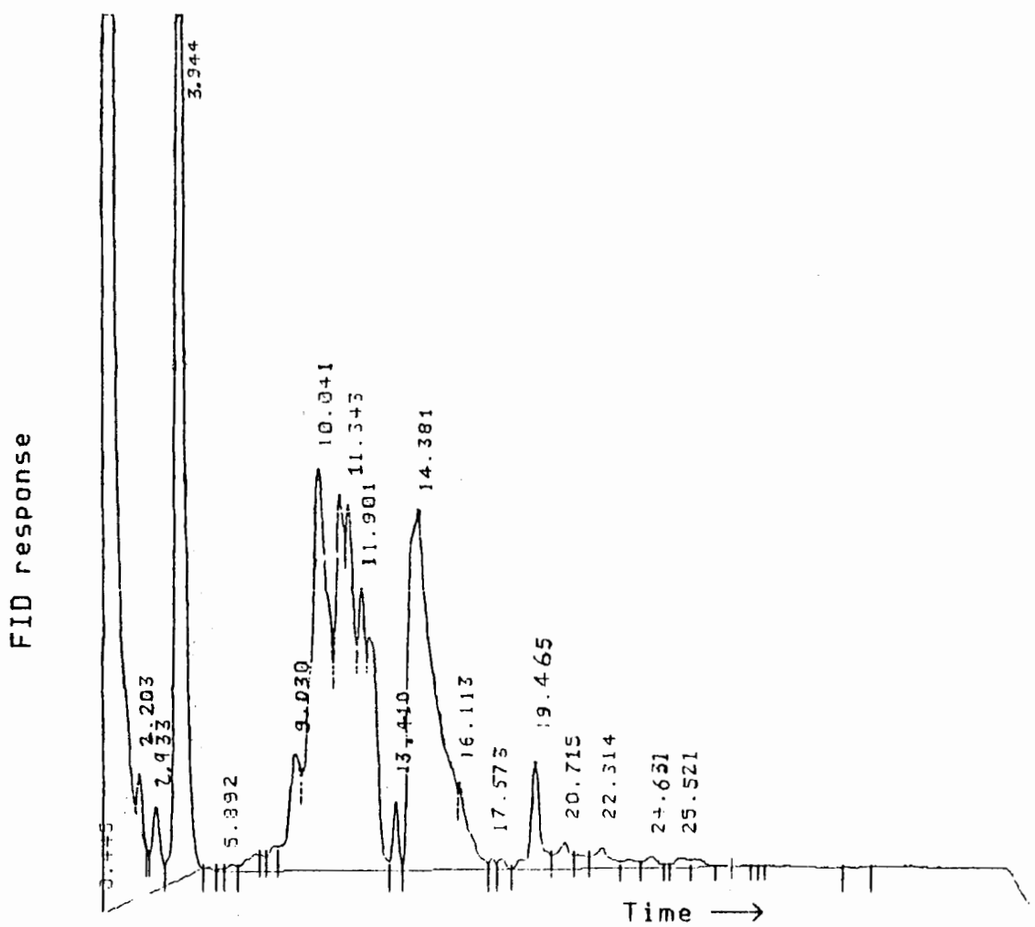

Figure A1.2. GC/FID response for hexane layer from control.

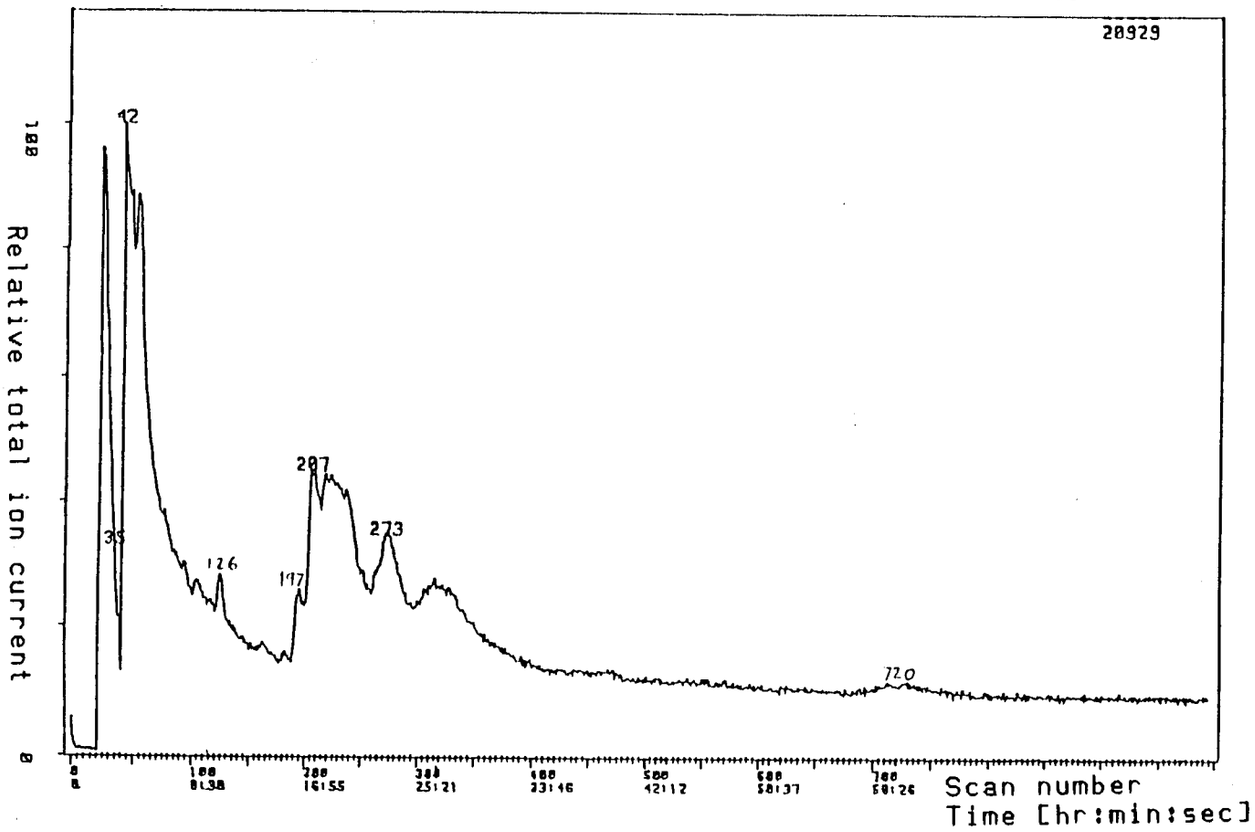

Figure A1.3. GC/MS total ion current profile for hexane layer with anion resin foulants.

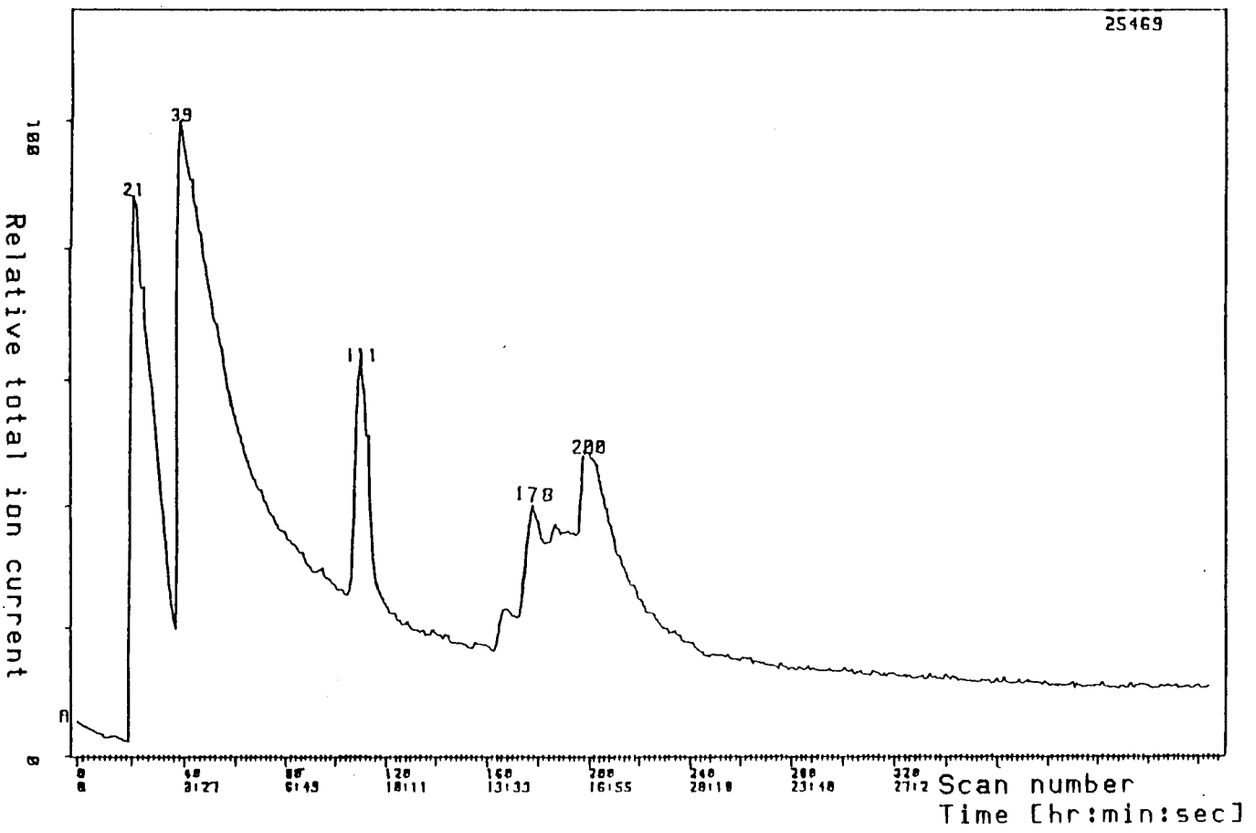

Figure A1.4. GC/MS total ion current profile for hexane layer from control.

best illustrated with an example. Aliphatic methyl esters typically fragment to produce large quantities of the ion $[CH_2CH_2COOCH_3]^+$. It is formed by the breaking of the third C-C bond from the carbonyl group. The ion has a molecular mass of 87 and a constant m/e profile for m/e = 87 is essentially a way of selectively monitoring the output of the GC column for this ion. There are other ions with a mass of 87 but since the presence of methyl esters was expected, they were unlikely to have made a large contribution to the results in this case.

The mass spectrometer scans for all ions (m/e values) every 5 seconds. The data is stored in a computer for later reconstruction. The computer looks at each scan and reads the detector current for when the detector was receiving ions with a molecular mass of 87. It notes the highest reading and prints it in the top right hand corner of the graph. It then assigns this detector reading with a value of 100% and scales all the other readings accordingly. The black curve on figure A1.5 is the result. The detector reading on the 126th scan at m/e = 87 had a value of 448 electrons. Figure A1.6 shows the equivalent profile for the control. The ion current at scan 111 was very high at 2399. The other results were therefore proportionally scaled down. Bearing this scale down factor in mind, the m/e = 87 profiles for the fouled resin and its control were very similar. Scan 126 on figure A1.5 corresponds to scan 111 on figure A1.6. Likewise 43 corresponds to 40 and 267 corresponds to 200. The lack of direct correlation between the scan numbers was due to a late start of the temperature programming for the sample with anion resin foulants. Also the GC/MS runs were started at 60 °C instead of 90 °C, so the retention times were longer than they were for the GC/FID runs.

The other m/e value monitored in figures A1.5 and A1.6 was m/e = 180. This m/e value is characteristic of a wide range of compounds mostly containing benzene rings, such as trichlorobenzenes, substituted phthalic acids and anthraquinone. The m/e = 180 profile for the control sample shows no response. This indicates clearly that there are at least 3 foulants from the bleaching effluent at scans 300 - 350, 460 - 510 and 690 - 770.

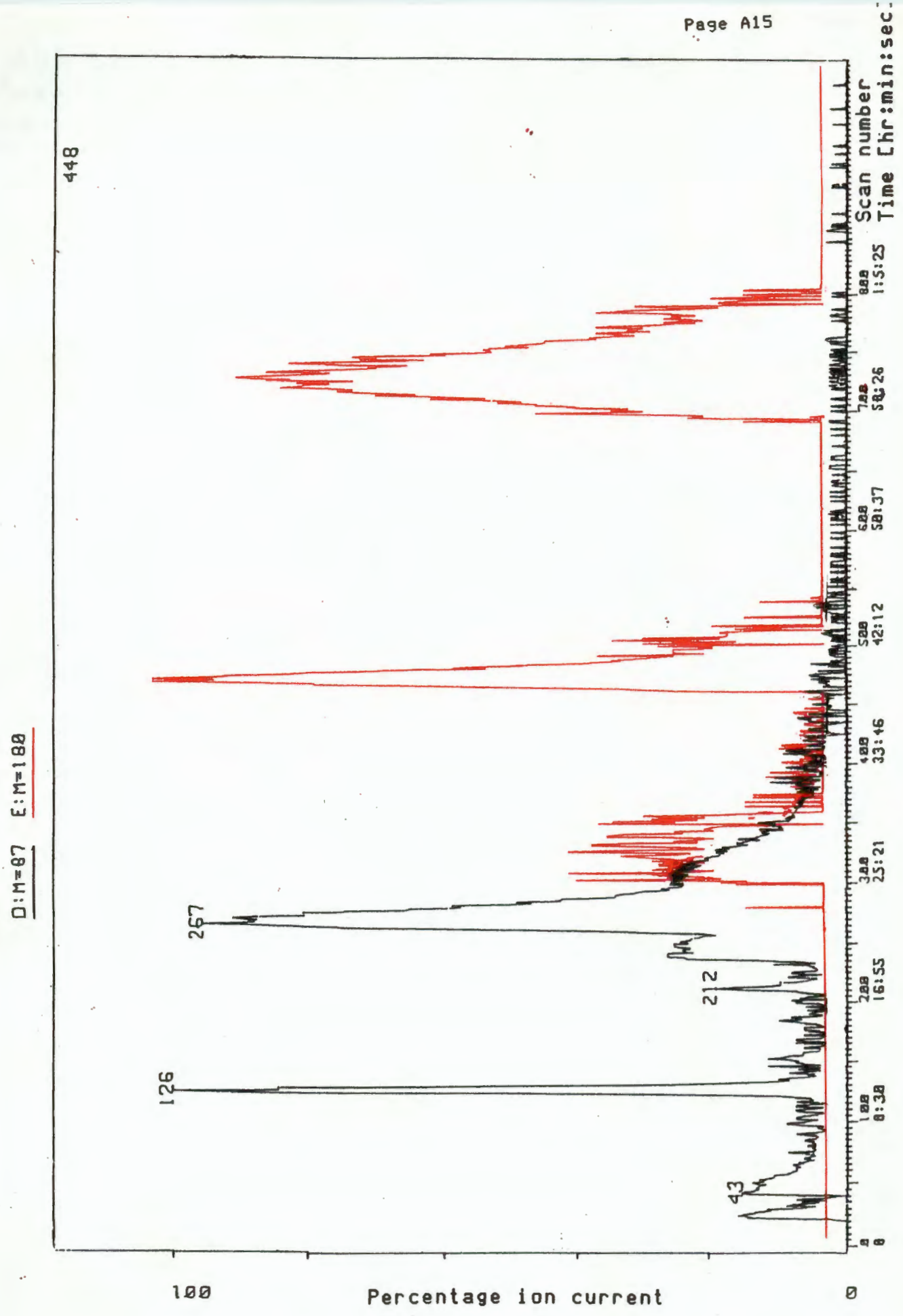

Figure A1.5. Mass spectrometry. Constant m/e profile for m/e = 87 and m/e = 180. Sample with anion resin foulants.

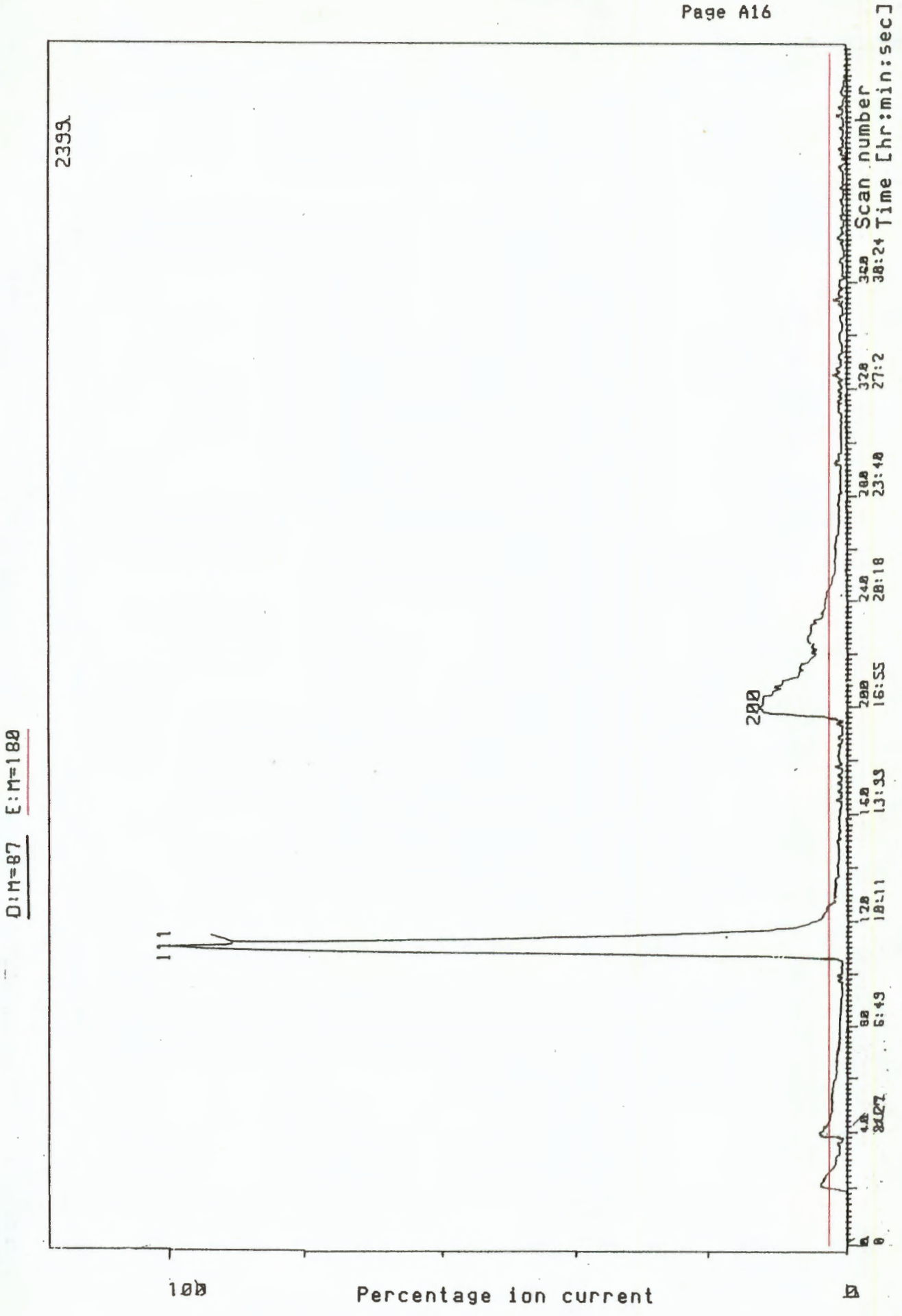

Figure A1.6. Mass spectrometry. Constant m/e profile for m/e = 87 and m/e = 180. Control sample.

SIM profiles were slow to construct because the computer had to reconstruct them from a large amount of data. Only five were performed. The other three were shown in figures A1.7 and A1.8. The m/e value of 74 was characteristic of methyl esters and was due to the ion $[CH_3OCOH{:}CH_2]^+$ (Budzikiewicz et al, 1967). The higher ion current from the sample with the foulants indicated that the concentration of methyl esters was increased on the fouled resin. The forth m/e profile was for m/e = 194. This could have been produced by a compound such as 2-methoxycarbonyl-diphenylmethane or 2,4 di-isocyanato chloro-benzene. The presence of this m/e value in the control at scans 412 - 436 showed that the compounds at scans 520 - 590 for the fouled sample were not necessarily from the bleaching effluent. The m/e = 194 and m/e = 222 profiles showed that there were at least two anion resin foulants present at scans 270 to 350.

The final identification of the compounds had to be made by manually comparing the mass spectra from the various scans with charts of published spectra. In Mass spectrometry data centre (1974), charts of spectra characteristic of 31 000 common compounds were published. The characteristic spectra quoted below came from this source unless stated otherwise.

Figures A1.9 - A1.16 show eight examples of mass spectra, all taken from the fouled resin sample. The first is taken from scan 126 and is very similar to scan 111 from the control sample. Looking at figure A1.3 it can be seen that the peak at scan 126 is small compared to the surrounding total ion current. This means that the spectra for this scan also contains a large response due to tailing of previous peaks and bleed from the GC column and other parts of the instrument such as the carrier-gas separator. Bleed has many causes and is almost impossible to eliminate. It is particularly bad from GC columns with fresh packing. Other sources of bleed are compounds from previous experiments that were strongly adsorbed and are slowly released during subsequent experiments. The best way to minimize it is to operate the instrument over-night or over a week-end at a high temperature. The effect of bleed and tailing can be largely eliminated from the results by subtracting two spectra from neighbouring scans. The spectra in figure A1.9 is the result of subtracting scan 121 from scan 126.

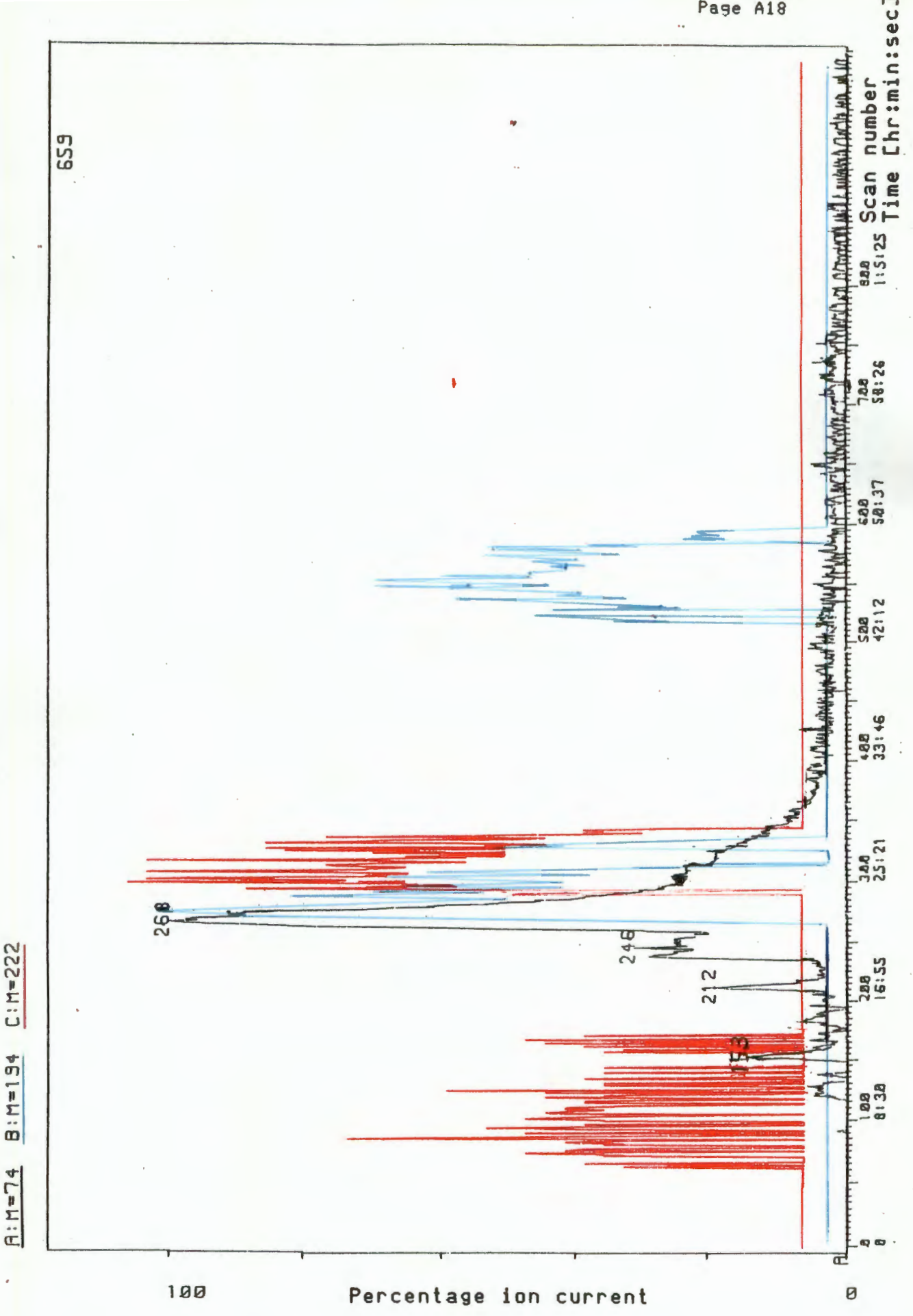

Figure A1.7. Mass spectrometry. Constant m/e profile for m/e = 74 , m/e = 194 and m/e = 222. Sample with anion resin foulants

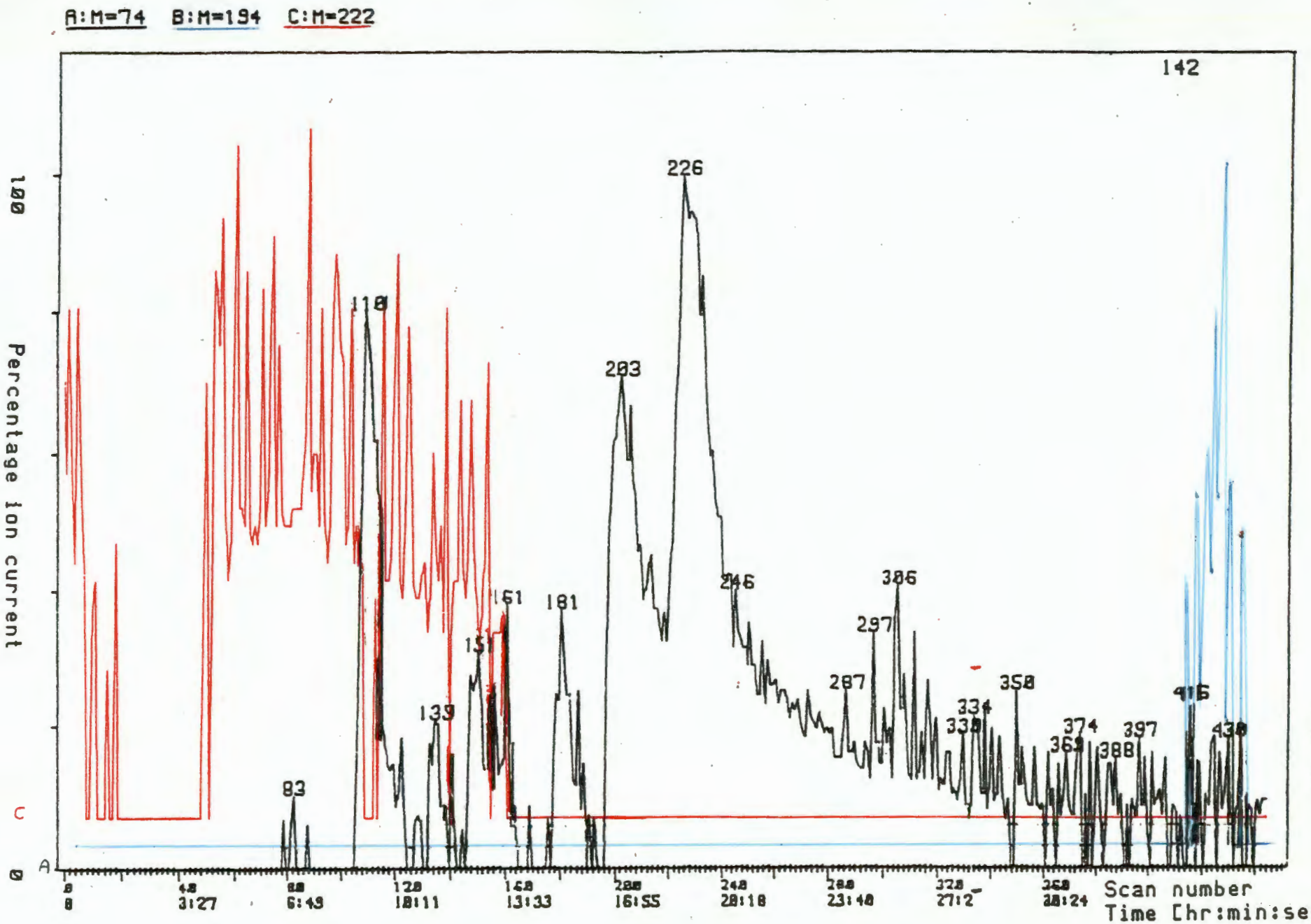

Figure A1.8. Mass spectrometry. Constant m/e profile for m/e = 74 m/e = 194 and m/e = 222.. Control sample.

The most abundant ion at scan 126 had a mass of 87. The difference in the ion current due to m/e = 87 at scan 126 and scan 121 was 411. (Printed in the top right hand corner.) This value was assigned to 100% relative abundance and the other values were all scaled accordingly. The most probable compound responsible for this scan was methyl 2-ethylhexanoate. The literature spectra was m/e = 87 at 100%, followed by m/e = 102 (89), 57 (53), 41 (39), 15 (32), 27 (29), 55 (28). These figures only corresponded roughly with the results reflected in figure A1.9. This was probably due to a combination of two or three factors.

i) Subtracting scan 121 did not completely eliminate the interference.

ii) There was more than one compound present.

iii) The spectra was due to another compound.

Points i) and ii) were almost certainly true, so the truth of the third point could not be verified.

The spectra shown in figure A1.10 was produced by subtracting scan 201 from scan 206. Possible compounds were:
o-benzylhydroxylamine;
91 (100)%, 77 (24), 105 (16), 108 (14), 51 (13), 79 (12), 107 (11) or,
3-ethyl-3-phenylpentane;
91 (100%), 105 (72), 147 (41), 41 (11), 117 (10), 115 (9), 27 (8), 77 (8) or,
6-phenyldodecane;
91 (100%), 161 (13), 105 (12), 175 (10), 41 (10), 92 (8), 43 (7), 104 (6).
This example gives an idea of how difficult it was to interpret the spectra.

Figure A1.11 came from subtracting scan 260 from scan 272. The most abundant ion was m/e = 74 and it had an ion current of 453. The next most abundant peak was m/e = 87 (66%). The prominence of these two peaks was a strong indication of an aliphatic carboxylic acid. The compound most likely present here was methyl palmitate [$CH_3(CH_2)_{14}CO_2CH_3$], derived from palmitic (or hexadecanoic) acid. The literature for methyl palmitate was m/e = 74 (100%), 87 (66%), 43 (38%), 41 (24%), 55 (24%), 57 (16%), 75 (16%), 29 (14%), and the molecular ion at 270 was 4.2%. The spectra in

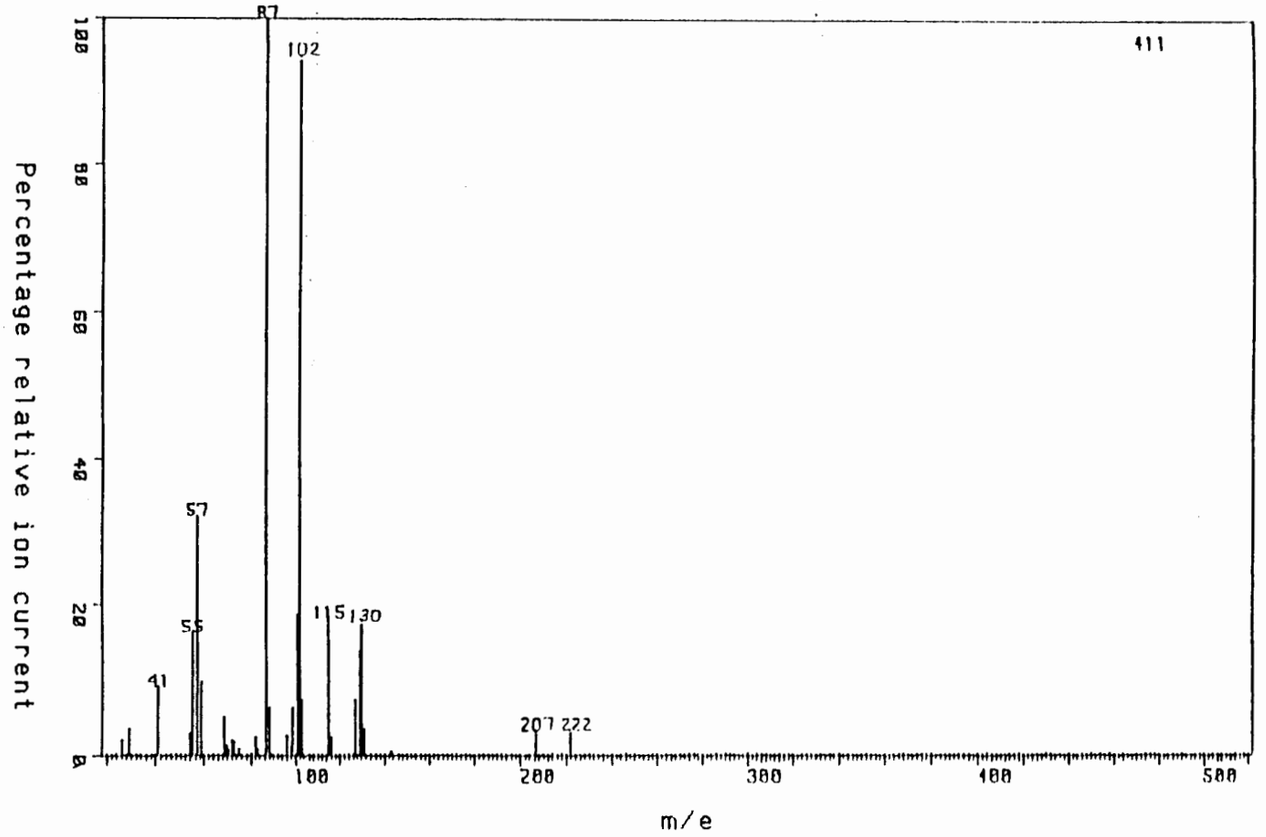

Figure A1.9. Mass spectrograph scan number 126 on sample with foulants. (Methyl 2-ethylhexanoate)

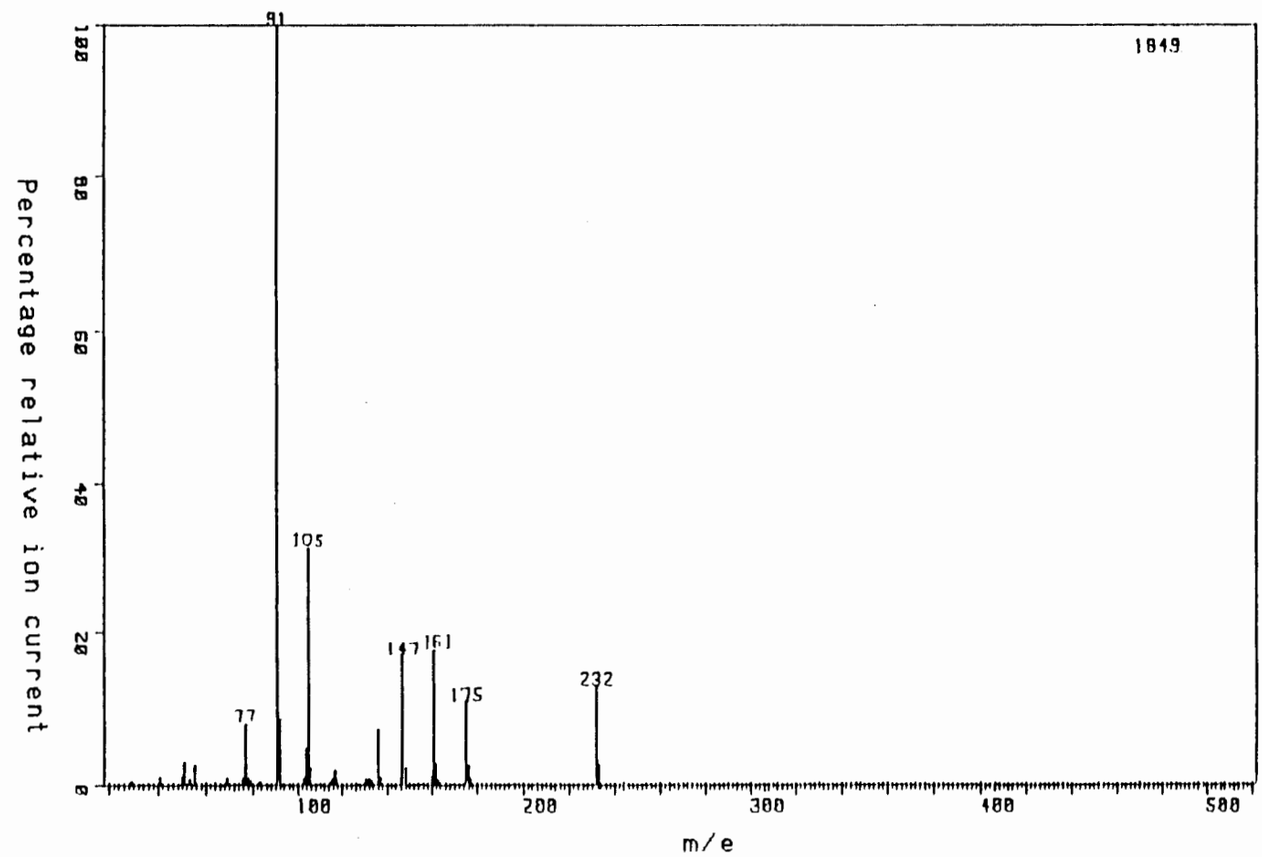

Figure A1.10. Mass spectrograph scan number 206 on sample with foulants. (Unknown)

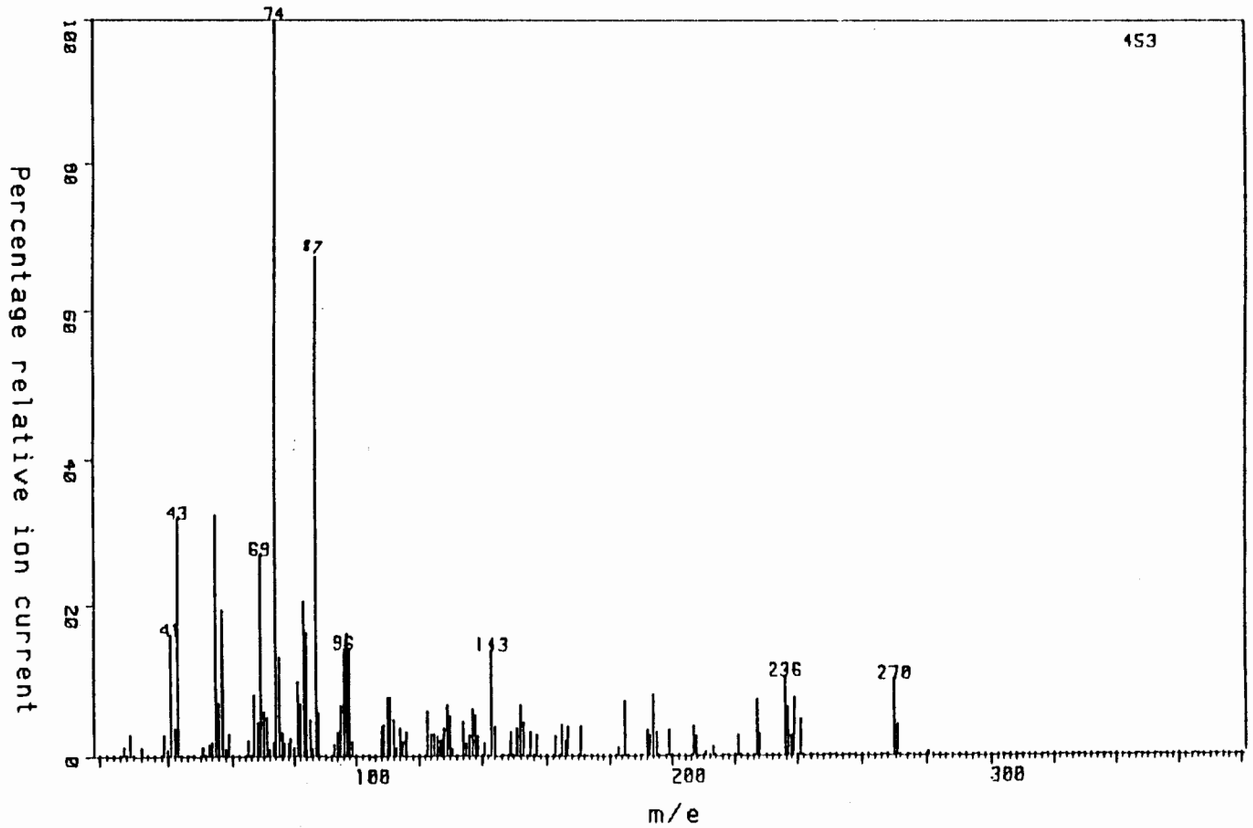

Figure A1.11. Mass spectrograph scan number 272 on sample with foulants. (Methyl palmitate)

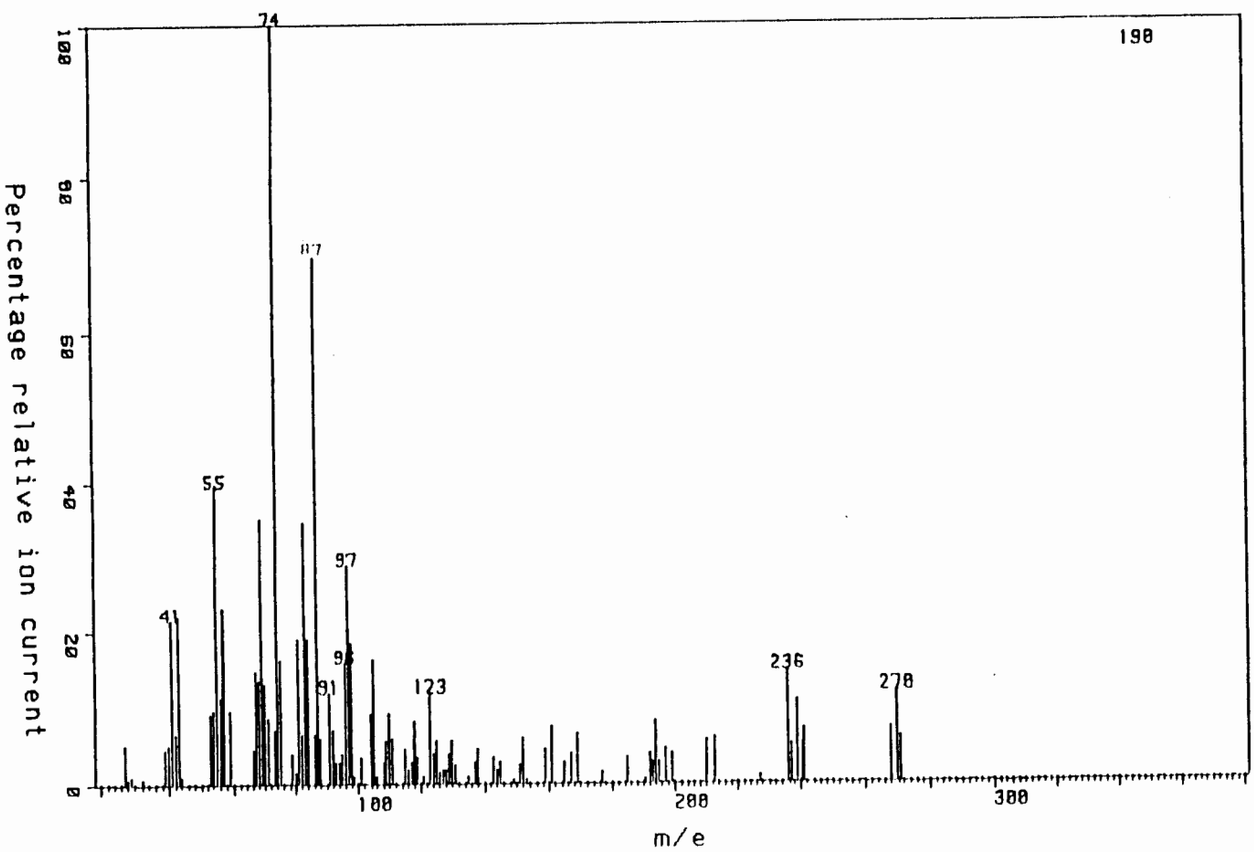

Figure A1.12. Mass spectrograph scan number 282 on sample with foulants. (Undetermined methyl ester)

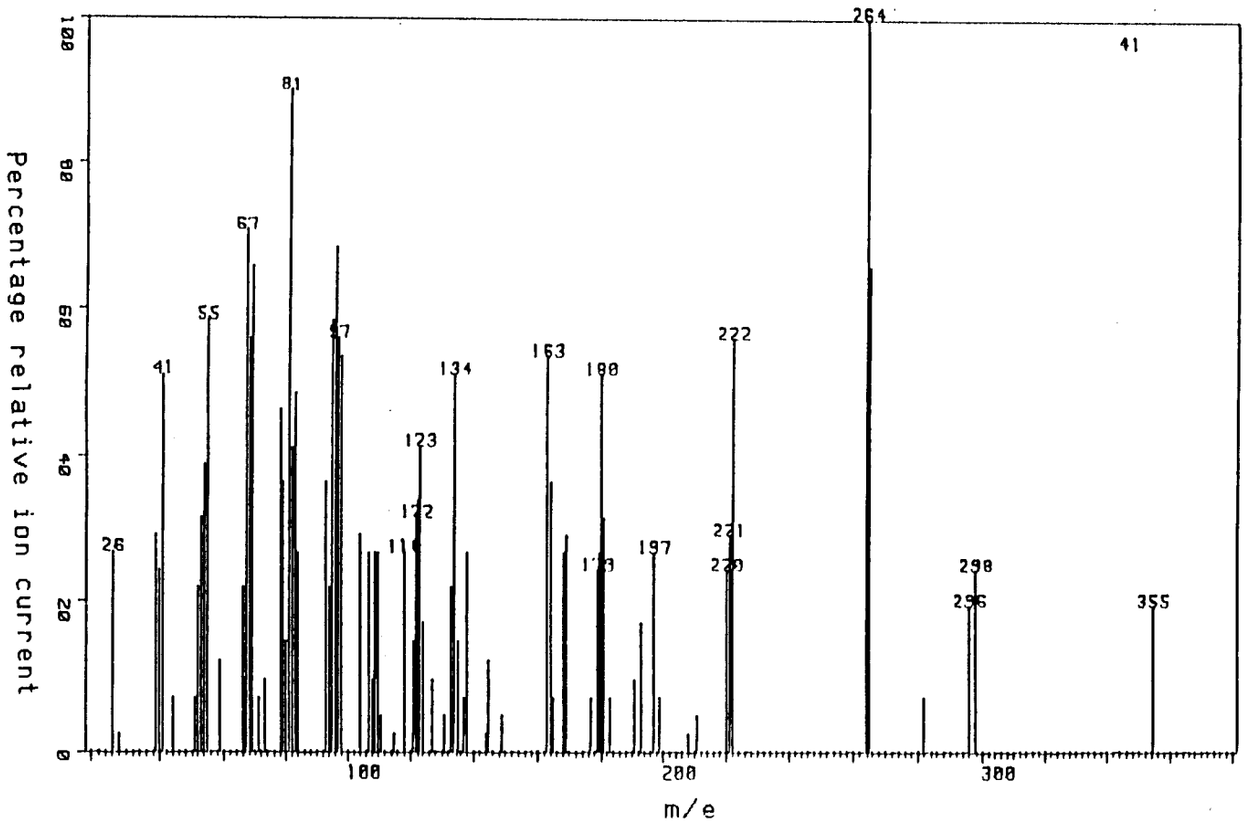

Figure A1.13. Mass spectrograph scan number 310 on sample with foulants. (Unknown)

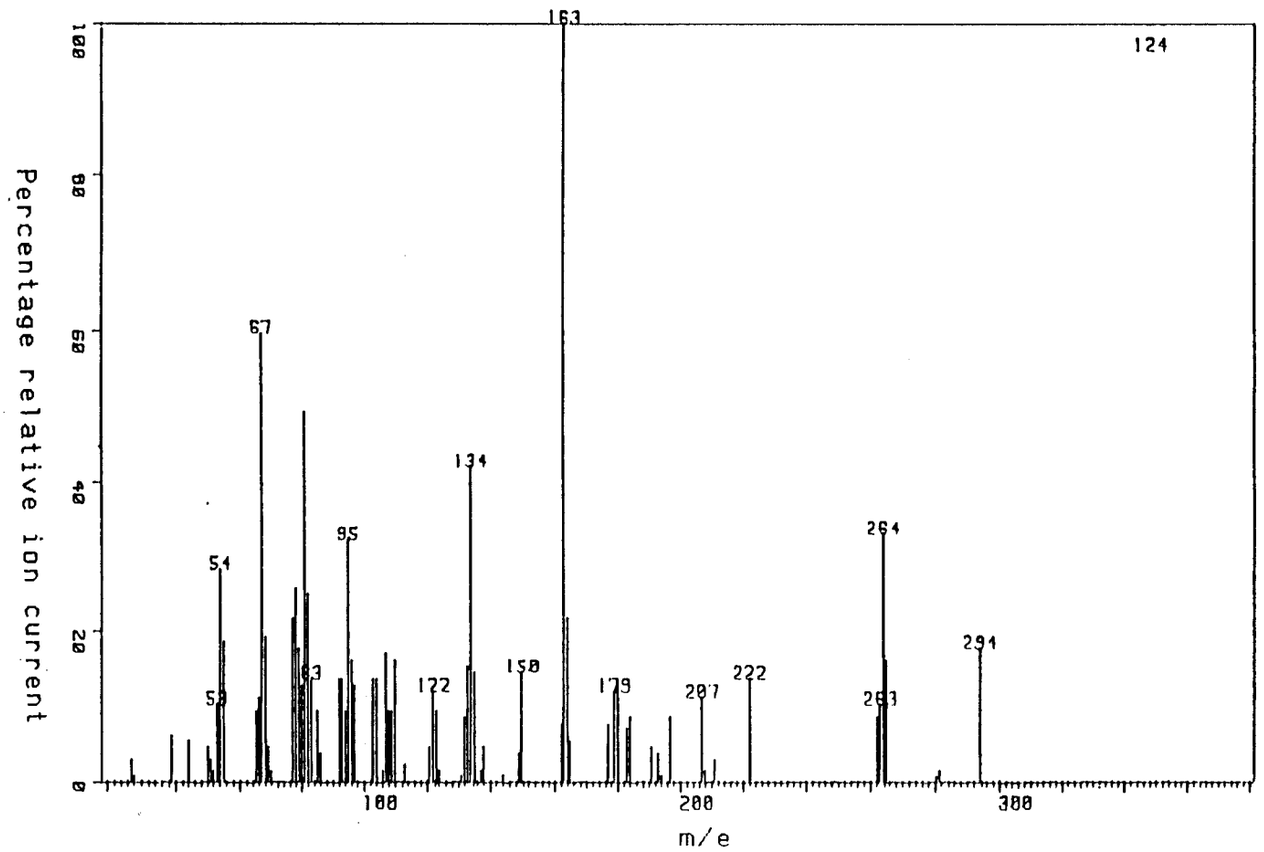

Figure A1.14. Mass spectrograph scan number 330 on sample with foulants. (Possibly dimethyl isophthalate)

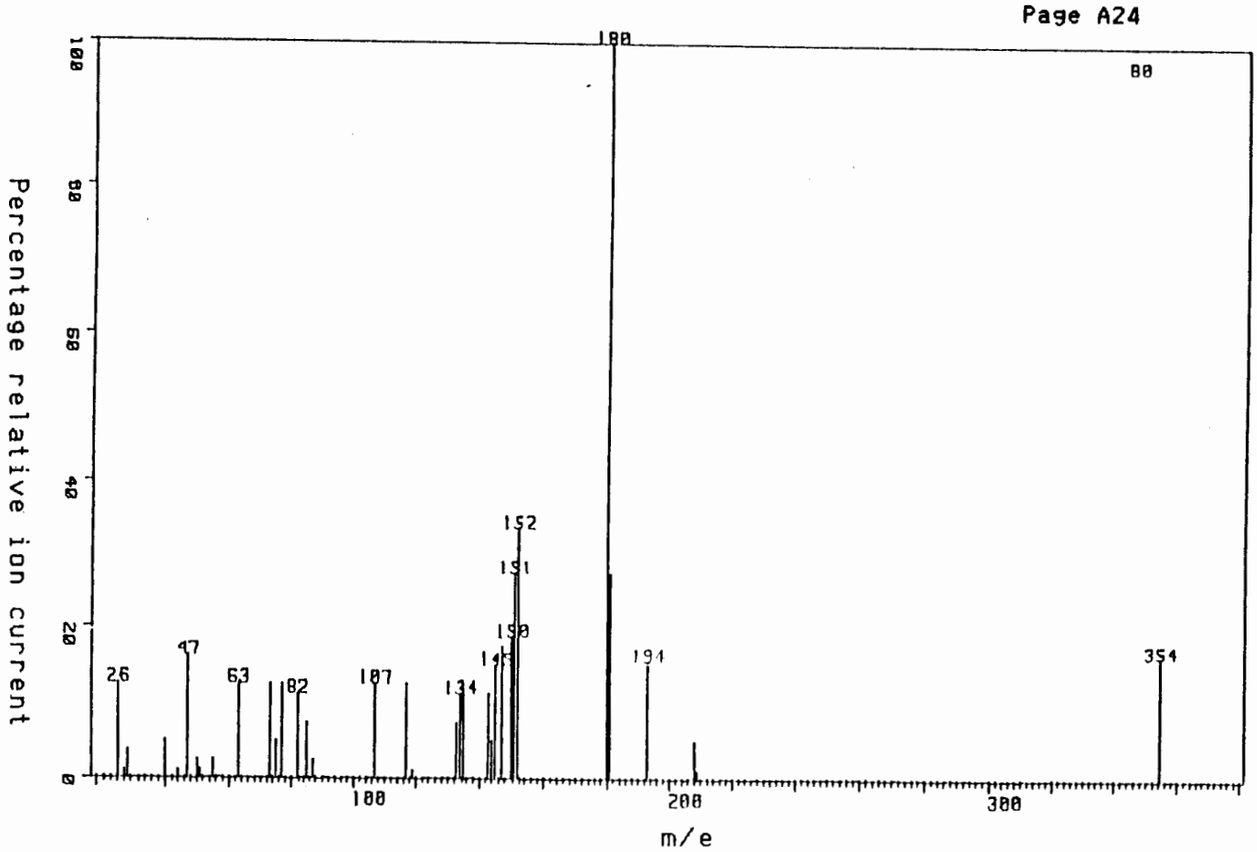

Figure A1.15. Mass spectrograph scan number 468 on sample with foulants. (Undetermined aromatic)

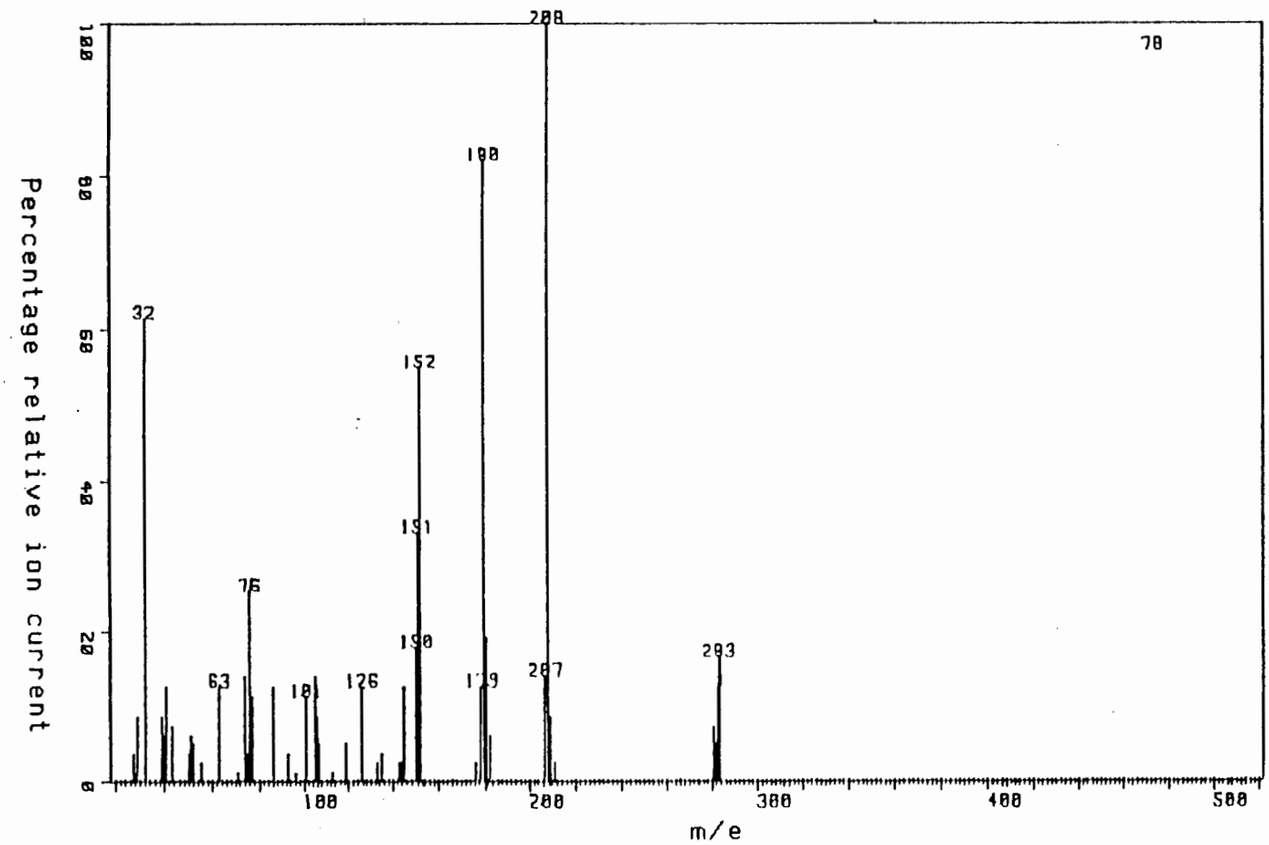

Figure A1.16. Mass spectrograph scan number 720 on sample with foulants. (Anthraquinone)

figure A1.11 agreed closely with this, but it also agreed with the published data for methyl-14-methylhexadecanoate. Since Keith (1976) found palmitic acid in paper mill effluents, it was assumed that this was the compound present at scan 272. Keith explained how the spectra was produced. There was a molecular ion at 270 due to the loss of an electron from the original molecule, and a smaller peak at 271 due to the heavy isotopes of hydrogen, and carbon. The parent ion then broke at points along the carbon chain to produce m/e values of 241 (loss of C_2H_5), 227, 213, 199, 185, 171, 157, 143, 129, 115, 101 and 87. The base peak of 74 was produced by the ion $[CH_3OCOH{:}CH_2]^+$. The un-explained m/e values were probably due to the tailing of neighbouring peaks. i.e. the system had not completely separated the different but similar compounds. Also there was probably incomplete compensation for bleed.

Figure 1.12 was the result of subtracting scan 260 from scan 282. It best matched the data for methyl 12-hydroxylaurate: 74 (100%), 87 (42), 98 (35), 84 (29), 55 (23), 43 (23), 75 (21), 69 (21).

The result of subtracting scan 292 from scan 310 was difficult to interpret (Figure A1.13). Possible compounds were beta-bisabolol, methyl oleate, Anthraquinone-1,6-dicarboxylic acid, methyl octadec-i-ene-1,8-dioate, 3-methyl cyclohexane, 1-m-chloro-2-p-dimethyl aminophenyl-1-cyano cyclopropane or a number of others. There were probably several compounds present and some of them may have been one of those mentioned above.

Figure A1.14 shows the result of scan 330 - scan 292. Possible compounds were methyl 13 beta-abietan-18-oate, methyl vinyl terephthalate, dimethylisophthalate, 2-carbomethoxy-2'-methyl benzophenone.

Figure A1.15 (scan 468 - 450) was a good example of a spectra that was proved to be unique to the fouled anion resin by the m/e = 180 SIM profiles. Possible compounds were 9,10-phenanthraquinone, 2,4-diformyl-3,5-dihydroxytoluene or 9-fluorenone.

Figure A1.16 shows the most positive result obtained from this section of work. The result was anthraquinone m/e=208 (100%), 180 (70), 152 (45), 57 (37), 76 (35), 151 (22), 207 (15), 209 (15). The absence of an m/e = 57 value on the figure was very probably due to its high value at scan 680 which was used as the background. Anthraquinone was also found in bleaching effluents by van der Klashorst (1984).

Method 2; The results of the GC/MS run with the butyl derivatives were spoiled by the mass spectrograph losing calibration. This was a pity because the method showed a lot of promise. Looking at figure A1.3 showed that there were many compounds that came off the GC column before the peak at scan 126. These were probably smaller molecules than methyl 2-ethylhexanoate which was probably responsible for the peak at this scan. Although the control showed that many of these compounds were not from the effluent, there may have been significant results from this region.

Method 3; The results indicated the presence of monosaccharides. Although little confidence can be placed on these results, because no control was done and because the mass peaks did not match well, sorbitol and dulcitol may have been present.

Finally to check if there were any high boiling compounds that would not pass through the column at the 250 °C limit of SP2330, the hexane layer from boron trifluoride methylation method and its control were passed through an OV101 column which was set at temperatures of up to 300 °C. The results were similar to the previous ones, and no new compounds were identified.

Fouling of A378 Resin by oxalic acid

A2.1) Aim of experiment

i) To check if oxalic acid fouls the anion resin. Is it an important chemical to watch in the pilot plant?

ii) To establish a procedure for testing possible anion resin foulants.

iii) To determine if the resin life testing apparatus at Enstra was suitable for such tests.

A2.2) Method

It was assumed that the A378 resin had a capacity of about 1.7 eq/l. A convenient quantity of resin for this experiment was 0.150 l with an assumed capacity of 0.255 eq.

A2.2.1) Conditioning the resin

To wash any dirt from the resin and to stabilize its behaviour, the resin should be conditioned by regenerating it with sodium hydroxide, then loading it with hydrochloric acid repeatedly until no change in capacity is detected. To do this, a 0.1 M solution of sodium hydroxide was prepared by dissolving 10.2 g NaOH in 2.55 l of deionized water. This solution was pumped through the column, but the effluent pH was 12.8 (0.1 below the influent pH) indicating that the resin was already fully regenerated.

Next 0.1 M hydrochloric acid was prepared by dissolving 0.026 l of 30-33 % w/v hydrochloric acid in deionized water and making the volume up to 2.55 l. The resin was then regenerated again and rinsed with deionized water.

A2.2.2) Oxalic acid fouling.

0.05 M oxalic acid (0.1 eq/l) was prepared by dissolving 16.06 g in 2.55 l water. The acid was pumped through the column at 0.05 l/min.

A 0.05 M calcium hydroxide slurry was prepared by adding 9.45 g to 5 l water. 5 litres was the volume of the container available. The lime slurry was pumped at a higher rate of 0.070 l/min to save time.

The resin was loaded twice and regenerated once.

A2.3) Results and discussion:

When the hydrochloric acid was pumped through the column, the pH of the effluent dropped from 10.6 to 7.4. The high pH was caused by excess sodium hydroxide in the bed being washed out. When the column was regenerated with sodium hydroxide, the pH rose from 2.2 to 11.3 during the cycle. The low initial pH was due to an excess of chloride ions being washed out of the resin. The high final pH was caused by the sodium hydroxide passing straight through the column which indicated that it was regenerated. The conditioning of the resin was stopped here because of the shortage of time.

The results of pumping the oxalic acid through the bed are reported in table A 2.1.

Table A2.1

First loading cycle of oxalic acid on resin

Bed volumes	equivalents	pH	Conductivity [ms/cm]
1.7	0.0255	10.9	0.23
6.3	0.0945	5.0?	0.089
11.3	0.17	9.4	0.045
15	0.225	9.6	0.039
17	0.255	9.0	0.033

The feed acid had a pH of 1.9 and a conductivity of 74 ms/cm. The low conductivity of the effluent shows that break-through did not occur.

The results of regenerating the bed with calcium hydroxide are shown in table A2.2.

Table A2.2

First lime regeneration cycle

Bed volumes	equivalents	pH	Conductivity [ms/cm]
2.5	0.019	10.0	0.1
10	0.075	9.3	0.49
21	0.158	12.3	17.0
28	0.21	12.1	16.5

The high pH of the effluent shows that there are no oxalate ions in it. They must either have been removed by the resin or precipitated as calcium oxalate.

The results of the second loading with oxalic acid are shown in table A2.3.

Table A2.3

Second loading cycle with oxalic acid

Bed volumes	equivalents	pH	Conductivity [ms/cm]
5	0.075	10.7	0.30
8	0.12	9.8	0.16
11	0.17	4.0	0.23
14	0.21	2.2	14.2

Break-through occurred before 0.21 eq of acid passed through the bed, while previously there was no break-through after 0.255 eq. This indicated a 20% loss of capacity after just one cycle. The loss in capacity appeared to be due to the inability of the lime to regenerate the resin fully. The accumulation of the calcium oxalate precipitate also caused a blockage in the bed, making pumping difficult. This problem would not occur in a fluidized bed under the correct conditions.

There was not enough time to get the on-line instrumentation with the life-testing apparatus working, so readings had to be taken from aliquots of the effluent. Readings could therefore not be taken often enough to allow accurate timing of the break-through. The apparatus is suitable for determining the anion resin fouling potential of different compounds. However, some time needs to be spent getting it fully functional again.

Results of isotherm measurements on XAD-8

As an example of how the isotherms were calculated from the experimental results, the first two points measured for the cation exchanged D1/D2 isotherm are calculated in detail below.

The empty bottle weighed 19.576 g and after adding wet resin it weighed 71.854g. Before the second weighing, a sample of the resin was taken from the bottle and placed in a weighed glass beaker. The beaker was reweighed and placed in an oven overnight. The mass of resin in the beaker was 7.350 g before drying and 2.227 g after drying. The dry mass of resin in the bottle was therefore 15.840 g.

After adding cation exchanged effluent to the bottle, it weighed 267.58 g which means 195.73 g of effluent was added. Accounting for the water that was carried with the resin, the total mass of liquid in the bottle was 232.16 g. After turning the bottle on the wheel for 1 day, the concentration was measured to be 12.57% of the original concentration: $\bar{c}$ = 0.1257. The total amount of solute remaining in solution was therefore 0.1257 × 232.16 = 29.18 g×$\bar{c}$. A control experiment where only water was added to the XAD-8 showed that there was no need to correct for contaminants coming off the resin.

The amount of solute adsorbed comes from the difference between the total solute added and the solute remaining in solution after equilibrium has been reached. The total solute added (units of g×$\bar{c}$) is the same as the mass of effluent added since $\bar{c}$ = 1. The amount adsorbed is then 166.55 g×$\bar{c}$. If the density of the solution is assumed to be 1000 g/l then the amount adsorbed converts to 0.16655 l×$\bar{c}$ and the specific adsorbence (or solid phase concentration) is 0.0105 l×$\bar{c}$/g XAD-8. If the initial concentration is known, the solid phase concentration is easily converted to grams per gram by multiplying the figure given here by the initial concentration expressed in grams per litre.

After measuring its concentration, the solution was transferred from the first bottle into the second bottle. The first bottle was re-weighed to check how much solution had been retained by the resin (which was not transferred). The results was 37.54 g, so the amount of solute retained in the resin pores was 37.54 × 0.1257 = 4.72 g×$\bar{c}$. More effluent was then added and on weighing the bottle, the amount added was calculated to be 201.29 g. After another day on the wheel, the concentration was measured again and was 0.1894 $\bar{c}$. The formula used this time to calculate the total solute adsorbed was:

Total solute added + residue in pores + solute already adsorbed − solute remaining in solution.
ie. 201.29 + 4.72 + 166.55 − 45.23 = 327.32 g×$\bar{c}$.

Solid phase concentration = 0.020663 l×C̄/g.

The full list of results is shown below in table A3.1. The room temperature for all readings was 18 °C. The pH of the equilibrium solution is given in the last column of the table.

Table A3.1

Isotherm of cation exchanged D1/D2 effluent on XAD-8

Mass dry XAD-8 [g]	Effluent added [g×C̄]	Residue in pores [g×C̄]	Total liquid mass [g]	Effluent in soln [g×C̄]	Effluent adsorbed [g×C̄]	Equilib. effluent conc. [C̄]	Adsorbed [l×C̄/ g XAD-8]	pH
15.84	195.72	0	232.16	29.1829	166.5430	0.1257	0.010514	1.72
15.84	201.29	4.71928	238.83	45.2351	327.3171	0.1894	0.020663	1.61
15.84	202.78	7.08998	240.21	56.7625	480.4245	0.2363	0.030329	-
15.84	195.87	8.87270	233.42	62.2074	622.9649	0.2665	0.039328	1.65
15.84	202.07	10.16536	240.21	72.0881	763.1120	0.3001	0.048176	1.65
15.84	200.46	11.55491	238.96	80.0528	895.0742	0.335	0.056507	1.61
4.57	232.9	3.59174	243.62	96.7665	398.0931	0.3972	0.087066	1.61
4.57	234.31	4.55657	245.78	109.2991	527.6605	0.4447	0.115403	-
4.57	233.19	5.18591	244.85	118.6306	647.4059	0.4845	0.141593	-
15.13	22.61	0	215.46	15.3629	7.2492	0.0713	0.000479	1.78
15.13	35.64	2.59955	224.64	27.4071	18.0847	0.122	0.001195	-
15.13	45.20	4.39435	227.32	35.7815	31.9040	0.1574	0.002108	1.67
15.13	49.32	5.71818	221.42	40.9643	45.9870	0.185	0.003039	1.66
15.13	56.19	6.71343	223.53	47.4573	61.4368	0.2123	0.004060	1.62
5.62	63.92	2.83500	204.17	50.5126	39.0879	0.2474	0.006948	1.61
5.62	88.14	3.40764	235.69	67.5734	63.0688	0.2867	0.011212	-
5.62	99.381	3.97474	237.34	76.4247	90.0004	0.322	0.016000	-
16.60	12.073	0	208.28	10.2058	1.8680	0.049	0.000112	-
16.60	21.885	2.02630	220.74	20.0213	5.7585	0.0907	0.000346	1.75
16.60	28.549	3.70446	222.22	27.3556	10.6565	0.1231	0.000641	1.69
16.60	32.439	4.79020	214.26	32.6965	15.1899	0.1526	0.000914	1.63
6.25	37.668	2.22929	192.03	34.7590	20.3286	0.181	0.003252	1.61
6.25	44.705	2.83242	196.34	42.3916	25.4745	0.2159	0.004075	-
18.35	7.346	0	192.98	6.1946	1.1513	0.0321	0.000062	2.13
18.35	15.341	1.3909	212.48	14.2999	3.5842	0.0673	0.000195	1.81
18.35	21.207	2.9242	215.73	21.5299	6.1861	0.0998	0.000337	1.67
7.50	24.950	1.7472	181.00	24.9246	7.9588	0.1377	0.001060	1.62
7.50	30.087	2.51538	184.49	30.4604	10.1013	0.1651	0.001345	-
18.52	4.466	0	182.51	3.9971	0.4689	0.0219	0.000025	2.34
18.52	10.679	0.99266	204.01	10.4456	1.6957	0.0512	0.000091	1.83
13.85	2.700	0	151.29	2.5115	0.1885	0.0166	0.000013	2.5

To illustrate the method for accounting for contaminants from the resin, the first point on the oxalic acid isotherm curve is calculated in detail below.

The dry mass of XAD-8 was calculated as before using its wet mass and the fraction of water retained in a sample of resin withdrawn at the same time. 0.1 l of 1E-5 M oxalic acid was added to the bottle, so the amount of acid added comes to 1 µmole. After reaching equilibrium, the UV absorbence indicated a concentration of 1.258E-5 M.; higher than the solution added. To calculate how much oxalic acid really did remain in solution, the results from the control experiment were used. The control bottle contained 16.00 g of XAD-8 and 136.8 g of water. The concentration as indicated by UV absorbence after 1 day was 4.82E-6 M of oxalic acid. This converts to 0.0412 µmole/g of XAD-8. The bottle with the oxalic acid solution in it contained 31.79 g XAD-8. The total contamination estimated to have been released by this resin was therefore 1.31 µmole. The indicated amount of oxalic acid remaining in solution was 173.1 g × 1.258E-5 M. If the density of the solution was 1000 g/l, this comes to 2.18 µmole of oxalic acid. Subtracting the contamination, the true quantity of acid remaining in solution was estimated at 0.868 µmole. The true equilibrium concentration was then estimated by dividing this figure by the total mass of solution.

The conversion from moles to grams was done using the molecular weight of the bi-hydrate molecule which is 126.07. The full results are shown below in table A3.2.

Table A3.2

Isotherm of Oxalic acid on XAD-8 measured by UV absorption.

Mass dry XAD-8 [g]	Oxalic added [μmole]	Measured conc [mmol/l]	Residue in pores [μmole]	Total mass soln [g]	Oxalic in soln [μmole] [g]	Oxalic adsorb [μmole]	Adsorbed [g/ g XAD-8]	Equilib. solution conc. [g/l]
31.79	1	0.01258	0	173.1	0.86785	0.13215	5.242E-07	6.322E-04
17.57	2	0.011	0	240.4	1.92051	0.07948	5.705E-07	1.007E-03
9.85	2	0.00977	0	222.7	1.76971	0.23028	2.946E-06	1.002E-03
6.49	2	0.00912	0	214.9	1.69245	0.30754	5.975E-06	9.931E-04
31.79	10	0.04464	0.9482	175.4	6.71720	4.36347	1.731E-05	4.829E-03
17.57	20	0.07983	0.4521	241.1	18.6320	1.89952	1.363E-05	9.745E-03
9.85	20	0.08868	0.2286	223.4	19.4661	0.99275	1.270E-05	1.099E-02
6.49	20	0.08958	0.1440	215.8	19.1041	1.34745	2.618E-05	1.116E-02
31.79	50	0.3091	3.3658	175.4	54.2161	3.51319	1.394E-05	3.898E-02
17.57	100	0.4309	3.2810	241.1	103.889	1.29054	9.262E-06	5.434E-02
9.85	100	0.4584	2.0751	223.4	102.406	0.66130	8.461E-06	5.780E-02
6.49	100	0.4711	1.2362	215.8	101.663	0.92028	1.788E-05	5.941E-02
31.79	500	2.983	23.306	175.4	523.218	3.60113	1.428E-05	3.762E-01
17.57	1000	4.194	17.709	241.1	1011.17	7.82713	5.618E-05	5.289E-01
9.85	1000	4.492	10.726	223.4	1003.51	7.87506	1.008E-04	5.664E-01
6.49	1000	4.656	7.4433	215.8	1004.76	3.59886	6.991E-05	5.871E-01
31.79	5000	26.83	224.91	175.4	4705.98	522.537	2.073E-03	3.383E+00
17.57	10000	39.82	172.37	241.1	9600.60	579.598	4.160E-03	5.021E+00
9.85	10000	43.73	105.11	223.4	9769.28	343.705	4.397E-03	5.514E+00
6.49	10000	45.57	73.564	215.8	9834.00	243.157	4.724E-03	5.746E+00
31.79	50000	259.5	2022.9	175.4	45516.3	7029.21	2.788E-02	3.272E+01
17.57	100000	400.3	1636.6	241.1	96512.3	5703.87	4.094E-02	5.048E+01
9.85	100000	438.6	1023.2	223.4	97983.2	3383.74	4.329E-02	5.531E+01
6.49	100000	457.2	720.00	215.8	98663.7	2299.40	4.467E-02	5.765E+01

Table A3.3 below shows the results of the electrical conductivity measurements performed on the same bottles as those reported in table A3.2 above.

Table A3.3

Isotherm of Oxalic acid on XAD-8 measured by conductivity.

Mass dry XAD-8 [g]	Oxalic added [µmole]	Measurd conc mmole/l	Residue in pores	Total mass soln	Oxalic in soln [µmole]	Oxalic adsorb [µmole]	Adsorbed [g/ g XAD-8]	Solution conc [g/l]
31.79	1	0.00157	0	173.1	0.27176	0.72823	2.889E-06	1.980E-04
17.57	2	0.00151	0	240.4	0.36300	1.63699	1.175E-05	1.904E-04
9.856	2	0.00267	0	222.7	0.59460	1.40539	1.798E-05	3.367E-04
6.491	2	0.0036	0	214.9	0.77364	1.22636	2.382E-05	4.540E-04
31.79	10	0.02302	0.11838	175.4	4.03770	6.80890	2.701E-05	2.903E-03
17.57	20	0.06775	0.06206	241.1	16.3345	5.36453	3.850E-05	8.543E-03
9.856	20	0.0826	0.06248	223.4	18.4528	3.01503	3.857E-05	1.042E-02
6.491	20	0.09072	0.0569	215.8	19.5773	1.70586	3.314E-05	1.144E-02
31.79	50	0.2939	1.73571	175.4	51.5500	6.99455	2.774E-05	3.706E-02
17.57	100	0.4233	2.78452	241.1	102.057	6.09142	4.372E-05	5.338E-02
9.856	100	0.4486	1.9328	223.4	100.217	4.73063	6.052E-05	5.657E-02
6.491	100	0.4638	1.25193	215.8	100.088	2.86976	5.575E-05	5.849E-02
31.79	500	2.922	22.1601	175.4	512.519	16.6358	6.599E-05	3.685E-01
17.57	1000	4.159	17.3976	241.1	1002.73	20.7541	1.490E-04	5.244E-01
9.856	1000	4.473	10.4972	223.4	999.268	15.9596	2.042E-04	5.640E-01
6.491	1000	4.633	7.3280	215.8	999.801	10.3964	2.020E-04	5.842E-01
31.79	5000	26.32	220.319	175.4	4616.53	620.426	2.461E-03	3.319E+00
17.57	10000	39.15	170.935	241.1	9439.06	752.624	5.402E-03	4.937E+00
9.856	10000	43.07	104.668	223.4	9621.84	498.789	6.382E-03	5.431E+00
6.491	10000	45.34	73.201	215.8	9784.37	299.226	5.813E-03	5.717E+00
31.79	50000	254.1	1984.53	175.4	44569.1	8035.81	3.188E-02	3.204E+01
17.57	100000	393.3	1609.06	241.1	94824.6	7537.06	5.409E-02	4.960E+01
9.856	100000	424.3	1007.84	223.4	94788.6	6718.01	8.595E-02	5.350E+01
6.491	100000	446	716.37	215.8	96247	4768.80	9.264E-02	5.624E+01

Isotherms for Malonic acid were measured and interpreted by exactly the same procedure used for oxalic acid. The molecular weight of Malonic acid is 104.06 g/mole. The room temperature rose from 19 to 21 °C during the determination. The detailed results from the UV absorbence measurements are reported in table A3.4. The results from the conductivity measurements are reported in table A3.5.

Table A3.4

Isotherm of Malonic acid on XAD-8 measured by Ultraviolet absorption.

Mass dry XAD-8 [g]	Malonic added [µmole]	Meas. conc mmole /l	Residue in pores [µmole]	Total liquid mass [g]	Malonic in soln [µmole]	Malonic adsorbd [µmole]	Malonic adsorb [g / g XAD-8]	Malonic conc [g/l]
27.55	1	0.088	0	162.5	0.525	0.475	1.794E-06	3.041E-04
14.76	2	0.018	0	233.5	-3.177	5.177	3.650E-05	-
16.6	2	0.024	0	237.7	-2.5952	4.5952	2.881E-05	-
10.08	2	0.016	0	222.9	-1.4736	3.4736	3.586E-05	-
27.55	10	0.087	5.5792	163.4	5.9769	9.6022	3.627E-05	3.443E-03
14.76	20	0.040	0.6012	233.4	5.0223	15.5788	1.098E-04	2.025E-03
16.6	20	0.037	0.9144	238.1	3.9011	17.0133	1.067E-04	1.542E-03
10.08	20	0.053	0.3744	223.4	8.9480	11.4264	1.180E-04	3.770E-03
27.55	100	0.570	5.5259	163.4	84.6077	20.9182	7.901E-05	4.873E-02
14.76	200	0.781	1.3523	233.4	177.843	23.5087	1.657E-04	7.171E-02
16.6	200	0.767	1.4211	238.1	177.467	23.9538	1.502E-04	7.015E-02
10.08	200	0.830	1.2540	223.4	182.344	18.9099	1.952E-04	7.682E-02
27.55	1000	4.581	36.1633	163.4	747.213	288.950	1.091E-03	4.304E-01
14.76	2000	7.329	26.1088	233.4	1709.88	316.228	2.229E-03	6.895E-01
16.6	2000	7.092	29.2265	238.1	1687.81	341.418	2.140E-03	6.671E-01
10.08	2000	7.923	19.4290	223.4	1769.51	249.914	2.580E-03	7.455E-01
27.55	8070	36.8	290.435	163.4	6013.12	2347.31	8.866E-03	3.463E+00
14.76	16140	61.09	244.788	233.4	14258.4	2126.38	1.499E-02	5.749E+00
16.6	16140	59.56	270.205	238.1	14181.2	2228.97	1.397E-02	5.605E+00
10.08	16140	66.34	185.398	223.4	14820.3	1505.04	1.554E-02	6.243E+00

Table A3.5

Isotherm of pure Malonic acid on XAD-8 measured by conductivity.

Mass dry XAD-8 [g]	Malonic added µmole	Meas. conc mmole /l	Residue in pores [µmole]	Total liquid mass [g]	Malonic in soln [µmole]	Malonic adsorb. [µmole]	Malonic adsorbed [g / g XAD-8]	Malonic conc [g/l]
27.55	1	0.004	0	162.5	0.6012	0.3987	1.506E-06	3.482E-04
14.76	2	0.004	0	233.5	0.934	1.066	7.515E-06	3.765E-04
16.6	2	0.004	0	237.7	0.9508	1.0492	6.577E-06	3.765E-04
10.08	2	0.005	0	222.9	1.2259	0.7740	7.991E-06	5.176E-04
27.55	10	0.010	0.23458	163.4	0.0218	10.2127	3.857E-05	1.258E-05
14.76	20	0.036	0.1336	233.4	7.6335	12.5001	8.813E-05	3.078E-03
16.6	20	0.032	0.1524	238.1	6.6946	13.4577	8.436E-05	2.646E-03
10.08	20	0.060	0.1287	223.4	12.8014	7.32726	7.564E-05	5.393E-03
27.55	100	0.406	0.64985	163.4	64.9302	35.7196	1.349E-04	3.740E-02
14.76	200	0.768	1.2191	233.4	178.490	22.7292	1.602E-04	7.197E-02
16.6	200	0.750	1.23063	238.1	177.888	23.3427	1.463E-04	7.031E-02
10.08	200	0.841	1.40423	233.4	187.331	14.0735	1.453E-04	7.892E-02
27.55	1000	4.586	25.7277	163.4	749.270	276.458	1.044E-03	4.316E-01
14.76	2000	7.614	25.6478	233.4	1777.06	248.584	1.753E-03	7.166E-01
16.6	2000	7.387	28.5978	238.1	1758.79	269.803	1.691E-03	6.952E-01
10.08	2000	8.28	19.6747	223.4	1849.72	169.953	1.754E-03	7.792E-01
27.55	8070	38.42	290.752	163.4	6277.83	2082.92	7.867E-03	3.616E+00
14.76	16140	63.25	254.307	233.4	14762.5	1631.76	1.150E-02	5.953E+00
16.6	16140	61.14	281.445	238.1	14557.4	1864.01	1.168E-02	5.754E+00
10.08	16140	68.39	193.75	223.4	15278.3	1055.42	1.090E-02	6.436E+00

The detailed isotherm results for phenol are shown below in table A3.6. The conductivity of the phenol solutions was very close to that of the distilled water used to prepare the solutions. Conductivity was therefore not used to measure concentration. The pH of all solutions was between 5.2 and 5.6. The molecular weight of phenol is 94.11 g/mole. The room temperature was 19°C.

Table A3.6

Isotherm of pure Phenol on XAD-8 measured by UV absorption.

Mass dry XAD-8 [g]	Phenol added µmole	Measur conc mmole/l]	Residue in pore [µmole]	Total liquid mass [g]	Phenol in soln [µmole]	Phenol adsorb [µmol]	Phenol adsorbed [g / g XAD-8]	Phenol conc [g/l]
33.94	1	0.0080	0	177.7	0.26799	0.7320	2.030E-06	1.419E-04
18.68	2	0.0026	0	242.8	-0.0065	2.0065	1.011E-05	-
15.11	2	0.0022	0	234.6	0.00590	1.9941	1.242E-05	2.366E-06
5.391	2	0.0014	0	212.3	0.11626	1.8837	3.289E-05	5.154E-05
33.94	10	0.0041	0.62175	176.8	0.09239	10.529	3.123E-05	4.918E-05
18.68	20	0.0023	0.11081	242.4	0.19896	19.912	1.104E-04	7.725E-05
15.11	20	0.0025	0.07664	235	0.29665	19.780	1.356E-04	1.188E-04
5.391	20	0.0060	0.01735	212.6	1.18635	18.831	3.616E-04	5.252E-04
33.94	100	0.0077	0.32401	177.1	0.91290	99.411	3.069E-04	4.851E-04
18.68	200	0.0203	0.09780	241.1	4.64957	195.44	1.095E-03	1.815E-03
15.11	200	0.0256	0.08594	233.3	5.78264	194.30	1.346E-03	2.333E-03
5.391	200	0.0664	0.07456	212.1	14.0149	186.06	3.610E-03	6.219E-03
33.94	1000	0.0954	0.60140	178.2	12.7243	987.88	3.046E-03	6.720E-03
18.68	2000	0.3993	0.87012	243.3	94.7982	1906.1	1.070E-02	3.667E-02
15.11	2000	0.5291	0.88783	234.6	122.225	1878.6	1.305E-02	4.903E-02
5.391	2000	1.97	0.81696	212.9	418.734	1582.1	3.123E-02	1.851E-01
33.94	10000	1.734	7.41102	177.8	291.647	9715.7	2.999E-02	1.544E-01
18.68	20000	12.87	17.0900	241.7	3101.51	16915	9.592E-02	1.208E+00
15.11	20000	17.73	18.3079	235.1	4160.91	15857	1.118E-01	1.666E+00
5.391	20000	53.85	24.231	213.2	11478.2	8546.0	1.804E-01	5.067E+00
33.94	20000	10.41	134.73	176.9	1792.14	18342	8.085E-02	9.534E-01
18.68	40000	77.52	550.83	242.5	18771.4	21779	2.057E-01	7.285E+00
15.11	40000	95.455	613.46	234.8	22390.8	18222	2.253E-01	8.975E+00

Sodium oxalate solutions were prepared by dissolving oxalic acid in a 0.1 N solution of sodium hydroxide. For the higher oxalate concentrations, extra solid sodium hydroxide was added to adjust the pH to 11.4. The results are given in table A3.7.

Table A3.7

Isotherm of sodium oxalate on XAD-8 at pH = 11.4

Mass dry resin [g]	oxalic acid added [mmole]	Measured conc [mmol/l]	Total liquid mass	Solute in soln	Solute adsorbed [mmole]	Solute conc [g/l]	Adsorbed [g/g]
35.75	0.01368	0.0821	220.43	0.0116	0.00205	0.00665	7.254E-06
35.22	0.02819	0.136	223.20	0.0239	0.00421	0.01354	1.510E-05
33.54	0.07121	0.3870	221.06	0.0794	-0.00826	0.04532	-
32.90	0.14546	0.7577	222.41	0.1625	-0.01711	0.09215	-
32.03	0.29416	1.4570	222.56	0.3184	-0.02432	0.18040	-
35.75	0.01368	1.8727	220.43	0.1709	-0.15721	0.09774	-
35.22	0.02819	0.7921	223.20	-0.0615	0.08971	-0.03474	3.211E-04
33.54	0.07121	1.4302	221.06	0.0892	-0.01799	0.05087	-
32.90	0.14546	1.6113	222.41	0.1357	0.00972	0.07694	3.725E-05
32.03	0.29416	2.2288	222.56	0.2792	0.01486	0.15820	5.850E-05
35.75	0.68445	2.7465	220.43	0.3635	0.24333	0.20790	8.580E-04
35.22	1.4097	5.9178	223.20	1.0825	0.37412	0.61144	1.339E-03
33.54	2.8484	16.3424	221.06	3.3857	-0.55045	1.93085	-
34.89	7.143	23.2876	224.35	4.9886	2.15436	2.80321	7.784E-03
32.90	14.546	111.5845	222.41	24.5950	-10.0527	13.94125	-
32.03	29.416	185.3524	222.56	41.0359	-11.6246	23.24460	-

The stearic acid solution was prepared by adding a known amount (2.5 mg) of solid acid to 1 litre of water and heating it until it dissolved. The concentration was measured using UV, but the absorbence of the almost saturated solution was only 0.057 in a 4 cm cell at 200 nm. The results are reported in table A3.8. The room temperature was 20 °C.

Table A3.8

Isotherm of Stearic acid on XAD-8

Mass dry resin [g]	Mass acid added [mg]	Measured conc. [mg/l]	Total liquid mass [g]	acid in soln [mg]	Acid adsorbed [mg]	Acid conc. [g/l]	Adsorbed [g/g]
0.4089	0.5216	30.2	209.59	4.130	-3.60876	1.971E-02	-
0.0703	0.5496	10.48	220.02	1.927	-1.37808	8.761E-03	-
0.4089	0.5262	15.2	211.42	1.587	-4.67037	7.510E-03	-
0.0703	0.5251	3.9	210.20	0.540	-1.39323	2.570E-03	-

Palmitic acid is very similar to stearic acid. The UV absorbence of the almost saturated solution (6 mg/l) was 0.134 which was still not enough to compare with the absorbence of the contaminants from the resin. See table A3.9 for the results.

Table A3.9

Isotherm of Palmitic acid on XAD-8

Mass dry resin [g]	Mass acid added [mg]	Measured conc. [mg/l]	Total liquid mass [g]	acid in soln [mg]	Acid adsorbed [mg]	Acid conc. [g/l]	Adsorbed [g/g]
0.6254	1.2600	38.26	211.40	4.652	-3.39206	2.201E-02	-
0.0527	1.2636	11.78	210.72	2.192	-0.92892	1.040E-02	-
0.6254	1.2017	23.9	201.69	2.308	-4.49903	1.145E-02	-
0.0527	1.2532	6.21	208.99	1.086	-0.76172	5.197E-03	-

Phthalic acid also also had to be dissolved in hot water. See table A3.10 for isotherm results.

Table A3.10

Isotherm of Phthalic acid on XAD-8

Mass dry resin [g]	Mass acid added [mg]	Measured conc. [mg/l]	Total liquid mass [g]	acid in soln [mg]	Acid adsorbed [mg]	Acid conc. [g/l]	Adsorbed [g/g]
0.1853	1.984	7.89	198.87	1.569	0.41546	7.890E-03	2.242E-03
0.3494	0.857	3.26	215.25	0.676	0.18151	3.142E-03	5.195E-04
1.0167	0.169	0.9	214.44	0.153	0.01625	7.157E-04	1.599E-05
0.1853	9.396	37.9	215.44	8.157	1.65440	3.786E-02	8.926E-03
0.3494	10.243	33.15	235.18	7.782	2.64273	3.309E-02	7.563E-03
1.0167	9.531	20.77	220.39	4.536	5.01159	2.058E-02	4.929E-03

Benzoic acid is more soluble than phthalic acid (3400mg/l compared to 20mg/l) so its isotherm was measured over a wider range. See table A3.11 for results.

Table A3.11

Isotherm of Benzoic acid on XAD-8

Mass dry resin [g]	Mass acid added [mg]	Measured conc. [mg/l]	Total liquid mass [g]	acid in soln [mg]	Acid adsorbed [mg]	Acid conc. [g/l]	Adsorbed [g/g]
2.9439	40.801	44.8	210.61	9.435	31.36642	4.480E-02	1.065E-02
1.8704	17.098	17.96	217.92	3.914	13.18478	1.796E-02	7.049E-03
6.3786	3.154	5.92	211.46	1.251	1.90265	5.920E-03	2.983E-04
1.8704	426.61	1113	217.49	242.0	197.7177	1.113E+00	1.057E-01
6.3786	385.35	299	206.98	61.88	325.3675	2.990E-01	5.101E-02

Table A3.12 below shows the results of the isotherm of untreated D1/D2 effluent on XAD-8.

Table A3.12

Isotherm of untreated D1/D2 effluent on XAD-8

Mass dry XAD-8 [g]	Effluent added [g*C]	Residue in pores	Total liquid mass [g]	Effluent in soln [g*C]	Effluent adsorbed [g*C]	Equilib effluent conc [C]	Adsorbed [l*C/ g XAD-8]
3.426	250	0	257.85	154.19	95.81	0.598	0.02796
3.426	250	4.69	257.85	164.25	186.25	0.637	0.05436
3.426	250	5.00	257.85	187.20	254.05	0.726	0.07415
3.426	250	5.70	257.85	195.96	313.79	0.76	0.09159
3.426	250	5.96	257.85	202.41	367.34	0.785	0.10722
3.426	250	0	257.85	154.71	95.29	0.6	0.02781
3.426	250	4.71	257.85	166.57	183.43	0.646	0.05354
3.426	250	0.00	257.85	153.93	96.07	0.597	0.02804
3.426	250	4.68	257.85	165.02	185.73	0.64	0.05421
3.426	250	5.02	257.85	184.88	255.87	0.717	0.07468
3.426	250	5.63	257.85	195.96	315.54	0.76	0.09210
3.426	250	5.96	257.85	200.09	371.41	0.776	0.10840
3.426	250	6.09	257.85	198.80	428.70	0.771	0.12513
2.574	250	0	255.89	164.80	85.20	0.644	0.03310
2.574	250	3.80	255.89	185.27	153.73	0.724	0.05972
2.574	250	4.27	255.89	196.27	211.73	0.767	0.08225
2.574	250	4.52	255.89	196.27	269.98	0.767	0.10488
3.426	250	0	257.85	159.86	90.14	0.62	0.02630
3.426	250	4.86	257.85	179.72	165.28	0.697	0.04824
3.426	250	5.47	257.85	190.03	230.72	0.737	0.06734
3.426	250	5.78	257.85	189.52	296.98	0.735	0.08668

Table A3.13 shows both the loading and the regeneration results for cation exchanged DC effluent on activated carbon.

Table A3.13

Isotherm of cation exchanged DC effluent on activated carbon

Mass Activ. carbon [g]	Effluent added [g]	Residue in pores [g×C̄]	Total Liquid Mass [g]	Solute in liquid g×C̄	Adsorbed GAC [g*C]	Equilib. Conc. [C/Co]	Adsorbed Adsorbenc [g×C̄/g]
45.602	181.352	0	181.35	1.9948	179.3571	0.011	3.933097
16.849	182.887	0	182.89	4.3892	178.4977	0.024	10.59396
86.901	163.396	0	163.39	0.8169	162.5790	0.005	1.870853
31.466	164.145	0	164.14	2.7904	161.3545	0.017	5.127901
9.759	170.07	0	170.07	5.4422	164.6277	0.032	16.86932
0.598	195.596	0	195.59	113.44	82.1503	0.580	137.3751
86.901	130.02	0.28028	186.07	1.8607	291.0185	0.010	3.348851
31.466	170.11	0.57148	203.73	5.5006	326.5353	0.027	10.37740
9.759	223.92	0.38345	235.90	28.308	360.6228	0.120	36.95284
0.598	175.5	0.79808	176.87	132.65	125.7914	0.750	210.3535
86.901	129.39	0.64886	194.27	2.7198	418.3375	0.014	4.813955
31.466	185.68	0.74646	213.33	8.1064	504.8554	0.038	16.04447
9.759	207.87	1.37556	219.33	48.253	521.6151	0.220	53.44965
0.598	152.8	1.107	154.27	124.96	154.7348	0.810	258.7539

Regeneration data

Mass Activ. carbon [g]	Effluent added [g]	Solute on carbon [g×C̄]	Total Liquid Mass [g]	Solute in liquid g×C̄	Adsorbed GAC [g*C]	Equilib. Conc. [C/Co]	Adsorbed Adsorbenc [g×C̄/g]
86.901	0	0.89972	181.97	14.5580	404.6791	0.08	4.65678
31.466	0	1.21284	194.76	25.3197	480.7485	0.13	15.27835
9.759	0	2.57906	206.01	129.788	394.4060	0.63	40.41459
0.598	0	1.41426	211.61	107.924	48.22494	0.51	80.64371

Kinetics of adsorption: experimental results

The 3 tables below show the results of contacting 10.338 grams of XAD-8 with 0.25 l of phenol solution in the spinning basket. Table A4.1 is the data for the first part of the experiment where 0.001 M phenol was contacted with clean XAD-8. Table A4.2 shows the data for the next part of the experiment where 0.01 M phenol was contacted with the resin from the first experiment. The equivalent results for 0.1 M phenol are in Table A4.3.

Table A4.1

Adsorption rate with 0.001 M phenol

time [sec]	actual conc. [C/C_0]	predicted: const diff.	predicted: variable diff.
0.00	1.000000	1.00000	1.000000
10.00	0.800213	0.82009	0.803660
20.00	0.684378	0.70747	0.619036
40.00	0.543039	0.56368	0.480726
60.00	0.456961	0.47180	0.404594
90.00	0.377258	0.37917	0.334581
120.00	0.330499	0.31780	0.289764
180.00	0.267800	0.24070	0.233239
240.00	0.232731	0.19628	0.199072
360.00	0.190223	0.14715	0.158018
660.00	0.146652	0.09726	0.110080
1200.00	0.116897	0.07397	0.082149

Table A4.2

Adsorption rate with 0.01 M phenol

time [sec]	actual conc. [C/C_0]	predicted: const diff.	predicted: variable diff.
0.00	1.000000	1.000000	1.000000
10.00	0.855473	0.848751	0.824842
20.00	0.759830	0.762187	0.744594
40.00	0.635494	0.648663	0.648583
60.00	0.560043	0.573011	0.585050
90.00	0.484591	0.492115	0.518766
120.00	0.434644	0.434211	0.470281
180.00	0.366631	0.353661	0.403762
240.00	0.324123	0.301321	0.357580
360.00	0.272051	0.236448	0.297800
660.00	0.216791	0.175446	0.226775
1200.00	0.183847	0.148357	0.181678

Table A4.3

Adsorption rate with 0.1 M phenol

time [sec]	actual conc. [C/C_0]	predicted: const diff.	predicted: variable diff.
0.00	1.000000	1.000000	1.000000
10.00	0.902232	0.877430	0.870681
20.00	0.838470	0.810694	0.838775
40.00	0.758767	0.742431	0.772350
60.00	0.714134	0.701079	0.730390
90.00	0.662062	0.663009	0.684067
120.00	0.625930	0.637902	0.649947
180.00	0.582359	0.617558	0.627426
240.00	0.553666	0.605951	0.605151
360.00	0.518597	0.599649	0.592894
660.00	0.487779	0.594475	0.587383
1200.00	0.478215	0.590492	0.583083

Table A4.4 shows the data for a similar experiment performed with oxalic acid. The only difference was that 0.2 l of solution was used. The first set of results are for 0.126 g/l (0.001 M) acid, the second for 1.26 g/l acid and the third for 12.6 g/l acid. The predicted concentrations were made using the 3-parameter Dubinin isotherm. Table A4.5 shows the same data, but the data was fitted using the 2-parameter isotherm.

Table A4.4

Rate of adsorption of oxalic acid on XAD-8: 3-parameter isotherm

time [sec]	actual conc. [C/C$_0$]	predicted conc
0.000000E+000	1.000000E+000	1.000000E+000
5.000000E+000	9.325932E-001	9.409326E-001
1.000000E+001	9.199048E-001	9.195731E-001
2.000000E+001	9.119746E-001	9.038068E-001
1.200000E+002	7.906423E-001	8.919535E-001
0.000000E+000	1.000000E+000	1.000000E+000
5.000000E+000	9.587629E-001	9.750816E-001
1.000000E+001	9.460745E-001	9.612192E-001
2.000000E+001	9.365583E-001	9.498428E-001
4.000000E+001	9.365583E-001	9.415281E-001
1.200000E+002	8.485329E-001	9.345565E-001
6.000000E+002	8.556701E-001	9.287523E-001
0.000000E+000	1.000000E+000	1.000000E+000
5.000000E+000	9.444885E-001	9.569682E-001
1.000000E+001	9.294211E-001	9.400485E-001
2.000000E+001	9.175258E-001	9.277976E-001
4.000000E+001	9.103886E-001	9.173135E-001
6.000000E+001	9.088025E-001	9.104706E-001
1.200000E+002	8.747026E-001	9.048215E-001
6.000000E+002	8.651864E-001	9.002058E-001

Table A4.5

Rate of adsorption of oxalic acid on XAD-8: 2-parameter isotherm

time [sec]	actual conc. [C/C_0]	predicted conc
0.000000E+000	1.000000E+000	1.000000E+000
5.000000E+000	9.325932E-001	9.008107E-001
1.000000E+001	9.199048E-001	8.689660E-001
2.000000E+001	9.119746E-001	8.520437E-001
1.200000E+002	7.906423E-001	8.410718E-001
0.000000E+000	1.000000E+000	1.000000E+000
5.000000E+000	9.587629E-001	9.219520E-001
1.000000E+001	9.460745E-001	8.991680E-001
2.000000E+001	9.365583E-001	8.843348E-001
4.000000E+001	9.365583E-001	8.728006E-001
1.200000E+002	8.485329E-001	8.639989E-001
6.000000E+002	8.556701E-001	8.576345E-001
0.000000E+000	1.000000E+000	1.000000E+000
5.000000E+000	9.444885E-001	9.537279E-001
1.000000E+001	9.294211E-001	9.326043E-001
2.000000E+001	9.175258E-001	9.158259E-001
4.000000E+001	9.103886E-001	9.029961E-001
6.000000E+001	9.088025E-001	8.922514E-001
1.200000E+002	8.747026E-001	8.834579E-001
6.000000E+002	8.651864E-001	8.778656E-001

Table A4.6 shows the data for the contact between cation exchanged D1/D2 effluent and XAD-8. The first set of results are for effluent that had had its concentration reduced to 0.0984 C/C_0 by adsorption on XAD-8. The initial concentration for the second set of results was 0.239 C/C_0. The last two sets of results show how the resin adsorbed effluent that had not had its concentration reduced by a previous adsorption step. 0.25 l of effluent was added to 10.338 g XAD-8.

Table A4.6

Rate of adsorption of cation exchanged D1/D2 effluent on XAD-8

time [sec]	actual conc. [C/C_0]	predicted conc
0.000000E+000	1.000000E+000	1.000000E+000
1.000000E+001	9.237805E-001	9.583425E-001
2.000000E+001	9.085366E-001	9.433968E-001
3.000000E+001	9.004065E-001	9.327291E-001
4.000000E+001	8.932927E-001	9.243182E-001
6.000000E+001	8.841463E-001	9.112466E-001
9.000000E+001	8.750000E-001	8.974383E-001
1.200000E+002	8.699187E-001	8.870098E-001
1.800000E+002	8.607724E-001	8.715517E-001
2.400000E+002	8.577236E-001	8.601552E-001
3.600000E+002	8.556911E-001	8.440590E-001
6.600000E+002	8.475610E-001	8.234958E-001
0.000000E+000	1.000000E+000	1.000000E+000
1.000000E+001	9.288703E-001	9.332189E-001
2.000000E+001	8.995816E-001	8.948775E-001
3.000000E+001	8.828452E-001	8.661050E-001
4.000000E+001	8.535565E-001	8.434623E-001
6.000000E+001	8.284519E-001	8.079779E-001
9.000000E+001	7.991632E-001	7.704596E-001
1.200000E+002	7.824268E-001	7.448307E-001
1.800000E+002	7.615063E-001	7.098717E-001
2.400000E+002	7.405858E-001	6.879983E-001
3.600000E+002	7.154812E-001	6.587333E-001
6.600000E+002	6.820084E-001	6.238730E-001
0.000000E+000	1.000000E+000	1.000000E+000
1.000000E+001	8.310000E-001	8.830326E-001
2.000000E+001	7.350000E-001	7.941862E-001
3.000000E+001	6.650000E-001	7.221188E-001
4.000000E+001	6.140000E-001	6.627860E-001
6.000000E+001	5.400000E-001	5.714240E-001
9.000000E+001	4.780000E-001	4.812546E-001
1.200000E+002	4.240000E-001	4.257078E-001
1.800000E+002	3.740000E-001	3.653442E-001
2.400000E+002	3.410000E-001	3.367705E-001
3.600000E+002	2.980000E-001	3.106831E-001
6.600000E+002	2.530000E-001	2.904013E-001
0.000000E+000	1.000000E+000	1.000000E+000
1.000000E+001	8.790000E-001	8.919517E-001
2.000000E+001	7.970000E-001	8.075108E-001
3.000000E+001	7.410000E-001	7.386855E-001
4.000000E+001	7.010000E-001	6.819043E-001
6.000000E+001	6.310000E-001	5.944227E-001
9.000000E+001	5.700000E-001	5.083301E-001
1.200000E+002	5.240000E-001	4.557761E-001
1.800000E+002	4.600000E-001	3.998962E-001
2.400000E+002	4.260000E-001	3.746757E-001
3.600000E+002	3.850000E-001	3.532601E-001
6.600000E+002	3.280000E-001	3.383107E-001

Table A4.7 shows the result of contacting D1/D2 effluent with XAD-8 resin beads with diameters between 5 and 8.5E-4 m. Table A4.8 shows similar results for 3 to 4.25E-4 m XAD-8 and table A4.9 is for 1.8 to 3E-4 m XAD-8. The contacts were performed in Xactics bottles.

Table A4.7

Rate of adsorption of D1/D2 effluent on 5 to 8.5E-4 m size fraction of XAD-8.

time [sec]	actual conc. [C/C_0]	predicted conc
0.000000E+000	1.000000E+000	1.000000E+000
6.000000E+001	9.520000E-001	9.488162E-001
1.800000E+002	8.830000E-001	8.940468E-001
4.200000E+002	8.250000E-001	8.224213E-001
1.020000E+003	7.530000E-001	7.357375E-001
2.640000E+003	6.790000E-001	6.669427E-001
9.240000E+003	6.000000E-001	6.374006E-001
0.000000E+000	1.000000E+000	1.000000E+000
1.200000E+002	8.980000E-001	9.351510E-001
3.600000E+002	8.270000E-001	8.598198E-001
9.600000E+002	7.680000E-001	7.731905E-001
2.760000E+003	7.110000E-001	7.110786E-001
6.360000E+003	6.770000E-001	6.942359E-001
2.022000E+004	6.460000E-001	6.861330E-001

Table A4.8

Rate of adsorption of D1/D2 effluent on 3 to 4.25E-4 m size fraction of XAD-8.

time [sec]	actual conc. [C/C_o]	predicted conc
0.000000E+000	1.000000E+000	1.000000E+000
6.000000E+001	9.020000E-001	9.180514E-001
1.800000E+002	8.040000E-001	8.327569E-001
4.200000E+002	7.350000E-001	7.375104E-001
9.600000E+002	6.750000E-001	6.585980E-001
2.460000E+003	6.270000E-001	6.234574E-001
5.640000E+003	5.970000E-001	6.122374E-001
0.000000E+000	1.000000E+000	1.000000E+000
1.200000E+002	8.790000E-001	8.984890E-001
3.600000E+002	7.940000E-001	7.943666E-001
9.000000E+002	7.300000E-001	7.144111E-001
2.700000E+003	6.730000E-001	6.882870E-001
6.360000E+003	6.480000E-001	6.828608E-001
1.854000E+004	6.400000E-001	6.799086E-001

Table A4.9

Rate of adsorption of D1/D2 effluent on 1.8 to 3E-4 m size fraction of XAD-8.

time [sec]	actual conc. [C/C_o]	predicted conc
0.000000E+000	1.000000E+000	1.000000E+000
1.200000E+002	8.720000E-001	8.846679E-001
3.000000E+002	8.040000E-001	8.079436E-001
6.600000E+002	7.450000E-001	7.267879E-001
1.560000E+003	7.120000E-001	6.639548E-001
5.160000E+003	6.720000E-001	6.458523E-001
2.400000E+004	6.670000E-001	6.398345E-001
7.944000E+004	6.440000E-001	6.363606E-001
0.000000E+000	1.000000E+000	1.000000E+000
1.200000E+002	9.170000E-001	9.321302E-001
3.000000E+002	8.730000E-001	8.685594E-001
6.600000E+002	8.230000E-001	8.022061E-001
1.560000E+003	8.000000E-001	7.553474E-001
5.160000E+003	7.670000E-001	7.451289E-001
2.298000E+004	7.670000E-001	7.427038E-001

Tables A4.10 and A4.11 show the results of contacting activated carbon with cation exchanged D1/D2 effluent in the Xactics bottles. Run 1 used 2.33 g carbon in 0.2 l effluent and run 2 used 2.589 g carbon in 0.2 l. The results in column 3 are those predicted using the diffusion model, and those in column 4 are from the second order empirical model. Not all points could be modeled satifactorily using the empirical model.

Table A4.10

Rate of adsorption of cation exchanged D/C effluent on activated carbon, run 1.

Time [sec]	Measured conc [C/C_0]	Predicted conc: Diff model	Predicted conc: empirical
0	1.0	1.0	1.0
180	0.984	0.984	0.988
780	0.959	0.950	0.965
1980	0.912	0.915	0.921
4560	0.847	0.868	0.834
17400	0.712	0.747	0.531
66600	0.57	0.57	
169920	0.464	0.446	
243240	0.405	0.403	

Table A4.11

Rate of adsorption of cation exchanged D/C effluent on activated carbon: run 2.

Time [sec]	Measured conc [C/C_0]	Predicted conc: Diff model	Predicted conc: empirical
0	1.0	1.0	1.0
180	0.988	0.986	0.987
480	0.968	0.968	0.974
1560	0.913	0.929	0.930
3300	0.868	0.893	0.863
16200	0.733	0.760	
65400	0.588	0.588	
168780	0.480	0.453	
242040	0.410	0.407	

A second order empirical rate equation

The two connected rate equations used were re-written below for convenience.

$$\frac{dq}{dt} = K_q (q_e - q) \qquad (2.35)$$

$$\frac{dC_p}{dt} = K_p (C - C_p) \qquad (2.36)$$

These equation were solved by numerical integration. An analytical solution may have been possible, but no attempt was made to find one since numerical integration allowed additional complicating factors to be accounted for later without undue difficulty.

The differential equations were solved by Euler's rule because higher order numerical methods were found to be unstable. The program first updated the pore solution concentration using the analog derived from equation 2.36;

$$C_p = C_p + K_p (C - C_p)\, \Delta t$$

Using the new value of C_p it updated q_e using the isotherm equation. It then updated the solid phase concentration using the analog derived from equation 2.35.

$$q = q + K_q (q_e - q)\, \Delta t$$

The bulk liquid concentration was found using a mass balance between the bulk liquid and the liquid in the resin pores.

$$\Delta C = \Delta C_p / (1 - \epsilon_m)$$

where ϵ_m = mass of liquid/total mass.

The two rate constants that fitted each set of experimental data were found using a Nelder-Mead numerical search. It was found that both rate constants were concentration dependent. For the Enstra D1/D2 effluent on XAD-8 they were $K_p = 2585\ C$ and $K_q = 5{,}88 / C_p$. This model was not used further because it had no ability to predict adsorption kinetics if any of the conditions were changed. It also failed to fit the data over a wide time range.

Horizontal arrangement of CCIX columns

The Cloete-Streat column is usually constructed by placing each stage on top of the next. The column is therefore very tall, but the stage separating plates are easy to build and install in the column. Cost estimates for the proposed Sappi pilot plant include a substantial sum for the tall support structure. This could be drastically reduced if each stage were next to the other horizontally. It does, however, add a cost for top and bottom closing ends, and interconnecting piping. A larger floor area is also required.

A horizontally mounted series of three columns was built and tested. Each stage was 0.09 m ID and 0.5 m high. Each stage contained the same separator plate as used in the vertical column, but with an additional section below for liquid flow distribution. Figure A5.1 illustrates the final arrangement.

The stages were first interconnected with lengths of 0.0095 m ID polyethylene tubing between 1.0 and 1.2 m long. To measure the pressure in the stages, manometers were mounted on the sides of each stage.

The resin storage tank was first loaded with resin. Flow of water was then directed down this tank and into the columns below. This downward flow of water transported the resin into stage 3, then 2 then 1. The flow direction was then switched to normal, and the stages were fluidized. When steady state was reached, the flow was reversed again to transport resin through the stages. This cycle was repeated a number of times.

Problems experienced were:

i) uneven transfer of resin because the reverse flow did not carry the same amount of resin into each stage;

ii) difficulty in refluidizing the system after transport of the resin because of the resin 'bridging' in the pipes;

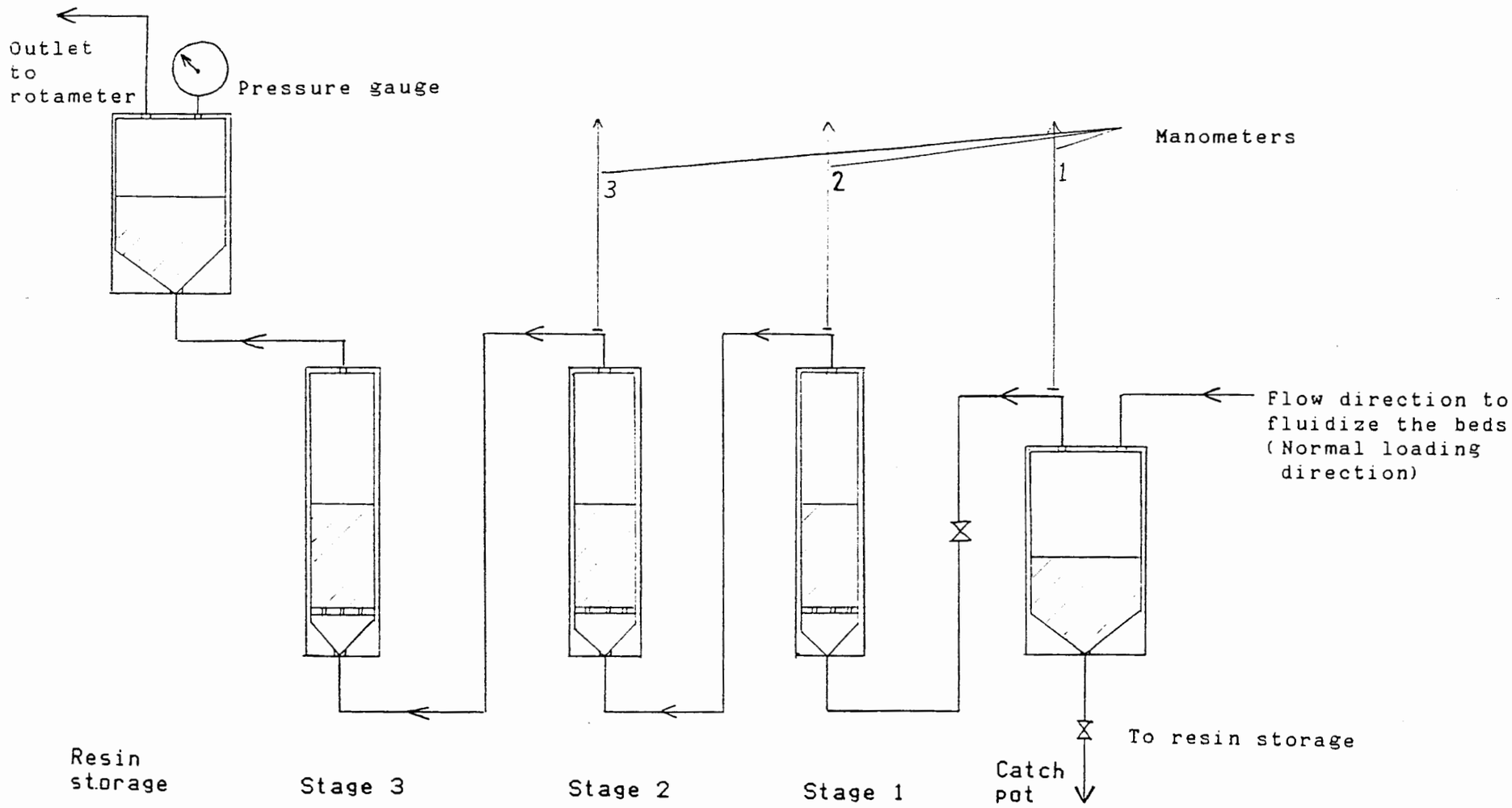

Figure A5.1. Horizontal arrangement of continuous counter-current contacting columns

iii) resin transport was slow due to friction in the pipes, and the pressure required was high at over 20 meters water head (mWh). Shortening the pipes made little difference.

Flexible 0.019 m ID by 1.0 m long tubing was then fitted between the stages, and the storage tank was placed above stage 3 instead of beside it. The pressure required for all operations was drastically reduced. The pressure to transport resin was reduced from +20 mWh to 4 mWh, and the pressure for refluidization was reduced from a +10 mWh to 3 mWh. It was found that if air was trapped in the interconnecting tubing the pressure required for forward flow was increased.

The column was finally set up as shown in Figure A5.1. Rigid PVC pipes 0.016 m ID with sharp elbows were used to connect stages. The manometers were moved to the highest point in the interconnecting piping and thus served the additional function of letting any air out.

The rigid pipes with the elbows made both resin transport and refluidizing the stages much easier. The elbows broke up the tendency for the resin to bridge in the pipes. The pressure required to transport the resin (reverse flow) was about a 1 to 2 mWh plus 0.1 mWh per stage. The pressure used to refluidize the stages after transporting the resin was 2.5 mWh on the first stage, and 2 mWh on the second stage. These pressures were sufficient to transfer the resin at satisfactory rates. Bridging of resin in the stages was observed during refluidization. To overcome this, water was allowed to flow out through the manometers (resin was prevented from escaping by screens at the base of each manometer). This had the effect of preventing excess back pressure, and of allowing the stages to refluidize sequentially. The process took about one minute per stage. Once all the stages were refluidized, the operating pressure was about 0.02 mWh per stage. It would therefore only require a 2.5 m head to refluidize 10 stages in series, and the operating pressure would be little more than that required to operate a single stage. This can be compared with the minimum 10 m operating head required for a vertical column with ten 1 m deep stages.

Table A6.1

Physical property data

Compound	mol. weight [g/mole]	Solubility in water [g/l]	temp [°C]	pKa at 25°C	refractive index [ν_D]	melting point [°C]	Density [kg/m^3]
Sodium hydroxide	40.00	420	0			318.4	2130
		3470	100				
Calcium hydroxide	74.09	1.43	0				2240
Solubility depends		1.38	10				
on size of solid		1.29	25				
crystals. Data for		1.21	30				
fine crystals		1.07	40				
Sodium chloride	58.44	357	0			801	2165
Calcium chloride	110.99	745	20			782	2150
Sodium formate	68.01	972	20			253	1920
Calcium formate	130.12	162	0				2015
		166	20				
		170.5	40				
Sodium acetate	82.03	1190	0			324	1528
Calcium acetate	158.17	374	0				
		347	20				
		342	25				
		338	30				
		327	60				
Acetic acid	60.05	oo	-		1.372	16.6	1049
Calcium n butyrate	268.32	203.1	0				
$Ca(C_4H_7O_2).3H_2O$		182	20				
		177.2	25				
		172.5	30				
		164	40				
Sodium benzoate	144.11	660	20				
Calcium benzoate	336.36	22.3	0				1436
$Ca(C_7H_5O_2)_2.3H_2O$		27.2	20				
		30.2	30				
		34.3	40				
Benzoic acid	122.13	3.0	18	4.20	1.504	122.4	1266
		3.4	25				
		6.3	42				
Sodium fumerate		972	20				
Calcium fumerate	208.18	21.1	30				
Calcium maleate	172.15	28.9	25				
Sodium oxalate	134.00	37	20			250-270	2340
Calcium oxalate	128.10	.0067	13				2200
		.0058	18				
		.007	20				
		.008	24				
		.0083	30				
		.014	95				
Oxalic acid	126.07	55.6	10	pKa_1	-	157	1650
(.$2H_2O$)		65.0	15	1.27		(sublim)	
		80.8	20	pKa_2			
		94.0	25	4.28			
		168	40				

Compound	mol. weight [g/mole]	Solubility in water [g/l]	temp [°C]	pKa at 25°C	refractive index [ν_D]	melting point [°C]	Density [kg/m^3]
Calcium malonate (.4H_2O)	214.19	2.9	0				
		3.3	10				
		3.65	20				
		3.96	30				
		4.22	40				
Malonic acid	104.06	705.0	10	pKa_1		134,9	1630
		767.8	20	2.86			
		827.5	30	pKa_2			
		883.4	40	5.65			
		897.6	50				
Sodium succinate	270.15	214.5	20				
Calcium succinate	212.22	12.2	10				
$CaC_4H_6O_4.3H_2O$		12.8	20				
		12.9	25				
		11.8	40				
Succinic acid	118.09	40	10	4.16	1.45	183	1572
		63	20	5.61			
		95	30				
		138	40				
Hexanoic acid	116.16	10.7	20	4.88	1.416	-3.9	923
Phenol	94.11	72.0	10	9.99	1.541	43	1632.55 -
		76.2	20				0.8188T -
		78.3	25				0.0067T^2
		80.7	30				
		87.6	40				
		105.3	50				
m-phthalic acid (isophthalic)	166.14	.13	25	3.62		347/8	
				4.60			
o-phthalic acid (phthalic)	166.14	7.06	25	2.95		191	1593
		10.12	35	5.41			
		14.67	45				
Calcium palmitate	550.93	0.028*	20				
Hexadecanoic acid (Palmitic)	256.43	0.0046	0	4.9§	1.433	62.7	853^{62}
		0.0072	20				
		0.0083	30				
		0.010	45				
Calcium stearate	607.04	0.04*	20			179	
Octadecanoic acid (stearic)	284.50	0.0018	0	4.9§	1.430	71.2	941
		0.0029	20				
		0.0034	30				
		0.0042	45				

* = Suspect data since Raptson (1942) stated that calcium salts of fatty acids were essentially insoluble.

§ = Estimated value

T = Temperature °C

Computer program for fitting diffusion coefficients to kinetic data

The program for determining the diffusion coefficients that best fit the experimental data is printed below. The data required by the program includes: isotherm data using the 2 or 3 parameter Dubinin or the Freundlich isotherm; data for the adsorbent such as its particle radius, porosity, density of dry adsorbent, total mass, and concentration of solute already adsorbed. The program uses the volume of solution added to calculate the system voidage. It also assumes that the adsorbent has its pores filled with solution in equilibrium with any solute already adsorbed. This allows it to estimate the concentration dependence of the surface diffusion coefficient from experiments where solutions of increasing concentration have been contacted with the same adsorbent. The program reads the data from disk or prompts the user for the required data. It can also prompt the user for first guesses of the diffusion coefficients. If a fit using a fixed surface diffusion coefficient is desired, the initial guess of the concentration dependence term can be set to zero.

```
program pdevp;    {curve fitting with the simplex algorithm}
                  {Variable Ds, and eta}
      const    m      = 3;     {number of parameters to fit}
               n      = 4;     {m+1}                                  {N.B.}
               nvpp   = 2;     {total number of vars per data point}
               mnp    = 200;   {maximum number of data points}
               alfa   = 1.0;   {reflection coefficient, >0}
               beta   = 0.5;   {contraction coefficient, 0to1}
               maxiter = 80; {max iterations for simplex ~ 20*m^2}
               max_iter = 15;{max iterations for Gauss-Seidal}
               tstep = 5;    {No of divisions between each reading}
               gamma = 2.0;  {expansion coefficient, >1}
               lw    = 5;    {width of line in data fields +1}
               root2 = 1.414214;
               assumedzero = 1E-20;
               ngrid  = 41;            {number radial steps +1}
               cGas   = 0.0083144;     {Gas constant}

      type     vector=array[1..n] of real;
               matrix = array[1..n] of vector;
               vec = array[1..ngrid] of real;

      var      done,
               Boundary  :boolean;           {convergence test}
               sets,                         {No of sets of data}
               i,j,k,
               conv,
               iso,
```

```
niter   :byte;                 {number of iterations}
h,l     :array[1..n] of byte;{number high/low paramts}
next,                          {new vertex to be tested}
center,                        {center of hyperplane described
        by all vertexes of the simplex excluding the worst}
mean,  err,
maxerr,                        {maximum error accepted}
p,sq,                          {to compute first simplex}
step    :vector;               {input starting steps}
cConst,
rad,
aCoeff,bCoeff,cCoeff,
raCoeff,rcCoeff,
gridconst,
sumq,
deltm,
etapt,
q,qold,                          {Adsorbent conc }
rrr,
rConst,
Cp,Cprev,                        {Pore conc}
qprev   :vec;
simp    :matrix;               {the simplex}
np      :array[0..30] of byte;{No of points in a data set}
data    :array[1..30,1..2,1..7] of real;  {the data}
sherwood,
Dg,Dgc,
qe,                             {In Equilib with original Cl}
qorig,                          {Original resin conc}
Corig    :array[1..7] of real; {Original solution conc}
fname    :string[14];           {File with data}
ans      :string[1];
din,
dout     :text;                 {input}
y,dy     :array[1..30,1..7]of real;{Predicted values & error}
Delq,DeltS,DelCp,               {Concentration step changes}
Cl,ClOld,                       {Conc bulk soln}
lnsat,Lkf,
deldelq1,deldelq2,
delq2,
delR,
eta,etap,                        {Voidages}
RhoSat,GasT,
qrhosat,
Mr,Vl,                           {Mass resin, Volume liquid}
delt,                            {Time step}
R,Rhos,
Rhoa,
B,nd,
wsat,
nf,Kf,                           {Freundlich constants}
sat,Temp,                        {Solubility, [C]}
etapore,
deltc,deltc1 : real;   {Time step consts}

{$R+}                                        {Enable range checking }
{$I-}                                        {Disable I/O checking }

{~~~~~~~~~~~~~~~~~~~~~~~~~~~~~~~~~~~~~~~~~~~~~~~~~~~~~~~~~~~~~~~~~~~~~~~~~~~~}
```

```
Procedure isotherm(iso : byte; qo : real; var Ci,q : real);
var    apotent    :   real;
begin
  Case iso of
    1 :
      Ci := exp((ln(q*qo)-Lkf)/nf)/qo;
    2 :
      Ci := exp(lnsat-sqrt(-B * ln(q * qRhoSat))/GasT) /qo;
    3 :
      Ci := exp(lnsat-exp((1/nd) * ln(-B * ln(q * qRhoSat)))/GasT)
              /qo;
    4 :
      q := exp(nf * ln(Ci * qo) + Lkf) / qo;
    5 :
    begin
      apotent := GasT * ln(Sat/qo/Ci);
      q := Rhosat * (exp(-apotent * apotent / B)) / qo;
    end;
    6 :
    begin
      apotent := GasT * ln(Sat/qo/Ci);
      q := Rhosat * exp(-exp(nd*ln(apotent)) / B) / qo;
    end;
  end;
end;

{~~~~~~~~~~~~~~~~~~~~~~~~~~~~~~~~~~~~~~~~~~~~~~~~~~~~~~~~~~~~~~~~~~~~~~~~~~}

procedure intg1(Co,qo : real);
                                          {Integrates between data points}
                                          {Boundary layer present}
var
         i,jj     :    byte;
begin
  conv := 1;
  while conv < max_iter do
  begin
    qold := q;
    q[1] := rConst[1] * q[2] - etapt[1] * (Cp[1] - Cprev[1]) + bCoeff[1];
    if q[1] < assumedzero then q[1] := assumedzero;
    for i := 2 to ngrid - 1 do
    begin
      q[i] := raCoeff[i] * q[i-1]  + rcCoeff[i] * q[i+1]  +  bCoeff[i]
              + etapt[i] * (Cprev[i] - Cp[i]);
      if (q[i-1] - q[i]) > assumedzero then
      begin
        q[i] := (q[i]+etapt[i]*Cp[i])*(1+rrr[i])/(1+rrr[i]+etap*Cp[i]
                /qold[i]);
        if (q[i-1] - q[i]) > assumedzero then
          q[i] := q[i-1];
      end;
      if q[i]  > 1 then  q[i] := 1;
      if q[i] < assumedzero then q[i] := assumedzero;
      isotherm(iso,qo,Cp[i],q[i]);
                                          {Update Cp using isotherm}
    end;
    q[ngrid] := bCoeff[ngrid];
    for jj := 2 to ngrid - 1 do
      q[ngrid] := q[ngrid] - (q[jj] + etap * Cp[jj]) * sumq[jj];
```

```
    q[ngrid] := q[ngrid] / sumq[ngrid];
    if q[ngrid] > 1 then
    begin
      conv := max_iter;
      boundary := false;
    end
    else
    begin
      isotherm(iso,qo,Cp[ngrid],q[ngrid]);
                                          {Update Cp using isotherm}
      if (abs(q[ngrid-1] - qold[ngrid-1])
          + abs(q[ngrid] - qold[ngrid])) < 1E-9 then
        conv := max_iter
      else
        conv := succ(conv);
    end;
  end;
  if Cp[ngrid] * qo/Co  >  C1 then
    boundary := false;
end;

{~~~~~~~~~~~~~~~~~~~~~~~~~~~~~~~~~~~~~~~~~~~~~~~~~~~~~~~~~~~~~~~~~~~~~~~~~~~~~~~~}

procedure intg2(Co,qo,Dgd : real);
                                          {Integrates between data points}
                                          {No boundary layer}
var
        i,jj     :    byte;
        delqAv   :    real;

begin                                          {Intg 2}
  conv := 1;
  while conv < max_iter do
  begin
    qold := q;
    q[1] := rConst[1] * q[2] - etapt[1] * (Cp[1] - Cprev[1]) + bCoeff[1];
    if q[1] < assumedzero then q[1] := assumedzero;
    for i := 2 to ngrid - 1 do
    begin
      q[i] := raCoeff[i] * q[i-1]  + rcCoeff[i] * q[i+1]  +  bCoeff[i]
            + etapt[i] * (Cprev[i] - Cp[i]);
      if (q[i-1] - q[i]) > assumedzero then
      begin
        q[i] := (q[i]+etapt[i]*Cp[i])*(1+rrr[i])/(1+rrr[i]+etap*Cp[i]
                /qold[i]);
        if (q[i-1] - q[i]) > assumedzero then
          q[i] := q[i-1];
      end;
      if q[i] > 1 then    q[i] := 1;
      if q[i] < assumedzero then   q[i] := assumedzero;
      isotherm(iso,qo,Cp[i],q[i]);
                                          {Update Cp using isotherm}
    end;
    delqAv := sumq[ngrid] * (delq + etap * delCp);
    for jj := 2 to ngrid - 1 do
      delqAv := delqAv +
              sumq[jj] * (q[jj] - qprev[jj] + etap*(Cp[jj] - Cprev[jj]));
    C1 := C1old - Dgd * delqAv;
                    {Mat balance on vessel}
```

```
    if c1 < assumedzero then
    begin
      c1 := assumedzero;
      writeln(' Bulk concentration below zero; check model.');
    end;
    Cp[ngrid] := C1 * Co / qo;
    isotherm(iso+3,qo,Cp[ngrid],q[ngrid]);
    delq := q[ngrid] - qprev[ngrid];
    delCp := Cp[ngrid] - Cprev[ngrid];
    deldelq1 := q[ngrid] - qold[ngrid];
    if conv > 1 then
    begin
      If abs(deldelq1) > abs(deldelq2) then
      begin
        delq := 0.25 * delq + delq2 * 0.75;
        q[ngrid] := delq + qprev[ngrid];
        isotherm(iso,qo,Cp[ngrid],q[ngrid]);
        for i := 1 to ngrid - 1 do
        begin
          q[i] := 0.25 * q[i] + 0.75 * qold[i];
          isotherm(iso,qo,Cp[i],q[i]);
        end;
        deldelq2 := abs(delq2 - delq);
        delq2 := delq;
      end                 else
      deldelq2 := abs(delq2 - delq);
    end                   else
      deldelq2 := deldelq1;
    delq2 := delq;
    deldelq1 := abs(deldelq1) + abs(q[ngrid-1] - qold[ngrid-1]);
    if deldelq1 < 1E-9 then
      conv := max_iter
    else
      conv := succ(conv);
  end;
  If deldelq1 > 1E-9 then
  begin
    delqAv := sumq[ngrid] * (delq + etap * delCp);
    for jj := 2 to ngrid - 1 do
      delqAv := delqAv +
            sumq[jj] * (q[jj] - qprev[jj] + etap*(Cp[jj] - Cprev[jj]));
    C1 := Clold - Dgd * delqAv;
  end;
  Clold := C1;
  qprev := q;
  Cprev := Cp;
end;                                                    {Intg 2}

{~~~~~~~~~~~~~~~~~~~~~~~~~~~~~~~~~~~~~~~~~~~~~~~~~~~~~~~~~~~~~~~~~~~~~~~~~~~~~~~~}

procedure sum_of_residuals (var x : vector);
                  {computes the sum of the squares of the residuals}
                  {x(1..m) passes parameters. Results returned in x(n)}
                  {x[1] = Kf.           x[2] = Ds.}
  label    astep;
  var      i,j,ii,jj   : byte;
begin
  x[n] :=0.0;
  for j := 1 to sets do
```

```
begin
  boundary := true;                              {Boundary layer present}
  Sherwood[j] := x[1]*R/Dg[j]/x[2];
  If not (iso = 1) then
    qrhosat := qe[j]/rhosat;
  C1 := 1;                                       {Initial starting conc}
  C1old := 1;
  isotherm(iso,qe[j],Cp[ngrid],qorig[j]);
                                                 {Assumed in equilibrium}
  for i := 1 to ngrid do
  begin
    q[i] := qorig[j];                            {Starting resin conc}
    qprev[i] := q[i];
    Cprev[i] := Cp[ngrid];
    Cp[i] := Cp[ngrid];
  end;
  for i := 2 to np[j] do
  begin
    DelT := (data[i,1,j] - data[i-1,1,j])/tstep;{Time step (variable)}
    If boundary then                               {Boundary layer present}
    begin
      for k := 1 to tstep do
      begin
        for ii := 1 to ngrid do
          deltm[ii] := x[2]*exp(x[3]*q[ii]/Rhosat*qe[j])*delT/R/R;
                                                   {Dimensionless time}
        deltC := DelTm[ngrid]*Dgc[j]*sherwood[j];
        delts := Sherwood[j] * deltm[ngrid];
        rrr[1] := 3 * deltm[1] / delr/delr;
        rConst[1] := rrr[1]/(1+rrr[1]);
        etapt[1] := etap/(1 + rrr[1]);
        for ii := 2 to ngrid - 1 do
        begin
          rrr[ii] := deltm[ii]/delr/delr;
          rConst[ii] := rrr[ii] / 2 / (1+rrr[ii]);
          etapt[ii] := etap/(1 + rrr[ii]);
          raCoeff[ii] := aCoeff[ii] * rConst[ii];
          rcCoeff[ii] := cCoeff[ii] * rConst[ii];
        end;
        bCoeff[1] := (qprev[1]+rrr[1]*(qprev[2]-qprev[1]))/(1+rrr[1]);
        for ii := 2 to ngrid - 1 do
          bcoeff[ii] := (qprev[ii] + rrr[ii]/2*(aCoeff[ii]*qprev[ii-1]
                        - 2*qprev[ii] + cCoeff[ii]*qprev[ii+1]))
                        /(1 + rrr[ii]);
        bCoeff[ngrid] :=  delts * (C1old - Cprev[ngrid]*qe[j]/Corig[j]);
        for ii := 2 to ngrid do
          bCoeff[ngrid] := bCoeff[ngrid] +
                           sumq[ii] * (qprev[ii] + etap * Cprev[ii]);
        C1 := C1old - deltC * (C1old - Cprev[ngrid] * qe[j]/Corig[j]);
                                                   {Material balance on vessel}
        if Cp[ngrid] * qe[j] / Corig[j]  >  C1 then
        begin
          boundary := false;
          writeln(c1:11);
          C1 := C1old;
          delq := 0;
          DelCp := 0;
          goto astep;
        end;
```

```
          intg1(Corig[j],qe[j]);                    {New bulk soln conc}
          if not boundary then
          begin
            writeln(cl:11);
            Cl := Clold;
            delq := 0;
            DelCp := 0;
            q := qprev;
            Cp := Cprev;
            goto astep;
          end;
          Clold := Cl;
          qprev := q;
          Cprev := Cp;
        end;
      end             else            {Boundary layer insignificant}
      begin
        for k := 1 to tstep do
        begin
          astep:
          for ii := 1 to ngrid do
            deltm[ii] := x[2]*exp(x[3]*q[ii]/Rhosat*qe[j])*delt/R/R;
                                                   {Dimensionless time}
          rrr[1] := 3 * deltm[1] / delr/delr;
          rConst[1] := rrr[1]/(1+rrr[1]);
          etapt[1] := etap/(1 + rrr[1]);
          for ii := 2 to ngrid - 1 do
          begin
            rrr[ii] := deltm[ii]/delr/delr;
            rConst[ii] := rrr[ii] / 2 / (1+rrr[ii]);
            etapt[ii] := etap/(1 + rrr[ii]);
            raCoeff[ii] := aCoeff[ii] * rConst[ii];
            rcCoeff[ii] := cCoeff[ii] * rConst[ii];
          end;
          bCoeff[1] := (qprev[1]+rrr[1]*(qprev[2]-qprev[1]))/(1+rrr[1]);
          for ii := 2 to ngrid - 1 do
            bcoeff[ii] := (qprev[ii] + rrr[ii]/2*(aCoeff[ii]*qprev[ii-1]
                 - 2*qprev[ii] + cCoeff[ii]*qprev[ii+1]))/(1 + rrr[ii]);
          intg2(Corig[j],qe[j],Dgc[j]);
                                                {New bulk solution conc}
        end;
      end;
      y[i,j] := Cl;
      writeln(cl:12,'  ',data[i,2,j]:12);
      dy[i,j] := y[i,j] - data[i,2,j];          {Error in prediction}
      x[n] := x[n] + abs(dy[i,j]) / (1 - data[i,2,j]);   {Sum errors}
    end;
  end;
  write('  ',niter:3);
  For i := 1 to n do
    write('  ',x[i]:13);
  writeln;
end;                            {sum_of_residuals}

{~~~~~~~~~~~~~~~~~~~~~~~~~~~~~~~~~~~~~~~~~~~~~~~~~~~~~~~~~~~~~~~~~~~~~~~~~~~~}
procedure dimension;
begin
  Corig[sets] := data[1,2,sets];
  for i := 1 to np[sets] do
```

```
  begin
    data[i,2,sets] := data[i,2,sets] /corig[sets];
  end;                                              {adjust dimensionless}
  np[sets] := pred(np[sets]);
  isotherm(iso+3,1,Corig[sets],qe[sets]);
  Dg[sets] := rhos * qe[sets]/corig[sets];
  Dgc[sets] := dg[sets] * 3 * (1-eta)/eta;
end;
{~~~~~~~~~~~~~~~~~~~~~~~~~~~~~~~~~~~~~~~~~~~~~~~~~~~~~~~~~~~~~~~~~~~~~~~~~~~~~~~~}

procedure setup;      {Get the required parameters}

begin                                               {enter}
  assign(din,'KBD:');
  reset(din);
  assign(dout,fname);
  rewrite(dout);
  writeln(' Which isotherm do you want to use ?');
  iso := 1;
  writeln(' 1 = Freundlich');
  writeln(' 2 = 2-parameter Dubinin');
  writeln(' 3 = 3-parameter Dubinin');
  readln(iso);
  writeln(dout,iso);
  If iso = 1 then
  begin
    Kf := 1.055;
    writeln(' Freundlich coefficient',Kf:12:6);
    readln(Kf);
    writeln(dout,Kf);
    rhosat := 1;
    LKf := Ln(Kf);
    nf := 3.04;
    writeln(' Freundlich exponent',nf:12:6);
    readln(nf);
    writeln(dout,nf);
  end
  else
  begin
    wsat := 1.3909E-4;
    writeln(' Adsorption capacity',wsat:12:6);
    readln(wsat);
    writeln(dout,wsat);
    B := 142.36;
    writeln(' Affinity coefficient',B:12:6);
    readln(B);
    writeln(dout,B);
    Temp := 296;
    writeln(' Temperature',Temp:12:6,' K');
    readln(temp);
    writeln(dout,temp);
    sat := 77.6;
    writeln(' Solubility',sat:12:6,' g/l');
    readln(sat);
    writeln(dout,sat);
    lnsat := ln(sat);
    Rhoa := 1073;
    writeln(' Density of solute',Rhoa:12:6);
    readln(Rhoa);
```

```
    writeln(dout,Rhoa);
    Rhosat := rhoa *  wsat;
    GasT := cGas * Temp;
    If iso = 3 then
    begin
      writeln(' Potential exponent',nd:12:6);
      readln(nd);
      writeln(dout,nd);
    end;
  end;
  R := 2.3E-4;
  writeln(' Particle radius',R:12:6,' metres');
  readln(R);
  writeln(dout,R);
  etapore := 0.56;
  writeln(' Particle porosity',etapore:12:6);
  readln(etapore);
  writeln(dout,etapore);
  Rhos := 528;
  writeln(' Density of resin',Rhos:12:6,' g/l');
  readln(Rhos);
  writeln(dout,Rhos);
  Mr := 10;
  writeln(' Mass of resin',Mr:12:6,' grams');
  readln(Mr);
  writeln(dout,Mr);
  Vl := 0.25;
  writeln(' Volume of solution added',Vl:12:6,' litres');
  readln(Vl);
  writeln(dout,Vl);
  eta := Vl/(Vl + Mr/rhos);
  sets := 1;
  np[sets] := 0;
  while not eof(din) do                          {Get the data}
  begin
    np[sets] := succ(np[sets]);
    writeln(' Input time [seconds] then concentration [g/l]
             (on same line)');
    writeln(' Start data with time = 0 and C = C orig');
    writeln(' End with time = 0 and C = 0');
                    {get the kinetic data (Time then Liquid conc)}
    readln(data[np[sets],1,sets],data[np[sets],2,sets]);
    writeln(dout,data[np[sets],1,sets],data[np[sets],2,sets]);
    if data[np[sets],2,sets] = 0.0 then
    begin
      dimension;
      writeln(' Input original solid phase concentration');
      writeln(' If no more data hit Ctl Z instead of Return');
      readln(din,qorig[sets]);
      writeln(dout,qorig[sets]);
      qorig[sets] := qorig[sets]/qe[sets];
      sets := succ(sets);
      np[sets] := 0;
    end;
  end;
  sets := pred(sets);
  close(dout);
  close(din);
end;
```

```
{~~~~~~~~~~~~~~~~~~~~~~~~~~~~~~~~~~~~~~~~~~~~~~~~~~~~~~~~~~~~~~~~~~~~~~~~~~~~~~~}

procedure enter;         {enters data from disk file fname
                          file must terminate with EOF immediately after
                          last number. }
begin
  sets := 1;                                    {First kinetic run}
  np[sets] := 0;                                {Count data points per run}
  read(din,iso);
  If iso = 1 then
  begin
    read(din,Kf,nf);
    Lkf := Ln(kf);
    rhosat := 1;
  end
  else
  begin
    read(din,wsat,B,temp,sat,Rhoa);
    Rhosat := rhoa *  wsat;
    lnsat := ln(sat);
    GasT := cGas * Temp;
    If iso = 3 then
      read(nd);
  end;
  read(din,R,etapore,Rhos,Mr,Vl);
  eta := Vl/(Vl + Mr/rhos);
  while not eof(din) do                               {Get the data}
  begin
    np[sets] := succ(np[sets]);
                          {get the kinetic data (Time then Liquid conc)}
    read(din,data[np[sets],1,sets],data[np[sets],2,sets]);
    if data[np[sets],2,sets] = 0.0 then
    begin
      dimension;
      read(din,qorig[sets]);
      qorig[sets] := qorig[sets]/qe[sets];
      sets := succ(sets);
      np[sets] := 0;
    end;
  end;
  sets := pred(sets);
end;                                                          {enter}

{~~~~~~~~~~~~~~~~~~~~~~~~~~~~~~~~~~~~~~~~~~~~~~~~~~~~~~~~~~~~~~~~~~~~~~~~~~~~~~~}

Procedure groups;                               {Calculate common groups}
begin
  step[1] := simp[1,1]/4;
  step[2] := simp[1,2]/4;
  step[3] := simp[1,3]/4;
  maxerr[1] := 0.000001;
  maxerr[2] := 0.000001;
  maxerr[3] := 0.000001;
  maxerr[4] := 0.000001;
  rad[1] := 0;
  delr := (1/(ngrid-1));
  for i := 2 to ngrid do
    rad[i] := rad[i-1] + delr;
  etap := etapore/rhos;
```

```
  cCoeff[1] := -1;
  for i := 2 to ngrid - 1 do
  begin
    aCoeff[i] := 1 - delr/rad[i];
    cCoeff[i] := 1 + delr/rad[i];
    sumq[i] := delr  * rad[i] * rad[i];
  end;
  sumq[ngrid] := delr / 2;
end;
{~~~~~~~~~~~~~~~~~~~~~~~~~~~~~~~~~~~~~~~~~~~~~~~~~~~~~~~~~~~~~~~~~~~~~~~~}

procedure writedisk(x : vector);                 {Writes results to disk}
  begin
    assign(din,fname);
    rewrite(din);
        writeln(din,'  Program exited after',niter:5,' iterations');
        write(din,'#':5,'  time (sec)   actual conc    predicted conc');
        writeln(din,'    error');
      for j := 1 to sets do
      begin
        y[1,j] := data[1,2,j];
        dy[1,j] := 0.0;
        for i := 1 to np[j] do
          writeln(din,i:3,' ',data[i,1,j]:13:2,'  ',data[i,2,j]:13:6,
                '  ',y[i,j]:13:6,'  ',dy[i,j]:9:6);
      end;
      writeln(din);
      writeln(din,'   Film Diff     Solid Diff      Conc factor
                   error.');
      for i := 1 to n do
      begin
        write(din,'  ',x[i]:13);
      end;
    close(din);
  end;

{~~~~~~~~~~~~~~~~~~~~~~~~~~~~~~~~~~~~~~~~~~~~~~~~~~~~~~~~~~~~~~~~~~~~~~~~}

procedure report;                          {Reports the results}
  var        j,i    : byte;

  begin
    sum_of_residuals(mean);
    writeln( '  Program exited after',niter:5,' iterations');
    writeln( '  The final simplex is ');
    for j := 1 to n do
    begin
      for i := 1 to n do
      begin
        if (i mod lw) = 0 then writeln;
        write('  ',simp[j,i]:12)
      end;
      writeln;
    end;
    writeln( '  The mean is');
    for i :=1 to n do
    begin
      if (i mod lw) = 0 then writeln;
      write('  ',mean[i]:12)
```

```
    end;
    writeln;
    writeln( '  The estimated fractional error is');
    for i := 1 to n do
    begin
      if (i mod lw) = 0 then writeln;
      write('  ',err[i]:12)
    end;
    writeln( ' #':4,'x':10,'y':15,'y"':15,'dy':15);
    for j := 1 to sets do
    begin
      y[1,j] := data[1,2,j];
      dy[1,j] := 0.0;
      for i := 1 to np[j] do
      begin
        writeln(i:4,' ',data[i,1,j]:13,'  ',data[i,2,j]:13,'
                  ',y[i,j]:13,'  ',dy[i,j]:13);
      end;
      writeln;
    end;
    writeln(' The average percentage error is  ',simp[1,n]/(np[j]-1):12);
    writedisk(mean);
  end;                                                    {report}

{~~~~~~~~~~~~~~~~~~~~~~~~~~~~~~~~~~~~~~~~~~~~~~~~~~~~~~~~~~~~~~~~~~~~~~~~~~~~~~~~}
procedure progrep;                          {check the starting values}
var   sigma  :  real;
      i,j    :  byte;
begin
  writeln(' #':4,'x':10,'y':15,'y"':15,'dy':15);
  for j := 1 to sets do
  begin
    y[1,j] := data[1,2,j];
    dy[1,j] := 0.0;
    for i := 1 to np[j] do
      writeln(i:4,' ',data[i,1,j]:13:2,'  ',data[i,2,j]:13:6,'
                ',y[i,j]:13:6, '  ',dy[i,j]:13);
  end;
  writeln(' The average percentage error is  ',simp[1,n]/(np[j]-1):12);
  writeln(' Press any key ');
  i := 0;
  While i < 253 do                          {Wait for an answer}
  begin
    If keypressed then
    begin
      writeln(' Do you want to change the starting values?  Y/N');
      readln(ans);
      while upcase(ans) = 'Y' do
      begin
        for i := 1 to m do
        begin
          write(simp[1,i]:12,'  New value ? ');
          readln(simp[1,i]);
        end;
        sum_of_residuals(simp[1]);
        progrep;
      end;
      i := 252;
      writeln(' File to save final results in ?');
```

```
      readln(fname);
    end;
    delay(1000);
    i := succ(i);
  end;
end;                                                    {ProgRep}

{~~~~~~~~~~~~~~~~~~~~~~~~~~~~~~~~~~~~~~~~~~~~~~~~~~~~~~~~~~~~~~~~~~~~~~~~~~~~~~~~}

procedure first;                          {Prints results for starting}
var   i,j  :  byte;
begin                                                     {simplex}
  writeln(' Starting simplex');
  for j :=1 to n do                                      {vertexes}
  begin
    write('simp[',j:1,']');
    for i :=1 to n do                                  {dimensions}
    begin
      if(i mod lw) =0 then writeln;
      write(simp[j,i]:12,'  ')
    end;                                               {dimensions}
    writeln                                              {vertexes}
  end;
  writeln                                                   {first}
end;

{~~~~~~~~~~~~~~~~~~~~~~~~~~~~~~~~~~~~~~~~~~~~~~~~~~~~~~~~~~~~~~~~~~~~~~~~~~~~~~~~}

procedure new_vertex;              {next in place of the worst vertex}
var   i,j  :  byte;
begin
  for i := 1 to n do
    simp[h[n],i] := next[i];
end;

{~~~~~~~~~~~~~~~~~~~~~~~~~~~~~~~~~~~~~~~~~~~~~~~~~~~~~~~~~~~~~~~~~~~~~~~~~~~~~~~~}

procedure order;                {gives high/low in each parameter}
                                {in simp. caution:not initialized}
  var i,j       : byte;

  begin
    for j :=1 to n do                              {all dimensiions}
    begin
      for i :=1 to n do                            {of all vertexes}
      begin                                  {find best and worst}
        if simp[i,j]< simp[l[j],j] then l[j] :=i;
        if simp[i,j]> simp[h[j],j] then h[j] :=i
      end                                                 {i loop}
    end                                                   {j loop}
  end;                                                     {order}

{~~~~~~~~~~~~~~~~~~~~~~~~~~~~~~~~~~~~~~~~~~~~~~~~~~~~~~~~~~~~~~~~~~~~~~~~~~~~~~~~}

begin             {simplex}
  writeln(' File name with old data or to save new data in ?');
  readln(fname);                        {Read data file name}
  writeln(' Do you want type in new data.  Y/N?');
  readln(ans);
```

```
if upcase(ans) = 'Y'  then
  setup
else
begin
  assign(din,fname);
  reset(din);
  enter;                                  {get the data}
  close(din);
end;
writeln(' File to save answers in ?');
readln(fname);
simp[1,1] := 1.7E-5;                      {Ks}
simp[1,2] := 5.9E-12;                     {Dso}
simp[1,3] := 0.1;                         {alpha}
writeln(' Change initial guess of diffusion coefficients ?   Y/N');
readln(ans);
if upcase(ans) = 'Y' then
begin
  writeln('  Film diffusion coefficient  ',Simp[1,1]:11);
  readln(simp[1,1]);
  writeln('  Surface diffusion coefficient  ',Simp[1,2]:11);
  readln(simp[1,2]);
  writeln('  Concentration dependence  ',Simp[1,3]:11);
  readln(simp[1,3]);
end;
writeln(' Do you want save a progress report to disk?  Y/N');
readln(ans);
groups;
sum_of_residuals(simp[1]);{first vertex  ie calculate function error}
                                          {on starting simplex}
if upcase(ans) = 'Y' then writedisk(simp[1]);
progrep;
for i :=1 to m do                         {compute offset of the vertexes}
begin                                      {of the starting simplex}
  p[i] :=step[i] * (sqrt(n) + m - 1) / (m * root2);
  sq[i] := step[i] * (sqrt(n) - 1) / (m * root2)
end;
for i :=2 to n do                           {all vertexes of the}
begin                                       {starting simplex}
    for j :=1 to m do simp[i,j] := simp[1,j] + sq[j];
  simp[i,i - 1] := simp[1,i - 1] + p[i - 1];
  sum_of_residuals(simp[i])                 {and their residuals}
end;
for i :=1 to n do                           {preset}
begin
  l[i]  := 1; h[i] :=1
end;
order;                                       {before calling}
first;                                       {to screen}
niter :=0;                                   {no iterations yet}
repeat                                       {keep iterating}
  done  :=true;                              {wish it were...}
  niter :=succ(niter);
  for i := 1 to n do center[i] :=0.0;
  for i := 1 to n do                        {compute centroid}
    if i <> h[n] then                         {excluding the worst}
      for j := 1 to m do
        center[j] := center[j] + simp[i,j];
  for i := 1 to n do                       {first attempt to reflect}
```

```
    begin
      center[i] := center[i] / m;
      next[i] := (1.0 + alfa) * center[i] - alfa* simp[h[n],i]
              {next vertex is the specular reflection of the worst}
    end;
    sum_of_residuals(next);

    if next[n] <=simp[1[n],n]then
    begin                                          {better than the best}
      new_vertex;                                  {accepted}
      for i :=1 to m do                            {and expanded}
        next[i] := gamma * simp[h[n],i] + (1.0 - gamma) * center[i];
        sum_of_residuals(next);                    {still beter}
        if next[n] <= simp[1[n],n] then new_vertex
      end                                          {expansion accepted}
    else                                        {if not better than the rest}
    begin
      if next[n] <= simp[h[n],n] then
        new_vertex                                 {better than worst}
      else                                         {worse than worst}
        begin                                      {then: contract}
          for i := 1 to m do
            next[i] := beta * simp[h[n],i] + (1.0 - beta) * center[i];
          sum_of_residuals(next);
          if next[n] <= simp[h[n],n] then
            new_vertex                              {contraction accepted}
          else                                      {if still bad}
            begin                                  {shrink all bad vertexes}
              for i := 1 to n do
              begin
                for j := 1 to m do
                  simp[i,j] := (simp[i,j] + simp[1[n],j]) * beta;
                  sum_of_residuals(simp[i])
              end                                     {i loop}
          end                                         {else}
        end                                           {else}
    end;                                              {else}
    order;
    for j := 1 to n do                             {check for convergence}
    begin
      if abs(simp[h[j],j]) < 1E-30 then simp[h[j],j] := 1E-30;
      err[j] := (simp[h[j],j] - simp[1[j],j]) / simp[h[j],j];
      if done then
        if err[j] > maxerr[j] then done := false;
    end;
  until  (done or (niter = maxiter));
  for i := 1 to n do                            {average each parameter}
  begin
    mean[i] := 0.0;
    for  j := 1 to n do  mean[i] := mean[i] + simp[j,i];
    mean[i] := mean[i] / n;
  end;
  report;                                          {to console or disk}
end.
```

Counter-current column modeling program

The program for modeling counter-current adsorption columns is shown below. It contains default values (for the pilot plant using XAD-8) of the required column operating data. These values can be changed by the user by changing the code, or by selecting the appropriate option when the program is started. Using a personal computer, the program writes its answers to the screen. However, since it is usually necessary to run the program overnight, a simple procedure for writing the output to disk may be desired.

The program does an overall mass balance after each pull-down where it determines how much solute has accumulated within the whole column since the previous pull-down. This solute accumulation figure should approach zero as the column approaches steady state. This figure was found to be a valuable cross-check of the correct operation of the program since it is independent of the numeric simulation of the adsorption kinetics. Therefore, if it does not approach zero it indicates a fault in the program.

```
PROGRAM columnp (input,output);
      CONST   endtime  = 800;                (Maximum time period)
              ngrid    = 41;               (Number of radial steps)
              nstage   = 6;               (Number of column stages)
              qorig    = 1E-15;              (Original resin conc)
              assumedzero = 1E-18;
              max_iter = 15;    Max iterations for Gauss-Seidal)

      TYPE    vecstag  = ARRAY[1..nstage] OF real;
              vecrad   = ARRAY[1..ngrid] OF real;
              matrix   = ARRAY[1..nstage] OF vecrad;

       VAR    i,                                (index for stages)
              j,                             (index for radial step)
              conv,                           (number of iterations)
              Numpulldown,                    (index for pull downs)
              Pred,
              k,
              timecount : INTEGER;              (index for time)

              Ans  :  STRING[4];
              Boundary  :ARRAY[1..NSTAGE] OF BOOLEAN;(convergence test)

              Re,                                    (Renolds number)
```

```
                rhoe,                   {Effective density of beads}
                rhos,                           {Density dry resin}
                d,                                 {Diameter beads}
                Dcol,                          {diameter of column}
                Vr,Vt,Vres,                   {stage volumes m^3}
                Mr,     {Masses of resin, pore liquid, bulk liq}
                settl_h,                   {height of settled bed}
                Xarea,           {Cross sectional area of column}
                time,LKf,
                Clstart,              {Original bulk liquid conc}
                Corig,
                Eta,etap,                               {Voidages}
                deltm, Delt, tau,                    {times steps}
                deldel1,deldel2,
                Delq1,delq2,
                DelCp1,DelCp2,
                delR,Delrt,
                Dgd,Dgf,
                Cpav,qAv,
                pulldowns,                     {Max no pull-downs}
                Clmax,Fl,height,
                Rhof,Rhor,
                Etapore,R,
                Dso,Delds,Ks,
                Kf,nfr,                        {Freundlich coeffs}
                deltD,
                DeltS,             {Concentration step changes}
                Stanton,Stant,
                qe,Visc,
                Recov,Cycletime,accum,
                Lastpulldown,Inflow,
                Coutav,Coutotal,
                Er,El,Em          :  REAL;              {voidages}

                Clold,
                Cl     :  ARRAY[0..nstage] of REAL;

                Delq              :  vecstag;

                sumq,DelCp,
                qold,
                aCoeff,cCoeff      :  vecrad;

                bCoeff,
                raCoeff,rcCoeff,
                etapt, Nf,
                rrr,rConst,
                Cp,Cprev,
                q,                     {point conc prev G-S iter.}
                qprev        :  Matrix;{Point conc on resin (time step)}

{~~~~~~~~~~~~~~~~~~~~~~~~~~~~~~~~~~~~~~~~~~~~~~~~~~~~~~~~~~~~~~~~~~~~~}

PROCEDURE default;
BEGIN
  Clmax := 0.15;
  Fl := 0.29;
  Delt := 8;
  Pred := 1;
```

```
  height := 1.0;
  Rhof := 998;
  Rhor := 1200;
  Etapore := 0.56;
  R := 2.3E-4;
  Dso := 5.9E-12;
  Delds := 0.1;
  Ks := 1.7E-5;
  Kf := 1.055;
  nfr := 3.04;
  Dcol  := 0.4;
  visc :=  1.0E-3;
END;

{~~~~~~~~~~~~~~~~~~~~~~~~~~~~~~~~~~~~~~~~~~~~~~~~~~~~~~~~~~~~~~~~~~~~~~~~~~~~~~~~}

PROCEDURE setup;
BEGIN
  WRITELN('Out-flow concentration at which to start pull-down:',Clmax:9:5);
  READLN(Clmax);
  WRITELN('Flow rate of effluent into column:',Fl:9:5,' litres/second');
  READLN(Fl);
  WRITELN('Time step for numerical model:',Delt:9:1,' seconds');
  READLN(Delt);
  WRITELN('Multiple of time step for report to screen:',Pred:4);
  READLN(Pred);
  WRITELN('Height of a column stage:',Height:9:4,' metres');
  READLN(Height);
  WRITELN('Density of effluent in column:',Rhof:9:2,' g/l or Kg/m^3');
  READLN(Rhof);
  WRITELN('Viscosity of effluent:',Visc:10:6,' Kg/m s');
  READLN(Visc);
  WRITELN('Matrix density of adsorbent:',Rhor:9:2,' g/l');
  READLN(Rhor);
  WRITELN('Porosity of adsorbent:',Etapore:9:4);
  READLN(Etapore);
  WRITELN('Radius of adsorbent particles:',R:10:5,' metres');
  READLN(R);
  WRITELN('Solid phase diffusion coefficient:  ',Dso:9,' m^2/s');
  READLN(Dso);
  WRITELN('Concentration factor for diffusion coefficient:  ',Delds:9);
  READLN(Delds);
  WRITELN('Film diffusion coefficient:  ',Ks:9,' m/s');
  READLN(Ks);
  WRITELN('Freundlich isotherm coefficient:',Kf:9:4);
  READLN(Kf);
  WRITELN('Freundlich exponent:',nfr:9:4);
  READLN(nfr);
END;

{~~~~~~~~~~~~~~~~~~~~~~~~~~~~~~~~~~~~~~~~~~~~~~~~~~~~~~~~~~~~~~~~~~~~~~~~~~~~~~~~}

PROCEDURE bedexp;  {Calculates the bed expansion, and voidage of stages}
CONST     Emf  =  0.41;                                  {Minimum voidage}

VAR       n,Uc,Ui   :  real;
          Uo  :  array[1..3] of real;
BEGIN
  Uo[2] := 0.008;                          {1st guess of free falling vel.}
```

```
  WRITELN('Diameter of adsorption column',Dcol:9:4,' m');
  READLN(Dcol);
  Xarea := 3.1416/4.0*Dcol*Dcol;
  Uc    := Fl/Xarea/rhof;              {Superficial fluidization velocity}
  rhoe  := (Etapore*rhof+(1-Etapore)*rhor);
  REPEAT                                                  {Iterate to find Uo}
    Uo[1] := Uo[2];
    Re := Uo[1]*d*rhof/visc;
    Uo[2] := d*d*(rhoe-rhof)*9.81/(18*visc*(1.0+0.15*exp(0.687*ln(Re))));
  UNTIL abs(Uo[1]-Uo[2]) < 0.00001;
  Ui  :=  EXP((ln(Uo[2])/ln(10)-d/Dcol)*ln(10));
                                {falling vel corrected for column diameter}
                                                    {Ui = 10E(logUo -d/Dcol)}
  n  :=  (4.4 + 18*d/Dcol)*EXP(-0.1*LN(Re));  {exponent for bed expansion}
  Eta  :=  EXP((LN(Uc) - LN(Ui)) /n);           {Voidage of fluidized bed}
  IF Eta < Emf THEN Eta := Emf;               {Check that bed is fluidized}
  Vt := xarea*height;                            {Total volume of stage }
  Vres := Vt*0.95*(1 - Eta);                {volume of beads (assumed solid)}
  settl_h := Vres/(1 - Emf)/Vt*height;          {settled height of resin}
  Vr := Vres*(1 - Etapore);                      {Volume of resin matrix}
  Mr := Vr*rhor;                               {Mass of resin (dry)  [Kg]}
  rhos := Mr/Vres;                                  {Density dry resin}
  Eta := (Vt - Vres)/Vt;                          {Adjust for 95% full}
  WRITELN;
  WRITELN(' Superficial settling vel = ',Uc:12,'  Renolds = ',Re:12);
  WRITELN(' Settled height resin = ',settl_h:12,'  Mass resin = ',Mr:11);
  WRITELN(' Is diameter of column correct');
  READLN(Ans);
  If upcase(ans) = 'N' THEN bedexp;
END;                                                              {bedexp}

{~~~~~~~~~~~~~~~~~~~~~~~~~~~~~~~~~~~~~~~~~~~~~~~~~~~~~~~~~~~~~~~~~~~~~~~~~~~~~~~~}

PROCEDURE pulldown;                    {Pulls the resin down one stage}
BEGIN
  Numpulldown := SUCC(Numpulldown);
  time := DelT / 60 * (pred * (timecount - 1) + k);
  Cycletime := time - lastpulldown;
  lastpulldown := time;
  Coutav := Coutotal * Delt/Cycletime/60;
  Inflow := Cycletime*60*Fl/rhof;
  Accum := Inflow*(1-Coutav);
  WRITELN;
  WRITELN('   Solute removed from effluent in last cycle = '
            ,Accum:11:5,' [Kg]');
  Recov := (Inflow - Xarea*settl_h + Vr)/Inflow;
  WRITELN('   Fraction of water recovered = ',Recov:11:4);
  WRITELN;
  WRITELN(' Stage#         Cl            Cpav            qav');
  WRITELN;
  FOR i := 1 TO nstage DO
  BEGIN
    qAv := 0;
    Cpav := 0;
    FOR j := 2 TO ngrid DO
    BEGIN
      qAv := qAv + sumq[j] * q[i,j];
      CpAv := CpAv + sumq[j] * Cp[i,j];
    END;
```

```
    qAv := qAv * 3 / 2 * delr;
    CpAv := CpAv * 3 / 2 * delr;
    IF i = 1 then
      Accum := Accum - (Mr*qav + Vres*Etapore*Cpav)*qe
                     - (Xarea*settl_h-Vres)*Cl[1]*Cl[0];
    WRITELN(i:5,'  ',Cl[i]:13:5,'  ',Cpav:13:5,'  ',qAv:13:6);
  END;
  WRITELN;
  WRITELN('   Time = ',time:9:3,' [minutes]');
  WRITELN('   Cycle time = ',Cycletime:9:3);
  WRITELN('   Average ouput conc = ',Coutav:11:6);
  Coutotal := 0;
  WRITELN('  Accumulation of solute in column during last cycle = '
         ,Accum:10:5,' [Kg]');
  WRITELN;
  Recov := (Xarea*settl_h-Vres)/(Vt - Vres);
  FOR i := 1 TO (nstage-1) DO
  BEGIN
    Cl[i] := Recov * Cl[i+1] + (1-recov) * Cl[i];     {Pull resin down}
    Clold[i] := Cl[i];
    boundary[i] := true;
    FOR j := 1 TO ngrid DO
    BEGIN
      q[i,j] := q[i+1,j];
      Cp[i,j] := Cp[i+1,j];
    END;
  END;
  FOR j := 1 TO ngrid DO
  BEGIN
    q[nstage,j] := qorig;                          {Regenerated resin in}
    Cp[nstage,j] := Corig;
  END;
  boundary[nstage] := true;
  Cl[nstage] := Clstart*Recov + (1-recov) * Cl[nstage];
  Clold[nstage] := Cl[nstage];
END;                                                              {pulldown}

{~~~~~~~~~~~~~~~~~~~~~~~~~~~~~~~~~~~~~~~~~~~~~~~~~~~~~~~~~~~~~~~~~~~~~~~~~~~~}

procedure intg2;                          {Integrates between data points}
                                                    {No boundary layer}
Var          delqAv,delqmax   :    real;

BEGIN                                                              {Intg 2}
  conv := 1;
  WHILE conv < max_iter DO
  BEGIN
    FOR j := 1 TO ngrid DO
      qold[j] := q[i,j];
    delq2 := delq1;
    delq1 := delq[i];
    delCp2 := delCp1;
    delCp1 := delCp[i];
    q[i,1] := rConst[i,1] * q[i,2] - etapt[i,1] * (Cp[i,1] -
              Cprev[i,1]) + bCoeff[i,1];
    IF q[i,1] < assumedzero THEN q[i,1] := assumedzero;
    FOR j := 2 to ngrid - 1 DO
    BEGIN
```

```
    q[i,j] := raCoeff[i,j] * q[i,j-1]  + rcCoeff[i,j] * q[i,j+1]
              +  bCoeff[i,j]  + etapt[i,j] * (Cprev[i,j] - Cp[i,j]);
                                              {new solid phase conc.}
    IF (q[i,j-1] - q[i,j]) > assumedzero THEN
    BEGIN
      q[i,j] := (q[i,j]+etapt[i,j]*Cp[i,j]) *
                (1+rrr[i,j])/(1+rrr[i,j]+etap*Cp[i,j]/qold[j]);
      IF (q[i,j-1] - q[i,j]) > assumedzero THEN
        q[i,j] := q[i,j-1];
    END;
    IF q[i,j] > 1 THEN q[i,j] := 1;
    IF q[i,j] < assumedzero THEN
      q[i,j] := qprev[i,j];
    Cp[i,j] := exp((ln(q[i,j] * qe)-Lkf)/nfr)/qe;
                                          {Update Cp using isotherm}
  END;
  deldel1 := q[i,ngrid-1] - qold[ngrid-1];
  IF conv > 1 THEN
  BEGIN
    IF abs(deldel1) > abs(deldel2) THEN            {not converging}
    BEGIN
      FOR j := 1 TO ngrid - 1 DO
      BEGIN
        q[i,j] := 0.25 * q[i,j] + 0.75 * qold[j];
        if q[i,j] < assumedzero then q[i,j] := qprev[i,j];
        Cp[i,j] := exp((ln(q[i,j] * qe)-Lkf)/nfr)/qe;
      END;
      delq[i] := 0.25 * delq[i] + 0.75 * delq2;
      delCp[i] := 0.25 * delCp[i] + 0.75 * delCp2;
      deldel2 := q[i,ngrid-1] - qold[ngrid-1];
    END                ELSE
    deldel2 := deldel1;
  END                  ELSE
    deldel2 := deldel1;
  delqAv := (delq[i] + etap * delCp[i]);
  FOR j := 2 to ngrid - 1 DO
    delqAv := delqAv +
          sumq[j]*(q[i,j] - qprev[i,j] + etap*(Cp[i,j] - Cprev[i,j]));
                                          {Mat balance on particle}
  Cl[i] := (Clold[i] * DeltD + Cl[i-1] - Delrt * delqAv) * Dgd;
                                            {Mat balance on vessel}
  IF Cl[i] < assumedzero THEN
  BEGIN
    conv := SUCC(conv);
    Cl[i] := Clold[i]/conv;
    delqmax := (Clold[i]*Deltd+Cl[i-1])/delrt-Clold[i]/conv/Dgd/Delrt;
    delqmax := delqmax/delqav;
    FOR j := 1 TO ngrid -1 DO
    BEGIN
      q[i,j] := (q[i,j] - qprev[i,j]) * delqmax + qprev[i,j];
      Cp[i,j] := (Cp[i,j] - Cprev[i,j]) * delqmax + Cprev[i,j];
    END;
    q[i,ngrid] := exp(nfr * ln(Clold[i] * Cl[0]/conv) + Lkf)/qe;
    Cp[i,ngrid] := Clold[i] *  Cl[0] / qe / conv;
    delq[i] := q[i,ngrid] - qprev[i,ngrid];
    delCp[i] := Cp[i,ngrid] - Cprev[i,ngrid];
    deldel1 := 1;
  END
  ELSE
```

```
    BEGIN
      q[i,ngrid] := exp(nfr * ln(Cl[i] * Cl[0]) + Lkf)/qe; {Surface conc}
      Cp[i,ngrid] := Cl[i] *  Cl[0] / qe;                    {"}
      delq[i] := q[i,ngrid] - qprev[i,ngrid];   {update estimate of step}
      delCp[i] := Cp[i,ngrid] - Cprev[i,ngrid];             {"}
      deldel1 := abs(deldel2) + abs(q[i,ngrid] - qold[ngrid]);
      IF deldel1 < 1E-9 THEN
        conv := max_iter
      ELSE
        conv := SUCC(conv);                    {Reset for next iteration}
    END;
  END;
  IF (deldel1 > 1E-9) THEN
  BEGIN
    delqAv := (delq[i] + etap * delCp[i]);
    FOR j := 2 TO ngrid - 1 DO
      delqAv := delqAv +
           sumq[j]*(q[i,j] - qprev[i,j] + etap*(Cp[i,j] - Cprev[i,j]));
                                                {Mat balance on particle}
    Cl[i] := (Clold[i] * DeltD + Cl[i-1] - Delrt * delqAv) * Dgd;
    IF Cl[i] < assumedzero THEN
    BEGIN
      Cl[i] := (Clold[i] * DeltD + Cl[i-1]) * Dgd;
      FOR j := 1 TO ngrid DO
      BEGIN
        q[i,j] := qprev[i,j];
        Cp[i,j] := Cprev[i,j];
      END;
    END;
  END;
END;                                                          {Intg 2}

{~~~~~~~~~~~~~~~~~~~~~~~~~~~~~~~~~~~~~~~~~~~~~~~~~~~~~~~~~~~~~~~~~~~~~~~~~~~~~~~~}

PROCEDURE nobcon;                                  {No boundary layer}
BEGIN
  FOR j  := 1 TO ngrid DO
    Nf[i,j] := Dso * exp(DelDs * q[i,j] * qe) * tau * Dgf / R / R;
                                                   {Dimensionless groups}
  rrr[i,1] := 3 * Nf[i,1] * deltm / delr/delr;  {& common combinations}
  rConst[i,1] := rrr[i,1]/(1+rrr[i,1]);
  etapt[i,1] := etap/(1 + rrr[i,1]);
  FOR j := 2 TO ngrid - 1 DO
  BEGIN
    rrr[i,j] := deltm * Nf[i,j] / delr / delr;
    rConst[i,j] := rrr[i,j] / 2 / (1+rrr[i,j]);
    etapt[i,j] := etap / (1 + rrr[i,j]);
    raCoeff[i,j] := aCoeff[j] * rConst[i,j];
    rcCoeff[i,j] := cCoeff[j] * rConst[i,j];
  END;
  bCoeff[i,1] := (qprev[i,1] + rrr[i,1]*(qprev[i,2] -
                 qprev[i,1]))/(1 + rrr[i,1]);
  FOR j := 2 TO ngrid - 1 DO
    bcoeff[i,j] := (qprev[i,j] + rrr[i,j]/2*(aCoeff[j]*qprev[i,j-1] -
              2*qprev[i,j] + cCoeff[j]*qprev[i,j+1]))/(1 + rrr[i,j]);
  intg2;                                           {Find all new concs.}
  Clold[i] := Cl[i];
END;                                                          {nobcon}
```

```
{~~~~~~~~~~~~~~~~~~~~~~~~~~~~~~~~~~~~~~~~~~~~~~~~~~~~~~~~~~~~~~~~~~~~~~~~}

procedure intg1;                              {Integrates between data points}
                                                  {Boundary layer present}
BEGIN
  conv := 1;
  WHILE conv < max_iter DO
  BEGIN
    FOR j := 1 to ngrid DO
      qold[j] := q[i,j];
    q[i,1] := rConst[i,1] * q[i,2] - etapt[i,1] * (Cp[i,1] -
              Cprev[i,1]) + bCoeff[i,1];
    FOR j := 2 TO ngrid - 1 DO
    BEGIN
      q[i,j] := raCoeff[i,j] * q[i,j-1]  + rcCoeff[i,j] * q[i,j+1]
              +  bCoeff[i,j]  + etapt[i,j] * (Cprev[i,j] - Cp[i,j]);
                                                {new solid phase conc.}
      IF (q[i,j-1] - q[i,j]) > assumedzero THEN
        q[i,j] := (q[i,j]+etapt[i,j]*Cp[i,j]) *
                  (1+rrr[i,j])/(1+rrr[i,j]+etap*Cp[i,j]/qold[j]);
      IF q[i,j] > 1 THEN q[i,j] := 1;
      IF q[i,j] < assumedzero THEN q[i,j] := assumedzero;
      Cp[i,j] := exp((ln(q[i,j] * qe)-Lkf)/nfr)/qe;
                                              {Update Cp using isotherm}
    END;
    q[i,ngrid] := bCoeff[i,ngrid] - etap * Cp[i,ngrid];
    FOR j := 2 TO ngrid - 1 DO
      q[i,ngrid] := q[i,ngrid] - ((q[i,j] + etap * Cp[i,j]) * sumq[j]);
                                                   {new surface conc.}
    IF q[i,ngrid] < assumedzero THEN
    BEGIN                                          {assume no adsorption}
      FOR j := 1 TO ngrid DO                         {for this time step}
      BEGIN
        q[i,j] := qprev[i,j];
        Cp[i,j] := Cprev[i,j];
      END;
      Cl[i] := (Cl[i-1] + Clold[i] * DeltD) * Dgd;
      conv := max_iter;
    END
    ELSE
    BEGIN
      Cp[i,ngrid] := (exp((ln(q[i,ngrid]*qe)-LKf)/nfr))/qe;
                                              {Update Cp using isotherm}
      deldel1 := (abs(q[i,ngrid-1] - qold[ngrid-1])
                + abs(q[i,ngrid] - qold[ngrid]));
      IF deldel1 < 1E-9 THEN
        conv := max_iter
      ELSE
        conv := conv + 1;
    END;
  END;
  IF Cp[i,ngrid] * qe / Cl[0]  >  Cl[i] THEN
    boundary[i] := false;
END;                                                            {intg1}

{~~~~~~~~~~~~~~~~~~~~~~~~~~~~~~~~~~~~~~~~~~~~~~~~~~~~~~~~~~~~~~~~~~~~~~~~}

PROCEDURE boundcon;
BEGIN
```

```
  FOR j  := 1 TO ngrid DO
      Nf[i,j] := Dso * exp(DelDs * q[i,j] * qe) * tau * Dgf / R / R;
                                                  {Dimensionless groups}
  rrr[i,1] := 3 * Nf[i,1] * deltm / delr/delr; {& common combinations}
  rConst[i,1] := rrr[i,1] / (1+rrr[i,1]);
  etapt[i,1] := etap / (1 + rrr[i,1]);
  FOR j := 2 TO ngrid - 1 DO
  BEGIN
    rrr[i,j] := deltm * Nf[i,j] / delr / delr;
    rConst[i,j] := rrr[i,j] / 2 / (1+rrr[i,j]);
    etapt[i,j] := etap / (1 + rrr[i,j]);
    raCoeff[i,j] := aCoeff[j] * rConst[i,j];
    rcCoeff[i,j] := cCoeff[j] * rConst[i,j];
  END;
  bCoeff[i,1] := (qprev[i,1] + rrr[i,1]*(qprev[i,2] -
                 qprev[i,1]))/(1 + rrr[i,1]);
  FOR j := 2 TO ngrid - 1 DO
    bcoeff[i,j] := (q[i,j] + rrr[i,j] / 2 * (aCoeff[j]*q[i,j-1] -
                2 * q[i,j] + cCoeff[j] * q[i,j+1]))/(1 + rrr[i,j]);
  bCoeff[i,ngrid] :=  delts * (Clold[i] - Cp[i,ngrid] * qe/C1[0]);
  FOR j := 2 TO ngrid DO
    bCoeff[i,ngrid] := bCoeff[i,ngrid] +
                     sumq[j] * (q[i,j] + etap * Cp[i,j]);
                                                  {Mat balance on vessel}
  C1[i] := (C1[i-1] + Clold[i] * DeltD  - Stant
        * (Clold[i] - Cprev[i,ngrid] * qe/C1[0])) * Dgd;
  IF Cp[i,ngrid] * qe / C1[0]  >  C1[i] THEN
  BEGIN
    boundary[i] := false;
    WRITELN('Switch to no B.L., C1 =',c1[i]:11);{Boundary insignificant}
    delq[i] := 0;
    DelCp[i] := 0;
    C1[i] := Clold[i];
  END
  ELSE
  BEGIN
    intg1;                                        {Find all new concs.}
    IF NOT boundary[i] THEN
    BEGIN                                        {Boundary insignificant}
      C1[i] := Clold[i];
      WRITELN('Switch to no B.L., C1 =',c1[i]:11);
      FOR j := 1 TO ngrid DO
      BEGIN
        q[i,j] := qprev[i,j];
        Cp[i,j] := Cprev[i,j];
      END;
      Delq[i] := 0;
      DelCp[i] := 0;
    END;
    Clold[i] := C1[i];                            {Reset for next time}
  END;
END;

{~~~~~~~~~~~~~~~~~~~~~~~~~~~~~~~~~~~~~~~~~~~~~~~~~~~~~~~~~~~~~~~~~~~~~~~~~~~~~~~~}

BEGIN
  default;
  WRITELN(' Do you want to change the column conditions ?  Y/N');
  READLN(ans);
```

```
IF UPCASE(ans) = 'Y' THEN  setup;
d := 2 * R;
bedexp;
Lkf := LN(Kf);                                          {Ln of Kf}
C1[0] := 1;                                    {feed concentration}
qe := 1;
etap := etapore/rhos;
tau := Vt * rhof / Fl;
Dgf := rhos * qe * (1 - Eta) / C1[0] / eta;
Stanton := Ks * tau * (1 - Eta) / R / eta;
Stant := 3 * eta * Stanton;
deltm := delt / tau / Dgf;
Dgd := Dgf*Deltm /(eta + Dgf * deltm);
DeltD :=  eta / (deltm * Dgf);
Delr := 1 / (ngrid - 1);
Delrt := 3 * eta * delr / 2 / deltm;
delts := 2 * Stanton * deltm / delr;
FOR j := 2 TO ngrid DO
BEGIN
  aCoeff[j] := 1 - 1 / (j - 1);
  cCoeff[j] := 1 + 1 / (j - 1);
  sumq[j] := 2 * (j-1) * (j-1) * delr * delr;
END;
sumq[ngrid] := 1;
Corig := exp((ln(qorig * qe)-Lkf)/nfr)/qe;
FOR i := 1 TO nstage DO
BEGIN
  FOR j := 1 TO ngrid DO
  BEGIN
    Cp[i,j] := Corig;
    q[i,j] := qorig;
    qprev[i,j] := qorig;
    Cprev[i,j] := Corig;
  END;
  C1[i] := Corig*qe/C1[0];          {Column initialized : fully loaded}
  C1old[i] := C1[i];                 {with clean water and clean resin}
  boundary[i] := TRUE;
END;
C1start := C1[nstage];
timecount := 0;
Numpulldown := 0;
Lastpulldown := 0;
Coutotal := 0;
REPEAT                                          {Iterate until finished}
  timecount := SUCC(timecount);
  FOR k := 1 TO pred DO                  {Iterate up to next print out}
  BEGIN
    FOR i := 1 TO nstage DO
      IF boundary[i] THEN
      BEGIN
        boundcon;
        IF NOT boundary[i] THEN
          nobcon;
      END
      ELSE
        nobcon;
    Coutotal := Coutotal + C1[nstage];
    IF c1[nstage] > clmax THEN pulldown;{Test for pull down conditions}
    qprev := q;
```

```
      Cprev := Cp;
    END;
    time := timecount * DelT / 60.0 * pred;
    WRITELN(' Outflow = ',cl[nstage]:12,' [g/l]   Time = ',
      time:7:3,' [min]');
  UNTIL ((Numpulldown > pulldowns) OR (timecount > endtime));
END.
```

Table A8.1 below shows the results from the program for a column with 6 stages, 0.4 m diameter, 1 m high, with a flow of 0.29 l/s of effluent. The column was set to pull-down at an out-flow concentration of 0.15.

Table A8.1

Computer simulation of 6 stage XAD-8 column

Time to pull-down [min]	Time between pull-downs	Stage number	Conc in stage at pull-down	Average conc in stages	Solid phase conc	Pore soln conc
233.1	-	1	0.454	0.405	0.0767	0.422
321.3	88.2					
406.8	85.5	2	0.300	0.272	0.0240	0.288
492.0	85.2					
577.2	85.2	3	0.238	0.221	0.0124	0.232
662.4	85.2					
747.7	85.3	4	0.203	0.191	0.0079	0.200
833.1	85.3					
		5	0.177	0.165	0.0052	0.175
		6	0.150	0.127	0.0030	0.146

The second column shows that the cycle time rapidly stabilised. The results for the last pull-down tested showed that there was a net accumulation of 0.00037 Kg of solute in the column, and that 1.298 Kg of solute was removed from the effluent stream. This indicated that the column had reached steady state and that the program was operating correctly. Comparing the figures in the forth and seventh columns shows that the pore solution was very nearly in equilibrium with the bulk solution. Since each stage came close to equilibrium, the graphical column design method should be accurate for XAD-8 columns. A test was performed with the data for activated carbon on the same sized column using 2E-4 m diameter particles and 10 stages. The pore solution concentration was 0.0010 and the bulk was 0.0506 indicating a very poor approach to equilibrium (the time between pull-downs was 42 minutes).

```
{~~~~~~~~~~~~~~~~~~~~~~~~~~~~~~~~~~~~~~~~~~~~~~~~~~~~~~~~~~~~~~~~~~~~~~~}

procedure intg1;                          {Integrates between data points}
                                               {Boundary layer present}
BEGIN
  conv := 1;
  WHILE conv < max_iter DO
  BEGIN
    FOR j := 1 to ngrid DO
      qold[j] := q[i,j];
    q[i,1] := rConst[i,1] * q[i,2] - etapt[i,1] * (Cp[i,1] -
               Cprev[i,1]) + bCoeff[i,1];
    FOR j := 2 TO ngrid - 1 DO
    BEGIN
      q[i,j] := raCoeff[i,j] * q[i,j-1]  + rcCoeff[i,j] * q[i,j+1]
                 +  bCoeff[i,j]  + etapt[i,j] * (Cprev[i,j] - Cp[i,j]);
                                                  {new solid phase conc.}
      IF (q[i,j-1] - q[i,j]) > assumedzero THEN
        q[i,j] := (q[i,j]+etapt[i,j]*Cp[i,j]) *
                  (1+rrr[i,j])/(1+rrr[i,j]+etap*Cp[i,j]/qold[j]);
      IF q[i,j] > 1 THEN q[i,j] := 1;
      IF q[i,j] < assumedzero THEN q[i,j] := assumedzero;
      Cp[i,j] := exp((ln(q[i,j] * qe)-Lkf)/nfr)/qe;
                                              {Update Cp using isotherm}
    END;
    q[i,ngrid] := bCoeff[i,ngrid] - etap * Cp[i,ngrid];
    FOR j := 2 TO ngrid - 1 DO
      q[i,ngrid] := q[i,ngrid] - ((q[i,j] + etap * Cp[i,j]) * sumq[j]);
                                                     {new surface conc.}
    IF q[i,ngrid] < assumedzero THEN
    BEGIN                                           {assume no adsorption}
      FOR j := 1 TO ngrid DO                         {for this time step}
      BEGIN
        q[i,j] := qprev[i,j];
        Cp[i,j] := Cprev[i,j];
      END;
      Cl[i] := (Cl[i-1] + Clold[i] * DeltD) * Dgd;
      conv := max_iter;
    END
    ELSE
    BEGIN
      Cp[i,ngrid] := (exp((ln(q[i,ngrid]*qe)-LKf)/nfr))/qe;
                                              {Update Cp using isotherm}
      deldel1 := (abs(q[i,ngrid-1] - qold[ngrid-1])
                 + abs(q[i,ngrid] - qold[ngrid]));
      IF deldel1 < 1E-9 THEN
        conv := max_iter
      ELSE
        conv := conv + 1;
    END;
  END;
  IF Cp[i,ngrid] * qe / Cl[0]  >  Cl[i] THEN
    boundary[i] := false;
END;                                                            {intg1}

{~~~~~~~~~~~~~~~~~~~~~~~~~~~~~~~~~~~~~~~~~~~~~~~~~~~~~~~~~~~~~~~~~~~~~~~}

PROCEDURE boundcon;
BEGIN
```

```
  FOR j  := 1 TO ngrid DO
      Nf[i,j] := Dso * exp(DelDs * q[i,j] * qe) * tau * Dgf / R / R;
                                                    {Dimensionless groups}
  rrr[i,1] := 3 * Nf[i,1] * deltm / delr/delr; {& common combinations}
  rConst[i,1] := rrr[i,1] / (1+rrr[i,1]);
  etapt[i,1] := etap / (1 + rrr[i,1]);
  FOR j := 2 TO ngrid - 1 DO
  BEGIN
    rrr[i,j] := deltm * Nf[i,j] / delr / delr;
    rConst[i,j] := rrr[i,j] / 2 / (1+rrr[i,j]);
    etapt[i,j] := etap / (1 + rrr[i,j]);
    raCoeff[i,j] := aCoeff[j] * rConst[i,j];
    rcCoeff[i,j] := cCoeff[j] * rConst[i,j];
  END;
  bCoeff[i,1] := (qprev[i,1] + rrr[i,1]*(qprev[i,2] -
                 qprev[i,1]))/(1 + rrr[i,1]);
  FOR j := 2 TO ngrid - 1 DO
    bcoeff[i,j] := (q[i,j] + rrr[i,j] / 2 * (aCoeff[j]*q[i,j-1] -
                2 * q[i,j] + cCoeff[j] * q[i,j+1]))/(1 + rrr[i,j]);
  bCoeff[i,ngrid] :=  delts * (Clold[i] - Cp[i,ngrid] * qe/Cl[0]);
  FOR j := 2 TO ngrid DO
    bCoeff[i,ngrid] := bCoeff[i,ngrid] +
                       sumq[j] * (q[i,j] + etap * Cp[i,j]);
                                                {Mat balance on vessel}
  Cl[i] := (Cl[i-1] + Clold[i] * DeltD  - Stant
        * (Clold[i] - Cprev[i,ngrid] * qe/Cl[0])) * Dgd;
  IF Cp[i,ngrid] * qe / Cl[0]  >  Cl[i] THEN
  BEGIN
    boundary[i] := false;
    WRITELN('Switch to no B.L., Cl =',cl[i]:11);{Boundary insignificant}
    delq[i] := 0;
    DelCp[i] := 0;
    Cl[i] := Clold[i];
  END
  ELSE
  BEGIN
    intg1;                                        {Find all new concs.}
    IF NOT boundary[i] THEN
    BEGIN                                       {Boundary insignificant}
      Cl[i] := Clold[i];
      WRITELN('Switch to no B.L., Cl =',cl[i]:11);
      FOR j := 1 TO ngrid DO
      BEGIN
        q[i,j] := qprev[i,j];
        Cp[i,j] := Cprev[i,j];
      END;
      Delq[i] := 0;
      DelCp[i] := 0;
    END;
    Clold[i] := Cl[i];                            {Reset for next time}
  END;
END;

{~~~~~~~~~~~~~~~~~~~~~~~~~~~~~~~~~~~~~~~~~~~~~~~~~~~~~~~~~~~~~~~~~~~~~~}

BEGIN
  default;
  WRITELN(' Do you want to change the column conditions ?  Y/N');
  READLN(ans);
```

```
IF UPCASE(ans) = 'Y' THEN  setup;
d := 2 * R;
bedexp;
Lkf := LN(Kf);                                          {Ln of Kf}
C1[0] := 1;                                    {feed concentration}
qe := 1;
etap := etapore/rhos;
tau := Vt * rhof / Fl;
Dgf := rhos * qe * (1 - Eta) / C1[0] / eta;
Stanton := Ks * tau * (1 - Eta) / R / eta;
Stant := 3 * eta * Stanton;
deltm := delt / tau / Dgf;
Dgd := Dgf*Deltm /(eta + Dgf * deltm);
DeltD :=  eta / (deltm * Dgf);
Delr := 1 / (ngrid - 1);
Delrt := 3 * eta * delr / 2 / deltm;
delts := 2 * Stanton * deltm / delr;
FOR j := 2 TO ngrid DO
BEGIN
  aCoeff[j] := 1 - 1 / (j - 1);
  cCoeff[j] := 1 + 1 / (j - 1);
  sumq[j] := 2 * (j-1) * (j-1) * delr * delr;
END;
sumq[ngrid] := 1;
Corig := exp((ln(qorig * qe)-Lkf)/nfr)/qe;
FOR i := 1 TO nstage DO
BEGIN
  FOR j := 1 TO ngrid DO
  BEGIN
    Cp[i,j] := Corig;
    q[i,j] := qorig;
    qprev[i,j] := qorig;
    Cprev[i,j] := Corig;
  END;
  C1[i] := Corig*qe/C1[0];          {Column initialized : fully loaded}
  C1old[i] := C1[i];                 {with clean water and clean resin}
  boundary[i] := TRUE;
END;
C1start := C1[nstage];
timecount := 0;
Numpulldown := 0;
Lastpulldown := 0;
Coutotal := 0;
REPEAT                                          {Iterate until finished}
  timecount := SUCC(timecount);
  FOR k := 1 TO pred DO                  {Iterate up to next print out}
  BEGIN
    FOR i := 1 TO nstage DO
      IF boundary[i] THEN
      BEGIN
        boundcon;
        IF NOT boundary[i] THEN
          nobcon;
      END
      ELSE
        nobcon;
    Coutotal := Coutotal + C1[nstage];
    IF c1[nstage] > clmax THEN pulldown;{Test for pull down conditions}
    qprev := q;
```

```
      Cprev := Cp;
    END;
    time := timecount * DelT / 60.0 * pred;
    WRITELN(' Outflow = ',cl[nstage]:12,' [g/l]   Time = ',
      time:7:3,' [min]');
  UNTIL ((Numpulldown > pulldowns) OR (timecount > endtime));
END.
```

Table A8.1 below shows the results from the program for a column with 6 stages, 0.4 m diameter, 1 m high, with a flow of 0.29 l/s of effluent. The column was set to pull-down at an out-flow concentration of 0.15.

Table A8.1

Computer simulation of 6 stage XAD-8 column

Time to pull-down [min]	Time between pull-downs	Stage number	Conc in stage at pull-down	Average conc in stages	Solid phase conc	Pore soln conc
233.1	-	1	0.454	0.405	0.0767	0.422
321.3	88.2	2	0.300	0.272	0.0240	0.288
406.8	85.5	3	0.238	0.221	0.0124	0.232
492.0	85.2	4	0.203	0.191	0.0079	0.200
577.2	85.2	5	0.177	0.165	0.0052	0.175
662.4	85.2	6	0.150	0.127	0.0030	0.146
747.7	85.3					
833.1	85.3					

The second column shows that the cycle time rapidly stabilised. The results for the last pull-down tested showed that there was a net accumulation of 0.00037 Kg of solute in the column, and that 1.298 Kg of solute was removed from the effluent stream. This indicated that the column had reached steady state and that the program was operating correctly. Comparing the figures in the forth and seventh columns shows that the pore solution was very nearly in equilibrium with the bulk solution. Since each stage came close to equilibrium, the graphical column design method should be accurate for XAD-8 columns. A test was performed with the data for activated carbon on the same sized column using 2E-4 m diameter particles and 10 stages. The pore solution concentration was 0.0010 and the bulk was 0.0506 indicating a very poor approach to equilibrium (the time between pull-downs was 42 minutes).